

**Nanotech France 2017**

**NanoMaterials for Energy & Environment**

**NanoMatEn 2017 – NanoMetrology 2017**

**Joint International Conferences and Exhibition**

**28 - 30 June, 2017**

**Paris – France**

# **Book of Abstracts**

Organizer



**SETCOR**  
Conferences & Exhibitions

**Nanotech France 2017**  
**Plenary session I**

# Combined experimentation and simulation on mechanical failure of metal/ceramic interfacial regions

X. Zhang<sup>1</sup>, B. Zhang<sup>1</sup>, Y. Mu<sup>1</sup>, S. Shao<sup>1</sup>, C.D. Wick<sup>2</sup>, B.R. Ramachandran<sup>2</sup>, W.J. Meng<sup>1,\*</sup>

<sup>1</sup>Louisiana State University, Baton Rouge, Louisiana 70803, U.S.A.

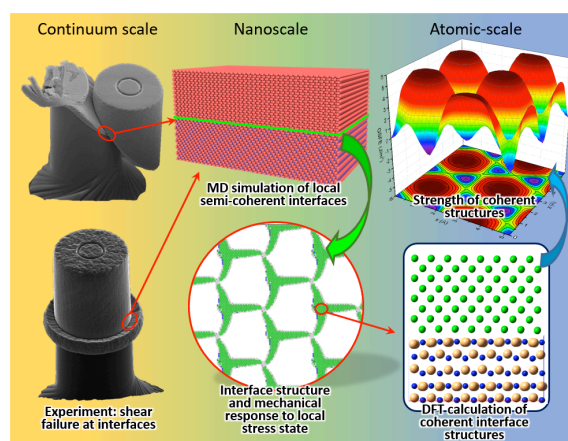
<sup>2</sup>Louisiana Tech University, Ruston, Louisiana 71272, U.S.A.

## Abstract:

We present new experimentation and modeling/simulation results on mechanical integrity of metal/ceramic interfacial regions. This study is relevant to Nanotech France 2017 Conference Topics of *Advanced Nanomaterials - Nanostructured coatings, Surfaces and Membranes and Nanomaterials Fabrication, Characterization and Tools - Nanoscale Materials Characterization*

Shear failure of the interfacial regions of two ceramic coating / metal adhesion layer / substrate systems, CrN/Cu/Si and CrN/Ti/Si, was measured quantitatively and observed directly through in-situ microscale compression of cylindrical micro-pillars with concurrent electron microscopy observations. Results indicate, for the first time to our knowledge, that shear failure of the interfacial region occurs in two stages: an initial shear deformation of the entire metal interlayer followed by an unstable dynamic shear failure close to one metal/ceramic interface. The experimentally observed dynamic shear failure is suggested to be concomitant with the metal/ceramic interface going from being “locked”, with no relative displacement between materials on the two sides of the interface, to being “unlocked”, with significant relative displacements. Density functional theory (DFT) and molecular dynamics (MD) studies on a related, Ti/TiN metal / ceramic interface provided further insights into this behavior. It was shown, for the first time to our knowledge, that a weak interaction plane exists in the metal layer near the chemical interface in a coherent Ti/TiN structure. Consequently, the free energy as well as the theoretical shear strength of the semi-coherent Ti/TiN interface is found to depend on the physical location of the misfit dislocation network (MDN). The minimum energy and strength of the interface occur when the MDN is near, but not at the chemical interface. The movement of this dislocation network as a critical stress level is reached provides a likely physical mechanism through which the unstable interfacial dynamic shear failure is achieved. The present results point to means of effective interface engineering in the future.

**Keywords:** Mechanical integrity of metal/ceramic interfaces, in-situ microscale mechanical testing, coating/substrate interfaces, density functional theory, molecular dynamics, dislocation mediated interfacial failure.



The figure above illustrates the scope of our combined experimentation and simulation studies on the mechanical integrity of metal/ceramic interfacial regions under shear loading. In-situ microscale mechanical testing reveals the two-stage interfacial shear failure. Combining DFT calculations with MD simulations, the energetics of coherent metal/ceramic interfaces in tension and shear are related to the shear response of MDNs at different physical locations relative to the metal/ceramic chemical interface. The movement of the MDN at a critical shear stress provides a physical mechanism for the experimentally observed unstable dynamic shear failure.

## References:

1. Y. Mu, J.W. Hutchinson, W.J. Meng, Micro-pillar measurements of plasticity in confined Cu thin films, *Extreme Mechanics Letters* 1, 62-69 (2014).
2. Y. Mu, X. Zhang, J.W. Hutchinson, W.J. Meng, Measuring critical stress for shear failure of interfacial regions in coating/interlayer/substrate systems through a micro-pillar testing protocol, *J. Mater. Res.* 32, doi:10.1557/jmr.2016.516 (2017).

# Relating elasticity and graphene folding conformation

Barry J. Cox, Duangkamon Baowan<sup>#</sup>, Wolfgang Bacsas<sup>^</sup> and James M. Hill<sup>\*</sup>

Nanomechanics Group, School of Mathematical Sciences, The University of Adelaide, South Australia 5005 Australia,

<sup>#</sup>Department of Mathematics, Faculty of Science, Mahidol University, Rama VI; Centre of Excellence in Mathematics, CHE, Si Ayutthaya Rd, Bangkok 10400 Thailand,

<sup>^</sup>CEMES-CNRS and University of Toulouse, 29 rue Jeanne Marvig, 31055 Toulouse, France,

<sup>\*</sup>School of Information Technology and Mathematical Sciences, University of South Australia, Mawson Lakes, South Australia 5095 Australia

## Abstract:

The variational calculus is employed to determine the folding behaviour of a single graphene sheet. Both elastic and van der Waals energies are taken into account, and from these considerations the shape of the curve is determined. By prescribing that the separation distance between the folded graphene in the parallel region is  $3.32\text{ \AA}$ , an arbitrary constant  $\beta$  arising by integrating the Euler-Lagrange equation is determined. Furthermore, the full parametric representations for the folding conformation is derived, so that the folded graphene may be depicted graphically. Using typical values of the bending rigidity in the range of 0.800 - 1.60 eV, the shortest stable folded graphene sheets are required to be at least 6.5 - 10 nm in length for the folded conformation.

**Keywords:** grapheme folding; elasticity; variational calculus; Euler-Lagrange equations;

## References:

1. B. J. Cox, D. Baowan, W. Bacsas and J. M. Hill, "Relating elasticity and graphene folding conformation." *RSC Advances*, **5** (2015) 57515-57520.
2. J. S. Bunch, A. M. van der Zande, S. S. Verbridge, I. W. Frank, D. M. Tanenbaum, J. M. Parpia, H. G. Craighead and P. L. McEuen, Electromechanical resonators from grapheme sheets, *Science*, 2007, 315, 490–493.
3. K.-T. Lam, C. Lee and G. Liang, Bilayer graphene nanoribbon nanoelectromechanical system device: a computational study, *Appl. Phys. Lett.*, 2009, 95, 143107.
4. M. Poetschke, C. G. Rocha, L. E. F. Foa Torres, S. Roche and G. Cuniberti, Modeling graphene-based nanoelectromechanical devices, *Phys. Rev. B: Condens. Matter Mater. Phys.*, 2010, 81, 193404.
5. X. Sun, Z. Liu, K. Welsher, J. T. Robinson, A. Goodwin, S. Zaric and H. Dai, Nanographene oxide for cellular imaging and drug delivery, *Nano Res.*, 2008, 1, 203–212.
6. H. Jiang, Chemical preparation of graphene-based nanomaterials and their applications in chemical and biological sensors, *Small*, 2011, 7, 2413–2427.

# Static Multiple Light Scattering as a tool to monitor size evolution of nanoparticles during wet milling, comparison with laser diffraction and DLS

C. Tisserand, G. Brambilla, P. Bru, G. Meunier

Formulation, 3-5 Rue Paule Raymondis, 31200 Toulouse, France

## Abstract:

Nano suspensions or emulsions are widely used in the industry but their real dispersion state remains unknown or not well characterized in their native and concentrated form. Indeed, it is well known that aggregation and agglomeration may exist in concentrated regime.

A technique of Static Multiple Light Scattering (SMLS) is proposed to measure mean particles size in a large range of concentration between 0.0001 and 95%, for sizes between 10 nm and 100  $\mu\text{m}$  by Turbiscan LAB technology. Turbiscan consists in sending a light source (880nm) and acquiring backscattered and transmitted signal. The signal intensity enables to measure directly the mean spherical equivalent diameter ( $d$ ), knowing refractive index of continuous ( $n_f$ ) and dispersed phase ( $n_p$ ) and the particles concentration ( $\varphi$ ) according to the Mie theory:

$$d = f(BS \text{ (or } T), \varphi, n_p, n_f)$$

with BS for Backscattering Intensity and T for Transmission Intensity.

This technique has the advantage to measure in one click, without sample preparation or dilution, the mean particles size and so the dispersibility efficiency particularly for concentrated suspensions. Other optical techniques such as DLS, PTA or laser diffraction can perform this measurement but only at a very high dilution which denatures the agglomerates and give an erroneous size of the native particles.

In this work, we present a complete study of size measurement of silica particles exposed to wet milling and going from micro to nanometers. This size is measured with SMLS and compared with DLS and Laser Diffraction.

We propose also to present comparison of SMLS with SEM/TEM microscopy size measurement.

**Keywords:** SMLS, silica particles, nanoparticles, DLS, laser diffraction, static multiple light scattering, aggregation, dispersibility, mean size

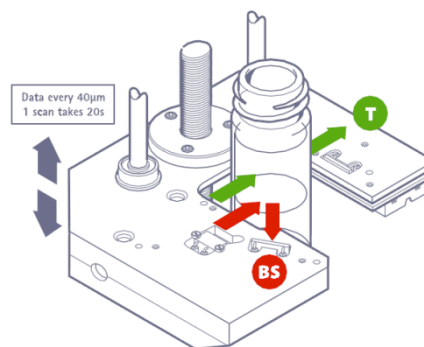


**Figure 1:** Principle of measurement of Turbiscan®

## References:

1. M. Wulff-Pérez, J. de Vicente, A. Martín-Rodríguez, M. J. Gálvez-Ruiz, *Int. J. Pharm.*, 2012, 423, 161-166
2. A. Pizzino, M. Catté, E. Van Hecke, J.-L. Salager, J.-M. Aubry, *Coll. Surf.*, 2009, 338, 148-154
3. D. Seo, W. Yoon, S. Park, J. Kim, J. Kim, *Coll. Surf. A*, 2008, 313-314

# Measurement and modeling of the effective thermal conductivity of sintered silver pastes

Jose Ordonez-Miranda,<sup>1\*</sup> Sebastian Volz<sup>2</sup>

<sup>1</sup> Institut Pprime, CNRS, Université de Poitiers, F-86962, Futuroscope, France

<sup>2</sup> Laboratoire EM2C, CNRS, CentraleSupélec, Université Paris-Saclay, 92295 Chatenay, France

## Abstract:

Thermal interface materials, such as thermal pastes, are critical for optimizing the thermal contacts between two surfaces and improving the heat dissipation across them. In this work, the effective thermal conductivity of sintered porous pastes of silver is modeled through two theoretical methods and measured by means of three experimental techniques. The first model is based on the differential effective medium theory and provides a simple analytical description considering the air pores like ellipsoidal voids of different sizes, while the second one arises from the analysis of the scanning-electron-microscope images of the paste cross-sections through the finite element method. The predictions of both approaches are consistent with each other and show that the reduction of the thermal conductivity of porous pastes can be minimized with spherical pores and maximized with pancake-shaped ones, which are the most efficient to block the thermal conducting pathways. A thermal conductivity of 151.6 W/m K is numerically determined for a sintered silver sample with 22% of porosity. This thermal conductivity agrees quite well with the one measured by LaTIMA for a suspended sample and matches, within an experimental uncertainty smaller than 16%, with the values obtained by means of Raman thermometry and the  $3\omega$  technique, for two samples buried in a silicon chip. The consistence between our theoretical and experimental results demonstrates the good predictive performance of our theoretical models to describe the thermal behavior of porous thermal interface materials and to guide their engineering with a desired thermal conductivity.

**Keywords:** Thermal conductivity, sintered silver pastes, Raman thermometry,  $3\omega$  technique, effective medium theory, finite element method.

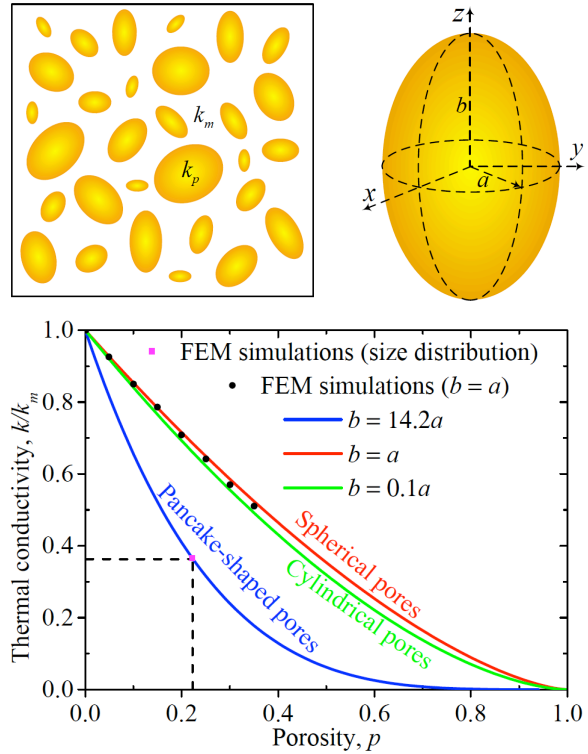


**Figure 1:** (a) Scheme of a porous paste made up of ellipsoidal pores of arbitrary size embedded in a matrix of thermal conductivity  $k_m$ , and (b) its normalized thermal conductivity as a function of porosity.

## References:

1. Ordonez-Miranda, J., Hermens, M., Nikitin, I., Kouznetsova, V. G., Van der Sluis, O., Abo Ras, M., Reparaz, J. S., Wagner, M., Sledzinska, R. M., Gomis-Bresco, J., Sotomayor Torres, C. M., Wunderle, B., Volz, S. (2016), Measurement and modeling of the effective thermal conductivity of sintered silver pastes, *Int. J. Thermal Sci.*, 108, 185-194.
2. Ordonez-Miranda, J., Alvarado-Gil, J. J. (2012), Effect of the pore shape on the thermal conductivity of porous media, *J. Mater. Sci.*, 47, 6733-6740.

# **Session I: Nanomaterials Fabrication / Synthesis**

# Effect of specific ions on the surface charge of silica nanoparticles and ion behaviour in silica gels

C. Sögaard<sup>1</sup>, J. Funehag<sup>2</sup>, Z. Abbas<sup>1</sup>

<sup>1</sup>University of Gothenburg, Department of Chemistry and Molecular Biology, Gothenburg, Sweden

<sup>2</sup>Chalmers University of Technology, Department of Geology and Geo-technique, Gothenburg, Sweden

## Abstract:

Use of silica nanoparticles as grouting material is an emerging environmentally friendly nanotechnology in tunnel construction. Low viscosity of silica nanoparticles suspension allows for the penetration of narrow fractures which cannot be grouted by cement. Use of silica nanoparticles as grouting material is based on the formation of gel. Usually gelling is induced by adding salt such as NaCl or KCl termed as an accelerator salt, see figure 1. It is well documented in literature that gel time of silica is highly salt specific and follows the direct Hofmeister series i.e.,  $\text{Li} < \text{Na} < \text{K} < \text{Rb} < \text{Cs}$  [1]. This can be rationalized by the affinity of counterions to the silica surface and hence the effectivity in screening the electrostatic forces between negatively charged silica particles.

There are some key issues such as long term stability and gel strength development, which need to be investigated before silica can find a wide spread use as grouting material. In this project, we are investigating the long term stability of silica by studying the aggregation, gelling of silica nanoparticles in different monovalent salts and by executing a long time leaching testes of silica gels formed by different accelerators and by varying the ionic composition of water and pH.

Results of potentiometric titrations clearly demonstrate the ion specific effects. It has been found that surface charge of silica nanoparticles increases in the presence of KCl compared with NaCl and LiCl as well as at high salt concentration. The stronger affinity of  $\text{K}^+$  for silica surface enhanced the screening of charged sites and hence deprotonation increases. The strong affinity of  $\text{K}^+$  for silica was also exhibited in the long time leaching tests which showed that leaching of  $\text{K}^+$  compared to  $\text{Na}^+$  was much lower. More results, especially with regard to ion effect on aggregation behaviour of the particles, will be presented for this ongoing research project.

**Keywords:** silica nanoparticles, silica sols, grouting, specific ion effect, acid-base titration, surface charge

## References:

1. Lyklema J. Simple Hofmeister series. *Chemical Physics Letters*. 2009;467(4–6):217-22.



**Figure 1:** Gel formed from silica sol upon introduction of salt accelerator.

# Rational Design of Mesoporous Silica Nanoparticles for Robust Immobilization of Lipase

M. Kalantari, M. Yu, C.Z. Yu

Australian Institute for Bioengineering and Nanotechnology, The University of Queensland, Brisbane, QLD 4072, Australia

## Abstract:

In recent years, the utilization of lipase (triacylglycerol ester hydrolases, EC 3.1.1.3) has gained important industrial applications, e.g., in pharmaceutical synthesis, food processing and biofuel production.<sup>[1]</sup> To overcome the limitations of native lipase including its proclivity to denaturation and the difficulty in recycling, immobilization of lipase including physical adsorption and chemical attachment approaches has been developed.<sup>[2]</sup> Even with promising achievements in the field of lipase immobilization, it remains an ongoing challenge to develop a simple approach with high loading, activity and stability.

Herein, hydrophobically modified mesoporous silica nanoparticles (MSN) with a high octadecylalkyl content of 19 wt% and adjustable pore sizes (1.6-13 nm) have been synthesized via a facile co-condensation approach. It is demonstrated that both the increased hydrophobic content and a tailored pore size ( $\sim 5$  nm) slightly larger than the size of enzyme are responsible for hyper-activation of immobilized lipase (Figure 1). The optimized C18-MSN exhibits a loading capacity of  $711 \text{ mg g}^{-1}$  with a specific activity 5.23 times than that of free enzyme with  $> 93\%$  of initial activity retained after 5 times' reuse, which is better than the best performance reported to date.<sup>[3]</sup> Our findings have paved the way towards robust immobilization of lipase for biocatalytic applications.<sup>[4]</sup>

**Keywords:** silica, hydrophobic, lipase immobilization, hyperactivation, pore size.

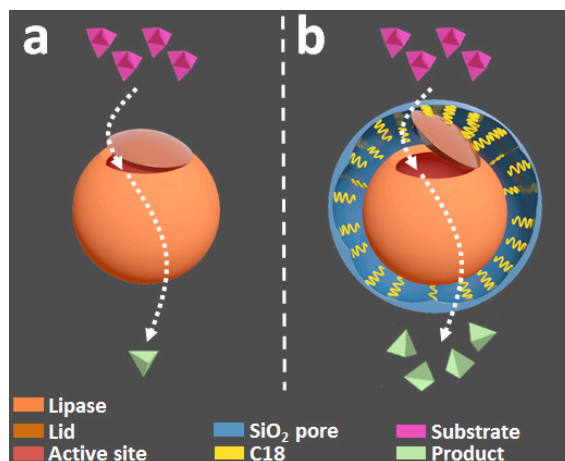


**Figure 1:** Schematic of the lid opening for lipase. For native lipase (a), the active site is partially covered by the lid. C-18MSNs (b) create a hydrophobic interface, causing the lid opening of immobilized lipase, a more accessible active site, and improved enzymatic activity to convert the substrate to the product. Objects are not drawn to scale.

## References:

1. P. Adlercreutz, P., (2013) *Chemical Society Reviews* **2013**, 42, 6406-6436.
2. Y. Zhang, J. Ge, Z. Liu, *ACS Catalysis* **2015**, 5, 4503-4513.
3. Z. Zhou, R. N. K. Taylor, S. Kullmann, H. Bao, M. Hartmann, *Advanced Materials* **2011**, 23, 2627-2632; Q. Jin, G. Jia, Y. Zhang, Q. Yang, Can Li, *Langmuir* **2012**, 28, 9788-9796; A. Rezaei, O. Akhavan, E. Hashemi, M. Shamsara, *Chem.Mater.* **2016**, 28, 3004-3016; M. Mathesh, B. Luan, T. O. Akanbi, J. K. Weber, J. Q. Liu, C. J. Barrow, R. H. Zhou, W. R. Yang, *ACS Catal.* **2016**, 6, 4760-4768.
4. M. Kalantari, M. Yu, Y. Yang, E. Strounina, Z. Gu, X. Huang, J. Zhang, H. Song, C. Yu, *Nano Research* **2016**, 1-13.

# The role of substrate rotation for growing metallic nanostructures prepared by glancing angle deposition

S. Liedtke,\* Ch. Grüner, B. Rauschenbach

Leibniz Institute of Surface Modification (IOM), Permoserstr. 15, D-04318 Leipzig, Germany

## Abstract:

Glancing angle deposition (GLAD) represents a powerful technique for sculpturing versatile nanostructure morphologies. Sensing, optics, energy and catalysis as well as biomedicine [1] are some of numerous potential application areas for such nanostructured films. As a matter of fact, the growth mechanisms of especially metallic nanostructures prepared by GLAD are only fragmentarily understood yet. Nevertheless, it is important to learn about these growth mechanisms in detail, because sub-nm scale morphology determines the properties of such nanostructured films significantly.

Here, Al, Ti, Cr and Mo are the selected metals because a wide range of melting points is covered (Al: 660 °C, Mo: 2617 °C). The metals are evaporated by an electron beam and deposited on flat Si(100) substrates at room temperature. The resulting films are investigated by scanning electron microscopy (SEM) and x-ray diffraction (XRD) measurements.

In a common physical vapor deposition process, the angle  $\theta$  between incoming particle flux and substrate normal is fixed to  $0^\circ$ , so there is no angular dependence. However, modifying the angle  $\theta$  plays a major role if the nanostructure morphology is to be influenced. When the substrate is tilted to an oblique angle of incidence  $70^\circ < \theta < 90^\circ$ , a highly porous film consisting of separated tilted columns is created. This is called oblique angle deposition (OAD), whereas GLAD is characterized by the combination of an oblique angle of incidence  $\theta$  and simultaneous substrate rotation. As the substrate rotates continuously, the apparent direction of the incoming particles is altered, which forces the columns to change their growth direction. Thus, varying the substrate rotation frequency allows the growth of spirals, screws and upright columns. On top of that, stepwise rotation is also possible. For example, zigzag structures can be created by first growing tilted columns, then rotating rapidly to  $180^\circ$  and again growing tilted columns etc.

It is observed that both the continuously and stepwise rotated nanostructures grow more

slowly in height compared to the not rotated nanostructures (Figure 1). A detailed study of rotated and not rotated nanostructures allows to identify how general growth mechanisms, such as nucleation process, self-shadowing and competitive growth, influence the morphology of the resulting film. Besides, XRD measurements reveal that the grown nanostructures are indeed crystalline, which brings further important growth factors such as crystalline structure and preferred growth orientation in focus of the presentation.

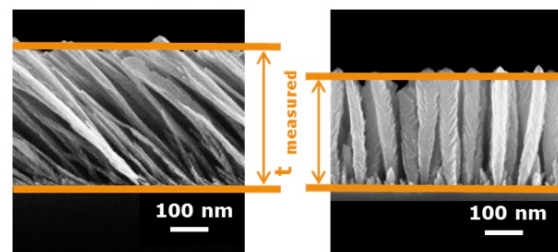


**Figure 1:** SEM images of not rotated (left) and rotated (right) Mo columns grown by evaporative glancing angle deposition on flat Si(100) substrates at room temperature.

**Keywords:** Glancing angle deposition, metallic nanostructures, scanning electron microscopy, x-ray diffraction, surface diffusion, self-organization

## References:

1. Srivastava, S. K., Shalabney, A., Khalaila, I., Grüner, C., Rauschenbach, B. and Abdulhalim, I. (2014) *Small*, 10, 3579–3587.

# Understanding the effects of Precursor Loading Factors on the Premixed Flame Synthesis of Titanium Oxide Nanoparticles

Xingming Lu\*, Jonathan Salvage, Khizer Saeed

Low Carbon Energy Research Group, School of Computing, Engineering and Mathematics,  
University of Brighton Lewes Road, Moulsecoombe, Brighton. BN2 4GJ. United Kingdom

## **Abstract:**

Premixed flame nanoparticles synthesis is emerging a promising method for large scale production of nanoparticle. This paper presents the work undertaken to investigate and establish the effects of precursor loading factors on the morphology of nanoparticles synthesized using premixed flame burner technique. Initially, a brief review of studies on the effect of precursor loading on flames based synthesis of nanoparticles was undertaken and presented. Experimental methodology of precursor loading in the new premixed flame nanoparticle synthesis system and used in the present work is presented. Next, the effects of precursor factors of precursor temperature and feed rate of Titanium isopropylate (TTIP) was undertaken and presented. The synthesis of titanium oxide ( $\text{TiO}_2$ ) nanoparticles were collected and analyzed by Scanning Transmission Electron Microscope (STEM). The effects of precursor factors on the size and morphology of end particles have been presented and discussed.

# Realization of Large-Area Wrinkle-Free Monolayer Graphene Films Transferred to Functional Substrates

Byeong-Ju Park<sup>1</sup>, Soon-Gil Yoon<sup>1</sup>

<sup>1</sup>Department of Materials Science and Engineering, Chungnam National University, Daeduk Science Town, 34134, Daejeon, South Korea

## Abstract:

Structural inhomogeneities, such as the wrinkles and ripples within a graphene film after transferring the free-standing graphene layer to a functional substrate, degrade the physical and electrical properties of the corresponding electronic devices. Here, we introduced titanium as a superior adhesion layer for fabricating wrinkle-free graphene films that is highly applicable to flexible and transparent electronic devices. The Ti layer does not influence the electronic performance of the functional substrates. Experimental and theoretical investigations confirm that the strong chemical interactions between Ti and any oxygen atoms unintentionally introduced on/within the graphene are responsible for forming the clean, defect-free graphene layer. Our results accelerate the practical application of graphene-related electronic devices with enhanced functionality. The large-area monolayer graphenes were prepared by a simple attachment of the Ti layer with the multi-layer wrinkle-free graphene films. For the first time, the graphene films were addressed for applications of superior bottom electrode for flexible capacitors instead of the novel metals.

**Keywords:** Graphene, wrinkle-free, Ti layer, BMNO capacitor

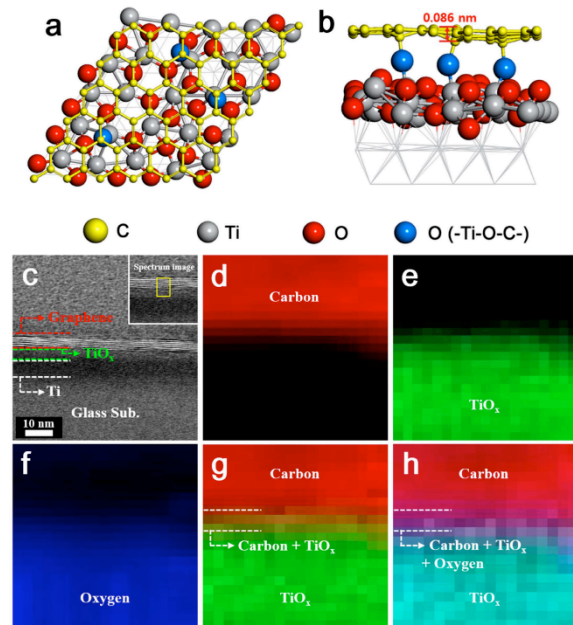


**Figure 1:** (a, b), The DFT-calculated morphologies at the interface; (c) the ADF image observed for the graphene film transferred to the Ti (10 nm)/glass. (d, e, and f). EELS mapping image observed at the bonding state of (g) (carbon and TiO<sub>x</sub>) and (h) (carbon, TiO<sub>x</sub>, and oxygen)

# The Effect of Polymer Functional Group on the Adsorption Behaviour of Polymers onto Graphene Oxide Nanosheets.

E. Al-Bermany, B. Chen,

University of sheffield, Department of Materials Science and Engineering, Sheffield, UK

## Abstract:

Polymer-graphene nanocomposites have shown high potential for a wide range of engineering and energy applications. This work aims to investigate the effect of polymer functional group on the adsorption behaviour of polymers onto graphene oxide (GO) nanosheets. Poly(methyl methacrylate) (PMMA), poly(methyl methacrylate-co-methacrylic acid) (PMM-MA) and poly(methacrylic acid) (PMAA) were used as the polymer models with different functional groups. GO was synthesised from graphite using a modified Hummers method which has functional groups including hydroxyl, epoxy and carboxylic acid. Various polymer-adsorbed GO nanohybrids were prepared using a solution processing method using N,N-Dimethylformamide (DMF) as the solvent. Fourier transform infrared spectroscopy (FT-IR), thermogravimetric analysis (TGA), differential scanning calorimetry (DSC), X-ray diffraction (XRD), contact angle measurements and scanning electron microscopy (SEM) were performed to characterise the structure and morphology of the nanohybrids. The characteristic peaks for the functional groups of both GO and the polymer were found in the FT-IR spectra of most nanohybrids. The TGA results showed that the polymers were adsorbed onto GO nanosheets with different ratios, and the maximum adsorption amount was 40 wt% for PMAA. DSC results showed increased glass transition temperatures of the polymers in the nanohybrids compared with the value of their neat polymer counterpart. The interlayer spacings increased in most nanohybrids according to the XRD results. The water contact angle of PMAA increased after mixing with GO whereas the values of PMMA and PMM-MA decreased. SEM images also confirmed the adsorption of the polymers onto GO. These results shed light on the adsorption behaviour of polymers of various functional groups onto GO nanosheets, which will be helpful for the investigation of the interfaces in polymer-GO nanocomposites as well as for monitoring the surface characteristics of GO nanosheets.

**Keywords:** graphene, nanocomposite, polymer, functional group, surface adsorption, structure.

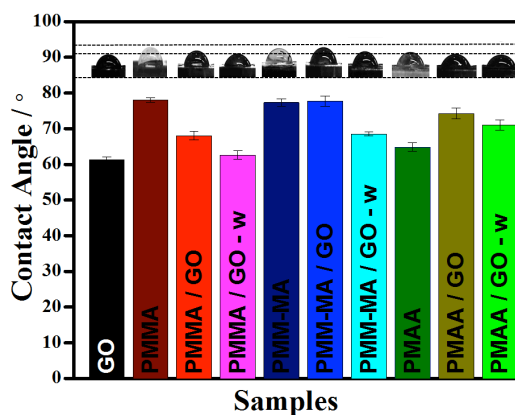


**Figure 1:** Contact angle of the GO, PMMA, PMMA/ GO, PMMA/ GO-w, PMM-MA, PMM-MA/ GO, PMM-MA/ GO-w, PMAA, PMAA/ GO and PMAA/ GO-w.: PMMA has been widely applied in many industrial and important applications such as dental fillers, tooth structure, bio-applications because it is amorphous thermoplastic and inexpensive [1,2]. In addition, its excellent chemical, physical, biological, and mechanical properties, has drawn considerable interest because of a desire to develop materials for applications in polymer-based memory devices [2].

## References:

1. Rajender, N. & Suresh, K. I. (2016), Surface-Initiated Atom Transfer Radical Polymerization (SI-ATRP) from Graphene Oxide: Effect of Functionalized Graphene Sheet (FGS) on the Synthesis and Material Properties of PMMA Nanocomposites. *Macromol. Mater. Eng.* 301, 81–92.
2. Ma, Z., Wu, C., Lee, D. U., Li, F. & Kim, T. W. (2016), Carrier transport and memory mechanisms of multilevel resistive memory devices with an intermediate state based on double-stacked organic/inorganic nanocomposites. *Org. Electron. physics, Mater. Appl.* 28, 20–24.

# Enhanced Blue Light Emission and Thermal Stability of Graphene oxide Hyperbranched Polyimide Nanocomposites

Asma Iqbal<sup>1,2</sup>, Humaira Masood Siddiqi<sup>1\*</sup>, Toheed Akhtar<sup>2</sup>, O.Ok.Park<sup>2</sup>

<sup>1</sup>Quaid-i-Azam University, Department of Chemistry, Islamabad, Pakistan

<sup>2</sup>Korea Advance Institute of Science and Technology, KAIST, Department of chemical and biomolecular Engineering, Daejeon, Republic of Korea

## Abstract:

In recent years, the use of graphene-based nanofillers for synthesis of a new class of advanced polymer composites with unique mechanical and thermal, and optical properties has been greatly investigated.

In this work, graphene oxide nanosheets were successfully surface modified by implanting imide linkage using a triphenylamine based tetra-amine and pyromellitic dianhydride in order to achieve better dispersion and charge transfer properties in PI-GO composites. The modified GO was then incorporated into the hyperbranched polyimide matrix. The polyimide was, in turn, synthesized from tetra-amine monomer and pyromellitic dianhydride by a two-step polymerization process. The development of organic functional groups on graphene sheets greatly enhanced the forces of attraction between GO and polyimide by formation of a charge transfer complex between polyimide and imide moieties on GO. The enhanced forces of attraction between two components suppressed the aggregation of GO. The resultant composites showed excellent thermal stability and photo-physical properties. In comparison to neat polyimide, the GO based nanocomposites demonstrated intense blue emission, bathochromic shift, and excitingly good PL quantum yields. Furthermore, higher HOMO levels, as compared to neat PI, were found as shown in Fig1. These properties indicate that our prepared nanocomposites may prove to be potential candidates for future flexible optoelectronic devices. This method could be of great interest for adjusting the electrochemical and photoluminescence properties for optoelectronics devices.

**Keywords:** triphenylamine, Surface modified GO, PI/MGO composites, blue light emitting, optoelectronics.

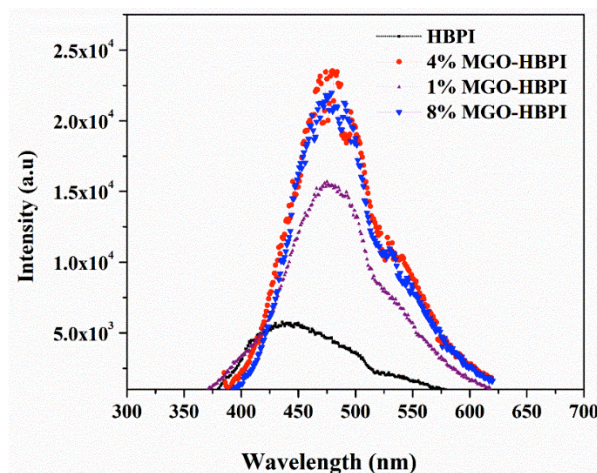


**Figure1:** PL emission of Neat polyimide and polyimide-GO nanocomposites

## References:

1. Li, Y.; Pei, X.; Shen, B.; Zhai, W.; Zhang, L.; Zheng, W. Polyimide/graphene composite foam sheets with ultrahigh thermostability for electromagnetic interference shielding. *RSC Advances*. **2015**, *5*, 24342-24351.
2. Ma, L.; Niu, H.; Cai, J.; Zhao, P.; Wang, C.; Bai, X.; Lian, Y.; Wang, W. Photoelectrochemical and electrochromic properties of polyimide/graphene oxide composites. *Carbon*. **2014**, *67*, 488-499.

# Tunable Au nanogaps via Layer by layer deposition of organic fillers and thiolated polyelectrolytes

A. Bellunato, C. de Sere, Zhanna Overchenko and G. F. Schneider  
Leiden University, Leiden Institute of Chemistry, Leiden the Netherlands

## Abstract:

Increasing research interest is focusing on nanogap technologies and their preparation<sup>[1,2]</sup>, particularly in the fields of molecular electronics and biosensors<sup>[3,4]</sup>. The perspective applications are many fold<sup>[5,6]</sup>, spacing from ultrafast transistors<sup>[7]</sup> up to DNA sequencers<sup>[8]</sup>.

Hereby, we report the achievement of tunable nanogaps between gold thin films via layer by layer deposition<sup>[9]</sup> of polyelectrolytes spacers.

More precisely, Au substrates are chemically functionalized using mixed Self-Assembly-Monolayers of amino-thiols and dodecanethiols and exposed to an acidic solution of polyelectrolytes, Figure 1. In acidic pH, the protonation of the amines attracts the oppositely charged polyelectrolytes that adhere on the substrate. Ultimately, the nanogap spacing is controlled by the subsequent deposition of alternatively charged polyelectrolytes, promoting the build-up of organic films by electrostatic interaction.

The assembly is terminated by a layer of thiolated polyelectrolytes and further coated by a Au thin film. As a result, the top layer of polyelectrolytes binds both the bottom organic assembly, via electrostatic interaction, and the Au top layer via thiol-Au covalent bond, ensuring the stability of the nanogap.

Afterwards, the nanogaps are transferred into a polymeric matrix and sectioned via microtomy<sup>[10]</sup>, producing nanometric polymer sections containing gold electrodes separated by a nanogap, Figure 2.

To conclude, the present talk demonstrates the versatility of polyelectrolyte multilayers to fabricate nanogaps between metallic electrodes. The number of polyelectrolytic layers determines the aperture of the gap, while the microtomy allows the facile preparation of nanogaps with controllable aspect ratio and transferrable on arbitrary substrates.

**Keywords:** nanogap, nanoskiving, microtomy, nanotechnology, layer by layer deposition, self-assembly-monolayer.

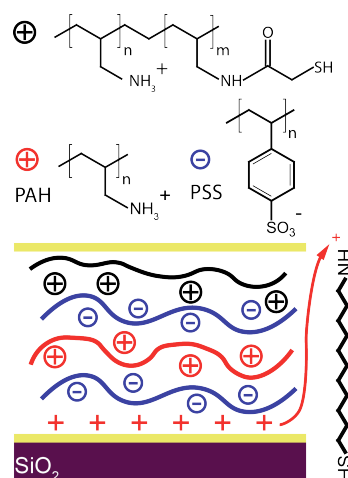


**Figure 1:** Assembly of a nanogap between Au thin films. A Au substrate is functionalized via SAM of aminothiols and dodecanethiols and coated by layer by layer deposition of polyelectrolytes. Lastly, a top-coating of Au is grown to ultimate the gap.

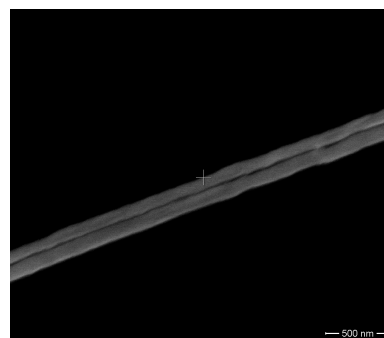


**Figure 2:** Nanogap between Au nanorods. The nanorods have been prepared via microtomy of the thin films separated by organic fillers. Scale bar: 500nm.

## References:

1. Z. Zhou, Z. Zhao, Y. Yu, B. Ai, H. Möhwald, R. C. Chiechi, J. K. W. Yang, G. Zhang, *Adv. Mater.* **2016**, *28*, 2956–2963.
2. A. Cui, Z. Liu, H. Dong, F. Yang, Y. Zhen, W. Li, J. Li, C. Gu, X. Zhang, R. Li, et al., *Adv. Mater.* **2016**, *28*, 8227–8233.
3. P. Pourhossein, R. K. Vijayaraghavan, S. C. J. Meskers, R. C. Chiechi, T. Kudernac, N. Katsonis, W. R. Browne, B. L. Feringa, T. Li, S. Seo, et al., *Nat. Commun.* **2016**, *7*, 11749.
4. M. Carlotti, M. Degen, Y. Zhang, R. C. Chiechi, *J. Phys. Chem. C* **2016**, *120*, 20437–20445.
5. X. Chen, Z. Guo, G.-M. Yang, J. Li, M.-Q. Li, J.-H. Liu, X.-J. Huang, *Mater. Today* **2010**, *13*, 28–41.
6. T. Li, W. Hu, D. Zhu, *Adv. Mater.* **2010**, *22*, 286–300.
7. A. Cui, H. Dong, W. Hu, *Small* **2015**, *11*, 6115–6141.
8. X. Liang, S. Y. Chou, *Nano Lett.* **2008**, *8*, 1472–1476.
9. G. Decher, J.-D. Hong, *Makromol. Chemie. Macromol. Symp.* **1991**, *46*, 321–327.
10. D. J. Lipomi, R. V. Martinez, G. M. Whitesides, *Angew. Chem. Int. Ed. Engl.* **2011**, *50*, 8566–83.

# Monitoring of Defect Formation in Epitaxial Graphene via Anodization

M. Vagin, I. Ivanov, R. Yakimova\*

<sup>1</sup> Linköping University, Department of Physics, Chemistry and Biology, Linköping, Sweden

## Abstract:

Epitaxial graphenes on SiC (EG) obtained via thermal decomposition set up a viable platform for a variety of applications, e.g. quantum metrology, sensorics and high frequency electronics. A main advantage compared to other graphenes is that no material transfer is needed. For device implementation it is critical to have large area graphene of monolayer thickness with controlled properties like carrier concentration, defects type and density, etc. High performance sensors require graphene structure modification that can be done by different ways but not an ultimately successful method has been proposed. By introducing defects in the graphene lattice an increased electrochemical activity can be obtained which leads to modulation of graphene properties. Anodization, a technique to induce defects into highly oriented pyrolytic graphite (HOPG), is an electrochemical approach to create defects also in the graphene lattice. Anodization at high potentials may remove contaminants from the surface hindering the kinetics of surface-sensitive redox processes and yielding anodized EG as an advanced sensing material. Here we report on real time observation of the anodization process, which is a key step of EG activation. The changes in capacitive, reactive and structural properties of the graphene are comparatively studied with Raman spectroscopy and electrochemical methods at conditions of electrocapacitive and redox processes. The combination of extreme smoothness, robustness and efficient surface cleaning and modification by reactive defects gives a significant increase of the reactivity and an up to 21 fold increase in charge storage capacity of graphene.

Raman spectroscopy showed that the defect formation surprisingly occurred only in the graphene monolayer (Figure 1), which represents about 80 % of the surface. The bilayer areas do not seem to contribute with any anodization induced defect formation. The defect density is estimated to be about 2 % of the carbon atoms in the monolayer area. This study brings new challenges in gra-

phene activation but also indicates high promises for practical applications of epitaxial graphene in bio-sensors due to the efficient surface modification/defect formation which is a prerequisite of proficient surface functionalization.

**Keywords:** epitaxial graphene, lattice defects, charge storage capacity, Raman spectroscopy, monolayer, bilayer.

## References:

1. Tzalenchuk, A., S. Lara-Avila, S., Kalaboukhov, A., Paolillo, S., Syvajarvi, M., Yakimova, R., Kazakova, O., Janssen, T.J.B.M., Fal'ko, V., Kubatkin, S. (2010), Towards a quantum resistance standard based on epitaxial graphene, *Nature Nanotechnology*, 5, 186-189.
2. Ivanov, I.G., Hassan, J.U., T. Iakimov, T., Zakharov, A.A., R. Yakimova, R., Janzen, E. (2014), Layer number determination in graphene on SiC by reflectance mapping, *Carbon*, 77 492-500.

# Graphene mechanics: defects, buckling and domain growth

Sandeep K. Jain,<sup>1,\*</sup> Gerard T. Barkema,<sup>2</sup>

<sup>1,\*</sup> Institute for Theoretical Physics, Utrecht University, Princetonplein 5, 3584 CC Utrecht, The Netherlands, \*s.k.jain@uu.nl

<sup>2</sup> Department of Information and Computing Science, Utrecht University, Princetonplein 5, 3584 CC Utrecht, The Netherlands

## Abstract:

We have developed a new semi-empirical potential for graphene [1], using DFT calculations for determining the various parameters, which for the first time includes a term for out-of-plane deformations. We have demonstrated the usefulness of this potential in studies of different kind of intrinsic defects (Stone-Wales defect, separating dislocations and grain boundaries). Our simulations show that the stress caused by these defects can be relieved by buckling, which extends to hundreds of nanometers. A detailed study of the formation energies of defects surprisingly revealed that the value for the formation energy depends on the type of boundary conditions [2]. Therefore it is necessary to specify the boundary conditions for the energy of the lattice defects in the buckled two-dimensional crystals to be uniquely defined. We have also theoretically described that the vibrational density of states (VDOS) can be used in probing the crystallinity of graphene samples [3]. The novel potential can be effectively combined with interlayer interaction, allowing the simulation of bilayer graphene and study the effect of twist angle on the structure and buckling [4]. Recently, we have described the universal shape behaviour of a graphene gas bubble irrespective of its size. We show that for small gas bubbles (~10 nm), the vdW pressure is in the order of 1 GPa [5].

**Keywords:** Graphene, buckling, defects, simulations, Moire-patterns, nanobubbles

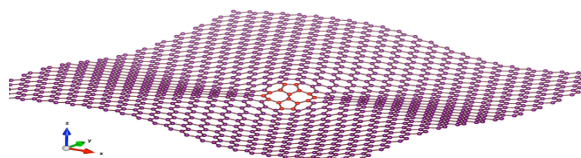


**Figure 1:** Buckled graphene with a Stone-Wales defect.

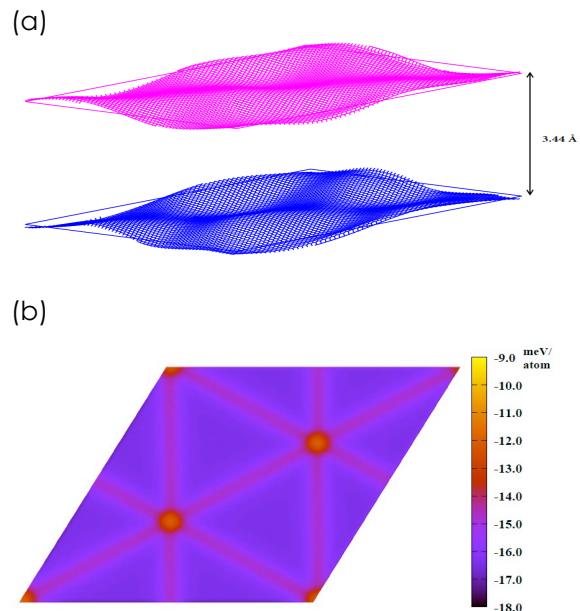


**Figure 2:** (a) Buckling in twisted bilayer graphene. (b) Energy distribution in twisted bilayer graphene and formation of vortices.

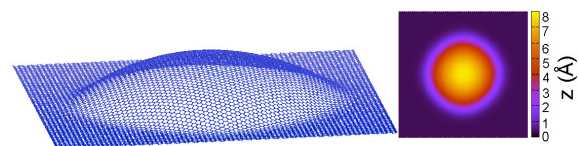


**Figure 3:** Structure of a graphene nanobubble. For small gas bubbles (~10 nm), the vdW pressure is in the order of 1 GPa.

## References:

1. S.K.Jain, et. al, JPCC, 199 (2015) 9646
2. S.K.Jain, et. al, PRB, 94 (2016) 020102(R)
3. S.K.Jain, et. al, JPCL, 6 (2015) 3897
4. S.K.Jain, et. al, 2D Mat., 4 (2016) 015018
5. S.K.Jain, et. al, PCCP, 19 (2017) 7465

# High Yield Exfoliation of Two-Dimensional Materials Based on the Control of Micellar Size of Surfactants

Sun Jin Yun,<sup>1,2,\*</sup> Changbong Yeon,<sup>1,2</sup> Jung Wook Lim<sup>1,2</sup>, Gil-Ho Kim,<sup>3</sup> Inyeal Lee<sup>3</sup>

<sup>1</sup> Electronics and Telecommunications Research Institute, 218 Gajeongno, Yuseong-gu, Daejeon 34129, Korea; <sup>2</sup> University of Science and Technology, 217 Gajeongno, Yuseong-gu, Daejeon 34113, Korea;

<sup>3</sup>School of Electronic and Electrical Engineering College of Information and Communication Engineering and Sungkyunkwan Advanced Institute of Nanotechnology (SAINT), Sungkyunkwan University, Suwon 16419, Korea. \*[sjyun@etri.re.kr](mailto:sjyun@etri.re.kr)

## Abstract:

Liquid exfoliation methods with no chemical reaction are cost-effective and scalable method to produce atomically thin flakes of two-dimensional (2D) materials such as graphene, MoS<sub>2</sub>, WS<sub>2</sub>, h-BN, etc. For the exfoliation in aqueous solutions, the use of surfactants is necessary because of hydrophobicity of 2D materials. In this work, the effect of micellar size of surfactants on the exfoliation of 2D materials was extensively studied. The surfactants utilized in this work were ionic sodium dodecyl sulfate (SDS) and non-ionic biocompatible block copolymer, Pluronic F-68.

For conventional surfactant-assisted exfoliations, the concentration of surfactants has been chosen in the range higher than critical micelle concentration (CMC). The molecules form spherical micelles at a concentration higher than CMC. However, the effect of micellar size on the exfoliation of 2D materials has not been studied until quite recently. We presents that the micellar size has a great influence on the exfoliation efficiency both with ionic SDS and non-ionic F-68.<sup>1,2</sup> The smaller size form such as unimer and very small micelle is much more efficient for obtaining a highly concentrated dispersion of atomically thin 2D materials than larger micelles. Thus, it should be very important to understand how the micellar size can be controlled in the exfoliation process.

We clarified that the exfoliation yield of graphene depended on the concentration of surfactant and the maximum yield could be obtained at a concentration much lower than CMC as shown in Figure 1. The size of micelles was also influenced by the addition of water-soluble alcohols. The results in Figure 2 showed that the exfoliation yields of MoS<sub>2</sub>, graphene, and h-BN strongly depended on the concentration of alcohols and showed the highest yields at the concentration of ethyl alcohol (EtOH), 50 vol.% at which unimers mainly exist. The role of

alcohols is a surface tension-reducing agent in the dispersion solution,<sup>1</sup> and to suppress the micelle-forming.<sup>2</sup> The results strongly insist that unimers and very small micelles are much more efficient for the exfoliation. When MoS<sub>2</sub> was exfoliated for 3 h in 50 vol.% EtOH solution of F-68, the exfoliation yield was 14.6% that is very high yield in aqueous solution among ever reported values.

We also suggested the dielectrophoresis (DEP) technique as a method of forming a film composed of 2D flakes. By DEP, MoS<sub>2</sub> flakes could be well deposited between two electrodes and showed a stable electrical connection and strong Raman peaks.

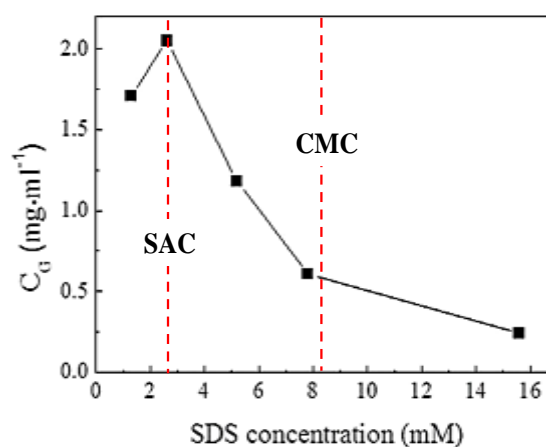


**Figure 1:** Concentraion of graphene in aqueous dispersions exfoliated at different concentration of SDS (SAC: surface aggregation concentration).

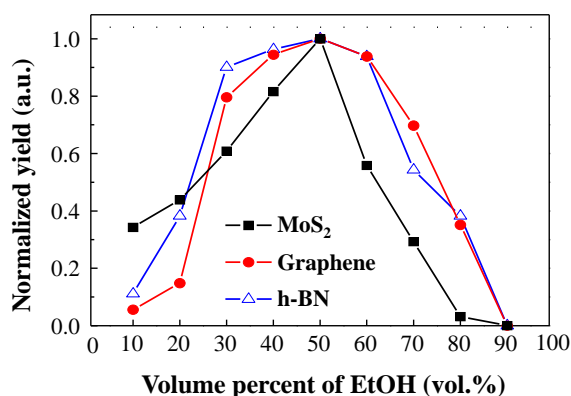


**Figure 2:** Average yield of MoS<sub>2</sub> (■), graphene (●), and h-BN (△) exfoliated for 1h in water/F-68/ethyl alcohol (EtOH) as a function of EtOH concentration.

**Acknowledgements:** This work was supported by Institute for Information & Communications Technology Promotion (IITP) grant funded by the Korea government (MSIP) (B0117-17-1003, Fundamental technologies of two-dimensional materials and devices for the platform of new-functional smart devices).

**Keywords:** liquid-phase exfoliation, surfactant, two-dimensional materials, MoS<sub>2</sub>, graphene, h-BN, surfactants, micellar size, unimer

#### References:

1. Yeon, C., Yun, S. J., Lee, K. -S., Lim, J. W. (2015) High-yield graphene exfoliation using sodium dodecyl sulfate accompanied by alcohols as surface-tension-reducing agents in aqueous solution, *Carbon*, 83, 136-143.
2. Yeon, C., Lee, I., Kim, G. H., Yun, S. J., (2017) Unimer-assisted exfoliation for high concentrated aqueous dispersion solutions of single- and few-layered van der Waals materials, *Langmuir*, DOI: 10.1021/acs.langmuir.6b04121.

# Controlling energy product of *hcp*-Cobalt nano-magnets

H. T. T. Nong<sup>1</sup>, K. Mrad<sup>1</sup>, F. Schoenstein<sup>1</sup>, N. Jouini<sup>1</sup>, B. Leridon<sup>2</sup>, J-Y. Piquemal<sup>3</sup>, and S. Mercone<sup>1</sup>

<sup>1</sup>Laboratoire des Sciences des Procédés et des Matériaux, CNRS-Université Paris 13, France

<sup>2</sup>LPEM-ESPCI Paris, PSL Research University, CNRS, Sorbonne Université, UMPC, 10 Rue Vauquelin, F-75005 Paris, France

<sup>3</sup>Interfaces Traitements Organisation et Dynamique des Systèmes, Université Paris Diderot, Sorbonne Paris Cité, CNRS UMR 7086, 15 rue J. A. de Baïf, 75205 Paris Cedex 13, France

## Abstract:

Co-based anisotropic nanowires are attracting scientific interest mainly for their possible applications as nano-magnets in (nano)medicine [1] as well as in recording media [2] and as building blocks in high energy nanostructured bulk permanent magnets [3]. In this latter case, a high magnetocrystalline anisotropy of the ferromagnetic nano-object is essential for high magnetic coercivity which are mandatory for obtaining a high magnetic energy product (namely  $BH_{max}$ ) and thus a good permanent magnet. In this frame, we studied the magnetic static properties of *hcp*-cobalt nanowires, which show a high shape anisotropy and magnetocrystalline anisotropy by using a standard Quantum Design MPMS SQUID magnetometer in the temperature range of 5 - 400K and with a magnetic field applied between -7 Tesla and +7 Tesla. The magnetic energy of these nanowires was studied as a function of the shape as well as of the stacking fault, respectively determined by HRTEM and X-Ray diffraction measurements. The optimum candidates were then sintered by non-conventional SPS technique and cobalt-based nanostructured materials were studied in view of magnetic energy optimization.

Our results show that the key parameter driving the magnetic energy product of the cobalt nanowires is the stacking fault density when the aspect ratio is optimized ( $L/d > 10$ ) [4]. No matter the dispersion and morphology of the nanowires, the stacking faults are completely driving the observed differences in the magnetic energy product behavior. A huge loss in the magnetic

energy is observed when the magnetic increases interactions between nanowires. A micromagnetic simulation is performed to study the local interactions of nanowires inside the like-bulk nanostructured samples. The micromagnetic simulation showed that the magnetic qualities of bulk nanostructured materials depend not only on the morphology and on the crystal structure

of nanowires, but also on the controlled arrangement of these latters inside the permanent magnet suggesting composites new magnet as a good alternative for future applications.

**Keywords:** nanowire, magnetic energy, stacking faults, *hcp* cobalt

## References:

1. A. Akbarzadeh, M. Samiei and S. Davaran (2012), Magnetic nanoparticles: preparation, physical properties, and applications in biomedicine, *Nanoscale Research Letters* 7, 144.
2. D. Weller and A. Moser (1999), Thermal Effect Limits in Ultrahigh-Density Magnetic Recording, *IEEE Trans. Magn.*, 35, 4423.
3. K. Gandha, K. Elkins, N. Poudyal, X. Liu and J. Ping Liu (2014), High Energy Product Developed from Cobalt Nanowires, *Scientific Reports*, 4, 5345.
4. S. Mercone, F. Zighem, B. Leridon, A. Gaul, F. Schoenstein and N. Jouini (2015), Morphology control of the magnetization reversal mechanism in Co<sub>80</sub>Ni<sub>20</sub> nano-magnets, *J. of Appl. Phys.*, 117, 203905.

# Study of Rapid Two Photon Polymerization for Cell Migration by Large Scale of Roughness and Hydrophobicity Controlled Surface

C. Y. Liu,<sup>1</sup> Q. W. Tang<sup>2</sup>, T. T. Chung,<sup>2</sup> A. B. Wang,<sup>1\*</sup>

<sup>1</sup>Institute of Applied Mechanics, National Taiwan University, Taipei 10617, Taiwan

<sup>2</sup>Department of Mechanical Engineering, National Taiwan University, Taipei 10617, Taiwan

## Abstract:

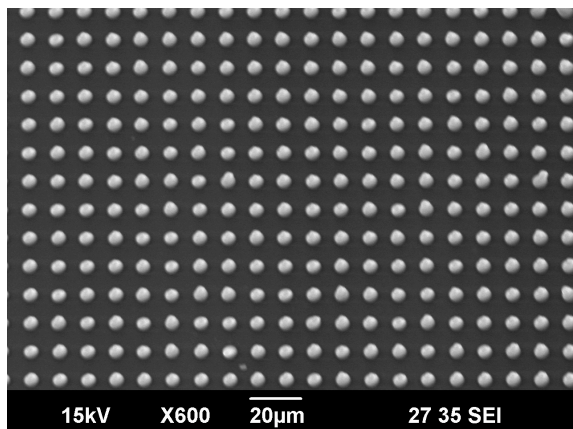
Surface properties are well-known to affect the extent of adhesion between two adjacent materials. However, imperfection caused roughness heterogeneity commonly leads to the difficulty in repeatability. In this study, the fundamental issues on the surface roughness homogeneity controlled by laser trajectories in rapid two-photon polymerization (TPP) were firstly addressed. Moreover, skipping the commonly used piezo-driven and upright optics in conventional two photon polymerization, the self-developed 4 W femtosecond laser based scanning system has increased the maximum fabrication speed up to 175 times (355 mm/sec) compared with that of conventional TPP method. By suitable selection of the fabrication parameters including of voxel distance, intensity and focusing point correction based on spherical aberration within an appropriate exposure time, a series of cube structures of  $6 \times 6 \text{ mm}^2$  surface area with roughness  $R_z$  ranging from 0.4 to  $1.3 \text{ }\mu\text{m}$  were designed and homogeneously polymerized. Meanwhile, hydrophobic structures inspired by the nature lotus effect has been made by this rapid TPP system for permanent surface modification. It is highly expected that the rapid fabrication of this level could fully fit the demands of various repeatability tests and devices in cell mechanics and tissue engineering applications.

**Keywords:** Two-photon polymerization, Surface modification, Voxel distance, Cell mechanics

**Figure 1:** Hydrophobic structures ( $2.5 \times 2 \text{ mm}^2$ ) made by rapid two photon polymerization: The size of pillar is  $4.35 \text{ }\mu\text{m}$  in diameter with  $75 \text{ }\mu\text{m}$  in height. The pitch distance between each pillar is  $10 \text{ }\mu\text{m}$ , which can be used as an identical parameter for further adjusting the surface hydrophobicity. The whole process was done within 3 min while the conventional TPP needs at least 8.7 hr to achieve this scale of products.

## References:

1. "Requirement for Both Micron and Submicron Scale Structure for Synergistic Responses of Osteoblasts to Substrate Surface Energy and Topography", G. Zhao, A.L. Raines, et al *Biomaterials*. 2007 June ; 28(18): 2821–2829.
2. "Translucent Titanium Coating Facilitates the Observation of Osteoblast Migration Behavior on a Titanium Surface", Yi Ho, Sang-Heng Kok, et al, *Int J Oral Maxillofac Implants*. 2012; 27(2):278-87.
3. "High-aspect 3D two-photon polymerization structuring with widened objective working range (WOW-2PP)", Kotaro Obata, et al, *light science & applications*. 2013; 2, e116.



# Deposition of Magnetic SmCo nanoparticles

L. Allocca<sup>°</sup>, U. Gambardella\* and A. Morone

Consiglio Nazionale delle Ricerche – Istituto di Struttura della Materia U.O. di Tito Scalo, Zona Industriale  
di Tito Scalo, I85050

<sup>°</sup> Istituto Motori, Viale Marconi 8, Napoli I80125

\*Istituto Nazionale di Fisica Nucleare, Sez. di Napoli, Via Cinthia I 80125

## **Abstract:**

SmCo is a permanent magnetic material having peculiar characteristics. It can be used in different application field: electronic, environmental control and medicine. SmCo nanoparticles could be used in hyperthermia, particular treatment of cancer cell. Hyperthermia is the procedure that increases the local temperature of cancer cells in the range of 40°- 43° C. Using this temperature management, the number of cancer cells could be reduced. SmCo nanoparticles will be produced by Pulsed Laser Ablation (PLD) or Matrix Assisted Pulsed Laser Deposition (MAPLE) techniques and the nanostructures will be characterized by using X-Ray Diffraction, Scanning Electron Microscopy and magneto-optics measurements. The analysis is proposed as attempt for the use of SmCo nanoparticles in the hyperthermia field.

# A versatile process toward amphiphobic surfaces

M. Blosi<sup>\*1</sup>, M. Raimondo<sup>1</sup>, F. Veronesi<sup>1</sup>, G. Boveri<sup>1</sup>, G. Guarini<sup>1</sup>,  
<sup>1</sup>ISTEC CNR, Institute of Science and Technology for Ceramics  
Via Granarolo, 64 – 48018 Faenza (Italy)

## Abstract:

The control of surface wettability has become an interesting area of investigation owing to its wide range of promising applications in different industrial sectors (maritime, aeronautic, hydraulic, energy, etc.) [1]. In order to create a surface allowing extreme repellence to water and oils and mimicking some living organisms (e.g. Lotus leaf, Taro leaf etc.) various approaches have been proposed in the literature [2]. It has been commonly agreed that biomimetic superhydrophobic surfaces can be achieved by a combination of micro and nanostructures with low surface energy. The replica of such natural surfaces allowed synthesizing coatings able to change the material response to different environments by the control of their wettability.

In this work we produced amphiphobic (super hydrophobic/oleophobic) surfaces by means of a multistep process which acts by following the double approach: nano-structuration and chemical modification. The same versatile process was successfully applied to different substrates: glass, ceramic tiles, metals and paper. The surfaces were treated with ceramic oxide nanoparticles prepared by a sol-gel method and applied by dip-coating. The treated surfaces were thermally cured at temperature between 150-400°C and then boiled in water. Finally properly selected fluorine-organic compounds were applied on the inorganic layer to introduce low energy functional groups. The so-treated substrates were widely characterized in terms of static and dynamic contact angle, microstructure observation (FESEM), surface chemistry (XPS) and durability. The results showed promising results with contact angles with water as high as 178°, CA hysteresis lower than 3° and CA with low surface tension liquids up to 150°. The microstructure evidenced a homogeneous *flower-like* structure (fig.1), with nanometric roughness, typically formed by inorganic lamellas randomly orientated and corresponding to a coating thickness of about 200-400 nm. Durability tests were performed on coated samples in severe environments (acid, basic, saline solutions, freezing, UV irradiation) to check their physico-chemical resistance. Results demonstrated that

the prepared coatings hold their properties over time. From the mechanical point of view, tape-test and scratch-test analyses evidenced a good adhesion of the coating to the different substrates, thus suggesting a wide range of potential applications.

**Keywords:** amphiphobic biomimetic surfaces, flower like nanostructure, sol-gel, versatile process

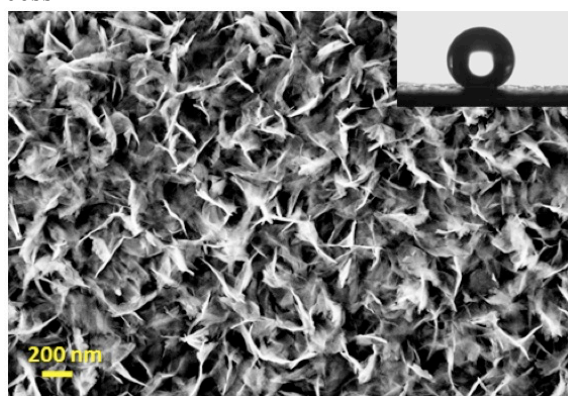


**Figure 1:** FESEM image of the flower-like nanostructure observed on aluminum surface. The inset shows a water drop on the same surface with a static contact angle of 175°, assessed by the sessile drop method.

## References:

1. Raimondo M., Blosi M., Caldarelli A., Guarini G., Veronesi F. (2014), Wetting behavior and remarkable durability of amphiphobic aluminum alloys surfaces in a wide range of environmental conditions. *Chem. Eng. Journal* 258, 101-108.
2. Yan, Y.Y., Gao, N., Barthlott, W. (2011), Mimicking natural superhydrophobic surfaces and grasping the wetting process: A review on recent progress in preparing superhydrophobic surfaces, *Advances in Colloid and Interface Science* 169, 80-105

# Preparation and Characterization of Transparent Alumina films by Novel Room Temperature Ceramic Coating Method

Jong-Hwan Park<sup>1</sup>, Seok-Hun Kim<sup>1</sup>, Jung-Kab Park<sup>1</sup>, Tae-Yoo Kim<sup>1,4,5</sup>, Jung-Woo Lee<sup>1</sup>, Sun-Woo Kim<sup>1</sup>, Se-Hee Shin<sup>1</sup>, Ho-Jun Choi<sup>1</sup>, Dong-Soo Park<sup>2</sup>, Chan Park<sup>3</sup>, Kyung-Sub Lee<sup>1</sup>, Su-Jeong Suh<sup>1,4,5</sup>

<sup>1</sup> Sungkyunkwan University, Suwon, Rep. of Korea

<sup>2</sup> Korea Institute of Materials Science, Changwon, Rep of Korea

<sup>3</sup> Pukyong National University, Busan, Rep. of Korea

<sup>4</sup> Advanced Materials and Process Research Center for IT, Suwon, Rep. of Korea

<sup>5</sup> Smart e-Plating Regional Innovation System, Suwon, Rep of Korea

## Abstract:

Granule Spray in Vacuum (GSV) is a novel ceramic coating method. Dense ceramic layer is deposited on various substrates (metal, polymer, ceramic) at room temperature in vacuum. Four raw powders of alpha alumina which have different mean particle sizes were selected for investigating relationship between the mean particle size and transmittance of alpha alumina films. Commercially available alpha alumina powders were used. A mean particle size was measured by a particle size analyzer. Mean particle size of four alpha alumina powders were 0.8  $\mu\text{m}$ , 0.84  $\mu\text{m}$ , 1.77  $\mu\text{m}$  and 4.44  $\mu\text{m}$ , respectively. It was confirmed through XRD (X-ray diffraction) that raw powders were in alpha phase. Transparent and dense alumina films were successfully deposited on slide glass by GSV. Phases of alumina films were determined alpha by SAD (selective area diffraction). Transmittances of alumina films were measured through UV visible spectrometer. The alumina film thickness was measured by an alpha step. As particle size of alumina raw powder increased, the transmittance of the alumina film decreased. Surface roughness of alumina films was measured by a surface profilometer. The microstructures and cross-sections of alumina films were observed by TEM (Transmission Electron Microscope). Alumina films have nanoscale microstructure and their grain size were mostly 5-10nm. But any consistent relationship between the grain size in alumina films and particle size of raw powder/transmittance was not found.

**Keywords:** Granule Spray in Vacuum, transparent, film, alumina, coating

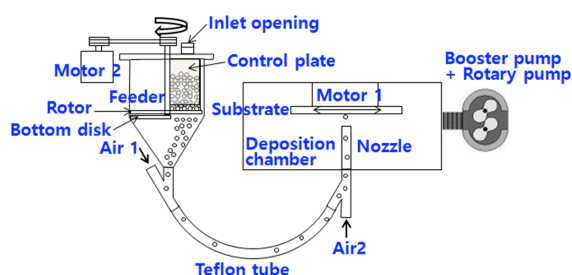


**Figure 1:** Schematics of GSV apparatus

## References:

1. M. Lebedev, S. Krumdieck. (2008) Optically transparent, dense alpha- $\text{Al}_2\text{O}_3$  thick films-deposited on glass at room temperature. Current Applied Physics, 8, 233-236

# Synthesis and characterization of nanocomposite polymer electrolytes with potential applications for Li-ion batteries.

J. Cardoso,<sup>1</sup> A. Mayrén,<sup>1</sup> I. C. Romero-Ibarra,<sup>2,\*</sup> D. P. Nava<sup>1</sup> and J. Vazquez-Arenas<sup>3</sup>

<sup>1</sup> Physics Department, Universidad Autónoma Metropolitana-Iztapalapa, Apartado Postal 55-534, 09340, México.

<sup>2</sup> Unidad Profesional Interdisciplinaria en Ingeniería y Tecnologías Avanzadas. Instituto Politécnico Nacional, Av. I.P.N. 2580, Gustavo A. Madero, 07340, Ciudad de México, México.

<sup>3</sup> Departamento de Química, Universidad Autónoma Metropolitana-Iztapalapa, C.P. 09340, Ciudad de México, México.

## Abstract:

The research and development of new materials for energy storage applications have become critical to meet the technological and environmental requirements demanded for sustainable power sources. Although the synthesis of new electrolytes for Li-ion batteries has drawn less attention compared to cathode materials, their performance is also crucial to avoid capacity fade mechanisms, providing electrochemical stability to electrodes (i.e. safety), limiting the power rate to some extent, and fabricating devices with non-toxic materials. Accordingly, various devices have been envisaged as nanocomposite organic/inorganic materials. Significant effort is focused on the ability to obtain control of the nanoscale structures via innovative synthetic approaches. The properties of nanocomposite materials depend not only on the properties of their individual precursors but also on their morphology and interfacial characteristics. This field is generating many exciting new materials with novel properties. The latter can derive by combining properties from the pristine constituents into a single material. The inorganic components can be three-dimensional framework systems such as zeolites, two-dimensional layered materials such as clays represents lamellar nanocomposites that can be divided into two distinct classes, intercalated and exfoliated. The intercalated nanocomposites are also more compound-like because of the fixed polymer/layer ratio, and they are interesting for their electronic and charge transport properties.

In this work novel poly(poly(ethylenglycol)methacrylate) (pPEGMA) nanocomposite electrolytes (NE) based on montmorillonite (MMT) and zeolite (ZSM-5) with a salt (LiTFSI) and an ionic liquid are synthesized. The salt was lithium bis(trifluoromethanesulfonyl)imide salt (LiTFSI) and 1-butyl-1-methylpyrrolidinium bis(trifluoromethylsulfonyl)imide as ionic liquid

(PYR 11 TFSI). During the synthesis the sonication technique is successfully used to introduce the fillers into the polymer matrix, provide uniform dispersion and shatter aggregates of nanofillers to ensure a polymer amorphous structure. The influence of the inorganic particle content (1, 3 and 5wt. %) and filler structure are discussed in terms of their thermal and morphological properties. SEM and TEM techniques reveal an efficient embedding of the fillers into pPEGMA, whereas analyses conducted with TGA/DSC, FTIR and XRD showed that for the binary systems BN-MMT and BN-ZSM-5 containing LiTFSI, the morphology of pPEGMA results into a crosslinking amorphous matrix where Li<sup>+</sup> ion motion is hindered. This behavior stems from a strong interaction between the surface of the anionic nanofiller with methylene (CH<sub>2</sub>) groups from pPEGMA, and particularly anionic nanofiller with Li<sup>+</sup>. The addition of ionic liquid PYR 11 TFSI to ternary systems TN-MMT and TN-ZSM-5 abates the aforementioned interactions and leads to an increase of the interfacial layer separation, which grants flexibility to the polymer chains. These effects stem significantly enhancements in the ionic conductivities of TN-MMT ( $4.0 \times 10^{-4} \text{ S cm}^{-1}$ ) and TN-ZSM-5 ( $9.4 \times 10^{-6} \text{ S cm}^{-1}$ ) at 30 °C. These materials present adequate morphological, thermal and mechanical properties, and a significant enhancement of Li<sup>+</sup> ion conductivity for green materials at room temperature to be considered as potential nanocomposite electrolyte for Li-ion batteries.

**Keywords:** ZSM-5, Montmorillonite clay, ionic liquid, nanocomposite polymer, polymer electrolytes, Li-ion batteries.

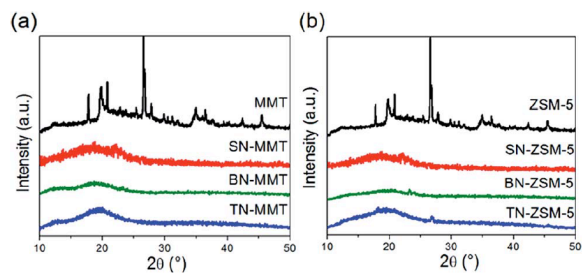


**Figure 1:** Figure illustrating the diffractograms of SN (pPEGMA-nanofiller), BN (pPEGMA nanofiller + LiTFSI) and TN (pPEGMA-nanofiller + LiTFSI + PYR11TFSI) nanocomposites: (a) MMT, SN-MMT, BN-MMT and TN-MMT, and (b) ZSM-5, SN-ZSM-5, BN-ZSM-5 and TN-ZSM-5

# Self-rectifying Resistive Switching Characteristics in the Au/Ni/FeO<sub>x</sub>-GO/Si<sub>3</sub>N<sub>4</sub>/n<sup>+</sup>-Si Structure

Se-I Oh<sup>1</sup>, Janardhanan R, Rani<sup>2</sup>, Jae-Hyung Jang<sup>1,2,3\*</sup>

<sup>1</sup>Gwangju Institute of Science and Technology, Department of WCU Nanobio Materials and Electronics, 123 Cheomdangwagi-ro, Buk-gu, Gwangju, 61005, South Korea

<sup>2</sup>Gwangju Institute of Science and Technology, School of Electrical Engineering and Computer Science, 123 Cheomdangwagi-ro, Buk-gu, Gwangju, 61005, South Korea

<sup>3</sup>Gwangju Institute of Science and Technology, Research Institute for Solar and Sustainable Energies, 123 Cheomdangwagi-ro, Buk-gu, Gwangju, 61005, South Korea

**Abstract:** Resistive random access memory (RRAM) has been extensively investigated as one of the most promising next-generation non-volatile memory devices, especially in the crossbar array (CBA) architecture, for future high-density memory application<sup>1</sup>. However, the necessary integration of a memory cell with selection devices, to alleviate the parasitic leakage currents in CBA is a major obstacle to realize three dimensional CBA structure<sup>2</sup>. The fabrication of discrete selection devices, such as Schottky diodes<sup>3</sup> and transistors<sup>4</sup>, and combining them with the memory cell are very difficult in the vertically integrated structure. In addition, the integrated bit cell results in large cell size, which hinders the realization of high-density CBAs. In order to circumvent these difficulties, recently, a memory cell containing self-rectification functionality is attracting a great deal of attention as an alternative method to eliminate the sneak currents without the need for selection devices<sup>5</sup>. Here, we demonstrate a memory cell having excellent bipolar resistive switching together with a self-rectifying characteristics, which is fabricated by inserting a silicon nitride (Si<sub>3</sub>N<sub>4</sub>) layer between bottom electrode (n<sup>+</sup>-Si) and solution-processed active material of an iron oxide embedded graphene oxide (FeO<sub>x</sub>-GO) layer (Figure 1). The memory cell exhibits high resistive switching ratio of  $4 \times 10^4$  and rectification ratio of  $2 \times 10^4$ . Moreover, during repetitive 100 cycles, the memory cell did not show any noticeable degradation with respect to the operating current levels including high-resistance state current ( $I_{HRS}$ ), low-resistance state current ( $I_{LRS}$ ), and rectifying current ( $I_R$ ) and SET voltage ( $V_{SET}$ ) indicating a resistive switching operation from HRS to LRS (Figure 2). Furthermore, we found that the FeO<sub>x</sub>-GO hybrid material acting as the resistive switching layer in the memory cell configuration provides lower  $V_{SET}$ , higher  $I_{LRS}$ , and lower  $I_R$  rather than the GO active layer

(Figure 3). This study realizes a simple and feasible method to achieve a highly uniform self-rectifying resistive switching RRAM cell for the CBA application. The experimental results and the discussion of analysis will be explained in detail, at the conference.

This work was supported by the National Research Foundation of Korea grant funded by the Korea government(MSIP) (No.2017R1A2B3004049).

**Keywords:** Crossbar array, sneak path, resistive random access memory (RRAM), self-rectifying RRAM, graphene oxide, iron oxide and graphene oxide hybrid, silicon nitride

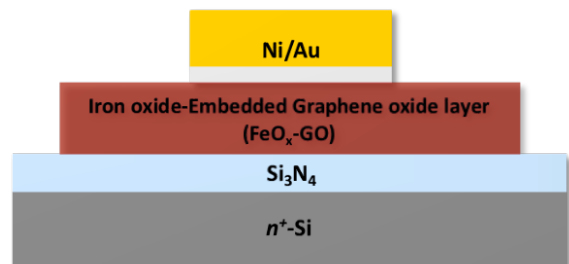


**Figure 1:** A schematic illustrating the cross section of the Au/Ni/FeO<sub>x</sub>-GO/Si<sub>3</sub>N<sub>4</sub>/n<sup>+</sup>-Si memory cell

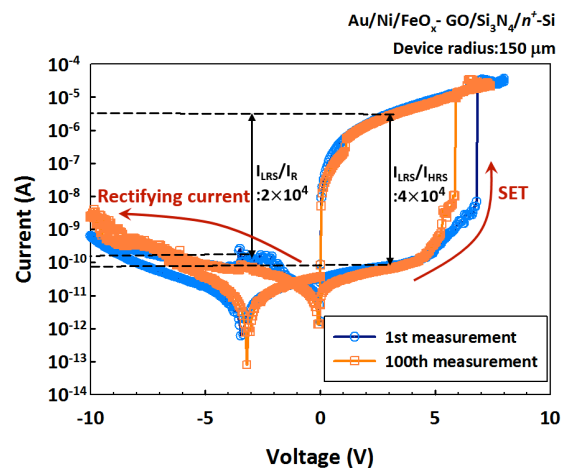


**Figure 2:**  $I$ - $V$  characteristics of Au/Ni/FeO<sub>x</sub>-GO/Si<sub>3</sub>N<sub>4</sub>/ $n^+$ -Si memory cell measured at first and 100<sup>th</sup> cycle after electroforming process ( $I_{LRS}$  and  $I_{HRS}$  were read at +3 V, and  $I_{LRS}$  and  $I_R$  were read at +3 V and -3 V, respectively).

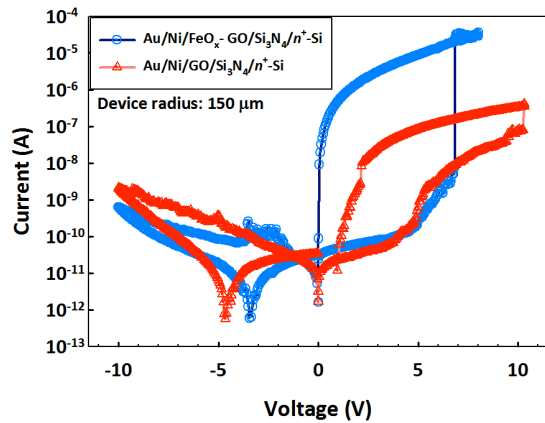


**Figure 3:** Comparison of the  $I$ - $V$  characteristics of Au/Ni/FeO<sub>x</sub>-GO/Si<sub>3</sub>N<sub>4</sub>/ $n^+$ -Si and Au/Ni/GO/Si<sub>3</sub>N<sub>4</sub>/ $n^+$ -Si memory cells

#### References:

1. Philip Wong, H. S., Lee, H.-Y., Yu, S., Chen, Y.-S., Wu, Y., Chen, P.-S., Lee, B., Chen, F. T., Tsai, M.-J. (2012), Metal-oxide RRAM, *Proc. IEEE*, 100, 1951-1970.
2. Lee, M.-J., Park, Y., Suh, D.-S., Lee, E.-H., Seo, S., Kim, D.-C., Jung, R., Kang, B.-S., Ahn, S.-E., Lee, C. B., Seo, D. H., Cha, Y.-K., Yoo, I.-K., Kim, J.-S., Park, B. H. (2007), Two series oxide resistors applicable to high speed and high density non-volatile memory, *Adv. Mater.*, 19, 3919-3923.
3. Kim, G. H., Lee, J. H., Hwan, J. H., Song, S. J., Seok, J. Y., Yoon, J. H., Yoon, K. J., Lee, M. H., Park, T. J., Hwang, C. S. (2012), Schottky diode with excellent performance for large integration density of crossbar resistive memory, *Appl. Phys. Lett.*, 100, 213508.
4. Cho, B. J., Song, S. H., Ji, Y. S., Kim, T.-W., Lee, T. H. (2011), Organic resistive memory devices: performance enhancement, integration, and advanced architectures, *Adv. Funct. Mater.*, 21, 2806-2829.
5. Yoon, J. H., Kim, K. M., Song, S. J., Seok, J. Y., Yoon, K. J., Kwon, D. E., Park, T. H., Kwon, Y. J., Shao, X., Hwang, C. S. (2015), Pt/Ta<sub>2</sub>O<sub>5</sub>/HfO<sub>2-x</sub>/Ti resistive switching memory competing with multilevel NAND flash, *Adv. Mater.*, 27, 3811-3816.

# Influence of flow rate in the structural and optical properties of nanostructured CeO<sub>2</sub> thin films deposited by spray pyrolysis

M.F. García Sánchez,<sup>1\*</sup> I. Ponce Rosas,<sup>1</sup> I.C.Romero Ibarra,<sup>1</sup> G. Santana,<sup>2</sup>

<sup>1</sup> Unidad Profesional Interdisciplinaria en Ingeniería y Tecnologías Avanzadas. Instituto Politécnico Nacional, Av. I.P.N. 2580, Gustavo A. Madero, 07340, Ciudad de México, México.

<sup>2</sup> Instituto de Investigaciones en Materiales, U.N.A.M., A.P. 70-360, Coyoacán, C.P. 04510, Ciudad de México, México.

## Abstract:

Recently, it has been demonstrated that nanostructured materials increase the transport properties of oxides used as electrolytes in SOFC [1-2]. This fact will allow a meaningful decrease of the devices operation temperature to intermediate temperature range (500-700°C), increasing its competitiveness [3]. However, the physical basis of this phenomenon it is not fully understood [4,5]. In this work, nanostructured ceria thin films have been prepared by ultrasonic spray pyrolysis using cerium acetylacetonate as metallo-organic precursor dissolved in anhydrous methanol. Two different flow rates was used and substrate temperature was varied in order to optimized the structural and optical properties. The morphology, structure and optical properties were studied by scanning electron microscopy, X-ray diffraction (XRD), X-ray photoelectron spectroscopy (XPS) and photoluminescence. The influence of thermal annealing at 900 °C on the films was studied. The spray conditions were optimized for obtaining smooth, dense and homogeneous nanocrystalline films with grains sizes smaller than 10 nm. By XPS were demonstrated the presence of Ce<sup>3+</sup>, even in treated films. The Ce<sup>3+</sup> concentration do not depend of the grown temperature and decrease with the thermal annealing. Variations on the flow rate modified the optimal grown temperature, change the texture coefficient of main reflections in XRD pattern and the defects distribution in the film.

The authors acknowledge financial support for this work from IPN with projects 20172276 and 20170488, CONACyT under project PN 1373 and “Red Temática de Almacenamiento” and SECITI 071-2016.

**Keywords:** Nanostructured materials, spray pyrolysis, thin films, cerium dioxide

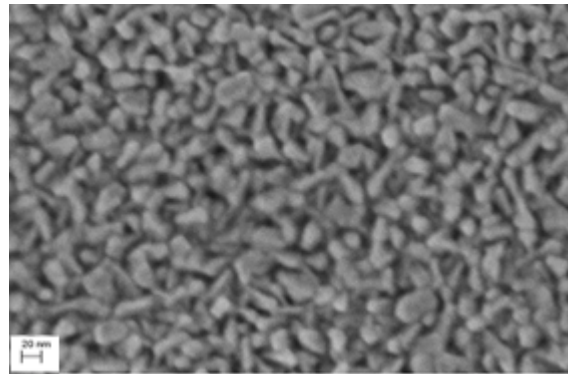


**Figure 1:** SEM images of CeO<sub>2</sub> thin films with grain size lower than 20 nm.

## References:

1. García-Sánchez, M. F., Peña, J., Ortiz, A., Santana, G., Fandiño, J., Cruz, F., (2008), Nanostructured YSZ thin films for solid oxide fuel cells by ultrasonic spray deposition *Solid State Ionics*, 179, 243.
2. García-Sánchez, M. F., Ortiz, A., Santana, G., Bizarro, M., Cruz Gandarilla, F., Aguilar-Frutis, M. A., Alonso J. C. (2010), Nanostructured CeO<sub>2</sub> thin films deposited by ultrasonic spray pyrolysis, *J. Am. Ceram. Soc.* 93, 155.
3. Shao, Z., Zhou, W., Zhu, Z. (2012) Advanced synthesis of materials for intermediate-temperature solid oxide fuel cells, *Progress Mater. Sci.* 57 804.
4. Rupp J. L. M. (2012), Ionic diffusion as a matter of lattice-strain for electroceramic thin films, *Solid State Ionics* 207 1.
5. Benítez-Rico A., García-Sánchez M. F., Picquart M., Monroy-Peláez B.M., Santana-Rodríguez G. (2015), Understanding the high ionic conductivity in nanostructured ytterbia stabilized thin films, *J. Nano-materials* 692648.

# **Session II: Nanomaterials synthesis and properties**

# Synthesis of size-controlled nanoparticles by tuning the support properties and varying the reduction temperature

B. Van Vaerenbergh,<sup>1</sup> K. De Vlieger,<sup>1</sup> J. Lauwaert,<sup>1</sup> J.W. Thybaut,<sup>1</sup> A. Verberckmoes,<sup>1</sup> J. De Clercq,<sup>1\*</sup> and P. Vermeir<sup>2</sup>

<sup>1</sup>Ghent University, Department of Materials, Textiles and Chemical Engineering, Ghent, Belgium

<sup>2</sup>Ghent University, Department of Applied Biosciences, Ghent, Belgium

## Abstract:

Heterogeneous catalysts are preferred over their homogeneous counterparts due to the ease in product separation and catalyst recycle. However, switching to heterogeneous catalysts often entails a loss in catalytic activity. To counter this disadvantage, nanocatalysis offers unique solutions. Over the last decade, nanomaterials and nanoparticles (NPs) in particular have emerged as remarkably performant materials due to their high surface/volume-ratio and quantum confinement. However, the use of NPs requires their stability against self-aggregation since the catalytic activity of the NPs is highly size-dependent (1-10 nm).<sup>1</sup>

In this work, NP stabilization is achieved by using hydrotalcites (HT), i.e., steric stabilization, and ion exchange resins (IEX), i.e., steric and electrostatic stabilization, as supports<sup>2, 3</sup> due to highly structural tunability of the former and the large variety of different types of functionalities of the latter. Size-controlled NPs were synthesized by tuning the HT structure as well as by varying the reduction temperature. Furthermore, the IEX functionality was varied in order to achieve well-controlled NP sizes.

First, the effect of calcining the HT material on the NP size was investigated. The HT supported NP catalysts were synthesized by using a co-precipitation (1.0 wt% Pd) method, followed by a reduction of the metal with NaBH<sub>4</sub> (20°C). TEM analysis showed that the largest NPs (6.9 nm) were found in the uncalcined catalyst, while for the calcined catalyst significantly smaller NPs (3.0 nm) were observed. This is attributed to the HT structure since calcination causes a structural collapse, resulting in a more pronounced confinement and, hence, smaller NPs with a narrow size distribution. In addition, the effect of the reduction temperature (0°C-20°C-60°C) on the NP size was studied for the uncalcined, co-precipitated NP catalyst. TEM analysis showed that while the smallest NPs were obtained at 60°C (4.1 nm), lower reduction temperatures, i.e., 0°C and 20°C (8.1 nm and 6.9 nm respectively) resulted in larger NPs. At low reduction temperatures, the nucleation rate is more limited preferring heterogeneous nucleation over homogeneous nucleation, which re-

sults in less but larger NPs. Upon higher reduction temperatures, a faster (homogeneous) nucleation occurs and, thus, the formation of smaller NPs is promoted.

Secondly, the effect of the resin functionality on the NP size was investigated.<sup>4</sup> Three different macroporous IEX were used as support: a sulfonic acid (Lewatit K2629, Lanxess), a thiol functionalized (Ambersep GT74, DOW Chemical), and a quaternary amine resin (Lewatit MP500OH, Lanxess). The NP catalysts (0.1 wt% Pd) were synthesized via an intermatrix synthesis, i.e., ion exchange and reduction (NaBH<sub>4</sub>, 20°C) method. TEM analysis showed that while the smallest NPs (1.3 nm) were found in the Ambersep GT74 resin, the Lewatit K2629 and Lewatit MP500 OH resins resulted in NPs of a similar size (2.4 and 2.6 nm respectively). The difference in NP size is attributed to the differences in the resin functionality, i.e., the Ambersep GT74 resin possess strong coordinating, weak exchange groups, in contrast to the Lewatit K2629 and Lewatit MP500OH resins which have both weak coordinating, strong exchange groups.

In this work, it is clearly shown that the support structure as well as functionality and the reduction temperature are effective factors to tune NP size, and, hence, need to be considered when developing NP catalysts.

**Keywords:** Heterogeneous catalysis, nanoparticles, hydrotalcite, ion exchange resins, transmission electron microscopy.

## References:

1. Schmid, G., (2003) General Introduction, in *Nanoparticles: From Theory to Application* (ed. G. Schmid), Wiley-VCH Verlag GmbH & Co. KGaA, Weinheim, 1-362.
2. Marrodan, C., Berti, D., Liguori, F., and Barbaro, P., (2012) *Catalysis Science & Technology*, **2**, 2279-2290.
3. Burrueco, M., Mora, M., Jimenez-Sanchidrian, C., and Ruiz, J., (2014) *Applied Catalysis a-General*, **485**, 196-201.
4. Van Vaerenbergh, B., Lauwaert, J., Bert, W., Thybaut, J.W., De Clercq, J. and Vermeir, P., (2017) *ChemCatChem*, **9**, 451-457.

# Control of the crystal shape and magnetic properties of Co nanorods through the stirring rate.

K. Mrad,<sup>1</sup> F. Schoenstein,<sup>1</sup> H. T. T. Nong,<sup>1</sup> E. Anagnostopoulou,<sup>2</sup> L. Mouton,<sup>3</sup> S. Merccone,<sup>1</sup> C. Ricolleau,<sup>4</sup> N. Jouini,<sup>1</sup> M. Abderraba,<sup>5</sup> G. Viau,<sup>2</sup> J.-Y. Piquemal<sup>3</sup>

<sup>1</sup>University Paris 13, LSPM, CNRS UPR 3407, 99 Avenue J.-B. Clément, 93430 Villetaneuse, France.

<sup>2</sup>University of Toulouse, LPCNO, UMR 5215 INSA CNRS UPS, 135 av de Rangueil, 31077 Toulouse Cedex 4, France.

<sup>3</sup>University Paris Diderot, Sorbonne Paris Cité, ITODYS, CNRS UMR 7086, 15 rue J.-A. de Baïf, 75205 Paris Cedex 13, France.

<sup>4</sup>University Paris Diderot, Sorbonne Paris Cité, MPQ, CNRS UMR 7162, 10, rue Alice Domon et Léonie Duquet, 75205 Paris Cedex 13, France.

<sup>5</sup>University of Carthage, LMMA, IPEST, route Sidi Bou Said, B.P :51 2075, La Marsa, Tunis7

## Abstract:

Nanomaterials development is mandatory for improving modern science and technology. The control over their crystal structure and shape allow the optimization of their properties and the development of new applications.

Our aim in this work is to show how the mechanical stirring applied during the polyol synthesis of cobalt nanorods<sup>1</sup> can help us to control the crystal structure as well as the complex shape of the nanorods.

Our results show that the cobalt nanowire morphology and the hexagonal structure piling up vary considerably with the stirring conditions. The highest stirring speed conditions impose a lower aspect ratio of the anisotropic nano-objects, and decrease the coherence of diffraction length along the *c* direction of the hexagonal structure (*hcp*). Also the particle morphology is strongly modified in this case: the nanorods have rough edges along the *c* axis of the *hcp* structure along which the particles grow ( see Figure 1 a). The case of low stirring speed, the structural and morphological characteristic go in the opposite way: nanowires present smooth lateral sides and the stacking faults densities is low (see Figure 1 b).

The magnetic properties of the particles have been measured by MPMS 3 magnetometer. Magnetic hysteresis cycles were measured by field cooling at 200 K the nanoparticles inside their synthesis solution under the application of a magnetic field of 70 kOe. The results showed that the increasing of the stirring

softened the magnetic behavior of the nanowires through the morphology and structural control.

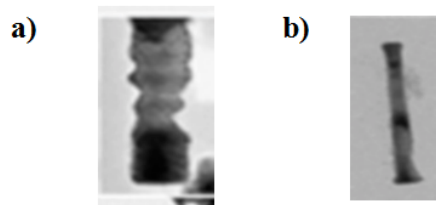


Figure 1 : TEM images of Co nanoparticles morphologies with two different stirring rates a) 300 rpm b) 50 rpm.

**Keywords:** Cobalt, anisotropy, magnetism, soft-chemistry synthesis, nanorod,

## References:

1. Pousthomis, M.; Anagnostopoulou, E.; Panagiotopoulos, I.; Boubekri, R.; Fang, W.; Ott, F.; Aït Atmane, K.; Piquemal, J. Y.; Lacroix, L. M.; Viau, G. Nano Research 2015.

# Intrinsic Conduction Mechanism in Polymer Nanofibers

K. H. Kim,<sup>1,2</sup> S. Lara-Avila<sup>2</sup>, S. Kubatkin<sup>2</sup>, Y. W. Park<sup>1,\*</sup>

<sup>1</sup>Seoul National University, Department of Physics and Astronomy, Seoul, Korea

<sup>2</sup>Chalmers University of Technology, Department of Microtechnology and Nanosciences, Gothenburg, Sweden

## Abstract:

Conductive polymers are an attractive route to cost effective and versatile nanoelectronics. Chemical synthesis of these materials offers possibility to chemically bottom-up engineer the electronic function of polymers at will, and yet produce them in large scale. As of now, several proof of concept devices based on conductive polymers have been shown that span a great range of applications including flexible field-effect transistors, actuators, sensors, and nano-optoelectronic devices. Insight in fundamental electron transport properties in these materials is of utmost importance for further practical development. Recent studies of I-V characteristics on pristine polymer nanofibers and carbonized polymer nanofibers show the similar power law scaling behavior despite the structural differences: the former quasi one-dimensional and the latter quasi-amorphous carbon networks of two- or three- dimensional. Both types of materials give apparent power law dependence of current with voltage and temperature and scaling of all measurements into a single universal curve. We have interpreted the power law scaling in carbonized polymer nanofibers as the manifestation of the Efros-Shklovskii variable range hopping (ES-VRH) in wide range of T and V parameters, which we suggest as the main transport mechanism of pristine polymer nanofibers<sup>1</sup>. The magneto resistance (MR), however, shows distinct behavior between the two materials. The pristine polyacetylene nanofibers show zero magneto resistance (ZMR) in high electric field<sup>2</sup>,  $E = 3 \times 10^4$  V/cm. But the MR of carbonized polyacetylene nanofibers remains positive which is typical for the VRH conduction. The applied electric power for the MR measurement of the pristine polyacetylene nanofibers in high electric field is  $P=1.2 \times 10^{-9}$  Watt, which is small enough to eliminate the heating effect. The ZMR observed in polyacetylene nanofibers in high electric field is explained with the de-confined conduction of spinless charged soliton which is a 1-D topological insulator<sup>3</sup>. A possibility to investigate the Majorana state in the polyacetylene nanofibers will be discussed.

**Keywords:** pristine polymer nanofibers, carbonized polymer nanofibers, power law scaling in I-V characteristic, zero magneto resistance in polyacetylene nanofibers, 1-D topological insulator, Majorana fermion

## References:

1. K. H. Kim, S. Lara-Avila, H. Kang, H. He, J. Eklof, S. J. Hong, M. Park, K. Moth-Poulsen, S. Matsushita, K. Akagi, S. Kubatkin and Y. W. Park, "Apparent power law scaling of variable range hopping conduction in carbonized polymer nanofibers", *Sci. Rep.* **6**, 37783 (2016)
2. Y. W. Park, "Magneto resistance of polyacetylene nanofibers", *Chem. Soc. Rev.* **39**, 2428-2438 (2010)
3. A. Choi, K. H. Kim, S. J. Hong, M. Goh, K. Akagi, R. B. Kaner, N. N. Kirova, S. A. Brazovskii, A. T. Johnson, D. A. Bonnell, E. J. Mele, and Y. W. Park, "Probing spin-charge relation by magnetoconductance in one-dimensional polymer nanofibers", *Phys. Rev. B* **86**, 155423 (2012).

# Low Temperature Electrical Resistivity and Magnetoresistance Measurement of Polyaniline and Carbon Nanotube Composites

Narendra Tanty,<sup>1\*</sup> Ananya Patra,<sup>1</sup> Krishana Prasad Maity<sup>1</sup> and V Prasad<sup>1</sup>  
<sup>1</sup>Indian Institute of Science, Department of Physics, Bangalore, India

## Abstract:

We report low temperature electrical resistivity and magnetoresistance (MR) measurements of conducting polyaniline (PANI) and multiwalled carbon nanotubes (MWCNT) composites. We have used in-situ oxidative polymerization method to synthesize hydrochloric acid doped PANI composites with MWCNT weight percentage 0%, 5%, 10%, 12%, 14% and 15%. The temperature dependence of resistivity is studied from room temperature to 4.2K and analysed by Mott Variable range hopping (VRH) model. The temperature dependence of resistivity shows five orders of magnitude change from  $1.1 \times 10^{-3} \Omega m$  at 300K to  $65.75 \Omega m$  at 4.2K for pure PANI, whereas for PANI composite with 15% MWCNT shows less variation from  $4.6 \times 10^{-4} \Omega m$  to  $3.5 \times 10^{-2} \Omega m$ . The huge change in resistivity is due to localization of charge carriers in presence of disorder. At 4.2K MR shows transition from positive to negative with higher MWCNT loading. Samples with 5% and 10% MWCNT shows positive MR, whereas 12%, 14% and 15% MWCNT loaded samples shows negative MR. Also at higher temperature like 10K, 20K and 30K both positive MR and negative MR is reduced to smaller value. The positive and negative MR is discussed in terms of wave function shrinkage effect and quantum interference effect on variable range hopping conduction.

**Keywords:** resistivity, variable range hopping, magnetoresistance

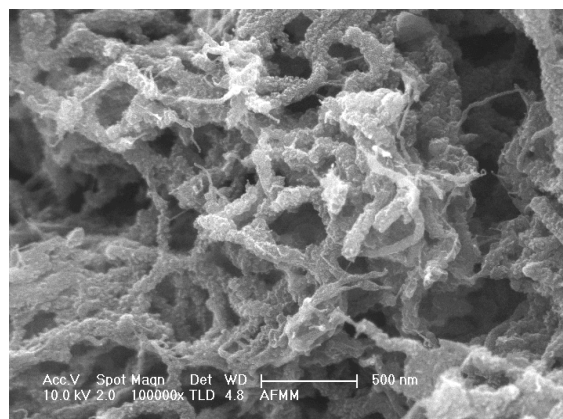


**Figure1:** Scanning electron microscope Image of PANI-CNT composite

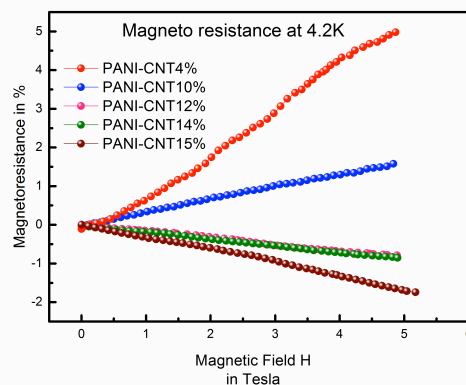


**Figure2:** Graph illustrating the transition of magnetoresistance from positive to negative with increase in Carbon nanotube content

## References:

1. Hongbu Gu, Jiang Guo et al Polymer 55(2014)4405-4419
2. Yunze Long et al Appl.phy.letters 85,1796(2004)
3. Y.Z. Long et al J.phys.Chem.C 2008,112,11507-11512

# Core-shell heterostructures combining photostrictive and piezo-magnetic properties

Adeline ADAM<sup>1\*</sup>, Mélanie POGGI<sup>1</sup>, Eric LARQUET<sup>1</sup>, Dmitry CHERNYSHOV<sup>2</sup>, Thierry GACOIN<sup>1</sup> and Isabelle MAURIN<sup>1</sup>

<sup>1</sup> Laboratoire de Physique de la Matière Condensée, CNRS-Ecole Polytechnique, 91128 Palaiseau Cedex, France

<sup>2</sup> The Swiss-Norwegian Beamlines, ESRF-The European Synchrotron, 71, Avenue des Martyrs, 38043 Grenoble Cedex, France

\*e-mail: [adeline.adam@polytechnique.edu](mailto:adeline.adam@polytechnique.edu)

## Abstract:

The optical control of the physical properties of a material is of interest for both fundamental and applied issues. The strategy that our group has developed in the past years is to design artificial core-shell heterostructures, which combines a photostrictive core with a piezomagnetic shell. These properties can be coupled via the transfer of mechanical stresses through the interface. Under light irradiation, the lattice of the core expands, exerting a pressure on the shell and in turn modifying its magnetic properties [1-3]. These photomagnetic effects could be exploited for a magneto-optical switching in optoelectronics or information storage devices.

The growth of such heterostructures has been optimized in the case of molecular crystals with a double perovskite structure derived from Prussian blue and of generic formula  $A_xM[M'(CN)_6]_y \cdot zH_2O$  (with A : alkali and M, M' : transition metal ions) [4-5]. In order to enhance the mechanical coupling between the core and the shell, we have studied a series of heteroepitaxial

$Rb_{0.5}Co[Fe(CN)_6]_{0.8} \cdot zH_2O @ K_xM[M'(CN)_6]_y \cdot z'H_2O$  (RbCoFe@KMM') core-shell particles involving a same RbCoFe photostrictive core and isostructural shell compounds with variable mismatch with the core lattice, from  $f = -2.6\%$  to  $-5.3\%$  with  $f$  defined as  $(a_{core} - a_{shell})/a_{core}$ .

Recent *in situ* X-ray powder diffraction (XRPD) experiments complemented by X-Ray absorption spectroscopy experiments performed at the Co K-edge to quantify the number of  $Co^{3+}-Fe^{2+}$  pairs converted into  $Co^{2+}-Fe^{3+}$  ones upon light irradiation provided a direct evidence for an effective transfer of the mechanical stresses across the interface within these heterostructures [6]. These measurements showed that the core expansion under light irradiation induces a partial deformation of the shell (figure 1). These effects are only due to the elastic coupling between the core and the shell as the investigated shell com-

pounds are optically inactive. Though, the presence of the shell significantly reduces the expansion of the core lattice under irradiation as well as the number of converted  $Co^{2+}-Fe^{3+}$  pairs. We also enhanced the fact that the mismatch has a strong effect on the efficiency of this elastic coupling.

**Keywords:** Prussian blue analogs, mechanical coupling, irradiation, lattice mismatch

**Figure 1:** Scheme of the expansion of the photostrictive core under light irradiation and the partial deformation induced in the shell (light green; dark green is not deformed)

## References:

1. Pajeroski et al., *J. Amer. Chem. Soc.* 2010, **132**, 4058.
2. Dumont et al., *Inorg. Chem.* 2011, **50**, 4295.
3. Risset et al., *Chem. Mater.* 2015, **27**, 38.
4. Presle et al., *New J. Chemistry*, 2011, **35**, 1296.
5. Presle et al., *J. Phys. Chem. C*, 2014, **118**, 13186.
6. Adam et al., submitted to *Chemistry of Materials*

# The effect of hybrid nanofillers on mechanical properties of carbon fibre epoxy composites.

Ayad Aied Mahuof,<sup>1,2,\*</sup> A.G.Gibson, George Kotsikos,<sup>1,2</sup>

<sup>1</sup>Newcastle University, School of Mechanical and Systems Engineering, Newcastle, UK

## Abstract:

In this study, graphene nanosheets (xGnP) and cup-stacked carbon nanotubes (CSCNT) were used to enhance the interlaminar shear strength properties of carbon fibre epoxy composites. The ball milling technique was used to disperse these two types of nanofillers into the epoxy matrix at different weight concentrations (0, 2.5, 4, 5, 6, 7) wt. %. Mechanical testing was performed to identify the optimum weight concentration for each type of nanophased matrix. The results showed that the highest mechanical strength was achieved after adding 5 wt. % of xGnP, 6 wt. % of CSCNT, and 4 wt. % of hybrid nanofillers (xGnP&CSCNT) to the epoxy resin. The optimum weight concentration for each type of nanocomposites was then used to modify the mechanical properties of carbon fibre composite. Three classes of carbon fibre epoxy composite hybrid produced with the following formulations, namely: a) xGnP/CF/epoxy composite, b) CSCNT/CF/epoxy composite, and c) xGnP-CSCNT/CF/ epoxy composite hybrid. Short beam shear testing was conducted on these three types of hybrid composites. The results showed that the interlaminar shear strength increased by approximately 28.73% in the xGnP/CF/ epoxy composite, and 34.34% in the CSCNT/CF/epoxy composite. In addition, there was a significant improvement by approximately 31.85% in the xGnP-CSCNT/CF/epoxy composite hybrid after combining of xGnP and CSCNT into the epoxy matrix. TEM and SEM was used to assess the dispersion of the nanofillers into the epoxy, and the fracture mechanism of carbon fibre composite. The microstructural details showed a reasonable dispersion of the nanofillers and good interlocking of the carbon fiber network with the nanofilled matrix.

**Keywords:** Ball milling technique, hybrid nanofillers, carbon fiber composite, nanocomposite, graphene, fibre nanotubes.

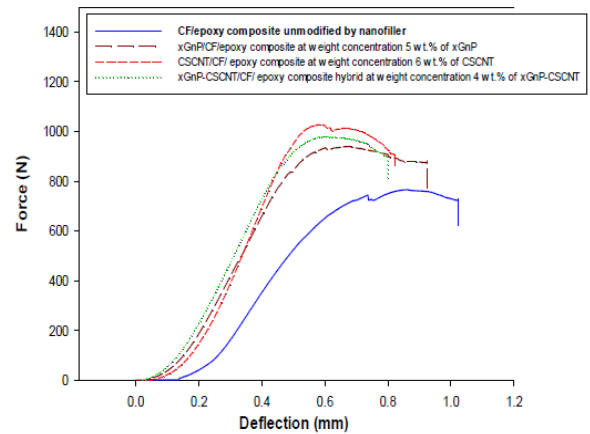


Figure: Typical force-deflection curves for short beam samples of carbon fibre composite modified with graphene, cup-stacked carbon nanotube, and hybrid nanofillers (xGnP&CSCNT).

## References:

1. Al-Saleh M H Electrical, "EMI shielding and tensile properties of PP/PE blends filled with GNP: CNT hybrid nanofiller", *Synthetic Metal* 217 (2016)322-330
2. Li, W., et al., On improvement of mechanical and thermo-mechanical properties of glass fabric/epoxy composites by incorporation CNT-Al<sub>2</sub>O<sub>3</sub> hybrids. *Composites Science and Technology*, 2014. 103 (0): P.36-43.

# Synthesis of zinc oxide/reduced graphene oxide nanocomposites and evaluation of its tribological properties in paraffin oil as energy efficient lubricant additive

R.B. Rastogi,<sup>1\*</sup> Kalyani,<sup>1</sup> V. Jaiswal,<sup>1</sup> D. Kumar<sup>2</sup>

<sup>1</sup>Department of Chemistry, Indian Institute Technology (Banaras Hindu University) Varanasi-221005, India

<sup>2</sup>Department of Ceramic Engineering, Indian Institute Technology (Banaras Hindu University) Varanasi-221005, India

## Abstract:

The reduced graphene oxide<sup>1</sup> (rGO), ZnO nanoparticles<sup>2</sup> and, reduced graphene oxide reinforced with ZnO nanoparticles (rGO/ZnO) were synthesized and characterized by various state-of-art techniques as powder-XRD, transmission electron microscopy, energy dispersive X-ray spectroscopy and Raman spectroscopic techniques. Friction and wear reducing properties of as-prepared rGO, ZnO and rGO/ZnO nanocomposite in liquid paraffin as base oil were investigated by the four-ball lubricant testing machine. All the tribological tests were carried out at an optimized additive concentration by varying the test durations at 392N load and by varying load for 30 min test duration. Various tribological parameters such as mean wear scar diameter (MWD), friction coefficient ( $\mu$ ), mean wear volume (MWV) and wear rate show that these nanoparticles act as efficient antiwear additives. The tribological results show the introduction of a small amount of these nanoadditives to the base lube could reduce friction and wear drastically under various test conditions. Among all the studied additives, rGO/ZnO exhibited superior lubrication behavior over its individual constituent rGO and ZnO nanoparticles in base oil. The pronounced tribological behavior of rGO/ZnO is due to entrapment of ZnO nanoparticles in between the multilayered rGO which enhanced the adherence property of rGO.<sup>3</sup> The rGO/ZnO nanoparticles act as nanobearings and/or form thin layer in between the steel-steel interface.<sup>4</sup> The surface morphology of the sliding surfaces has been analysed using SEM and AFM which exhibit there is huge reduction in surface roughness in presence of rGO/ZnO. Tribochemis-

try of the worn surface lubricated with rGO/ZnO has been investigated by XPS shows there is formation of protective *in-situ* tribochemical film/s made up of ZnO and Fe<sub>2</sub>O<sub>3</sub>/Fe<sub>3</sub>O<sub>4</sub>.

**Keywords:** rGO/ZnO nanocomposite, anti-wear additives, Surface characterization: SEM/EDX, AFM, XPS.

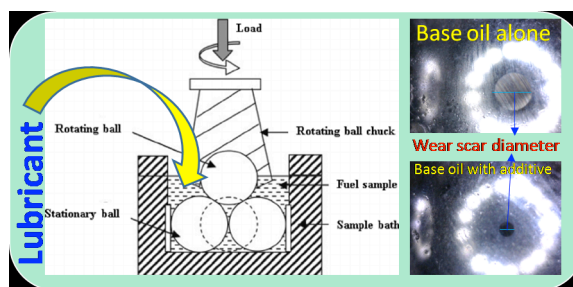


**Figure 1:** Zinc oxide/reduced graphene oxide nanocomposite significantly enhanced antiwear and load carrying properties of paraffin base oil.

## References:

1. D.C. Marcano, D.V. Kosynkin, J.M. Berlin, A. Sinitskii, Z. Sun, A. Slesarev, L.B. Alemany, W. Lu, J.M. Tour, *ACS Nano*, 2010, 4, 4806.
2. Kalyani, V. Jaiswal, R.B. Rastogi, D. Kumar, *Appl. Nanosci.*, 2015, DOI 10.1007/s13204-015-0471-1.
3. D. Berman, A. Erdemir, A.V. Sumant, *Materials Today*, 2014, 17, 32.
4. V. Jaiswal, R.B. Rastogi, R. Kumar, L. Singh, K.D. Mandal, *J. Mater. Chem. A.*, 2014, 2, 275-286.

# Polyurethane-MWCNT nanocomposite for RAM applications

I.J. Rajmohan<sup>1</sup>, M.I.Hussein<sup>1</sup>, Q.Clément<sup>2</sup>, N.Vukadinovic<sup>2</sup>

<sup>1</sup>UAE University, Department of Electrical Engineering, Abu Dhabi, UAE

<sup>2</sup>Dassault Aviation, 92552 Saint-Cloud, France

## Abstract:

A class of high performance composite, based on multi-wall carbon nanotubes (MWCNT), is explored for its applicability in developing new radar absorbing materials (RAMs) and shielding structures. Carbon nanotubes possess remarkable mechanical and physical performances and act as multifunctional nano-fillers for polymer fibers. It has great potential for wide range of applications owing to their large aspect ratio and high conductivity, with excellent absorption level and shielding effectiveness. In this study the MWCNT fillers are uniformly dispersed in polyurethane (PU) polymer matrix at different weight percentages (0.1%-5%). The performance of the composite aggregates at microwave frequency is governed by the electrical properties of the filling particles and polymer matrix. Higher aspect ratio of the MWCNT reconfirms the composite's electromagnetic absorption capabilities [1]. It is expected that conducting network inside the composites are created using small percentage of MWCNT content as the conduction paths are easily formed due to the contacts between the ends of the long tubes [2]. In order to measure the dielectric properties of the composite samples, open ended coaxial probe method is used. Dielectric Assessment Kit (DAK) from SPEAG is used to obtain the electrical properties for eleven samples with different weight percentages (w%) including 0%, 0.1%, 0.2%, 0.3%, 0.4%, 0.5%, 1%, 2%, 3%, 4% and 5%. The measurements are carried out at room temperature using R&S<sup>®</sup>ZVL 13.6 GHz Vector network Analyzer, with frequency range of (300MHz-13.6 GHz), as shown in Figure 1. It is observed that the real part of the electric permittivity is increasing with increasing w% concentration. A theoretical model is currently developed in order to describe the dielectric properties of the MWCNT composites with aim of fitting the measurements as best as possible. Moreover, reflection loss calculations have been done, based on the dielectric properties obtained for each w%, considering a slab of MWCNT composite laid on a perfect conductor. As shown in Figure 2 for a 2 w% MWCNT composite slab with a thickness of 10 mm, the reflection loss at normal incidence can have two min-

ima, respectively located around 3 GHz and 10 GHz, leading to a two-band RAM.

**Keywords:** multi-wall carbon nanotubes, radar absorbing materials, composite materials.

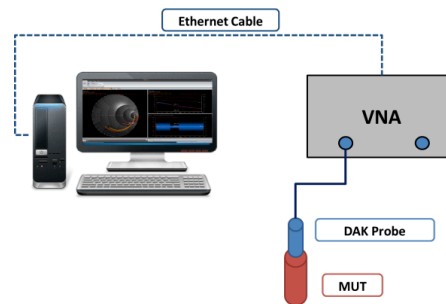


Figure 1: Measurement setup.

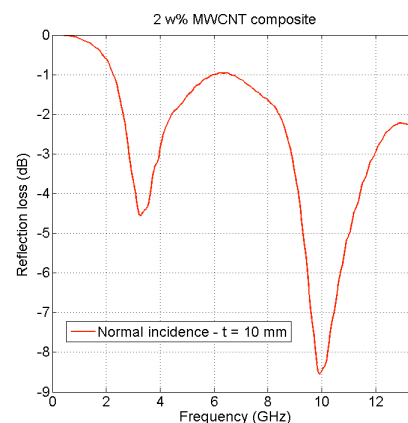


Figure 2: Reflection loss at normal incidence of a 2 w% MWCNT composite with a thickness of 10 mm.

## References:

- [1] D. Micheli, R. Pastore, M. Marchetti, G. Gradoni, F. Moglie and V. M. Primiani, "Modeling and measuring of microwave absorbing and shielding nanostructured materials," in *Electromagnetic Compatibility (EMC EUROPE)*, 2012.
- [2] A. Saib, L. Bednarz, R. Daussin, C. Bailly, X. Lou, J.-M. Thomassin, C. Pagnouille, C. Detrembleur, R. Jerome and I. Huynen, "Carbon nanotube composites for broadband microwave absorbing materials," *IEEE Transactions on Microwave Theory and Techniques*, vol. 54, no. 6, pp. 2745 - 2754, 2006.

# The Challenge of Nanoparticle Stabilization for the Preparation of Nanocomposites

T. Graule

Empa Swiss Federal Laboratories for Materials Science and Engineering, Laboratory for High Performance Ceramics, Dübendorf, Switzerland

## Abstract:

The efficient stabilization of ceramic based nanopowders is a prerequisite for the achievement of highly reliable ceramic materials and for the development of nanocomposites and nanostructured materials, e.g. on the basis of porous materials for filtration and catalysis.

Agglomeration or re-agglomeration due to Van der Waals forces can be avoided using different concepts to increase the separation barrier by electrostatic or steric means. Recently some studies applying anion type copolymers using alumina and zirconia submicron and nanoparticles were performed in order to develop a basic understanding of the mechanism of steric stabilisation in aqueous media [1-3]. We present here a review on the new concepts to apply anion type and cation type comb copolymers as a promising alternative in case of the stabilisation of titania [4, 5] and other oxides. The effectiveness of the dispersants was evaluated on the basis of adsorption, zeta potential measurements and particle size measurements.

**Keywords:** electrostatic stabilization, steric stabilization, colloid chemistry, surfactants, dispersants, ceramics, nanoparticles, adsorption, zeta potential

## References:

1. Y. De Hazan, J. Heinecke, A. Weber, T. Graule, High Solids Loading Ceramic colloidal Dispersions in UV Curable Media via Comb polyelectrolyte Surfactants, *J. Colloid Interf. Sci.* 337 (2009) 66–74.
2. M. Wozniak, Y. de Hazan, T. Graule, D. Kata, Rheology of UV curable colloidal silica dispersions for rapid prototyping applications, *J. Eur. Cer. Soc.* 2011, 31, 2221-2229.
3. Y. de Hazan, V. Märkl, J. Heinecke, C. Aneziris, T. Graule, Functional ceramic and nanocomposite fibers, cellular articles and microspheres via radiation curable colloidal dispersions, *J. Eur. Cer. Soc.* 2011, 31, 2601-2600.
4. V. Klimkevicius, T. Graule, R. Makuska, Effect of structure of cationic comb copolymers on their adsorption and stabilization of titania nanoparticles, *Langmuir* 2015, 31, 2074-2083.
5. V. Klimkevicius, T. Graule, R. Makuska, Rheological behaviour of alkaline concentrated titania nanoparticle dispersions stabilized by cationic comb copolymers, *Applied Rheology* 26 (2016) 15199.,

# Why are Rubber Nanocomposites so Exciting?

Anil K. Bhowmick

Rubber Technology Center, Indian Institute of Technology Kharagpur- 721302, India

Email: [anilkb@rtc.iitkgp.ernet.in](mailto:anilkb@rtc.iitkgp.ernet.in)/[anilbhowmick@gmail.com](mailto:anilbhowmick@gmail.com)

## Abstract:

Rubber nanocomposite is a field of extensive research in recent years. This is a class of organic-inorganic hybrid materials, where the inorganic component is uniformly distributed in nanometer scale ( $10^{-9}$  m) within the rubber matrix. The reinforcing components are mostly nanoclay, silica, expanded graphite, carbon nanotubes, nanofibers etc. Naturally occurring or synthetic clays are first modified into rubber compatible nanoclay and then dispersed in a matrix by any of the three different methods namely solution intercalation, in-situ polymerization and melt intercalation. Gallery spacing of clay could also be expanded without the use of an organic modifier, simply by using a synthetic approach. Graphitic layers have been delaminated to a few layers of graphene by modification. The present lecture will highlight some interesting observations in the area of modified nanomaterials and their nanocomposites. For instance, dispersion of a wide range of nanofillers can be enhanced by various compatibilization and dispersion techniques in different rubbers. The nanostructure – property relationship will be demonstrated in this lecture. The modified clays have been shown to improve the mechanical, thermal and swelling properties of these rubbers, depending on the nature of polymer matrix ( Fig. 1) . The results have been explained with the help of morphology, interaction between the components, adsorption phenomena, surface and cleavage energy balance and thermodynamics. On the basis of these, a new mechanism for polymer intercalation into clay galleries has been proposed. Tribological characteristics of rubber nanocomposites, performed by analyzing the debris and abraded surface, revealed that nanofillers arrested wear significantly. The mechanical, dynamic mechanical and tribological properties of ternary nanocomposites comprising polymer /nanofiller/carbon black exhibited synergistic improvements, within the high performance window of good wet skid and low rolling resistance. Thermal properties of various nanocomposites are shown to be improved considerably for hydrogenated nitrile rubber used in automotive applications. Thus, these nanocomposites have paved the way for various applications, which would be discussed.

**Keywords:** polymer, rubber, nanocomposites.

**Figure 1:** Mechanical properties of SBR nanocomposites

## References:

1. Sengupta, R., Bhattacharya, M., Bandyopadhyay, S., Bhowmick, A.K. (2011), A review on the mechanical and electrical properties of graphite and modified graphite reinforced polymer composites, *Progress in Polymer Science*, 36, 638–670.
2. Kotal, M., Bhowmick, A.K. (2015), Polymer nanocomposites from modified clays: Recent advances and challenges, *Progress in Polymer Science*, 51, 127-187.
3. Sadhu, S., Bhowmick, A.K. (2004), Preparation and Properties of Nanocomposites Based on Acrylonitrile–Butadiene Rubber, Styrene–Butadiene Rubber and Polybutadiene Rubber, *Journal of Polymer Science: Part B: Polymer Physics*, 42, 1573–1585.
4. Bhattacharya, M., Bhowmick, A.K. (2010), Correlation of vulcanization and viscoelastic properties of nanocomposites based on natural rubber and different nanofillers, with molecular and supramolecular structure, *Rubber Chem Technol*, 83, 16-34.
5. Ganguly, A., Bhowmick, A.K., Li, Y. (2008), Insights into Montmorillonite Nanoclay Based ex Situ Nanocomposites from SEBS and Modified SEBS by Small-Angle X-ray Scattering and Modulated DSC Studies, *Macromolecules*, 41, 6246-6253.

# Field emission propererties of Lanthanum Nickelate nanoparticles

Ananya Patra,<sup>1,\*</sup> Ramesh Kamble<sup>1,2</sup>, Narendra Tanty<sup>1</sup> and V. Prasad<sup>1</sup>

<sup>1</sup>Department of Physics, Indian Institute of Science, Bangalore 560012, Karnataka, India

<sup>2</sup>Department of Physics, College of Engineering, Pune 411005, Maharashtra, India

## Abstract:

Field emission posses tremendous applications in numerous technological aspects. To name a few are: electron sources in electron microscope, field emission displays, vacuum electronic devices etc. Excellent thermal stability, high electrical conductivity and low work function make lanthanum nickelate (LNO) an ideal candidate for potential electron field emitter. In the present work, we have prepared nanostructured LNO by sol-gel method and studied field emission properties.<sup>1</sup> We have analysed our results by Fowler-Nordheim (F-N) model which relates the emission current density (J) with applied electric field (E) by the following equation:<sup>2</sup>

$$J = \frac{A(\beta E)^2}{\phi} \exp\left(\frac{B\phi^{3/2}}{\beta E}\right)$$

(1)

Where  $A = 1.54 \times 10^{-6} \text{ eV/V}^2$  and  $B = 6.83 \times 10^9 \text{ AeV}^{3/2}/\text{V}^2$ ,  $\phi$  is work function of the material and  $\beta$  is the field enhancement factor which depends on the geometry of the tips. Notably,  $\beta$  signifies the enhancement of the local electric field at the tip of the emitter over the applied electric field.

Figure 1 shows the variation of J with E. We have theoretically fitted the data in the figure by Eqn. [1]. We have obtained from the fitting the threshold electric field,  $E_{TH} = 19.23 \text{ V}/\mu\text{m}$  and turn on field,  $E_{TO} = 16.91 \text{ V}/\mu\text{m}$  which are lower than the previously reported value.<sup>3</sup> The turn on field and threshold field are defined as the minimum field required to achieve a current density of  $0.1 \text{ mA}/\text{cm}^2$  and  $1 \text{ mA}/\text{cm}^2$  respectively. These comparatively low values of  $E_{TH}$  and  $E_{TO}$  are facilitated by the pyramidal and whisker shaped tips and sharp edges of nanostructured LNO.<sup>4</sup> We extracted a satisfactory value of  $\beta \sim 249.37$  from the slope of the graph  $\ln(J/E^2)$  vs  $1/E$ , shown in the inset of figure 1. Such observation can be attributed to low work function and topography of the surface. As efficiency of field emission can be tuned by varying the aspect ratio and shape of the emitter tips, the

nanostructured LNO of high purity can be a promising material for studying the field emission properties.

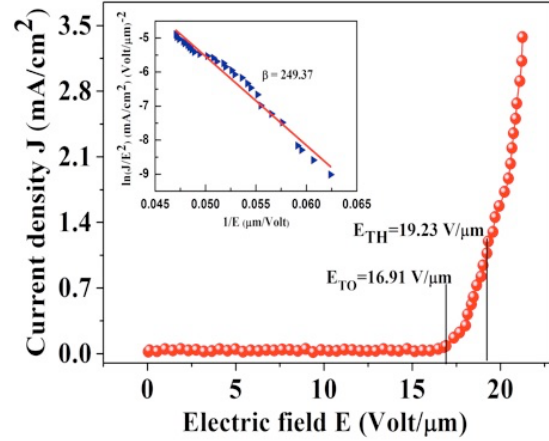


**Figure 1:** Variation of current density J as a function of electric field E. The inset shows Fowler-Nordheim plot ( $\ln(J/E^2)$  vs.  $1/E$ )

**Keywords:** Field emission study, emission current, nanostructure

## References:

1. Kamble, R. B., Tanty, N., Patra, A., Appl. Phys. Lett., 109, 083102 (2016)
2. Fowler, R. H. and Nordheim, L., R. Soc. London Ser. A, 119, 173 (1928)
3. Yang, T. H., Harn, Y. W., Chiu, K. C., Fan, C. L. and Wu, J. M., J. Mater. Chem. 22, 17071 (2012).
4. Utsumi, T., IEEE Transac. Electron Devices, 38, 2276 (1991).

# Superior Optical Properties of Single Perovskite Nanocrystals

Xiaoyong Wang,<sup>1\*</sup> Fengrui Hu,<sup>1</sup> Chunyang Yin,<sup>1</sup> Chunfeng Zhang,<sup>1</sup> and Min Xiao<sup>1,2\*</sup>

<sup>1</sup>National Laboratory of Solid State Microstructures, School of Physics, and Collaborative Innovation Center of Advanced Microstructures, Nanjing University, Nanjing 210093, China

<sup>2</sup>Department of Physics, University of Arkansas, Fayetteville, Arkansas 72701, USA

## Abstract:

Ever since the first synthesis of semiconductor perovskite nanocrystals (NCs) of cesium lead halides in 2015, they have attracted a lot of research interest due to the size- and composition-dependent emission colors from the quantum confinement effect. At the single-particle level, the quantum-emitter nature of perovskite NCs have been confirmed from the single-photon emission measurements. Here we show that, at room temperature and with low-power excitation, nonblinking photoluminescence (PL) is easily achieved in single perovskite CsPbI<sub>3</sub> (cesium lead iodide) NCs synthesized from a facile colloidal approach. With high-power excitation, PL blinking is triggered in single CsPbI<sub>3</sub> NCs by the photo-ionization effect that creates two types of charged excitons with opposite signs. The “grey” intensity level in the PL blinking time trace is related to the charged exciton with Auger-mediated weak fluorescence. Auger recombination in the other type of charged exciton is nearly eliminated so that its fluorescent photons contribute to the blinking “on” intensity level with a PL lifetime almost twice shorter than that of the neutral exciton. At cryogenic temperature and with low-power excitation, a resolution-limited PL linewidth of  $\sim 200$   $\mu\text{eV}$  is measured for single CsPbI<sub>3</sub> NCs without the spectral diffusion effect (Figure 1). Due to the suppressions of both PL blinking and spectral diffusion effects, bright-exciton fine structure splittings of single excitons and the appearance of optical emissions from neutral and charged biexcitons can be further demonstrated in single CsPbI<sub>3</sub> NCs.

**Keywords:** perovskite, nanocrystal, blinking, spectral diffusion, fine structure splitting, single-particle spectroscopy

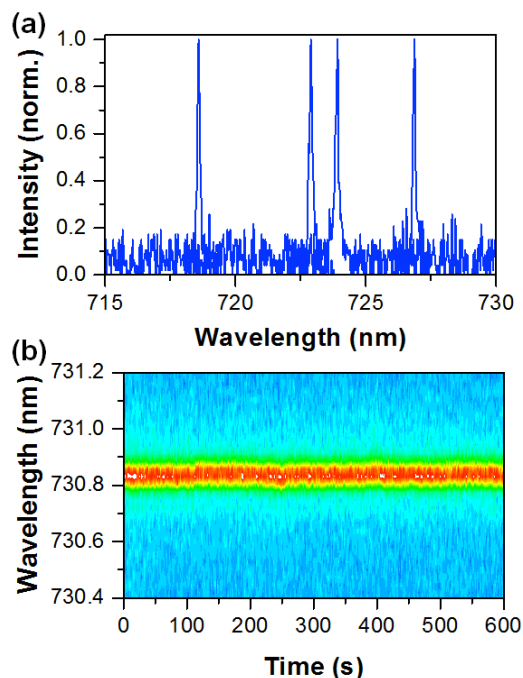


**Figure 1:** (a) PL spectra of four single CsPbI<sub>3</sub> NCs showing ultranarrow PL linewidths of  $\sim 200$   $\mu\text{eV}$  limited only by the system resolution. (b) Time-dependent PL spectral image of a single CsPbI<sub>3</sub> NC showing the suppressions of both PL blinking and spectral diffusion effects. The above measurements were performed at the cryogenic temperature of  $\sim 4$  K.

## References:

1. Hu, F., Zhang, H., Sun, C., Yin, C., Lv, B., Zhang, C., Yu, W. W., Wang, X., Zhang, Y., Xiao, M. (2015) Superior optical properties of perovskite nanocrystals as single photon emitters. *ACS Nano*, 9, 12410-12416.
2. Hu, F., Yin, C., Zhang, H., Sun, C., Yu, W. W., Zhang, C., Wang, X., Zhang, Y., Xiao, M. (2016) Slow Auger recombination of charged excitons in nonblinking perovskite nanocrystals without spectral diffusion. *Nano Lett.*, 16, 6425-6430.

# The Dielectric Studies of BT-CCT Nanocomposite Ceramic Synthesized by Solid State Route

K.D. Mandal\*, A. Khare

Indian Institute of Technology, (Banaras Hindu University), Department of Chemistry, Varanasi-221005, (U.P), India

## Abstract:

A nanocomposite ceramic with the composition close to  $0.9\text{BaTiO}_3 - 0.1\text{CaCu}_3\text{Ti}_4\text{O}_{12}$  (BT-CCT) was synthesized using a solid state method through sintering at  $950^\circ\text{C}$  for different time durations 3, 6, 9 and 12 h. The structural and microstructural details were studied by X-ray diffraction (XRD), scanning electron microscope (SEM) and transmission electron microscope (TEM) techniques. XRD analysis confirmed the existence of BT and CCT as the primary phases along with CuO and  $\text{CaTiO}_3$  as the minor aspects. The average grain sizes obtained by SEM analysis were found to be around 269 nm, 309 nm, 342 nm, and 734 nm for sintering durations 3, 6, 9 & 12 h respectively. TEM analysis showed the particle size in the range of  $35\pm 15$  nm. The surface morphology was analyzed by atomic force microscopy (AFM). The sample sintered for three h exhibited very high dielectric constant ( $\epsilon_r \sim 31967$ ) at 1 kHz and 333 K. The presence of semiconducting grains with the insulating grain boundaries significantly attributes to such a high dielectric constant value, supporting the internal barrier layer capacitance (IBLC) mechanism operative in BT-CCT nanocomposite.

**Keywords:** Solid state route; Nanocomposite; X-ray diffraction; Dielectric constant.

## References:

1. Bueno, P.R., Ribeiro, W.C., Ramirez, M.A., Varela, J.A., Longo, E. (2007) Separation of dielectric and space charge polarizations in  $\text{CaCu}_3\text{Ti}_4\text{O}_{12}/\text{CaTiO}_3$  composite polycrystalline systems, *Appl. Phys. Lett.* 90, 142912–142913.
2. Almond, D., Bowen, C. (2004) Anomalous power law dispersions in ac conductivity and permittivity shown to be characteristics of microstructural electrical networks, *Phys. Rev. Lett.* 92, 157601–157604
3. Ni, L., Chen, X.M., Liu, X.Q. (2010) Structure and modified giant dielectric response in  $\text{CaCu}_3(\text{Ti}_{1-x}\text{Sn}_x)$  4O12 ceramics, *Mater. Chem. Phys.* 124, 982–986
4. Kim, H.E., Choi, S.M., Lee, S.Y., Hong, Y.W., Yoo, S.I. (2013) Improved dielectric properties of  $\text{BaTiO}_3$ -added  $\text{CaCu}_3\text{Ti}_4\text{O}_{12}$  polycrystalline ceramics, *Electron. Mater. Lett.* 9, 325–330.

# Study of LDH Fabrication Method to Reduce Atmospheric CO<sub>2</sub> Concentration

JiHo Eom, SoonGil Yoon\*

Department of Materials Science and Engineering, Chungnam National University, Daeduk Science Town, 34134, Daejeon, Korea

## Abstract:

At present, there are many environmental pollution problems due to rapid industrial development and indiscreet use of fossil fuels. Among them, the effects of global warming due to the increase of atmospheric CO<sub>2</sub> concentration are very serious. Therefore, many researches and policies are in progress to solve this problem in various fields. Carbon capture and storage (CCS) is one of the most studied methods for reducing the concentration of atmospheric CO<sub>2</sub>. CCS is the technology that captures, transports, and stores CO<sub>2</sub> emitted from power plants or factories that can emit large amounts of CO<sub>2</sub>. However, it has cost disadvantages and required much research at the national level in the future. Hereby we propose a new method for reducing the atmospheric CO<sub>2</sub> concentration. We have succeeded in producing Zn-Al:LDH which is one of the Layered Double Hydroxide (LDH) materials currently being studied in electrical, mechanical and construction fields using Al doped ZnO (AZO) thin film and water. LDH is a structure that Carbonate ions (CO<sub>3</sub><sup>2-</sup>) are trapped in between two hydroxide layers. After LDH formation, the CO<sub>2</sub> concentration in water was decreased and then it was recovered again with time. These mechanisms can be used to reduce the atmospheric CO<sub>2</sub> concentration while creating LDH in the real industry. For this reason, we will confirm that possibility of LDH formation using Al-doped MgO and Al-doped Fe<sub>2</sub>O<sub>3</sub> etc. and compare the CO<sub>2</sub> consumption while making LDH using each material. We will also compare the LDH formation time with temperature and pressure. Through this study, it is expected to present a new direction for the environmental problem caused by the atmospheric CO<sub>2</sub> concentration.

**Keywords:** LDH, CO<sub>2</sub> reduction, FTS sputtering

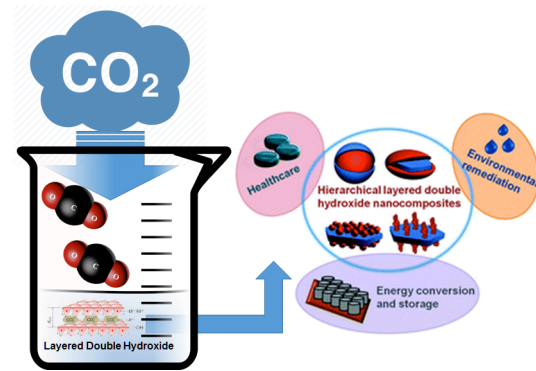


**Figure 1:** Fabrication of Layered Double Hydroxide using atmospheric carbon dioxide.

# Inexpensive and Rapid Synthesis Unilamellar Liposomes for Drugs Delivery

C. Has<sup>1\*</sup> and P. Sunthar<sup>1</sup>

<sup>1</sup>Indian Institute of Technology Bombay, Department of Chemical Engineering, Mumbai, India

## **Abstract:**

Liposomes (or vesicles) have been emerged as one of the most advantageous delivery vehicles for the various drugs. They are self-closed spherical lipid bilayer structures in which a volume of the aqueous solution is entrapped by inner core. They are usually formed because the accumulation of lipid molecule yields entropically favourable conditions of minimal free energy in an energetically favourable manner. To date there have been several methods for the liposomes synthesis but most of them involve complex and tedious technique. Here we present an inexpensive, simple, and rapid approach for preparing a wide range of unilamellar liposomes by a static phase interdiffusion method. This single step novel preparation technique is suitable for reliably synthesizing monodisperse and unilamellar vesicles with a wide range of size (150-500 nm) and low polydispersity (PDI < 0.2). In addition, the present technique doesn't require any post processing steps such as sonication, or extrusion. Liposomes can be observed within 10-15 min and have a long shelf life. The principle of vesicles formation is based on the diffusion driven process of two miscible phases. Process involves the self assembly of lipids into liposomes as ethanol speedily diffuses into aqueous phase. Moreover, size of the liposomes can be easily tuned by temperature and type of the lipid only. The experimental conditions in this method reveal that the lipid concentration, time duration of experiment, length of lipid phase, ethanol content, and pH have very little influence on the liposomes mean diameter. Furthermore, it is also shown that the rate of ethanol evaporation with time does not have any significant influence on the vesicles size, pointing out that the process is controlled by the rate of interdiffusion of the two miscible phases.

We anticipate that with this simple and efficient technique, the finding of novel liposomal formulations can be better investigated and more widely administered in clinical settings.

**Keywords:** Self-assembly, diffusive mixing, Unilamellar liposomes, drug encapsulation, biomedical applications.

# Real-time assessment of self-assembly of smart supramolecular systems by optical and biochemical methods

K.G. Shevchenko,<sup>1</sup> V.R. Cherkasov,<sup>1</sup> E.N. Mochalova,<sup>1</sup> A.V. Babenyshev,<sup>1</sup> M.P. Nikitin<sup>1,2</sup>

<sup>1</sup> Moscow Institute of Physics and Technology, Laboratory of Nanobiotechnology, Dolgoprudny, Moscow Region, Russia

<sup>2</sup> General Physics Institute, Russian Academy of Science, Moscow, Russia

## Abstract:

Biomedical agents based on self-assembly of nanoparticles via non-covalent molecular interfaces promise to become an important milestone in development of nanomedicine due to easily adjustable composition, size and functionality. Here, we demonstrate the capabilities of localized surface plasmon resonance (SPR) phenomenon to study non-covalent interactions not just between plasmonic particles, but between gold nanoparticles (AuNP) and non-plasmonic ones. We show its potential to study assembly and performance of a novel type of advanced smart materials, namely, biocomputing agents. These agents, self-assembled from nanoparticles via biomolecular interfaces such as proteins, DNA, etc., can analyze presence of biomolecular inputs according to Boolean logic and undergo the input-induced disassembly implementing the proper output action. Using UV-Vis spectroscopy to monitor the assembly/disassembly processes of the basic YES-gate structure that consists of a polymer core particle with and gold nanoparticles associated on its surface we found that the structure transformations are well-characterized by pronounced difference in SPR spectral band position (shifting up to 50 nm). This SPR shift correlates remarkably well with biochemical estimation of the of assembly/disassembly, and can provide valuable real-time kinetic analysis. We believe that the obtained data can be easily extended to other non-plasmonic nanoparticle systems with similar chemical and colloidal properties. SPR method can become a valuable addition to analytical toolbox for characterization of self-assembled smart nanosystems used in biosensing, imaging, controlled release and other applications.

**Keywords:** Surface plasmon resonance, gold nanoparticles, smart materials, self-assembling systems, molecular logic gates

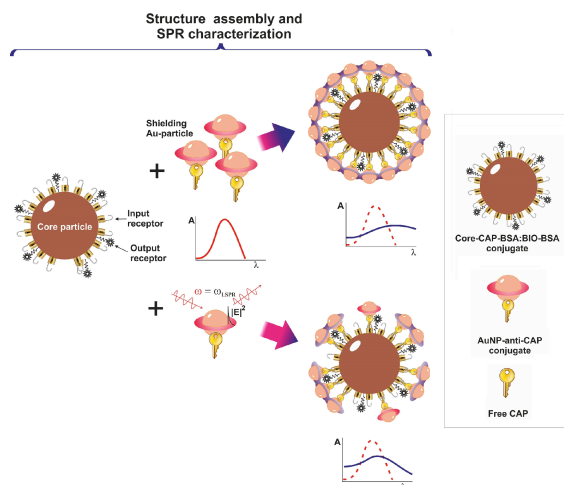


**Figure 1:** Illustration of SPR methods for characterization of assembly/disassembly of gold nanoparticles on the surface of the core particle: top – probing the density of surface coverage; bottom – fabrication of YES-gate structure and its operation.

## Acknowledgements:

Different aspects and parts of this multidisciplinary research were partially supported by the Russian Foundation for Basic Research (grants No 14-29-07271, 16-32-00791, 16-34-60230, 17-33-80176).

## References:

1. Nikitin, M.P., Shipunova, V.O., Deyev, S.M., Nikitin, P.I. (2014) Biocomputing based on particle disassembly. *Nat. Nanotechnol.*, 9, 716–722.
2. Shevchenko, K. G., Cherkasov, V. R., Tregubov, A. A., Nikitin, P. I., Nikitin, M. P. (2017) Surface plasmon resonance as a tool for investigation of non-covalent nanoparticle interactions in heterogeneous self-assembly & disassembly systems, *Biosens. Bioelectron.*, 88, 3-8.

# Scaling up nanoxerography by electrical micro-contact printing for photoluminescent anti-counterfeiting solutions

D. Poirot,<sup>1</sup> E. Palleau,<sup>1</sup> F. Guerin,<sup>1</sup> T. Alnasser,<sup>1</sup> L. Ressier<sup>1</sup>

<sup>1</sup> Université de Toulouse, LPCNO, INSA-CNRS-UPS, 135 avenue de Rangueil, F-31077 Toulouse, France

## Abstract:

Over the last decade, colloidal-based applications and nanodevices have been multiplied, benefiting from the miniaturization trend and the unique properties of used nano-objects appearing at the nanoscale. Their fabrication requires directing the assembly of colloidal nano-objects from their suspension onto predefined areas of rigid or flexible substrates. To achieve this step, our research team has been working on the so called nanoxerography technique, a process that uses electrostatic patterns written into electret thin films to trap charged and/or polarizable colloidal nanoparticles. It recently led to the conception of an anti-counterfeiting marker based on photoluminescent NaYF<sub>4</sub>:Yb:Er nanocrystals where charges patterns forming a micro QR code were written owing to an electrically polarized Atomic Force Microscope (AFM) tip [1]. Nevertheless, to scale up the fabrication of such anti-counterfeiting solutions, the sequential nature of the AFM charge writing is inappropriate since it cannot meet the needs of industrial production in terms of speed. The aim of this work was thus to adapt and optimize the charge writing step of the nanoxerography protocol to fulfill these industrial requirements.

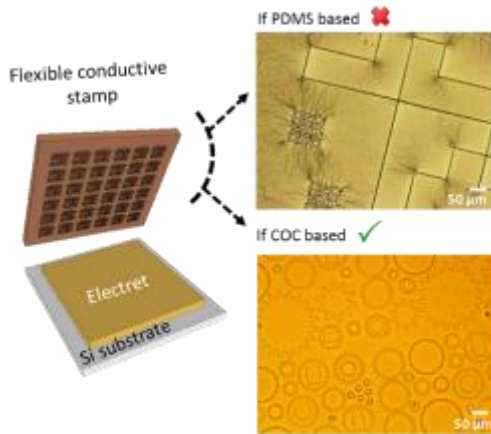
To tackle this technological bottleneck, we investigated the electrical micro-contact printing method (e- $\mu$ CP) originally developed by Jacobs and Whitesides [2]. In e- $\mu$ CP, the parallel injection of charge patterns is ensured by a conductive flexible stamp featuring bas relief micropatterns of desired geometries which then acts as the top electrode facing the electret thin film. Derived from the standard soft lithography micro-contact printing process, e- $\mu$ CP is consistent with fast and low-cost fabrication of colloidal-based structures since it exhibits large-area surface-patterning capabilities and experimental simplicity allowing parallel charge injection in one step over one centimeter square [2,3,4]. Nevertheless, the initial architecture of the flexible electrode- an Au coated-silicone PolyDiMethylSiloxane (PDMS) stamp- suffers from intrinsic drawbacks: a costly and complex metallization step, the formation of

wrinkles and/or cracks on the gold surface, the sagging/collapse of the structures and a low stamp durability. In order to overcome these limitations and step forward to mass production, we fabricated Au coated-thermoplastic stamps with higher Young's modulus and surface energy than PDMS to improve the mechanical resistance of the stamp and make the metallization cheaper and easier while reducing mechanical stress in the gold film. Consequently, we microstructured COC (Cyclic Olefin Copolymer) films by capillary force lithography [5] over substrates as large as a 4 inch diameter in few minutes and performed gold thin film deposition using cheap thermal evaporation. We demonstrated the capability of these thermoplastic-based stamps to inject electrical charges over 4 inch diameter surfaces with better geometric versatility and mechanical resistance than PDMS-based stamps. Finally, we were able to realize homogenous charge injections for hundreds of e- $\mu$ CP processes, paving the way of fast and low-cost fabrication of hundreds of thousands micro-sized anti-counterfeiting tags made of assembly of photoluminescent CdSe@CdS quantum dots.

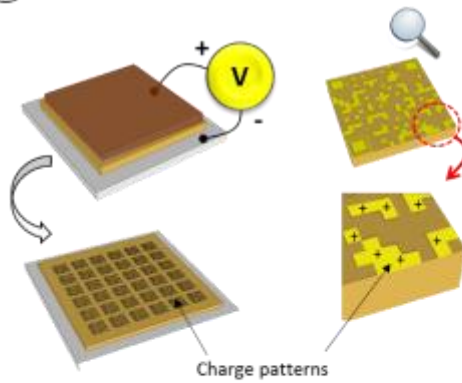
## Keywords:

Nanoxerography, electrical micro-contact printing, directed assembly, nano-objects, colloidal-based applications

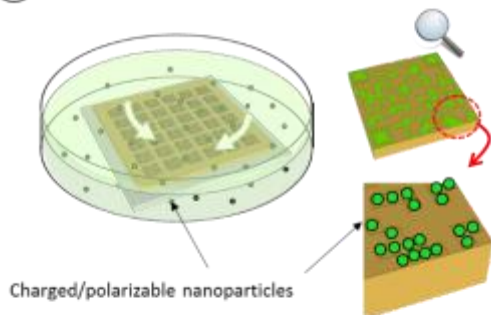
### 1 Fabrication of conductive flexible stamp



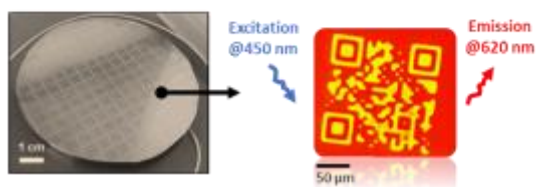
### 2 Parallel charge writing



### 3 Nanoparticle electrostatic trapping



### Photoluminescent CdSe/CdS Qdot based anticounterfeiting QR code



### References:

1. Sangeetha, N.M. *et al.* (2013) 3D assembly of upconverting NaYF<sub>4</sub> nanocrystals by AFM nanoxerography: creation of anti-counterfeiting microtags. *Nanoscale* 5, 9587
2. Jacobs, H.O. and Whitesides, G.M. (2001) Submicrometer patterning of charge in thin-film electrets. *Science* 291, 1763–1766
3. Wolfe, D.B. *et al.* (2004) Fabrication of planar optical waveguides by electrical microcontact printing. *Appl. Phys. Lett.* 84, 1623
4. Krinke, T.J. *et al.* (2002) , Nanostructured deposition of nanoparticles from the gas phase. *Particle & Particle Systems Characterization*. 19, 321-326
5. Suh, K.Y. and Lee, H.H. (2002) Capillary force lithography: large-area patterning, self-organization, and anisotropic dewetting. *Adv. Funct. Mater.* 12, 405–413

**Figure 1.** Fabrication of photoluminescent anti-counterfeiting markers through the optimization of the e-μCP nanoxerography process

# Eco-friendly Antibacterial films using Al doped ZnO based Thin Films by RF Sputtering

Hyung-Jin Choi<sup>1</sup>, Soon-Gil Yoon<sup>1</sup>

<sup>1</sup> Department of Materials Science and Engineering, Chungnam National University, 220 Gungdong, Yuseong-gu, Daejeon 34134, Korea

## Abstract:

Modern society has damaged by various types of bacteria and viruses occur, such as *Staphylococcus aureus*, *Salmonella*, and *E. coli*, are living while touching in our life. To prevent these hazards, a varieties of antibiotics and drugs have been developed for eliminated the disease caused by microbial infection. Silver nanoparticles (NPs) and ions are known to have a strong inhibitory effect on these microorganisms. As a result, have been produced various antibacterial products, it is widely are commercialized antimicrobial films using silver NPs and ions. Recently, the environmental problems have been raised by the Silver ions released in the water from antibacterial products. Therefore, instead of Ag NPs, most studies have focused mainly on ZnO NPs to accomplish an antibacterial effect. But, Zinc ions also above a limited amount that were released into the water from the ZnO films could be very harmful to humans. Some report addressed the strong drawbacks of Zn ion release when the ZnO films came into contact with water.

ZnO and Al doped ZnO (AZO) 30 nm-thick films deposited at room temperature onto a glass substrate by RF sputtering. The 30 nm-thick ZnO and AZO films showed a high transmittance (~ 91.3%) comparable to that of a glass substrate at a wavelength of 550 nm. The ZnO based films showed strong antibacterial activity more than 99.99% against *E. coli* and *S. aureus* bacteria by film attachment method (JIS Z 2801). However, in these cases of ZnO and low Al doped ZnO (Al 3 ~ 10 at%), it has a problem that Zn or Al is dissolved in the water and acid. Therefore, increasing the transparency and stability of ZnO thin film through a change of the Al doping amount to 0 ~ 90 at%, made an antibacterial films has not been dissolved in the water and acid. Also, this study discusses the characterization of Al doped ZnO based thin films and the mechanism of their antibacterial activity.

**Keywords:** Sputtering, Antibacterial Activity, Al doped ZnO, Zn release

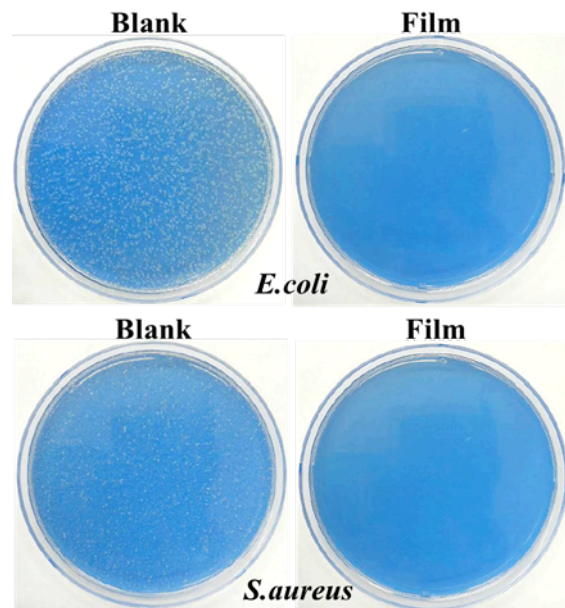


**Figure 1:** Actual images of the incubated bacteria onto AZO film and without films (Blank)

# Fabrication and Characterization of Graphene Reinforced Tungsten Carbide – Cobalt Composite

Gorti Vasu Kiran, Golla Sairam, B. Bhavani Shankar, Kantubhukta Jyothi, Kokkiligadda Jhansi, Ramesh S. Rao<sup>\*</sup>, and A.O. Surendranathan

Department of Metallurgical & Materials Engineering, National Institute of Technology Karnataka, Surathkal, P.O.Srinivasnagar-575025, India

<sup>\*</sup> R&D in Materials Sciences, Kennametal India Limited, Bangalore, India

## **Abstract:**

The attractive properties of tungsten carbide (WC) are high melting point, high hardness, high thermal and electrical conductivities, and relatively high chemical stability. However, it is a very brittle material. This in turn reduces the tool lives in industries due to the failures after a certain amount of time. The dispersion of brittle tungsten carbide particles into the ductile cobalt metal continuous phase has provided enhancing mechanical properties of hardness and toughness. However, the characteristic of the ductile cobalt binder that generate optimum toughness is yet to be adequately established. In this paper, the preparation of WC powder with 6% cobalt (Co) and graphene (0.2%) by high energy rate ball milling and ultrasonification is described. This powder mixture was sintered using spark plasma sintering at 1250°C for 10 minutes. The addition of graphene nanoplatelets (GNPs) improves the densification and fracture toughness of WC upto about 100% through mechanisms such as GNP bending, pull-out, grain wrapping, crack bridging, and crack deflection. The effects of graphene reinforcement and spark plasma sintering were studied by analyzing the physical (density), magnetic (coercivity, and magnetic saturation) microstructural (porosity) and mechanical properties (hardness, fracture toughness) of the composite.

**Keywords:** Fabrication, Characterization, Graphene, Tungsten Carbide, Cobalt, Composit

# **Session III: Nanocharacterisation / Nanometrology**

# Modelling the particle size dependent surface charging of nanoparticles

Z. Abbas

University of Gotheburg, Department of Chemistry and Molecular Biology, Gothenburg, Sweden

## **Abstract:**

Synthesis of nanoparticles of different sizes, determination of their surface/interfacial properties and modelling are challenging tasks. In the field of modelling inclusion of curvature at the particle solution interface and effects of enhanced screening due to the curvature of double layer are necessary to include in theory. A simple theory based on classical density functional approach so called Corrected Debye Hückel (CDH) theory will be presented. The feasibility of the CDH theory in accurately describing the surface charging behaviour of SiO<sub>2</sub>, TiO<sub>2</sub> and iron oxide nanoparticles of diameters ranging from 1 to 100 nm will be presented. The theoretical predictions of the CDH theory are that the particles of diameter less than 15 nm start to behave like molecules which leads to enhanced screening and increased surface charge density. The theoretical predictions are in very good agreement with the Monte Carlo simulations as well as with the experimental data.

**Keywords:** silica, nanoparticles, Corrected Debye-Hückel theory, surface charge

# Elastomeric nanofluidic devices for characterizing nanomaterials

Elena Angeli, Patrizia Guida, Denise Pezzuoli, Luca Repetto, Roberto Lo Savio, Giuseppe Firpo and Ugo Valbusa

Dipartimento di Fisica, Università degli studi di Genova, Genova, Italy

## Abstract:

The use of nanomaterials for the production of consumer goods such as food, cosmetics, medicines, hygiene products and clothing raises interesting questions about the effects of the interaction between nanomaterials with human body and environment. Thus, for these studies it is extremely important to have reliable and repeatable tools for measuring and characterizing nanometric objects that offer better performances than traditional analysis methods. Among classical techniques, electronic and atomic force microscopy are time consuming and need laborious sample preparation, particle tracking or dynamic light scattering require assumptions about shape and size distribution of the objects to be measured while methods inspired by Coulter counter systems cannot provide high resolution because of the short detection time.

Here, we report a novel technique [1] based on simultaneous optical and electrical detection of nanoparticles passing through a nanochannel patterned on a nanofluidic lab-on-chip device. We perform electrical measurements of nanoparticles passing, one at a time, through a 250 nm deep nanochannel and measure their optical traces while entering and exiting it. The combination of such two independent methods improves the reliability of size measurements and, at the same time, offers the possibility of investigating other properties such as the particle shape, surface charge, specific interactions with the walls of the device.

**Keywords:** nanofluidics, nanochannels, nanoparticles, electro-optical measurements, lab-on-chip, elastomeric material, PDMS

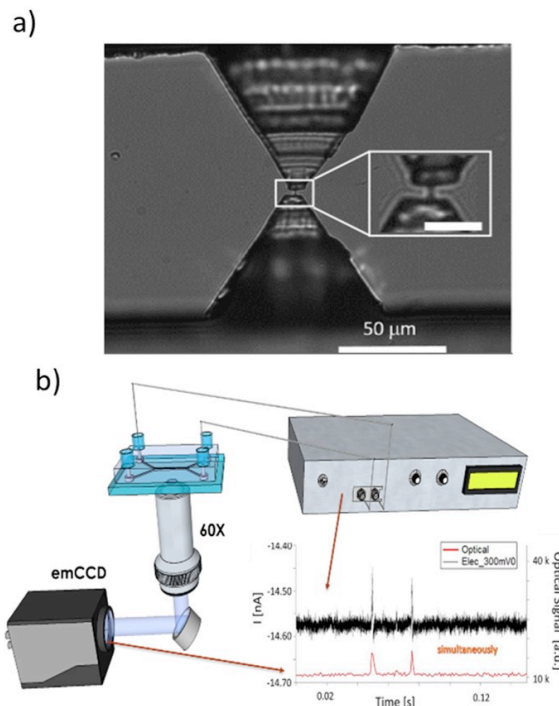


**Figure 1:** a) PDMS device with a single nanochannel connecting two microchannels, b) scheme of the experimental set-up for electro-optical measurements.

## References:

1. Angeli E., Volpe A., Fanzio P., Repetto L., Firpo G., Guida P., Lo Savio R., Wanunu M., Valbusa U. (2015) Simultaneous Electro-Optical Tracking for Nanoparticle Recognition and Counting, *Nano Letters* 15, 5696–5701

# Bristol NanoESCA Facility: a new platform for surface analysis

M. Cattelan,<sup>1</sup> N. A. Fox,<sup>1</sup>

<sup>1</sup>University of Bristol, School of Chemistry, Bristol, UK

## Abstract:

The Bristol NanoESCA Facility is the newest and one of the most advanced surface analysis instruments in UK. The facility is located at the Centre for NanoScience and Quantum Information at the University of Bristol in the quietest ultra-low noise laboratory in Europe.

The three main characterization techniques of the facility are: NanoESCA II Photoemission Electron Microscope (PEEM), high-resolution X-ray Photoelectron Spectroscopy (XPS) and Spot Profile Analysis Low Energy Electron Diffraction (SPA-LEED).

The NanoESCA II offers PEEM with a lateral resolution of 25 nm, image field of view can vary from 1100  $\mu\text{m}$  to 5  $\mu\text{m}$ . It is possible to analyze the band structure of the materials by means of Micron-scale Angle-Resolved Photoemission Spectroscopy ( $\mu$ -ARPES) in regions as small as 3  $\mu\text{m}$  with an energy resolution of 23 meV at 28 K.

The XPS ARGUS analyzer can operate in snapshot mode for real time analysis and mapping mode with resolution of 60  $\mu\text{m}$ . The overall energy resolution of the XPS is less than 300 meV. The SPA-LEED is used to determine strains and defects of single crystal materials by means of a quantitative 1D and 2D k-space analysis.

This facility has an extraordinary surface sensitivity therefore samples are usually prepared *in-situ* by annealing or sputtering with inert gases. It is also possible to transfer samples under ultra-high vacuum (UHV) conditions from and to other facilities, e.g. synchrotron beamlines, using a UHV suitcase.

The facility's aim is to help research groups and industries to investigate advanced materials using cutting edge instrumentation and a range of specialized light sources.

Examples of the latest studies are:

- analyses of commercial graphene and epitaxial graphene to observe the number of layers, quantify impurities and study the band structure by  $\mu$ -ARPES<sup>1</sup>;
- studies on new photovoltaic materials, such as CZTS, with work function maps and  $\mu$ -valence band spectroscopy,

- depth profiling XPS and valence band spectroscopy of uranium oxide/nitride interfaces. Moreover, we characterize by XPS a variety of materials such as: catalysts<sup>2</sup>, biosensors, stainless steel samples, reactor ashes, semiconductor films etc.

The Bristol NanoESCA facility is a unique tool to study materials at the nanoscale, its surface sensitivity makes it suitable to study innovative atomically thick 2D materials.

**Keywords:** X-ray Photoelectron Spectroscopy, Low Energy Electron Diffraction, Photoemission Electron Microscopy, work function maps,  $\mu$ - Angle-Resolved Photoemission Spectroscopy.

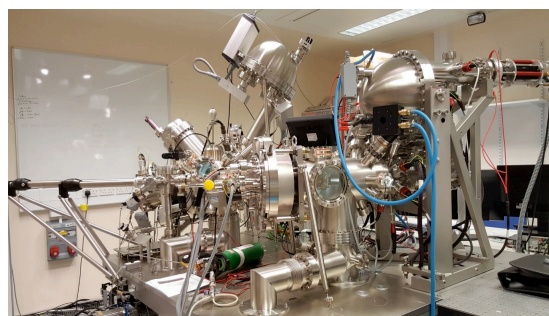


**Figure 1:** Picture of the Bristol NanoESCA Facility located in the ultra-low noise lab of the University of Bristol.

## References:

1. Ridene, M., Najafi, A., Iezhokin, I., Cattelan, M., Fox, N. A., Flipse, C. F. J. (2017) Origin of room temperature ferromagnetism in hydrogenated epitaxial graphene on silicon carbide. *In preparation*
2. Celorrio, V., Morris, L. J., Cattelan, M., Fox, N. A. (2017) Tellurium-doped lanthanum manganite as catalysts for the oxygen reduction reaction, *MRS Commun.*, DOI: 10.1557/mrc.2017.22.

# Mathematical modeling of nanoparticle growth and melting

Tim Myers,<sup>1,2</sup> Claudia Fanelli<sup>1,2</sup>, Helena Ribera<sup>1,2</sup>

<sup>1</sup> Centre de Recerca Matemàtica, Barcelona, Spain

<sup>2</sup> Universitat Politècnica de Catalunya, Barcelona, Spain

## Abstract:

The basis of nanotechnology is the nanoparticle. Due to the high ratio of surface to volume atoms, nanoparticles behave differently to their bulk counterparts: examples include enhanced mechanical strength; enhanced solar radiation absorption and superparamagnetism. These properties are size dependent and so in order to safely use the particles the ability to manufacture a specific size and also an understanding of their size dependent behaviour is critical.

In this talk we will describe two mathematically related issues regarding nanoparticle production and phase change:

### 1. Synthesis of monodisperse nanocrystal.

Due to its ease of use and flexibility, precipitation of nanoparticles from solution is one of the most widely used synthesis methods. The main disadvantage of this method is that the relationship between particle growth and system conditions is not fully understood. In practice, the optimal reaction conditions are usually ascertained empirically or intuitively. In this part of the talk we consider the impact of size focussing and defocussing (or Ostwald ripening) on the evolution of the nanoparticle size distribution and also strategies for optimal growth.

### 2. Nanoparticle melting

The mathematics of phase change is a well established field. However, as we move towards the nanoscale standard theories break down due to the size dependence of previously constant quantities. Here we describe a new model for nanoparticle melting that accounts for decreases in melt temperature, latent heat and surface energy. We also discuss the effect of non-Fourier heat transfer on the system.

In both cases the mathematical models involve diffusion (of heat or monomer in solution). The solution of the mathematical model allows us to propose improved methods for system control.

**Keywords:** Nanoparticle synthesis from solution, Size focusing, Optimal growth, Nanoparticle melting, Phase change, Diffusion.

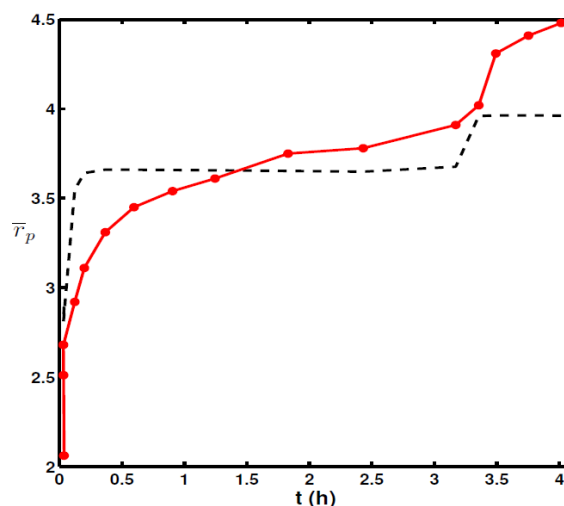


**Figure 1:** Evolution of the average radius in nm of a group of CdSe nanoparticles (dotted line) and corresponding experimental data (red line). Extra monomer is injected just after 3hrs.

## References:

1. Ribera H., Myers T.G. (2016) A mathematical model for nanoparticle melting with size-dependent latent heat and melt temperature. *Microfluid. Nanofluid.* DOI 10.1007/s10404-016-1810-6
2. Cregan V.C. et al (2017) Synthesis of monodispersed nanoparticles. *Proceedings of the 115<sup>th</sup> European Study Group with Industry.* In Press.

# Oblique Angle Deposition: A Ballistic Model and its Limits

Ch. Grüner<sup>1,\*</sup>, S. Liedtke<sup>1</sup>, J. Bauer<sup>1</sup>, S. Mayr<sup>1,2</sup>, B. Rauschenbach<sup>1,2</sup>

<sup>1</sup> Leibniz Institute of Surface Modification, Permoserstr. 15, 04318 Leipzig, Germany

<sup>2</sup> University Leipzig, Institute of Experimental Physics II, Linnéstr. 5, 04103 Leipzig, Germany

## Abstract:

Physical vapor deposition methods are commonly used to prepare high-quality thin films. If the vapor incidence angle is large ( $\theta > 70^\circ$ , with respect to the surface normal), nanocolumns are formed. This technique is referred to as oblique angle deposition (OAD). Hereby the self-shadowing effect is maximized, leading to a highly porous thin film consisting of separated thin nanostructures (Fig. 1). The characteristics of these nanostructures, like their tilt angle and survival rate as well as the porosity of the film, are linked to the angle of incidence and some material dependent parameters.

Understanding the relationship between the growth conditions and the physical properties of the resultant film is crucial for bringing the resultant OAD films to application. A few common models exist to describe the correlation between the angle of incidence and the nanostructure tilt angle. These are the empirical tangent and cosine rules, as well as the recently often discussed fan model [1,2]. However, these rules do not describe the observed relation sufficiently, as shown in Figure 2.

In this contribution, a model describing the growth of OAD nanostructures for the full angle of incidence range ( $0^\circ - 90^\circ$ ) is proposed. The model is linked to the fan model, taking the shape of a non-shadowed growth front into account. Predictions of this model for tilt angles and porosities are shown and compared to an off-lattice computer simulation as well as to deposited films of different materials (e.g. Si, Ge, Mo). It is discussed how surface diffusion influences the growth of the nanostructures and how far this can be covered by the proposed model. A look onto the limits of these kind of models in specific growth regimes is taken.

**Keywords:** oblique angle deposition, ballistic deposition, shadowing, overhangs, off-lattice simulations, nanostructure, self-organization, self-assembly, porosity

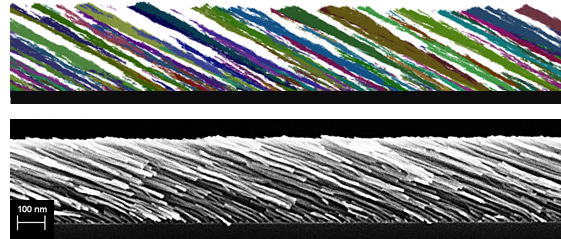


**Figure 1:** Simulated (top) and Ge (bottom) nanostructures. The obliquely deposited thin films are highly porous and consist of separated nanostructures, tilted toward the incoming particle beam.

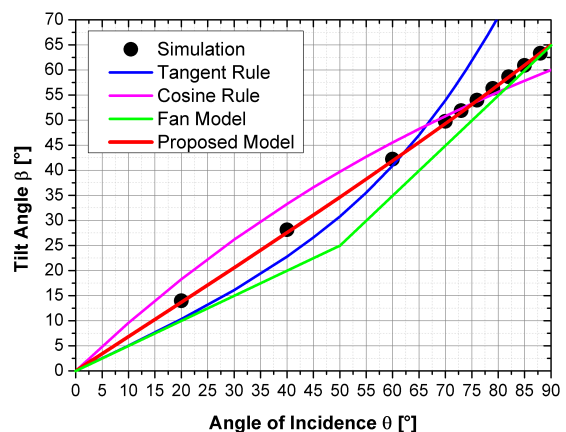


**Figure 2:** Different commonly used models for the relation between the angle of incidence and the tilt angle are shown and compared to values observed in a computer simulation. The prediction of the here proposed model is also inserted.

## References:

1. Ramanlal, P., Sander, L. M. (1985), Theory of Ballistic Aggregation, *Phys. Rev. Lett.*, 54 (16), 1828
2. Tanto, B., Ten Eyck, G., Lu, T.-M. (2010), A model for column angle evolution during oblique angle deposition, *Journal of Applied Physics*, 108, 026107

# The effect of the surfactant in the stability of NiO-nanofluids

Antonio Sánchez-Coronilla,<sup>1,\*</sup> Elisa I. Martín,<sup>2</sup> Javier Navas,<sup>3</sup> Teresa Aguilar,<sup>3</sup> Roberto Gómez-Villarejo,<sup>3</sup> Juan Jesús Gallardo,<sup>3</sup> Rodrigo Alcántara,<sup>3</sup> Desiré De los Santos,<sup>3</sup> Iván Carrillo-Berdugo,<sup>3</sup> Concha Fernández-Lorenzo<sup>3</sup>

<sup>1</sup>Seville University, Department of Physical Chemistry, Seville, Spain

<sup>2</sup>Seville University, Department of Chemical Engineering, Seville, Spain

<sup>3</sup>Cádiz University, Department of Physical Chemistry, Cádiz, Spain

## Abstract:

Concentrating Solar Power (CSP) is one of the most interesting options as renewable energy today. One option in order to improve the efficiency of these plants is to enhance the thermal properties of the heat transfer fluid (HTF) by using nanofluids. In this sense, this study presents an analysis of the stability of NiO nanoparticles on a base fluid composed of the eutectic mixture of diphenyl oxide and biphenyl with Benzalkonium Chloride (BAC) and 1-Octadecanethiol (ODT) as surfactants. The stability of the nanofluid was analysed using different techniques: UV-vis spectroscopy, particle size measurements using the dynamic light scattering technique and  $\zeta$  potential measurements. It is worth noting that the stability of the nanofluids improved with the use of BAC. To understand the role played by the surfactants in the stability of the nanofluid, DFT calculations were performed. The interaction of the surfactants with both the base fluid and the NiO (100) surface was performed. The interaction of the surfactants with the base fluid showed that hydrogen bond interactions favour the stability of the base fluid-surfactant mixture, what was attested by the QTAIM. The results of the interaction of the surfactants with the NiO (100) surface suggest that the favoured interaction site is on the Ni (Figure 1). Moreover, in concordance with experimental results, the theoretical results show that the nanofluid system with the BAC surfactant is the favoured one.

**Keywords:** nanofluids, Concentrating Solar Power, DFT, heat transfer fluid, surfactant, QTAIM, BAC, ODT, specific heat, thermal conductivity, nanoparticles.

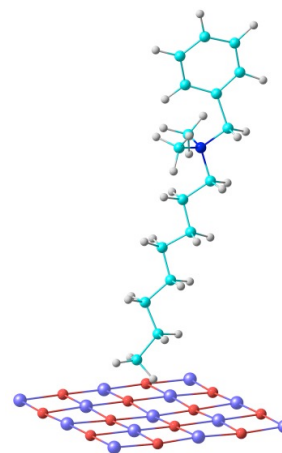


**Figure 1:** Interaction of BAC on the Ni site of NiO (100) surface.

## References:

1. Singh, D., Timofeeva, E. V., Moravek, M., Cingarapu, S. R., Yu, W. H., Fischer, T., Mathur, S. (2014) Use of the metallic nanoparticles to improve the thermophysical properties of the organic heat transfer fluids used in concentrated solar power, *Sol. Energy*, 105, 468-478.
2. Montoneri, F., Montoneri, E., Boffa, V., Sharts, O. (2011), Protein helical structure enhancement in fluorinated-phosphonate nanoporous silica glasses characterized by circular dichroism spectroscopy, *Int. J. Nanotech.*, 8, 471-491. Kasaeian, A., Eshghi, A. T., Sameti, M. (2015) A review on the applications of nanofluids in solar energy systems. *Renew Sust Energ Rev.*, 43, 584-598

# Taylor Dispersion Analysis: Extending the boundaries of nanoparticle characterization

D. A. Urban,<sup>1</sup> A. M. Milosevic,<sup>1</sup> D. Bossert,<sup>1</sup> F. Crippa,<sup>1</sup> C. Geers,<sup>1</sup> S. Balog,<sup>1</sup> B. Rothen-Rutishauser,<sup>1</sup> A. Petri-Fink<sup>1</sup>

<sup>1</sup>Adolphe Merkle Institute, University of Fribourg, Fribourg, Switzerland

## Abstract:

The characterization of nanoparticles has always proven to be a challenge, due to the manifold of core materials, shapes, sizes, and consequent issues these have on analytical techniques. Due to the rising interest to use nanoparticles in, for example medical applications (e.g. drug delivery systems, sensors), it is imperative to find instrumentations to cope with accurately characterizing nanoparticles in such complex environments, such as blood or cell culture media. In this project we show the capabilities of Taylor Dispersion Analysis to accurately measure hydrodynamic sizes of various types of nanoparticles, and the advantages this method has over conventional sizing techniques.<sup>1</sup>

Taylor Dispersion Analysis (TDA) was introduced in the 1950s, but only in recent years has it been discovered to have potential to characterize nanoparticle size in solution. In short, Taylor Dispersion Analysis is an analytical method to determine the diffusion coefficient of small molecules, proteins, or nanoparticles under flow conditions (Figure 1).<sup>2</sup>

In this project we expand upon the potential of TDA by measuring various particle materials, including proteins, silica, gold and iron oxide nanoparticles. Furthermore we show the advantages that this technique has over alternative measurement techniques, such as dynamic light scattering and electron microscopy. Among the advantages are the minimal use of sample volume, detection possibilities (absorbance, scattering), wide range of particle sizes that can be measured, and solvents that particles can be measured in. We further demonstrate the future potentials that this system has to offer for more complex nanoparticle characterization. We could show, for the multitude of samples that were measured, that we could reliably acquire sizes for all materials. Furthermore we could show that particles as small as 4 nm in diameter could be measured via TDA. We extend the study by showing that even very polydisperse samples from industrial applications could be

characterized to an extent, and that measuring nanoparticles in complex environments, such as complete cell culture media, is possible. In conclusion we could show that TDA could be a valuable standard tool for nanoparticle characterization in the future.

**Keywords:** Taylor Dispersion Analysis, nanoparticle characterization, hydrodynamic size, dynamic light scattering, electron microscopy, proteins.

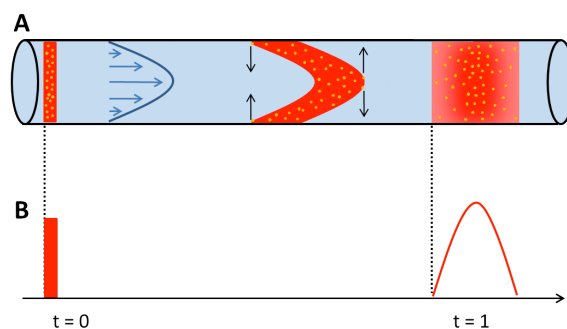


**Figure 1:** A) Schematic illustrating the principle of Taylor Dispersion Analysis. A nanoparticle sample introduced with a pressure driven flow into a narrow bore fused silica capillary, will be affected by convection (blue arrows) and subsequently increased radial diffusion (black arrows), causing a band broadening effect. The band broadening gives insight into the particles diffusion coefficient. B) Idealized signal obtained during a TDA measurement.

## References:

1. Lopez-Serrano (2014) Nanoparticles a global vision. Characterization, separation, and quantification methods. Potential environmental and health impact. *Anal. Methods*, 6, 38-56.
2. Alizadeh, A. (1980) The Theory of the Taylor Dispersion Technique for Liquid Diffusivity Measurements. *International Journal of Thermophysics*, 1, 3, 243-284.

# Evaluation of particle sizing by analytical centrifugation using real-world materials for the implementation of the EC definition of the term “nanomaterial”

C. Ullmann,<sup>1,\*</sup> D. Mehn,<sup>2</sup> D. Gilliland,<sup>2</sup> W. Wohlleben,<sup>3</sup> R. Koeber,<sup>4</sup> F. Babick<sup>1</sup>

<sup>1</sup> Dresden University of Technology, Dresden, Germany

<sup>2</sup> Joint Research Centre, Directorate F–Health, Consumers and Reference Materials F2, Ispra, Italy

<sup>3</sup> BASF SE, Ludwigshafen, Germany

<sup>4</sup> Joint Research Centre, Directorate F–Health, Consumers and Reference Materials F6, Geel, Belgium

## Abstract:

Analytical centrifugation (AC) is a powerful technique for the determination of particle size distributions. This study evaluates the performance for the grouping of particulate substances according to the European Commission’s recommendation on the definition of a nanomaterial, which is based on the number-weighted median size. The repeatability of the measurement and the method precision including sample preparation, measurement and conversion into number-weighted particle size distributions were compared.

Four instrument of analytical centrifugation technologies with turbidity detectors are tested [1]: Cuvette centrifuges LUMiSizer 610 (radiation at 470nm), LUMiSizer 651 (865nm), disc centrifuge DC24000UHR (405nm) and analytical ultracentrifuge XL-I ProteomeLab Version (670nm). Performance tests were carried out for a multimodal polystyrene mix and non-spherical real-world materials. The intermediate precision was determined according to ISO 5725 with two grades of barium sulfate (nano and non-nano). Measurements were performed in daily triplicates for five days and evaluated using analysis of variance (ANOVA). The radiation wavelengths of 470nm and 865nm have only a minor impact on the number-weighted median sizes, but clearly affects the intermediate precision that differs from 9.4% to 12.6% relative standard deviation (figure 1). The impact of sample preparation is obvious. The disc centrifuge shows a precision (10.3 – 10.9%) and advantages in detecting nanoparticles but troubles with broadly distributed particle size distributions. The AUC shows a good precision (4.6 - 7.2%) but the lowest number-weighted median.

Analytical centrifugation can be recommended for the classification of materials according to the ECs recommendation for the definition of a nanomaterial. This poster presents results of the European project NanoDefine, which has received funding from the EC's Seventh Frame-

work Programme under Grant Agreement n° 604347.

**Keywords:** analytical centrifugation, evaluation, intermediate precision, nanomaterial detection, particle size

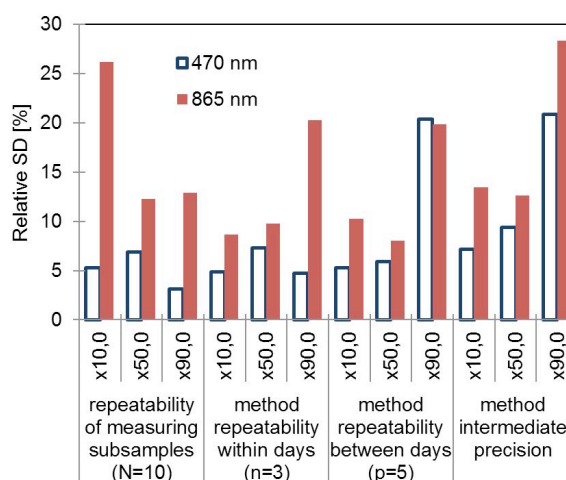


**Figure 1:** Figure illustrating the measurement precision with the method’s intermediate precision and the respective contributions from within-day and between-day effects for BaSO<sub>4</sub> particles ( $x_{50,0} \approx 42\text{nm}$ ) of the cuvette centrifuge.

## References:

1. ISO 13318-2:2007, Determination of particle size distribution by centrifugal liquid sedimentation methods – Part 2: Photocentrifuge method, Geneva, 2007
2. Babick, F.; Mielke, J.; Wohlleben, W.; Weigel, S.; Hodoroaba, V.-D.: How reliable can a material classified as a nanomaterial? Available particle sizing techniques at work. J Nanopart Res (2016)

# Monitoring the sintering of nanoparticles with Raman scattering

L. Saviot<sup>1\*</sup> S. Le Gallet<sup>1</sup> F. Demoisson<sup>1</sup> L. David<sup>2</sup> G. Sudre<sup>2</sup> A. Girard<sup>3</sup> J. Margueritat<sup>3</sup> A. Mermet<sup>3</sup>

<sup>1</sup>Laboratoire Interdisciplinaire Carnot de Bourgogne, UMR 6303 CNRS-Université de Bourgogne Franche-Comté, 9 av. A. Savary, BP 47870, F-21078 Dijon Cedex, France

<sup>2</sup>Ingénierie des Matériaux Polymères, Univ Lyon, Université Claude Bernard Lyon 1, CNRS UMR 5223, 15 bd A. Latarjet, F-69622, Villeurbanne, France

<sup>3</sup>Institut Lumière Matière, Univ Lyon, Université Claude Bernard Lyon 1, CNRS UMR 5306, F-69622 Villeurbanne, France

## Abstract:

Sintering nanoparticles (NPs) enables to make macroscopic samples while retaining the original properties resulting from the small size of the starting NPs. Ideally ceramics with nanograins and enhanced tenacity are obtained. However, sintering may also alter the NPs and/or the medium surrounding each of them which in turn alters their original functional properties. In this work, we consider 5-nm anatase TiO<sub>2</sub> and monoclinic ZrO<sub>2</sub> NPs and focus on the early stages of their sintering so that the size of the NPs is hardly changed. Inelastic light scattering measurements are used in addition to other experimental techniques (XRD, SAXS, BET, ... ) to follow the changes of the average size and surface area. In addition, the low-frequency Raman spectra enable to monitor the acoustic vibrations in the NPs. These confined vibrations are the original property of the NPs which we tried to preserve. Two challenges had to be overcome in this work: 1/ the synthesis of gram-quantity of monodisperse NPs was achieved using a continuous supercritical water setup and 2/ a fast sintering process (SPS) to avoid the growth of the NPs. We report a significant decrease of the scattered light intensity at low-frequency as the sintering temperature increases (Figure 1) and as the applied force increases. This is primarily due to the decrease of the quasielastic scattering intensity. This decrease quantitatively matches the decrease of the surface area as measured by the BET method. The relative intensity of the acoustic phonon peaks was also shown to decrease without any substantial change in the peak shapes. This has been assigned to the appearance of coupled inter-NP vibrations due to the formation of necks between neighbor NPs. At larger temperatures, the average size of the NPs increases. These results demonstrate that low-frequency inelastic light scattering is a suitable tool to study the onset of the formation of necks in the first stages of sintering of small NPs.

**Keywords:** nanoparticle, sintering, low-frequency inelastic light scattering.

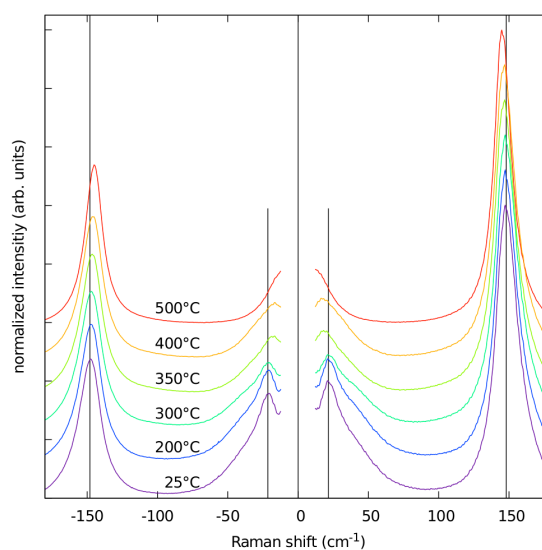


**Figure 1:** Low-frequency Raman spectra of an anatase TiO<sub>2</sub> nanopowder sintered at different temperatures in a SPS setup.

## References:

1. Saviot, L., Machon, D., Debbichi, L., Girard, A., Margueritat, J., Krüger, P., Marco de Lucas, M. C., Mermet, A. (2014), Optical and acoustic vibrations confined in anatase TiO<sub>2</sub> nanoparticles under high-pressure, *J. Phys. Chem. C.*, 118, 10495-10501.
2. Saviot, L., Murray, D. B., Caputo, G., Marco de Lucas, M. C., Pinna, N. (2013), THz nanocrystal acoustic vibrations from ZrO<sub>2</sub> 3D supercrystals, *J. Mat. Chem. C.*, 1, 8108-8116.

# HRTEM and STEM-EELS study of thin films Pt-CeO<sub>x</sub> nanocatalysts for on-chip fuel cell technology

Valérie Potin

Laboratoire Interdisciplinaire Carnot de Bourgogne, UMR 6303 CNRS - Université de Bourgogne  
Franche-Comté, Dijon, France

## Abstract:

Platinum (Pt) is a versatile element in catalysis that efficiently mediates a multitude of chemical reactions. Due to its high price exceeding that of gold, reducing amount of Pt is the major driving force in catalysis research. There are two strategies to tackle this challenge: to replace noble metal by others, less expensive materials; and to use platinum as efficiently as possible. In this study, we handle both of them by growing extremely porous Pt-CeO<sub>2</sub> structures.

In this study, nanometric Pt-ceria thin films were characterized by XPS and mainly by TEM after elaboration by physical and/or chemical vapor deposition. The deposited layers exhibited different morphologies linked to the different growth conditions. By the optimization and the suitable combination of materials we can tune the morphology of the catalysts. In addition to the substrate type, many effects as the formation of carbides or silicates at the interface, an interaction of ceria with platinum and the presence of the porosity influenced also the structure and the chemistry of the deposited layers [1,2].

In all samples, HRTEM study indicates that crystallites corresponding mainly to CeO<sub>2</sub> and to a less extent to CeC<sub>2</sub> crystallographic structures were observed. STEM-EELS measurements have been carried out on these nanometric layers. Data analysis of the M<sub>4,5</sub> white lines of cerium have pointed out a variation of cerium oxidation state from Ce<sup>4+</sup> to a mixture of Ce<sup>3+</sup> and Ce<sup>4+</sup> depending of the localization of the measurement. Experiments have also been performed after deposition on a TEM membrane grid to observe directly the pristine layer.

**Keywords:** cerium oxide, nanometric thin films, fuel cells, transmission electron microscopy, electron energy loss spectroscopy

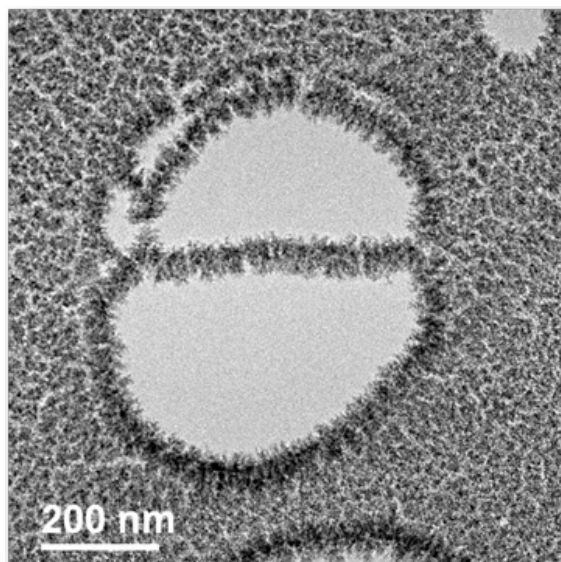


**Figure 1:** Platinum doped cerium oxide deposited on TEM membrane grid.

**Figure 2:** STEM-EELS linescan indicating that pristine layer is mainly Ce<sup>4+</sup>.

## References:

- [1] J. Lavkova et al, *Nanoscale* 7, 4038 (2015)
- [2] P. Simon et al, *Advanced Materials Interfaces* 4, 1600821 (2017)

# Self-organized nano-structures usable for the calibration and the traceability of AFM and TEM

D. Pachinger<sup>1,2</sup>

<sup>1</sup> E+E Elektronik Ges.m.b.H., Designated Laboratory (BEV/E+E), Engerwitzdorf, Austria

<sup>2</sup> Johannes Kepler University, Institute for Semiconductor and Solid State Physics, Linz, Austria

## Abstract:

The SiGe material system is widely used in the semiconductor industry and it is thus a very well explored material system even though reaching the quantum limit opens up further research potential. However the majority of the morphological characteristics at the micro- and nanometer scale are known and therefore these structures are useable as calibration standards for the nanometrological characterization methods like AFM and TEM. During the epitaxial fabrication process of SiGe based nano-structures it is possible to establish three different growth modes by changing the thermodynamical conditions. These modes comprise a 2D layer-by-layer growth mode (Frank-van der Merwe), 3D island growth mode (Volmer-Weber) and islands on wetting layer growth mode (Stranski-Krastanov). Thus, different structures, like islands with well defined size and facet angles or surface structures with steps of monolayer height can be realized. During the 3D growth mode the SiGe quantum dots show clearly defined facets. They switch from pyramids with only  $\{1\ 1\ 3\}$  facets to domes having  $\{1\ 1\ 3\}$ ,  $\{1\ 0\ 5\}$  and  $\{15\ 3\ 23\}$  facets with the corresponding angles of  $25.2^\circ$ ,  $11.3^\circ$  and  $33.6^\circ$ , respectively [1] (Figure 1). The facet angles measured with AFM and TEM can be used to establish a metrological connection between the two characterization methods. Structures that are fabricated according to the 2D layer-by-layer growth mode can be analysed with standard AFM where surface steps with one or two monolayer height can be resolved and used for the height calibration. Together with high-resolution TEM images, the SiGe nano-structures are perfectly suited to calibrate AFM or TEM and to trace them back to the Si lattice constant. Finally, two applications of nano-metrological measurements are presented. First, under certain conditions during Stranski-Krastanov growth a dislocation network is realized which is clearly visible in AFM measurements. High-resolution TEM images however, can additionally be used to measure the degree of strain relaxation through the evaluation of

Moiré fringes. Second, it is shown how TEM is used to measure the size and composition of nano-crystals which can thus also be used for the calibration of the microscope. [2]

**Keywords:** AFM, TEM, quantum dots, self-organization, nano-structures, nano-crystals, calibration, traceability.

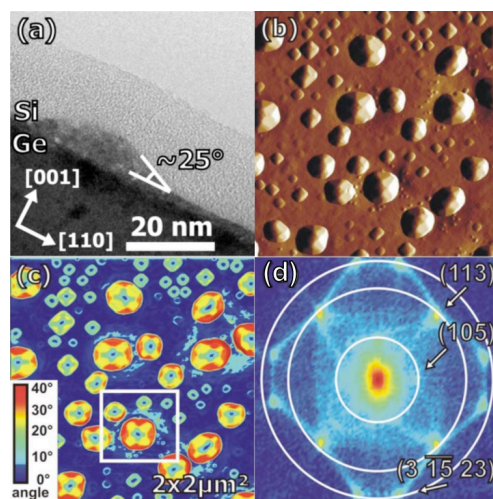


**Figure 1:** Figure illustrating the quantum dot characterization with AFM, the metrological connection to TEM and the traceability to the Si lattice constant.

## References:

1. Pachinger, D. et al., Stranski-Krastanov growth of tensile strained Si islands on Ge (001), APL 91 (23), 233106 (2007)
2. Kovalenko, M.V. et al., Colloidal HgTe nanocrystals with widely tunable narrow band gap energies: From telecommunications to molecular vibrations, JACS 128 (11), pp. 3516-3517 (2006)

# Probing electronic and magnetic structure of functionalized graphene compounds by Near Edge X-ray absorption Fine structure Spectroscopy and Confocal Raman Spectroscopy

Sharadha Sambasivan<sup>1</sup>, Nakeshma Cassel<sup>2</sup>, Darnel Allen<sup>2</sup>, Phil Smith<sup>2</sup>, Wayne Archibald<sup>2</sup>  
Daniel A. Fischer<sup>3</sup>

<sup>1</sup>Suffolk County Community College, Ammerman Campus, Selden NY, USA

<sup>2</sup>College of Science and Mathematics, University of the Virgin Islands, St Thomas, US Virgin Islands

<sup>3</sup>National Institute of Standards and Technology, Gaithersburg, MD, USA

## Abstract:

Graphene, a single sheet of graphite has attracted great attention due to its unmatched electrical transport, electronic, mechanical and thermal properties. This project investigated the electronic and morphological structural changes in transition metal doped graphene. Functionalization or doping induces electronic structure perturbations that substantially modify the properties of graphene to adapt its use for the optoelectronic industry. Primary spectroscopic technique that was utilized for this study was confocal Raman spectroscopy, Near Edge X-ray Absorption Fine Structure (NEXAFS) and atomic force microscopy (AFM). Additionally, previously measured Hall Effect carrier mobility and x-ray magnetic circular dichroism were compared with the recent results from Confocal Raman spectroscopic measurements. These complimentary techniques reveal the correlation of doping type (electron or hole doping) and density with the perturbations of the graphene  $\pi$  band evidenced in NEXAFS and XMCD. Both NEXAFS and Raman studies used to probe the perturbations of the graphene C- edge and G and 2D bands that portray the planarity and dopant effect in graphene electronic structure. Results from AFM, Raman and mobility experiment provided a novel methodology to understand extremely high ion mobility of Titanium doped graphene in comparison other transition metal graphene doped species. It was seen that Ti-Graphene films had higher surface roughness, strain evidenced by AFM measurements. Raman Spectroscopy of single layer CVD graphene doped with titanium and gold indicated that they are both P-type with moderate carrier mobility. Measurements will afford us information on how the Dirac point would shift with respect to the

Fermi level upon doping the graphene with various transition metals. Further analysis via Photoluminescence Spectroscopy (PL), NEXAFS will determine the band gap, chemical nature of Graphene metal interaction to create required size of the engineered bandgap.

## References:

1. J. Schultz, C. J. Patridge, V. Lee, C. Jaye, P. S. Lysaght, C. Smith, J. Barnett, D. A. Fischer, D. Prendergast and S. Banerjee, Nat. Commun., 2011, 2, 372
2. T. Abtew, B.C. Shih, S. Banerjee and P. Zhang, Nanoscale, 2013, 5, 1902

# Current Distribution Mapping of Carbon Nanotube-Embedded Polymer Using Conductive Probe Atomic Force Microscopy

G. Pascual, J. Pineda, B. Kim, and K. Lee

Park Systems Inc., 3040 Olcott Street, Santa Clara, CA 95054, United States of America

## Abstract:

By running an electrical current through a metal probe tip and a conductive sample, conductive probe atomic force microscopy (CP-AFM) can not only acquire the sample's topography but also correlate current distributions with specific observed spatial features.[1] Being able to identify nanoscale sized areas of high and low conductivity, has proven especially helpful in the semiconductor, photovoltaic, and hard disk drive manufacturing. These industries have developed ever-increasing material processing demands which have resulted in more and more devices with critical dimensions so small that bulk property values can no longer predict their behavior. In this investigation, we discuss topography and conductivity data acquired using a Park NX10 atomic force microscopy (AFM) system to characterize a polymer sheet sample embedded with carbon nanotubes (CNTs). The 1 x 1  $\mu\text{m}$  scan area, with the sample bias set to -0.3 V, revealed the presence of multiple tube-like structures present at multiple depths over a span of 30-40 nm on the sample surface. Given their geometry and their approximate diameters measuring in tens of nanometers, these structures were likely the CNTs embedded in the polymer sheet. Further evidence strengthening the argument that these structures are CNTs was provided in the corresponding current distribution image. Comparing the topography image to the simultaneously acquired current distribution image made it clear that the tube-like structures correlated to areas of conductivity in excess of 10 nA. These areas contrasted strongly with areas showing nearly no conductivity which are believed to be the polymer in which the CNTs were embedded in. A second 500 x 500 nm scan, also set to a sample bias of -0.3 V, was taken to provide a magnified view of the original scan area. This zoomed-in scan once again correlates the tube-like structures on the surface topography to areas of high conductivity, re-supporting the conclusion that they are CNTs.

**Keywords:** atomic force microscopy, AFM, conductivity, characterization, carbon nanotubes, CNT, conductive probe atomic force microscopy, CP-AFM, polymer, topography

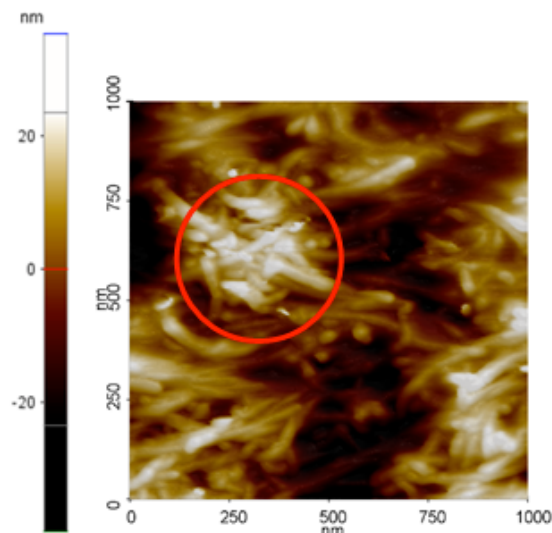


**Figure 1:** Topography of polymer-CNT sample imaged with CP-AFM. The inset red circle denotes a region of interest in the sample's topography. Here, multiple tendril-like structures flagged as potential CNTs have gathered into a large bundle representing some of the tallest peaks in the scan area. Scan size: 1 x 1  $\mu\text{m}$ , sample bias: -0.3 V.

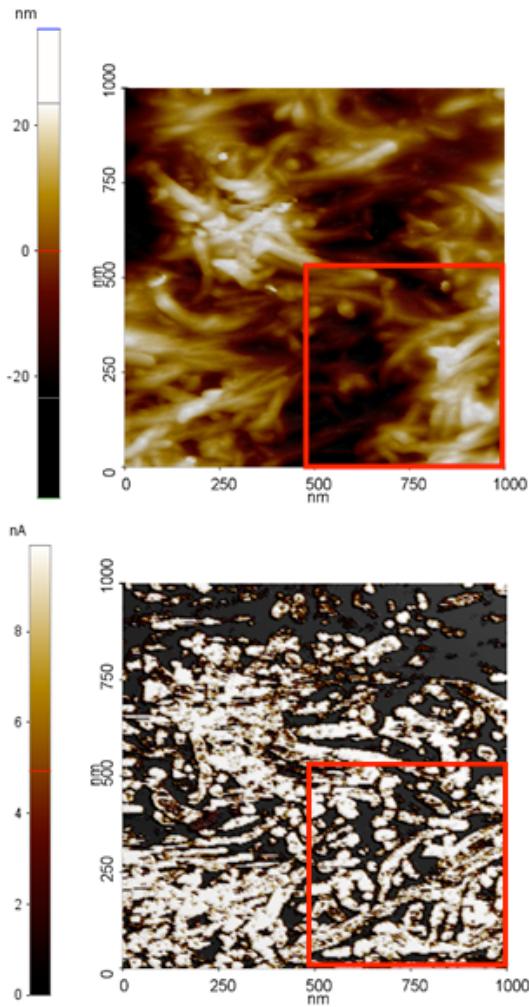


**Figure 2:** Polymer-CNT sample topography data (top, Figure 1) and current distribution data (bottom) all acquired with CP-AFM. The inset red squares in each image were later re-scanned (Figure 3) to demonstrate the resolution of this technique. Scan sizes: 1 x 1  $\mu\text{m}$ , sample bias: -0.3 V.

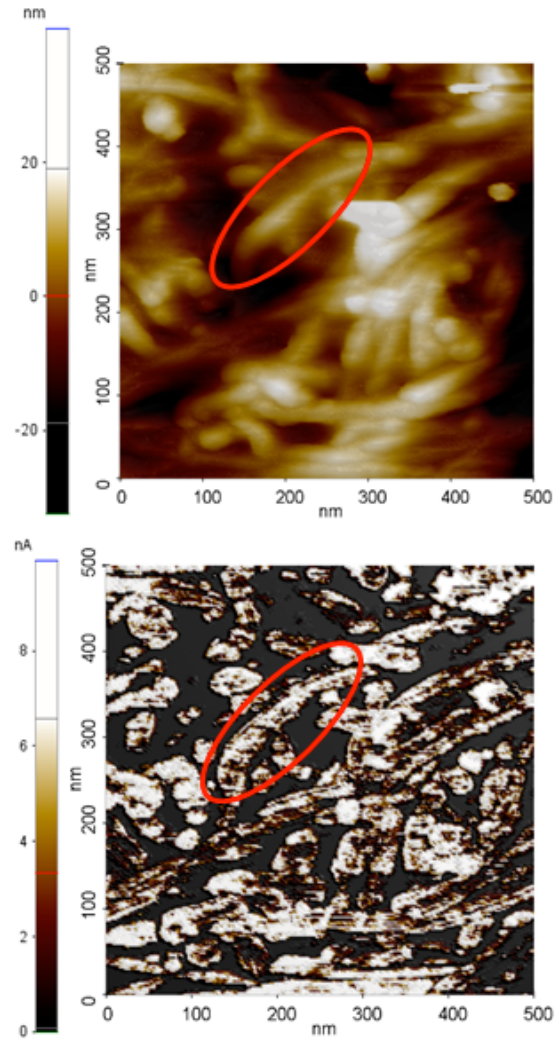


**Figure 3:** Polymer-CNT sample topography data (left) and current distribution data (right) acquired from the lower-right quadrant of Figure 2's scan area. The contrast levels of the current distribution data have been adjusted from Figure 2 to increase the visibility of the CNT outlines. Note that major visual landmarks (such as the tall CNT in the inset red circles) as well as other finer visual details not only match in these two images but have also been preserved from the earlier, larger scan in Figure 2. Scan sizes: 500 x 500 nm, sample bias: -0.3 V.

#### References:

1. Conductive AFM. (2016) Retrieved from <http://www.parkafm.com/index.php/park-spm-modes/94-electrical-properties/233-conductive-afm>

# Nanoscale material characterisation with the use of a modified DVD pickup in High-speed Atomic Force Microscopy

Freddie Russell-Pavier,<sup>1,2</sup> Oliver Payton<sup>1</sup>, Loren Picco<sup>1</sup>, John Day<sup>1</sup>, Tom Scott<sup>1</sup> and Andrew Yacoot<sup>2</sup>

<sup>1</sup> Interface Analysis Centre, University of Bristol, Bristol, UK

<sup>2</sup> National Physical Laboratory, Teddington, Middlesex, UK

## Abstract:

Optical pickups have been developed over several decades for reading and writing of optical discs such as CD, DVD and Blu-ray. In operation, optical pickups are conducting the complex task of automatically 3D tracking and reading a spiral of embedded pits on the underside of the optical disc that can extend up to several tens of kilometers in length and less than 500 nm in width. This is performed with the use of a compact laser and a single quadrant photodiode. The optical system makes use of an astigmatic lens, which has two focal planes in orthogonal axes that focus to different focal lengths. When the laser light is focused on the disc, the quadrant diode lies in between these two focal lengths. The quadrant photodiode can then be used to determine if the laser is losing focus by measuring which of the two focal lengths it is closer to.

We integrate a DVD optical pickup into high-speed atomic force microscope to create a novel instrument with low build cost and increased bandwidth, in addition to being able to perform angular monitoring of the cantilever. It has been shown in previous studies how optical pickups can be incorporated into a range of experimental set-ups [1-4], making use of the astigmatic detection system. This work builds upon the development of the world's fastest contact mode high-speed atomic force microscope conducted at the University of Bristol.

By making use of the high throughput and the sub-nanometer resolution achieved with a modified optical pickup within a bespoke instrument, outlined in Figure 1, surface properties and nanoparticle identification can be conducted on a sub-second timescale. This rapid analysis generates large statistical datasets allowing sample wide representative properties to be measured quickly. Work with the National Physical Laboratory (NPL) assesses the metrological capabilities of the pickup and seeks to ensure measurement traceability.

Main areas of research interests include bridging the nano to micro length scales. Specific applications include DNA imaging, characterisation of nanoparticles and materials.

## Keywords:

Optical pickups, nanotool, nanoparticles, nanometrology, 2D materials, DNA and high-speed AFM

## References:

1. F. Quecioli et al., Review of Scientific Instruments, 1999, Vol. 70, Issue 9, pp 3620-3624
2. K. Fan et al., Measurement Science and Technology, 2002, Vol. 14, pp 47-54
3. E. Hwu et al., Appl. Phys. Letters, Vol. 91, Issue 22, pp 221908:1-3
4. C. Chu et al., Measurement Science and Technology, 2007 Volume 18, Issue 7, pp 1831-1842

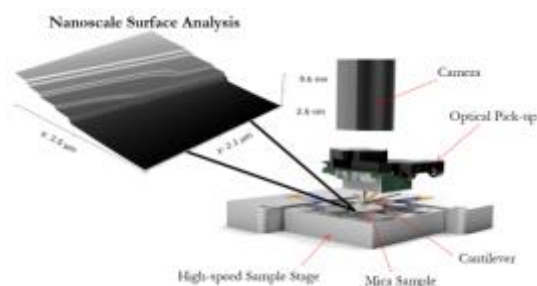


**Figure 1:** A schematic of the optical pickup based high-speed AFM used for rapid exploration of surface features and properties

# Dual-tip-based scanning probe microscopy

J. Šoltýs<sup>1</sup>, M. Precner<sup>1</sup>, K. Neilinger<sup>1</sup>, J. Dérer<sup>1</sup>, V. Cambel<sup>1</sup>  
<sup>1</sup>Institute of Electrical Engineering SAS, Bratislava, Slovakia

## Abstract:

Scanning probe microscopy (SPM) is a well established tool for the sample imaging and characterisation at nanoscale. Various SPM techniques have been developed over the years in order to study a wide range of physical properties. They rely on single cantilever-based probe that is adopted for concrete application. However, the single probe configuration suffers from some drawbacks. Therefore, it turns out that the use of dual-probe system is highly advantageous for some applications [1]. This work reports on two novel SPM methods which both use tailored dual AFM tips. In the first method, so called dual-tip magnetic force microscopy (DT-MFM), topological and magnetic scans are segregated using two different tips (Fig. 1). The non-magnetized tip is used for topography only, and the magnetized one is used for a magnetic field mapping only (it never touch the surface). Our experiments show that the dual-tip technique minimizes the perturbations of the magnetic tip. Introduced DT-MFM is perspective for exploring of magnetically soft samples.

The second method has been designed for bio-applications to study the mechanical properties of cells. It consists of two cantilevers; one having a sharp tip, the other having a spherically blunted tip (Fig. 2). The sharp tip is used for topography imaging with high resolution, while blunt tip is used for measuring of force distance curves. Various biophysical properties of cells can be obtained from force spectroscopy, such as elasticity, adhesion, hardness, friction, etc. [2]. The larger area of probe-cell contact results in averaging local variation in the cell rigidity compared to the one measured with a regular sharp probe. Therefore, the measurement time becomes shorter and, moreover, there is no risk that tip will penetrate into soft cell. The switching between sharp and blunt tip is realized by means of integrated magnetostrictive actuator.

**Keywords:** SPM tip prototype fabrication, magnetic force microscopy, force spectroscopy, cell indentation.

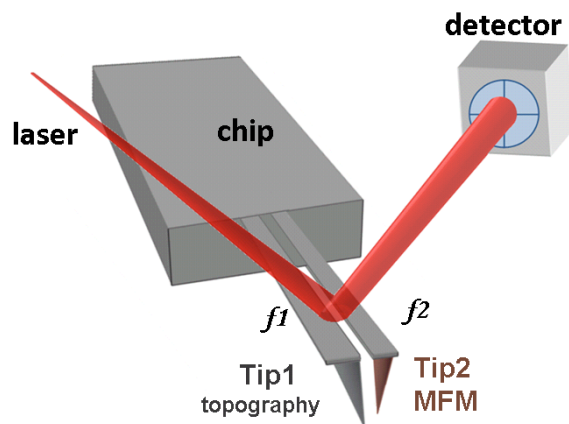


**Figure 1:** Principle of the dual-tip MFM technique. Topography is performed by non-magnetic Tip1 at the resonant frequency  $f_1$ , and the phase shift is evaluated by magnetic Tip2 at the resonant frequency  $f_2$ .

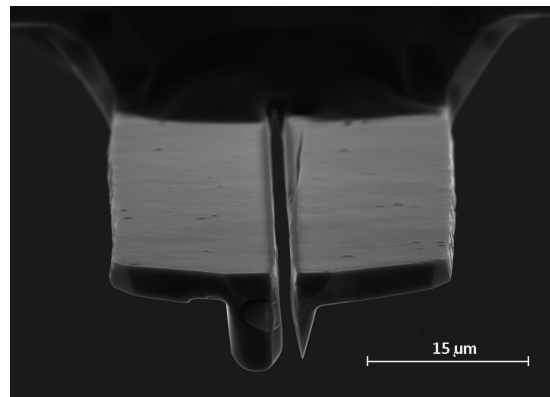


**Figure 2.** SEM micrograph of dual-tip designed for force spectroscopy. The sharper tip (right) is used for topography, and larger tip (left) is used for spectroscopy measurement.

## References:

1. M. Despont, H. Takahashi, S. Ichihara, Y. Shirakawabe, N. Shimizu et al., *Thirteenth IEEE International Conference on MEMS* January 23–27 (2000) 126.
2. Sokolov I. AFM in cancer cell research. In: Nalwa HN, Webster T, editors. *Cancer Nanotechnology*. Valencia, CA: American Scientific Publishers (2007) p. 1–17.

# First Principles-Based Molecular Dynamics Study of the Effect of Dielectric Polarization of Graphene in the Wetting of Graphitic Surfaces

Rahul Prasanna Misra and Daniel Blankschtein

Department of Chemical Engineering, Massachusetts Institute of Technology, Cambridge, Massachusetts 02139, USA

## Abstract

Graphene, an allotrope of carbon and the two-dimensional form of bulk graphite, consists of only a single layer of  $sp^2$  hybridized carbon atoms arranged in a honeycomb lattice. Owing to its atomic thickness and high mechanical strength, graphene has attracted widespread attention as a potential membrane for seawater desalination, nanopore-based osmotic power harvesting, and DNA sequencing applications. However, in order to realize the true potential of graphene in these applications, it is imperative to develop a deeper understanding of the way in which water molecules interact with graphene. Previous simulation studies on the wetting of graphene and highly-ordered pyrolytic graphite have assumed that water molecules interact with carbon atoms in graphene through weak pairwise additive dispersion interactions. However, when graphene comes in contact with a polar solvent like water, the water molecules exert a finite electric field on the carbon atoms in graphene. This electric field distorts the charge distribution in graphene and results in the generation of induced charges which then interact with the permanent dipoles of water molecules. In this talk, using force-field molecular dynamics simulations with parameters determined from first-principles calculations, we discuss the effect of the dielectric polarization of graphene on the contact angle of water on graphene and highly-ordered pyrolytic graphite. Our study, for the first time, reveals that the electric field felt by the carbon atoms in graphene depends on the orientation of water molecules in the interfacial layer, which results in a strong non-linear dependence of the electric field on the static dipole polarizability of graphene. Our results also show that polarization (permanent dipole – induced dipole interactions) has a more pronounced effect on the interfacial

entropy compared to dispersion (induced dipole – induced dipole interactions). As a result, these effects contribute differently to the wetting of graphitic surfaces. Our theoretical estimation of  $63^\circ$  for the contact angle of water on highly-ordered pyrolytic graphite is in excellent agreement with recent experimental data which report a contact angle value in the range of  $62-68^\circ$ .

## Keywords

Graphene, contact angle, ab-initio calculations, molecular dynamics simulations, dielectric polarization, electric field, wetting properties, interfacial phenomena.

# Quantitative Modeling of MoS<sub>2</sub>–Solvent Interfaces: Predicting Contact Angles and Exfoliation Performance Using Molecular Dynamics Simulations

Ananth Govind Rajan<sup>1</sup>, Vishnu Sresht<sup>1</sup>, Emilie Bordes<sup>2</sup>, Michael S. Strano<sup>1</sup>, Agilio A. H. Padua<sup>2</sup>, and Daniel Blankschtein<sup>1</sup>

<sup>1</sup>Department of Chemical Engineering, Massachusetts Institute of Technology, Cambridge, Massachusetts 02139, United States

<sup>2</sup>Institut de Chimie de Clermont-Ferrand, Universite Blaise Pascal and CNRS, 63176 Aubiere, France

## Abstract

The controlled synthesis of molybdenum disulfide (MoS<sub>2</sub>) using liquid-phase exfoliation, as well as several of its proposed applications, involve liquids coming into intimate contact with MoS<sub>2</sub> surfaces. Molecular dynamics (MD) simulations offer a robust methodology to investigate nanomaterial/liquid interactions involving weak van der Waals forces. However, MD force fields for MoS<sub>2</sub> currently available in the literature incorrectly describe not only the cohesive interactions between layers of MoS<sub>2</sub>, but also the adhesive interactions of MoS<sub>2</sub> with liquids such as water. In this talk, we outline the development of a set of force-field parameters that reproduce the properties of bulk 2H molybdenite, with special attention to the distinction between the covalent, intra-layer terms and the non-covalent, inter-layer Coulombic and van der Waals interactions. The resulting model is compatible with MD force fields for organic compounds, and can correctly describe the interactions of MoS<sub>2</sub> with liquids, yielding excellent agreement with experimental contact angles for water and diiodomethane. Potential of mean force (PMF) calculations using various solvents, including isopropanol (IPA), water (H<sub>2</sub>O), dimethyl sulfoxide (DMSO), dimethylformamide (DMF), and N-methyl-2-pyrrolidone (NMP), demonstrate that the use of our force field can explain the current selection of solvents used in experimental studies of the

liquid-phase exfoliation of MoS<sub>2</sub> flakes, as well as the observed colloidal stability of the resulting dispersion. Our new force field enables an accurate description of MoS<sub>2</sub> interfaces, thereby paving the way for the simulation-aided design in applications including membranes, microfluidic devices, and sensors. In addition, it enables a deeper understanding of the extent to which dispersion interactions and electrostatics determine the wetting and frictional properties of this material.

## Keywords

Wetting, contact angle, friction, water, MoS<sub>2</sub>, layered materials, exfoliation, solvents, colloidal dispersion

# Synthesis and characterization of iodinated polymer particles and use as a contrast agent for tomography using a spectral scanner

Joëlle Balegamire<sup>1\*</sup>, Daniel Bar-Ness<sup>2,3</sup>, Yves Chevalier<sup>1</sup>, Hatem Fessi<sup>1</sup>, Salim Si-Mohamed<sup>2,4</sup>, Monica Sigovan<sup>2,4</sup>, Marc Vandamme<sup>5</sup>, Emmanuel Chereul<sup>5</sup>, Loïc Bousset<sup>2,4</sup>, Philippe Douek<sup>2,4</sup>

<sup>1</sup>LAGEP, CNRS UMR 5007, UCB Lyon 1, 69622 Villeurbanne, France

<sup>2</sup>CREATIS, CNRS UMR 5220, INSERM U630, UCB Lyon 1, 69621 Villeurbanne, France

<sup>3</sup>CERMEP, 69677 Bron, France

<sup>4</sup>Hospices Civils de Lyon, Radiology Department, 69677 Bron, France

<sup>5</sup>VOXCAN, 69280 Marcy-l'Étoile, France

\*joelle.balegamireniv-lyon1.fr

## Abstract :

Contrary to conventional Computed Tomography (CT) that provide a single attenuation measurement, Dual Energy scanners (two attenuations at different energy ranges) and recent prototypes of Spectral Photon Counting CT (SPCCT), can discriminate between different elements by recording the energy spectrum of the tissues attenuation at each voxel of the image. This allows material decomposition that provides quantitative determination of the concentration of a specific element. Iodine-based materials are widely used and efficient contrast agents for CT scanners. Contrast agents in the form of nanoparticles that specifically bind to the tissue to be imaged, provide contrast enhancement in respect to small molecules. The purpose of this study is to combine the SPCCT technology and contrast agents as nanoparticles. In order to do so, iodinated polymer nanoparticles were designed, to be used as contrast agents for the SPCCT.

The iodinated polymer material was prepared by covalently linking an iodinated molecule onto Poly (vinyl alcohol) (PVAL 13 kDa) (Figure 1). The radiopaque moieties were successfully incorporated onto the polymer and the grafting rate (degree of substitution, DS), calculated from the <sup>1</sup>H NMR spectrum, was over 50 mol%. The iodine content determined from the DS was over 70 wt%. Elemental analysis for iodine content confirmed these results.

Nanoparticles of iodinated polymers were prepared using the Nano-precipitation method. Dynamic Light Scattering (DLS) and Cryogenic Transmission Electron Microscopy (Cryo-TEM) measured particle size. Nanoparticles were stable and well-separated (Figure 2) and their mean diameter was in the 40 – 200 nm range, depending on the concentration of polymer.

Radio-opacity of the contrast agents and sensitivity of the scanner for iodine were evaluated in-vitro on phantoms prepared with suspensions of contrast agents at different concentrations (Figure 3). Bio-distribution was studied in-vivo by experiments performed on small animals (intravenous injections to rabbits). Such measurements were performed on a conventional CT and on the SPCCT for the sake of comparison.

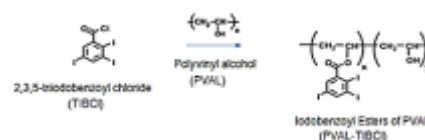


Figure 1. Iodinated polymer synthesis: covalent linkage of 2,3,5-triodobenzoic chloride onto

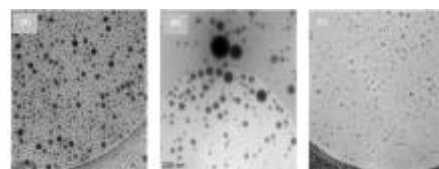


Figure 2. Cryo-TEM images of aqueous dispersions of iodinate polymer at different concentrations JB43 and JB48 (A & B) and block co-polymer PCL-b-PEG micelles (C).



Figure 3. Phantoms prepared with suspensions of iodinated polymer in water at different concentrations. (JB48).

“The project leading to this document has received funding from the European Union’s Horizon 2020 research and innovation program under grant agreement No 643694”.

[www.SPCCT.eu](http://www.SPCCT.eu)

# Fabrication and Dispersion of Super-paramagnetism Magnetite Nano Powder using Co-Precipitation Method for Magnetic Fluid.

Jung-Kab Park<sup>1</sup>, Ho-Jun Choi<sup>1</sup>, Jung-Ho Park<sup>1</sup>, Tae-Yoo Kim<sup>1</sup>, Seok-Hun Kim<sup>1</sup>, Sun-Woo Kim<sup>1</sup>, Jung-Woo Lee<sup>1</sup>, Se-Hee Shin<sup>1</sup>, Jong-Hwan Park<sup>1</sup>, Hwa-Sun Park<sup>1</sup>, Yong-Soo Oh<sup>1</sup>, Su-Jeong Suh<sup>1\*</sup>

<sup>1</sup> School of advanced Materials Science and Engineering, Sungkyunkwan University, Republic of Korea

## Abstract:

Magnetic fluid has three main constituents: super paramagnetism particle such as magnetite and composite ferrite, a surfactant, and base liquid such as water or oil. The surfactant coats the ferromagnetic particles, each of which has a diameter of 10 nm. In this study, magnetite powder is produced using the co-precipitation method. First  $\text{Fe}_2\text{Cl}\cdot 4\text{H}_2\text{O}$  (3.97 g, 0.02 mol) and  $\text{FeCl}_3\cdot 6\text{H}_2\text{O}$  (5g) are dissolved in 50 mL DI while stirring at 500 rpm for 30 min. Next, 2M  $\text{NH}_4\text{OH}$  aqueous solution is added dropwise, at a rate of 5 mL per minute. The color of the solution slowly turns from brown to black, and magnetite particles are formed. The powder is then washed 10 times by distilled water and is desiccated at 80°C for 10 hours in an atmosphere of  $\text{N}_2$ . The desiccated powder is altered with its concentration by using a fluorinate surfactant and dispersed by ultrasonic wave for 3 hours. By using ethanol and distilled water, the powder is washed and desiccated at 80°C for 10 hours in vacuum. The powder is then pulverized and dispersed magnetization value of the powder was measured as 79 emu/g by using Vibration Sample Magnetometer(VSM). The averages particles size of the powder was determined as 12 nm by using TEM. The magnetic fluid fabricated by the ball mill process had the shape of a spike, as was confirmed by applying a magnetic field.

**Keywords:** Magnetite, Dispersion, Super paramagnetism, Surfactant,

1. Buhe Bateer, Yang Qua, Chungui Tian, Shichao Du, Zhiyu Ren, Ruihong Wang, Kai Pan, Honggang Fu, *Materials Research Bulletin* 56 (2014) 34-38
2. Bing Tang, Liangjun Yuan, Taihong Shi, Linfeng Yu, Youchun Zhu, *Journal of Hazardous Materials* 163 (2009) 1173-1178

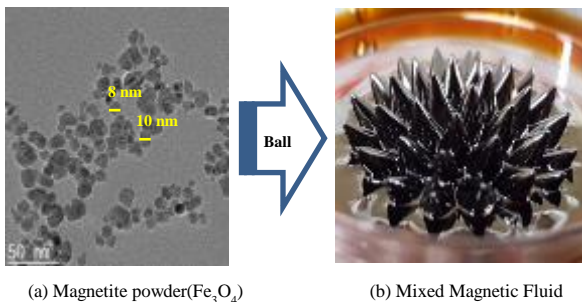


**Figure 1:** Fabrication of magnetic fluid using  $\text{Fe}_3\text{O}_4$  nano powder.

## References:

# Theoretical Analysis of the Optical Response of silicon/silica/gold Multishell Nanoparticle in Biological tissue

W. Chaabani,<sup>1,2,\*</sup> A. Chehaidar,<sup>1</sup> J. Proust,<sup>2</sup> J. Plain<sup>2</sup>

<sup>1</sup> Université de Sfax, Faculté des Sciences de Sfax, B.P. 1171, 3000 Sfax, Tunisia

<sup>2</sup> Université de Technologie de Troyes, Laboratoire de Nanotechnologie et d'Instrument Optique, , 12 rue marie Curie-CS 42060 – 1004 Troyes Cedex, France

## Abstract:

The scattering and absorption efficiencies of light by a single silicon/silica/gold spherical multishell in biological tissue are analyzed theoretically in the framework of Lorenz-Mie theory and finite-difference-time-domain formalism. We first revised the ideal case of a concentric silicon/gold nanoshell, then we analyzed the effect of growing a silica layer of uniform thickness around the silicon core, and finally we examined the effect of an offset of the gold-shell with respect to the center of the silicon/silica nanoshell. Our simulation showed that the silicon/gold nanoshell in the biological tissue supports significant absorption and scattering resonances in the biological spectral window. On the other hand, the growth of a silica layer on the silicon-core surface leads to a blue shift of these resonances accompanied by a slight increase of their magnitudes. The offset of the gold-shell with respect to the silicon/silica core results in a redshift of the absorption (Figure 1) and scattering resonances supported by the concentric silicon/silica/gold multishell within the biological window, accompanied by a decrease in their amplitudes. On the other hand, the gold-shell offset gives rise to a more prominent electric-field enhancement at the interface silicon/silica/gold multishell-biological tissue. Our simulation thus shows that the deviation from an ideal silicon/gold nanoshell due to the growth of a silica layer on the silicon surface and/or a gold-shell offset with respect to the silicon/silica core in no way diminishes the quality of its optical response within the biological spectral window, thus making these nanostructures potential candidates in bioimaging and photothermal-therapy applications.

**Keywords:** optical properties; silicon-silica-gold multishell nanoparticle; Mie theory; FDTD method; modeling and simulation.

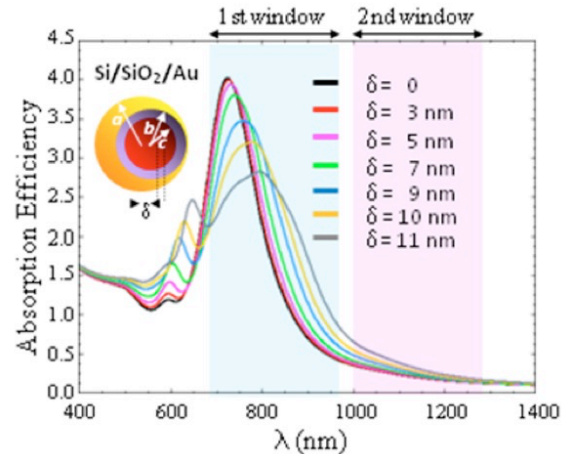


**Figure 1:** The absorption efficiency computed for a single Si/SiO<sub>2</sub>/Au eccentric multishell in biological tissue as a function of the incident light wavelength  $\lambda$  for different values of the gold-shell offset  $\delta$ .

## References:

1. Chaabani, W., Chehaidar, A., Plain, J. (2016) Comparative theoretical study of the optical properties of silicon/gold, silica/gold core/shell and gold spherical nanoparticles, *J. Plasmonics*, 11, 1525-1535.
2. Smith, A.M., Mancini, M.C., Nie, S. (2009) Bioimaging: Second window for in vivo imaging, *Nature Nanotechnology*, 4, 710-711.
3. Gobin, A.M. et al. (2007) Near-Infrared Resonant Nanoshells for Combined Optical Imaging and Photothermal Cancer Therapy, *Nano Lett.*, 7, 1929-1934.

**Nanotech France 2017**  
**Plenary session II**

# Medical Nanochemistry, the use of reactive inorganic nanoparticles in medicine.

Victor Puntès<sup>1,2,3\*</sup>

<sup>1</sup> Institut Català de Nanotecnologia, Campus UAB, Barcelona, Spain

<sup>2</sup> Vall d'Hebron Institute of Research, Barcelona, Spain

<sup>3</sup> Institut Català de Recerca i Estudis Avançats, Barcelona, Spain

## Abstract:

Chemical processes performed or promoted by inorganic nanoparticles in physiological conditions allows to monitor and manipulate biological states, from its catalytic properties, as ROS quenchers CeO<sub>2</sub> NPs, to coordination chemistry, for the pH controlled release of antitumoral agents, first developed with polymers and then gold NPs, or the use the aggregate state of a compound in the form of a NP which progressively dissolves or corrodes, as a carrier of itself, as curcumin or iron oxide nanoparticles, and providing cations and electrons when dissolving affecting cellular REDOX state (metabolism). A case that is already in the clinic is the use of feromuxitol to treat ferropenic anemia. Other more subtle alterations of the reactivity of the biomolecules is observed in the case of therapeutic antibodies linked to NPs. In this chemical approach is also important to unveil the special features that rise in the pharmacokinetic models when working with nanoparticles, very different from the small drug standard pharmacokinetic models.

Due to their higher percentage of surface atoms and their colloidal nature, NPs experience processes that transform them towards more stable thermodynamic states -driven by the minimization of their reactivity- which is translated into high rates of oxidation, dissolution, aggregation and interaction with proteins. Aggregation, that is colloidal stability, has a significant influence on the reactivity, bioavailability and pharmacokinetic of NPs, having long been recognized that the effective size can mediate their toxicity, as in the case of asbestosis, industrial aerosols and ambient particulate matter. Similarly, oxidative dissolution favors the chemical dissolution of the NPs, affecting their persistence and promoting the release of ionic species. The physicochemical state of the NPs also play a role in their interaction with media proteins, and the subsequent nature of the protein corona around them (the so-called soft and hard corona), inevitably providing them with new biological identity, which determines their physiological response including cellular uptake, biodistribution

and toxicity. Although the extent of each individual process, determined by the intrinsic properties of the NPs (material, size, shape, concentration, crystallinity, surface charge and coating) and the nature of the media in which they are dispersed (ionic strength, protein concentration, pH...), can be studied separately, the fact that the greatest NP transformation occur within the same time scale (from minutes to hours of exposure) it is translated into the overlapping and competition between all the different processes involved. Thus, it is common to observe that NPs are instable and tends to aggregate after their exposure to cell culture media and that they corrode while being coated by proteins. As a result of this complexity, it is critical to fully understand the transformation kinetics of NPs in biological systems. In this regard, the understanding of these transformations not only may help to better interpret the biological effects of NPs, but also assists in designing the desired NPs for specific purposes. Finally, a NP surface must have charges to organize surrounding ions and control interactions with the surrounding media (e.g.:Ca<sup>2+</sup> ions interferes between surfaces and proteins in implants). Indeed, drug penetration and distribution properties have been related to the electrostatic water envelop that surrounds it. This chemical approach will contribute to the development of tools for medicine and consequently nanomedicine.

---

<sup>1</sup> More than a century ago, Franz Hofmeister recognized that ions with identical charge precipitate proteins to differing extents. It was later discovered that equally charged ions exhibit opposite tendencies. Indeed, the Hofmeister series can be observed for many interfacial phenomena, usually when the Debye length is small, as in the NPs object of this study.

# Engineering porous silicon nanoparticles for smart drug delivery

N.H. Voelcker

Monash Institute of Pharmaceutical Sciences, Monash University, Parkville, VIC, Australia  
Melbourne Centre for Nanofabrication, Australian National Fabrication Facility, Clayton, VIC, Australia

## Abstract:

Targeted approaches to deliver anti-cancer drugs have the potential to achieve improved efficacy and at the same time reduced side effects. In fact, this is one of the cornerstones of nanomedicine.

We are exploring the use of high porosity biodegradable porous silicon and genetically engineered biosilica nanoparticles that are loaded with chemotherapy drugs or siRNA and also display on the particle's periphery targeting moieties such as cell-surface antibodies recognising cognate ligands highly expressed on the surface of tumour cells.

One approach centers around porous silicon nanodiscs. The process relies on a combination of colloidal lithography and metal-assisted chemical etching. Height and diameter of the pSi nanodiscs can be easily adjusted. The nanodiscs are degradable in physiological milieu and are non-toxic to mammalian cells. In order to highlight the potential of the pSi nanodiscs in drug delivery, we carried out an *in vitro* investigation which involved loading of nanodiscs with the anti-cancer agent camptothecin and functionalization of the nanodisc periphery with an antibody that targets receptors on the surface of neuroblastoma cells. The thus prepared nanocarriers were found to selectively attach to and kill cancer cells [1,2]. In a second approach, we used natural nanoporous biosilica from the diatom *Thalassiosira pseudonana*. The biosilica was genetically engineered to display GB1, an IgG binding domain of protein G, on the biosilica surface, which allowed for the attachment of cancer cell targeting antibodies and the adsorption of nanoparticles loaded with anti-cancer drugs. Adherent neuroblastoma cells and B lymphoma cells in suspension were selectively targeted and killed by drug-loaded biosilica displaying specific antibodies (Figure 1). In a subcutaneous mouse xenograft model of neuroblastomamice, regression of SH-SY5Y tumour growth was evident in immunodeficient Balb/c nude mice that were when treated with drug-loaded anti-p75NTR-labelled biosilica. Histological analysis confirmed accumulation of anti-p75NTR-labelled biosilica in the tumours. This result established the efficacy of targeted drug-

loaded-biosilica in a relevant clinical model [3]. In a final approach, we engineered porous silicon nanoparticles to deliver siRNA to successfully downregulate drug transporter proteins in brain tumour cells [4,5]. Coating of nanoparticles with cationic polymers improved sustained DNA and siRNA release and suppressed burst release effects. In addition, polymer coating significantly enhanced the uptake of nanoparticles across the cell membrane. Histopathological analysis of liver, kidney, spleen and skin tissue collected from mice receiving nanoparticles further demonstrates their biocompatible and non-inflammatory properties.

**Keywords:** drug delivery, nanoporous silicon, diatom biosilica.

## References:

1. H. Alhmoud, B. Delalat, A. Cifuentes, R. Elnathan, A. Chaix, O. Durand, M.-L. Rogers, N.H. Voelcker, Porous silicon nanodiscs for targeted drug delivery, *Advanced Functional Materials*, 25 (2015), 1137-1145.
2. M. Alba, B. Delalat, P. Formentín, M.-L. Rogers, L.F. Marsal, N.H. Voelcker, Silica Nanopills for Targeted Anticancer Drug Delivery, *Small*, 11 (2015), 4626-4631.
3. B. Delalat, V.C. Sheppard, S. Rasi Ghaemi, S. Rao, C.A. Prestidge, G. McPhee, M.-L. Rogers, J.F. Donoghue, V. Pillay, T.G. Johns, N. Kröger, N.H. Voelcker (2015) Targeted drug delivery using genetically engineered diatom biosilica, *Nature Communications*, 6 (2015), 8791.
4. Y. Wan, S. Apostolou, R. Dronov, B. Kuss, N. H. Voelcker. Cancer-targeting siRNA Delivery from Porous Silicon Nanoparticles, *Nanomedicine*, 9 (2014), 2309-2321.
5. M.H. Kafshgari, B. Delalat, W.Y. Tong, F. Harding, M. Kaasalainen, J. Salonen, N.H. Voelcker, Oligonucleotide delivery by chitosan-functionalized porous silicon nanoparticles, *Nano Research*, 8 (2015), 2033-2046.

# Solar Fuel: High Efficient Photocatalysts for CO<sub>2</sub> conversion into hydrocarbon fuels

SU-IL IN

Department of Energy Systems Engineering, DGIST, Republic of Korea

## Abstract:

Photocatalytic CO<sub>2</sub> conversion to fuel offers an exciting prospect for solar energy storage and transportation thereof. Several photocatalysts have been employed for CO<sub>2</sub> photoreduction; the challenge of realizing a low-cost, readily synthesized photocorrosion-stable photocatalytic material that absorbs and successfully utilizes a broad portion of the solar spectrum energy is as yet unmet. Herein, a mesoporous p-type/n-type heterojunction material, Cu<sub>x</sub>O–TiO<sub>2</sub> (x = 1, 2), is synthesized via annealing of Cu/Cu<sub>2</sub>O nanocomposites mixed with a TiO<sub>2</sub> precursor (TiCl<sub>4</sub>). Such an experimental approach in which two materials of diverse bandgaps are coupled provides a simultaneous opportunity for greater light absorption and rapid charge separation because of the intrinsic p–n heterojunction nature of the material. As detailed herein, this heterostructured photocatalyst demonstrates an improved photocatalytic activity. With the CO<sub>2</sub> reduction of our optimal sample (augmented light absorption, efficacious charge separation, and mesoporosity) that utilizes no metal cocatalysts, a remarkable methane yield of 221.63 ppm·g<sup>-1</sup>·h<sup>-1</sup> is achieved.

**Keywords:** CO<sub>2</sub> conversion, Photocatalyst, Solar energy, heterojunction, mesoporosity

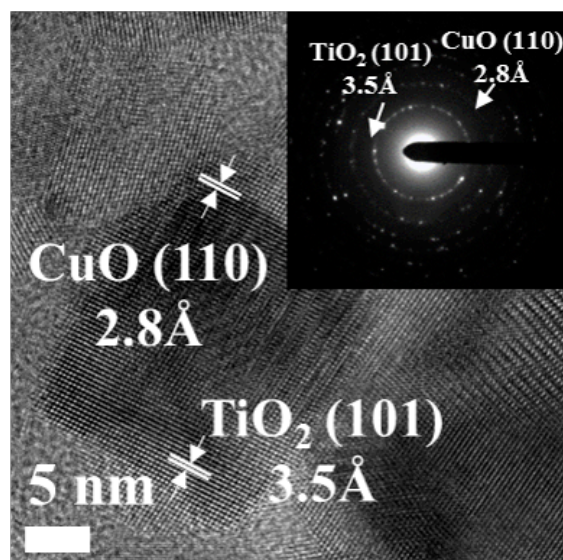


**Figure 1:** HR-TEM and SAED patterns (inset) confirming the presence of CuO and TiO<sub>2</sub> within the mesoporous Cu<sub>x</sub>O–TiO<sub>2</sub> composite.

## References:

1. ACS Omega 1 (2016) 868–875
2. RSC Advances 6 (2016) 38964–38967
3. Carbon 98 (2016) 537–544

# Progress in Quantum Dot Photonics: From Science to Practical Implementations

Yasuhiko Arakawa

Institute of Industrial Science, The University of Tokyo, Tokyo, Japan

## Abstract:

Recent advances in growth and physics of quantum dots have led to the commercialization of quantum dot lasers for telecommunications and other applications<sup>1-3</sup>. Moreover, single quantum dots coupled to photonic crystal nanocavities have enabled the investigation of fundamental physics such as solid-state cavity quantum electrodynamics (QED)<sup>4-5</sup>.

In this presentation, we discuss the current state of the art of quantum dot lasers, and also future prospects including their application to hybrid silicon photonics<sup>6-7</sup> and the development of ultra-small nanolasers<sup>8-12</sup>. We also describe the demonstration of a single photon emission from a III-Nitride nanowire-based quantum dot operating above room temperature<sup>13-14</sup>.

## References:

1. Y. Arakawa and H. Sakaki, *Appl. Phys. Lett.* **40**, 939 (1982)
2. J. Oshinowo, M. Nishioka, S. Ishida, and Y. Arakawa, *Appl. Phys. Lett.* **65** 1421 (1994)
3. K. Otsubo, N. Hatori, M. Ishida, S. Okumura, T. Akiyama, Y. Nakata, H. Ebe, M. Sugawara and Y. Arakawa, *Jpn. J. of Appl. Phys.* **43**, L1124, Express Letter (2004)
4. C. Weisbuch, M. Nishioka, A. Ishikawa, and Y. Arakawa, *Phys. Rev. Lett.* **69**, 3314 (1992)
5. Y. Arakawa, S. Iwamoto, M. Nomura, A. Tandechnurat, and Y. Ota, *IEEE J. of Selected Topics in Quantum Electronics* **18**, 1818 (2012)
6. Y. Urino, Y. Arakawa, *et al.* *Electron. Lett.* **50**, 1377 (2014)
7. B. Jang, Y. Arakawa *et al.*, *Appl. Phys. Ex* **9**, 092102 (2016)
8. M. Nomura, N. Kumagai, S. Iwamoto, Y. Ota, and Y. Arakawa, *Nature Physics* **6**, 279 (2010)
9. A. Tandechnurat, S. Ishida, D. Guimard, M. Nomura, S. Iwamoto, and Y. Arakawa, *Nature Photonics* **5**, 91-94 (2011)
10. Y. Ota, S. Iwamoto, N. Kumagai, and Y. Arakawa, *Phys. Rev. Lett.* **107**, 233602 (2011)
11. J. Tatebayashi, S. Kako, J. Ho, Y. Ota, S. Iwamoto, and Y. Arakawa, *Nature Photonics* **9**, 501(2015)
12. J. Ho, J. Tatebayashi, S. Sergent, C. F. Fong, S. Iwamoto, and Y. Arakawa, *Nano Letters* **16**, 2845 (2016)
13. M. J. Holmes, K. Choi, S. Kako, M. Arita, and Y. Arakawa. *Nano Lett.* **14**, 982 (2014)
14. M. J. Holmes, K. Choi, S. Kako, M. Arita, and Y. Arakawa. *ACS Photonics*, **3**, 543 (2015)

## Acknowledgement:

The work is supported by JSPS KAKENHI Grant-in-Aid for Specially Promoted Research (15H05700) and NEDO project.

**Session IV-1:  
NanoBioMedecine / Nanosafety**

# Gold Nanoparticles can shuttle Ions across Phospholipid Bilayer Membranes

M. Brust,\* M. Grzelczak

University of Liverpool, Department of Chemistry, Liverpool L69 7ZD, UK

## Abstract:

Gold Nanoparticles capped with mercaptocarborane ligands have a number of unusual properties that make them of interest as membrane transporters in biological and bio-mimetic systems.<sup>1</sup> Most pertinent for this application is the ability of the particles to adjust their hydrophilicity. The particles, as prepared, are negatively charged by excess electrons in the metal core. This charge is partially balanced by Na ions that reside within the voids of the ligand shell. The resulting net charge of the particles makes them dispersible in water. Under condition of less or no net charge, the particles become less hydrophilic and, if possible, preferentially associate with the phospholipid membrane of vesicles as shown in Figure 1. In the presence of a membrane potential and a remaining small net charge of the particles, the particles can be forced by the electric field to flip across the membrane. This process can lead to the transport of ions by the particle from one side of the membrane to the other. Here we will present the results of monitoring this process using two different experimental systems. The first is based on measuring the depolarization of a vesicle membrane as Na ions are shuttled across by the particles. The second system measures electrochemically the particle-mediated charge transfer across an artificial membrane supported by a small hole in a plastic cell. Both experimental setups give consistent and complementary information, and it is evident that the particles do not act as ion channels but as membrane potential dependent electrostatic shuttles. Examples of nanoparticles carrying charge across membranes are to date very scarce.<sup>2</sup>

**Keywords:** Gold Nanoparticles, Phospholipid Membranes, Charge Transfer, Vesicles, Electrochemistry, Mercaptocarborane, Ion Shuttles, Ion Channels, Transporters, Fluorescence Spectroscopy, Membrane Potential.

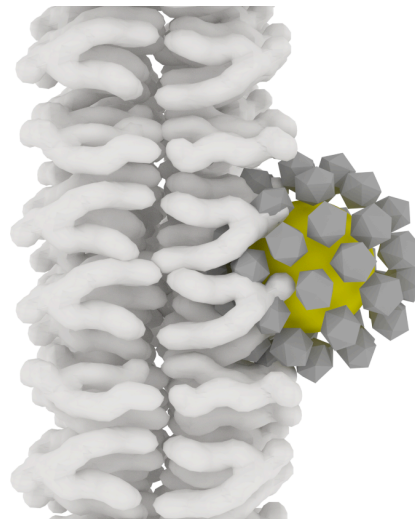


**Figure 1:** To-scale cartoon of a phospholipid bilayer membrane and a *ca.* 3 nm mercaptocarborane-capped gold nanoparticle. Note the open structure of the ligand shell, which allows for the inclusion of Li, Na or K ions counterbalanced by electronic charge in the metal core. Electrostatic charging of the particles makes them dispersible in water, while neutral particles are very hydrophobic and tend to bury into the nonpolar part of the membrane. This adaptable behaviour and the ability to carry cations in the ligand shell enables the particles to shuttle charge across the membrane.

## References:

1. Cioran, A. M., Musteti, A. D., Teixidor, F., Krpetić, Ž., Prior, I. A., He, Q., Kiely, C.J., Brust M., Viñas, C. (2012). Mercaptocarborane-capped gold nanoparticles: electron pools and ion traps with switchable hydrophilicity.. *Journal of the American Chemical Society*, 134, 212-221.
2. Grzelczak, M. P., Hill, A. P., Belic, D., Bradley, D. F., Kunstmann-Olsen, C., Brust, M. (2016). Design of artificial membrane transporters from gold nanoparticles with controllable hydrophobicity. *FARADAY DISCUSSIONS*, 191, 495-510.

# Nanomedicine for Molecular Imaging and Targeted Therapy of Cardiovascular Diseases

C.Chauvierre

INSERM Unit 698/1148 Paris, France

## **Abstract:**

One hundred years ago, Paul Ehrlich, the founder of chemotherapy, received the Nobel Prize in Physiology or Medicine. His postulate of creating ‘magic bullets’ for use in the fight against human diseases inspired generations of scientists to devise powerful molecular imaging agents and therapeutics. After the use of various synthetic polymers, natural polysaccharides have received a lot of attention in the biomedical field thanks to their biological properties and to recent progresses in polysaccharide chemistry and nanotechnologies. These new dedicated nanosystems may be designed to fight atherothrombotic pathology, which remains the main cause of morbidity and mortality in the industrialized world.

The presentation will intend to provide an overview on polysaccharide-based nanosystems as drug delivery systems and targeted contrast agents for molecular imaging with an emphasis on the treatment and imaging of cardiovascular pathologies

# Multilayer Nano-Films for Controlled Release of Therapeutics

Jinkee Hong\*, Uiyoung Han, Daheui Choi

Chung Ang University, School of Chemical Engineering and Material Science, Republic of Korea

## Abstract

Recent developments in biomedical engineering, novel cell culture techniques, and newly discovered chemicals as a replacement of the growth factors have opened new area toward the engineered technique of biomedical applications, for use in both research and clinical applications. Ideal bio-platform must be biocompatible that is to say, they should show both proper surface stability for the promotion of cell attachment and functions with drug delivery. However, plenty of challenges are still in progress, as the reason for the high compatibility of polymer film in cell culture environment and precisely controlled functional release of their drugs..

Layer-by-layer (LbL) self-assembly technic has been developed and used to prepared biocompatible multilayer films and polyelectrolyte capsules for drug delivery. Certain drug molecules, such as active proteins, cytokine, growth factors, enzymes, nucleic acids, and DNA, have been immobilized into nano-sized multilayer films. The advantages of LbL multilayer films as drug delivery systems include the sustained drug release through controlling the film physical & chemical properties, in addition multilayer films have the potential to protect drug molecules from losing their biological functions, and the film preparation process is simple and can be automated.

In this presentation, we prepared the cell friendly platform by take full advantages of LbL assembly with evenly distributed drug loading by nano-sized layer assembly. The nano-films are prepared by various materials including not only synthetic-, natural-polymers but also functional materials such as growth factors, cytokines which are resulting different film degradation profiles. These results lay a cornerstone for future studies to achieve the multi-functional nanofilms including programmed loading/release of drugs for therapeutic purposes

**Keywords:** multilayers, layer-by-layer, self-assembly, protein, growth factor, controlled release, nano-film

## References:

1. Choi, D., Hong, J., et al (2017) Cytoprotective self-assembled RGD peptide nanofilms for surface modification of viable mesenchymal stem cells, *Chemistry of Materials*, 29, 2055-2065.

# A targeted vaccine delivery system using functionalized gold nanocages and an intestinal Trojan horse

C. Yu,<sup>1,2,\*</sup> T. Tong,<sup>1</sup> Q. Wang,<sup>3</sup> C. Miller<sup>4</sup>

<sup>1</sup>Iowa State University, Department of Agricultural and Biosystems Engineering, Ames, IA 50010, USA

<sup>2</sup>National Seafood Engineering Center, Dalian Polytechnic University, Dalian, China

<sup>3</sup>Iowa State University, Department of Chemical and Biological Engineering, Ames, USA

<sup>4</sup>Iowa State University, Department of Biomedical Sciences, Ames, USA

## Abstract:

The intestinal epithelium forms an essential element of the mucosal barrier and plays a critical role in the pathophysiological response to different enteric disorders and diseases. It is also a barrier for oral vaccine delivery. Here, we demonstrated the feasibility of purposefully designing immunogen-carrying gold nanocages functionalized with  $\sigma$ -1 proteins from T1L reovirus to deliver immunogens across the mucosal barrier to enhance immunological responses. The immunogen delivery was further enhanced by a Trojan horse system. The Trojan horse system with the synergy of nanotechnology and host cells can achieve better therapeutic efficacy in specific diseases. Primary isolated intestinal stem cells were used to create these Trojan horses. M-cells, which are the targets for  $\sigma$ -1 functionalized nanocages, were induced in these Trojan horses to allow easy pass of the nano-vaccine complexes into the Trojan horses.

Here, we demonstrated this proof-of-concept intestinal Trojan horse nano-vaccine system that will have a wide variety of applications in the development of oral vaccines for infectious diseases.

**Keywords:**  $\sigma$ -1 protein, gold nanocages, nano-vaccines, intestinal stem cells.

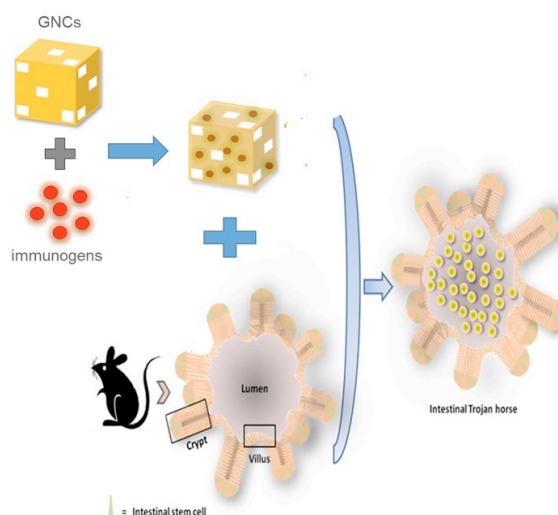


**Figure 1:** Figure illustrating the mechanism of targeted vaccine delivery using gold nanocages functionalized by  $\sigma$ -1 proteins from reovirus to deliver immunogens into Trojan horse made from small intestinal stem cell to facilitate vaccine delivery across mucosal barrier to stimulate strong immune-responses.

## References:

1. Chappell, J.D., A.E.Prota, T.S.Dermody, and T.Stehle. Crystal structure of reovirus attachment protein sigma1 reveals evolutionary relationship to adenovirus fiber. The EMBO Journal Vol 21. Nos 1 & 2 pp, 1-11, 2002.
2. Peng, H., C. Wang, X. Xu, C. Yu and Q. Wang, An Intestinal Trojan Horse for Gene Delivery. Nanoscale, DOI: 10.1039/C4NR06377E, published on line Jan 2015.
3. Ikoba, U., H. Peng, H. Li, C. Miller, C. Yu, Q. Wang, Nanocarriers in Therapy of Infectious and Inflammatory Diseases. Nanoscale, DOI: 10.1039/C4NR07682F, published online Feb 2015

# Asymmetric flow field-flow fractionation: A new approach for analysis of the protein corona

C. Weber,<sup>1</sup> K. Landfester,<sup>1</sup> S. Winzen<sup>1</sup>

<sup>1</sup>Max Planck Institute for Polymer Research Mainz, Ackermannweg 10, 55128 Mainz, Germany

## Abstract:

Targeted drug delivery by nanosized particles is a potent and promising medical concept, especially in cancer therapy. The synthesized drug carriers are injected in the blood stream and as soon as they enter any biological fluid proteins adsorb to its surface and form the so called “protein corona”. As a consequence the chemical identity of the particle only plays a minor role; instead the new biological identity is responsible for the fate of the nanoparticle in the body. (1)

To operate safely in nanomedicine, it is essential to understand and predict the *in vivo* behavior of the nanomaterial and therefore analyze the “protein corona”. However, this analysis is challenging, since there are not many methods to separate free proteins from those, which are forming the protein corona, without influencing the complex system. Right now, methods requiring a separation step provide access to the identification of only the strongly bound proteins, so that those methods have to be combined with other techniques that allow characterization directly in the biological medium. (2) Those techniques can give information about the loosely bound proteins, but not directly about the type of bound proteins.

A new approach to address this separation problem is the asymmetric flow field-flow fractionation (AF4). Hereby, very small particular species like single proteins can be separated from larger nanoparticle-protein complexes. The shear stress affecting the sample is very low in comparison to centrifugation, what makes it a rather mild method.

In our study, polystyrene-nanoparticles served as model systems which were incubated with human blood plasma.

After separation of the protein corona from free proteins by AF4, the obtained fractions are characterized with regards to size and protein composition by using dynamic light scattering, SDS-polyacrylamide gel electrophoresis and liquid-chromatography mass-spectrometry. We could show that the separation is possible using the above mentioned methods. Moreover, the composition of the protein corona separated by AF4 differed significantly from repetitive cen-

trifugation as the alternative separation method. Specifically, more serum albumin with a generally lower binding affinity was present in the extracted corona. This suggests that we were able to extract the nanoparticles with strongly as well as loosely bound proteins.

**Keywords:** nanoparticles, protein corona, drug delivery, asymmetric flow field-flow fractionation.

## References:

1. Monopoli, M. *et al.* (2012) Biomolecular coronas provide the biological identity of nanosized materials, *Nat Nanotechnol*, 7 (12), 779.
2. Winzen, S. *et al.* (2015) Complementary analysis of the hard and soft protein corona: sample preparation critically effects corona composition, *Nanoscale*, 7 (7), 2992

# Simultaneous Live Cell Monitoring and Gene Therapy with Multifunctional Carbon Nanoparticles

Morteza Aramesh<sup>1,\*</sup>

<sup>1</sup>Laboratory of Biosensors and Bioelectronics, Institute for Biomedical Engineering, ETH Zürich, Zürich 8092, Switzerland, \* maramesh@ethz.ch

## Abstract:

Light-emitting nanoparticles are emerging as promising imaging agents and therapeutic carriers for biological and medical applications.<sup>1, 2</sup> The ability to track light-emitting nanoparticles inside the living tissues and organisms opens a range of opportunities for in vivo or in vitro biosensing or targeted drug delivery.<sup>3, 4</sup> Functionalization of nanoscale light-emitting sources for selective and sensitive signalling allows observation and eventually engineering of biological processes at the subcellular level.<sup>5, 6</sup>

Detection of nucleic acids (NA) at the subcellular level is especially interesting due to their vital role in gene expression and disease diagnostics. Nanoparticle platforms with combined light-emitting properties and surface functionality are particularly suitable for intracellular NA sensing. The molecular interactions between the nanoparticles surfaces and fluorescently-tagged NA can provide a signalling system for sensing.

We report on a novel method for fabrication of carbon coated alumina nanoparticles (CANPs), using the plasma-induced carbonization method that effectively modifies the surface of the alumina nanoparticles, producing a conformal ultrathin carbon layer over the entire surfaces of the particles. The hybrid nanoparticles exhibit multiple functionalities, such as fluorescence, tuneable surface chemistry, quenching ability and water solubility. A proof of concept study is demonstrated to show that CANPs can be used as an effective fluorescent sensing platform for nucleic acid detection. The fluorescently-tagged probe nucleic acids quench upon adsorption on the surface of the CANPs and the fluorescence recovers after selective hybridization with target nucleic acids.

**Keywords:** carbon materials, surface modification, DNA sensing, cell imaging, Gene delivery.

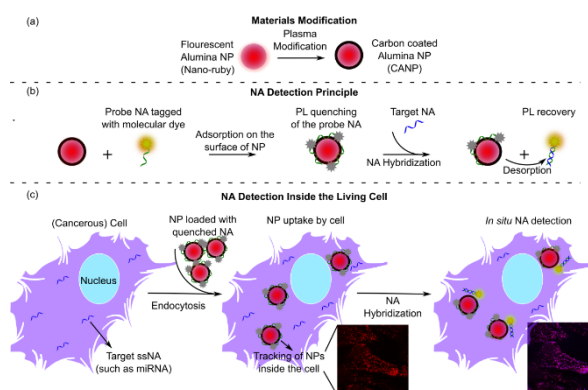


**Figure 1:** Schematic (not to scale) of the platform for simultaneous cellular monitoring and targeted gene release. NA loaded nanoparticles are internalized by the cell, and the NA releases from the surface of the particle upon hybridization with its complementary pair.

## References:

1. L. P. McGuinness, YanY, StaceyA, D. A. Simpson, L. T. Hall, MaclaurinD, PrawerS, MulvaneyP, WrachtrupJ, CarusoF, R. E. Scholten and L. C. L. Hollenberg, *Nat Nano*, 2011, 6, 358-363.
2. T.-J. Wu, Y.-K. Tzeng, W.-W. Chang, C.-A. Cheng, Y. Kuo, C.-H. Chien, H.-C. Chang and J. Yu, *Nat Nano*, 2013, 8, 682-689.
3. Z. Liu, S. Tabakman, K. Welsher and H. Dai, *Nano Res.*, 2009, 2, 85-120.
4. W. G. Kreyling, A. M. Abdelmonem, Z. Ali, F. Alves, M. Geiser, N. Haberl, R. Hartmann, S. Hirn, D. J. de Aberasturi, K. Kantner, G. Khadem-Saba, J.-M. Montenegro, J. Rejman, T. Rojo, I. R. de Larramendi, R. Ufartes, A. Wenk and W. J. Parak, *Nat Nano*, 2015, 10, 619-623.
5. G. Kucsko, P. C. Maurer, N. Y. Yao, M. Kubo, H. J. Noh, P. K. Lo, H. Park and M. D. Lukin, *Nature*, 2013, 500, 54-58.
6. O. A. Shenderova and G. E. McGuire, *Bio-interphases*, 2015, 10, 030802.

# Elaboration of nanohybrid based on titanate nanotubes for biomedical applications: new nanovectors of resveratrol derivatives

F. Sallem<sup>1,2</sup>, J. Boudon<sup>1</sup>, R. Haji<sup>3</sup>, D. Fasseur-Vervandier<sup>3</sup>, A. Megriche<sup>2</sup>, M. El Maaoui<sup>2</sup> and N. Millot<sup>1,\*</sup>

<sup>1</sup> Laboratoire Interdisciplinaire Carnot de Bourgogne ICB, UMR 6303 CNRS – Université Bourgogne Franche-Comté, 9 Avenue Alain Savary, BP 47870, 21078 Dijon, France

<sup>2</sup> Université de Tunis El Manar, Faculté des sciences de Tunis, UR11ES18 Chimie Minérale Appliquée, 2092, Tunis, Tunisie

<sup>3</sup> ICMUB UMR 6302 CNRS-Université Bourgogne Franche-Comté, Dijon, France

\* nadine.millot@u-bourgogne.fr

## Abstract:

Titanate nanotubes (TiONts) synthesized *via* hydrothermal processes have attracted extensive interest since their first synthesis owing to their physicochemical properties such a high aspect ratio<sup>1-2</sup>. In spite of their interesting physicochemical properties and their low cytotoxicity<sup>3-4</sup>, bare titanate nanotubes (TiONts) present some shortcomings such as strong aggregation and a poor suspension stability which limit their use as biomaterials. One needs to circumvent these drawbacks to turn TiONts into valuable nanohybrids<sup>5</sup>.

The aim of this work is to elaborate nanotubes-based nanohybrid materials suitable for biomedical uses. For this purpose, two essential features have been enhanced: colloidal stability and biocompatibility. The grafting of 3,4-dihydroxyhydrocinnamic acid (DHCA), amino acid 3,4-dihydroxy-L-phenylalanine (L-DOPA) and citric acid have been studied to enhance the long-term stability of TiONts under physiological conditions. A comparative study between the three types of grafting has been made.

The biocompatibility of TiONts in biological systems has also been improved through their surfaces modification with 3-aminopropyl triethoxysilane (APTES) and chitosan grafting, with two different methods.

Experimental conditions (pH, temperature, reaction time, molar ratio) have been tested and optimized in order to obtain the highest grafting efficiency for all the studied compounds. The obtained compounds were characterized by a large range of techniques (TEM, XPS, IR, Raman spectroscopy, zeta potential measurements, UV-vis, TGA, *etc.*).

Finally, an original study of TiONts functionalization with trans-resveratrol as a cancer therapeutic molecule will be also exposed with the results of the first bioassays.

**Keywords:** titanate nanotubes, surface functionalization, drug delivery, resveratrol derivative.

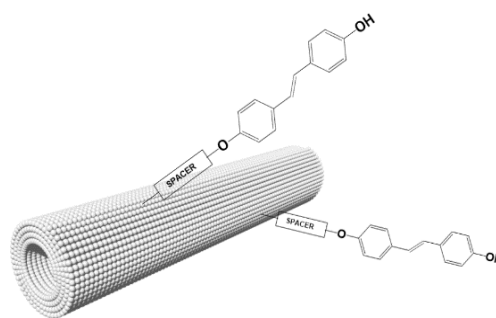


**Figure 1:** TiONts-trans-resveratrol nanohybrids

## References

1. J. Boudon, A.-L. Papa, J. Paris, N. Millot, in *Nanomedicine*, One Central Press, Manchester, 2014, pp. 403-428.
2. A.-L. Papa, N. Millot, L. Saviot, R. Chassagnon, O. Heintz, *J. Phys. Chem. C* 2009, 113, 12682
3. C. Mirjolet, A. L. Papa, G. Créhange, O. Raguin, C. Seignez, C. Paul, G. Truc, P. Maingon, N. Millot, *Radiother. Oncol.* 2013, 108, 136
4. A.L. Papa, L. Dumont, D. Vandroux, N. Millot, *Nanotoxicology* 2013, 7 (6), 1131.
5. A.L. Papa, J. Boudon, V. Bellat, A. Loiseau, H. Bisht, F. Sallem, R. Chassagnon, V. Berard, N. Millot, *Dalton Trans.* 2015, 44, 739.

# Enhancing transdermal delivery of hydrophilic compound via synergistic action of d-limonene loaded PEGylated lipid nanocarriers

W. Rangsimawong,<sup>1</sup> Y. Obata,<sup>2</sup> P. Opanasopit,<sup>1</sup> T. Rojanarata,<sup>1</sup> K. Takayama,<sup>2</sup> T. Ngawhirunpata,<sup>1\*</sup>

<sup>1</sup>Faculty of Pharmacy, Silpakorn University, Nakhon Pathom 73000, Thailand

<sup>2</sup>Department of pharmaceutics, Hoshi University, Shinagawa-ku, Tokyo 142-8501, Japan

## Abstract:

The aim of this study was to investigate the effect of d-limonene (DL) loaded three types of PEGylated lipid nanocarriers [liposomes (PL), niosomes (PN) and solid lipid nanoparticles (PSLN)] on the skin penetration of hydrophilic compound, sodium fluorescein (NaF). The physicochemical characteristics of nanocarriers and their effects on *in vitro* skin penetration were evaluated. Confocal laser scanning microscopy (CLSM) was used to visualize the penetration pathways. Fourier transform infrared spectroscopy (FTIR) was used to confirm the enhancing effect on stratum corneum lipids. The results showed that all formulations had small particle sizes in the range from 31 nm to 197 nm, which was in the order: PL-DL < PL < PN-DL < PN < PSLN-DL < PSLN. TEM image also showed the spherical in shape. This indicated that DL reduced the particle sizes of all nanocarriers. The percent entrapment efficiency of NaF was in the range from 21% to 51%, which was in the order: PL < PL-DL < PN < PSLN-DL < PN-DL < PSLN. For the skin penetration, the penetrated flux of NaF-loaded PL-DL was significantly higher (93-fold enhancement from NaF solution) than PN-DL, PL, PSLN, PN, PSLN-DL, and NaF solution, respectively. DL loaded PL and PN vesicles increased the NaF flux due to enhanced permeability of the stratum corneum. While DL loaded PSLN decreased the NaF flux, suggesting that DL might not be released from lipid particles to skin surface. CLSM images of NaF loaded PL-DL treated skin exhibited brighter fluorescence intensity of entrapped NaF and PL-DL vesicles both in the deeper skin layer and hair follicles than other formulations. The niosome and SLN formulations had little or no vesicles in the skin, suggesting that NaF may be released from these nanocarriers before permeation. For FTIR results, PL-DL provided a significant change in stratum corneum lipid, which DL-containing liposomes play an important role to deliver NaF by increasing the fluidity of stratum corneum intercellular lipid. In conclusion, PL-DL serves as a potentially effective strategy to transdermally deliver of hydrophilic compound. The combination of d-limonene (as a skin-penetration enhancer) and the

small size of liposome vesicles might provide a synergistic effect to enhance the skin permeability.

**Keywords:** skin penetration, d-limonene, lipid nanocarriers, liposomes, niosomes, solid lipid nanoparticles, hydrophilic compound

## References:

1. Rangsimawong, W., Opanasopit, P., Rojanarata, T., Ngawhirunpata, T. (2014) Terpene-containing PEGylated liposomes as transdermal carriers of a hydrophilic compound, *Bio. Pharm. Bull.*, 37(12), 1936–1943
2. Rangsimawong, W., Opanasopit, P., Rojanarata, T., Duangjit, S., Ngawhirunpata, T. (2016) Skin Transport of Hydrophilic Compound-Loaded PEGylated Lipid Nanocarriers: Comparative Study of Liposomes, Niosomes, and Solid Lipid Nanoparticles, *Bio. Pharm. Bull.*, 39(8), 1254-1262
3. Subongkot, T., Wonglertnirant, N., Songprakhon, P., Rojanarata, T., Opanasopit, P., Ngawhirunpata, T. (2013) Visualization of ultradeformable liposomes penetration pathways and their skin interaction by confocal laser scanning microscopy. *Int. J. Pharm.* 441(1-2), 151-161.

# Plasma Engineered Nanorough Substrates For Stem Cells In Vitro Culture

Melanie MacGregor-Ramiasa<sup>1,\*</sup>, Isabel Hopp<sup>2</sup>, Patricia Murray<sup>2</sup> and Krasimir Vasilev<sup>1</sup>

<sup>1</sup> Future Industries Institute, University of South Australia, Adelaide, Australia

<sup>2</sup> University of Liverpool, Liverpool, UK

## Abstract:

Stem cells based therapies are one of the greatest promise of new-age medicine due to their potential to help curing most dreaded conditions such as cancer, diabetes and even auto-immune disease. However, establishing suitable in vitro culture materials allowing to control the fate of stem cells remain a challenge.[1] Amongst the factor influencing stem cell behavior, substrate chemistry and nanotopography are particularly critical.[2] In this work we used plasma assisted surface modification methods to produce model substrates with tailored nanotopography and controlled chemistry.[3] Three different sizes of gold nanoparticles were bound to amine rich plasma polymer layers to produce homogeneous and gradient surface nanotopographies. The outer chemistry of the substrate was kept constant for all substrates by depositing a thin layer of our patented biocompatible polyoxazoline plasma polymer on top of the nanofeatures. For the first time, protein adsorption and stem cell behaviour (mouse kidney stem cells and mesenchymal stem cells) were evaluated on nanorough plasma deposited polyoxazoline thin films. Compared to other nitrogen rich coatings, polyoxazoline plasma polymer support the covalent binding of proteins.[4, 5] Moderate surface nanoroughness, in both size and density, triggers cell proliferation. In association with polyoxazoline coating, cell proliferation is further enhanced on nanorough substrates.[6] (Figure 1).

Results are discussed in term of substrates wetting properties. These findings provide valuable insights on the mechanisms governing the interactions between stem cells and their growth support.

**Keywords:** Nanotopography, stem cells, differentiation, plasma polymer, oxazoline

## Podocyte marker WT1

## Counter stain actin

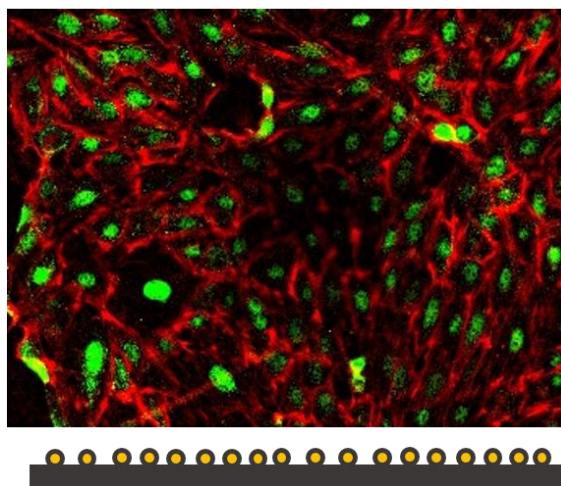


**Figure 1:** Kidney derived kidney stem cells grown on nanorough (decorated with 68 nm gold nanoparticles) plasma deposited polyoxazoline film.

## References:

1. MacGregor-Ramiasa, M.; Vasilev, K. (2016) Plasma polymer deposition: a versatile tool for stem cell research. In: *Adv. Mat. Book series, Advanced surface for stem cell research*. Wiley. Tiwari A, editor.
2. MacGregor-Ramiasa, M.; Hopp, I.; Murray, P.; Vasilev, K.; (2017) Surface Nanotopography guides Kidney-derived Stem Cells Differentiation into Podocytes. Under review *Acta Biomaterialia*.
3. Ramiasa-MacGregor, M.; Mierczynska, A.; Sedev, R.; Vasilev, K. (2016) Tuning and predicting the wetting of nanoengineered material surface. *Nanoscale*.;8:4635-42.
4. Ramiasa, M.; Cavallaro, A.A.; Mierczynska-Vasilev, A.; Christo, S.; Gleadle, J.; Hayball, J.D.; Vasilev, K. (2015) Plasma Polymerised PolyOxazoline Thin Films for Biomedical Applications. *Chem Commun*. 51, 4279
5. MacGregor-Ramiasa, M.N.; Cavallaro, A.A.; Vasilev, K. (2015) Properties and reactivity of polyoxazoline plasma polymer films. *J. Mat. Chem. B*. 3, 6327.
6. MacGregor-Ramiasa, M.N.; Cavallaro, A.A.; Visalakshan, R.M., Gonzalez, L; Vasilev, K. (2016) Plasma deposited Polyoxazoline coatings, a versatile new class of biomaterials. *CHEMECA 2016*. Adelaide,302-312.

# Providing an alternative to covalent stealth modification of nanomaterials by using tunable surfactants

S. Winzen,<sup>1,\*</sup> J. Müller,<sup>1</sup> K.N. Bauer,<sup>1</sup> J. C. Schwabacher,<sup>1</sup> D. Prozeller,<sup>1</sup> J. Simon,<sup>1</sup> V. Mailänder,<sup>1,2</sup> K. Landfester,<sup>1,\*</sup>

<sup>1</sup>Max Planck Institute for Polymer Research, Ackermannweg 10, 55128 Mainz, Germany

<sup>2</sup>Dermatology Clinic, University Medical Center Mainz, Langenbeckstraße 1, 55131 Mainz, Germany

## Abstract:

In the field of nanomedicine, nanocarriers are currently being investigated as potential drug delivery devices. Such nanocarriers will present a foreign interface to the body when applied into biological fluids such as blood. This results in the formation of a protein coating, called the 'protein corona'. In order to achieve a sufficient blood circulation time, unspecific cell uptake of the nanocarriers has to be avoided. Recently, it was shown that the covalent modification of the nanocarriers surface with poly(ethylene glycol) or biodegradable polyphosphoesters leads to an enrichment of specific 'stealth' proteins in the protein corona, which effectively reduced uptake in phagocytotic cells. (1) Furthermore, our group analyzed the influence of surfactants present on the nanocarriers surface after synthesis on the interaction with serum albumin. A significant correlation between surfactant concentration and protein binding affinity was found, which means that not only covalently bound functional groups will affect the protein corona. (2) Thus, we decided to take advantage of the properties of surfactants for providing an easy alternative to covalent 'stealth' modification. Therefore, different biodegradable poly(phosphoester) based surfactants were synthesized and characterized with regard to their thermodynamic binding properties on model nanocarriers. Depending on the length and structure of their hydrophilic and hydrophobic building blocks, their binding affinity could be maximized. It was found that with higher surfactant binding affinity also the tendency towards unspecific protein adsorption could be reduced. At the same time, all surfactants enabled an enrichment of the 'stealth' proteins clusterin and apolipoprotein A-I in the protein corona, which successfully reduced phagocytotic cell uptake. This non-covalent approach facilitates the tuning of protein adsorption and with it the biological fate of nanocarriers. Because of the surfactant adsorption principle, it can potentially be applied to any kind of nanomaterial with sufficient binding optimization. (3)

**Keywords:** nanoparticles, protein corona, surfactants, stealth effect, poly(ethylene glycol), poly(phosphoester)s, isothermal titration calorimetry.

## References:

1. Schöttler, S., Becker, G., Winzen, S., Steinbach, T., Mohr, K., Landfester, K., Mailänder, V., Wurm, F. R. (2016) Protein adsorption is required for stealth effect of poly(ethylene glycol)- and poly(phosphoester)-coated nanocarriers, *Nat. Nanotechnol.*, 11, 372-377.
2. Winzen, S., Schwabacher, J. C., Müller, J., Landfester, K., Mohr, K. (2016), Small surfactant concentration differences influence adsorption of human serum albumin on polystyrene nanoparticles, *Biomacromolecules*, 17, 3845-3851.
3. Müller, J., Bauer, K. N., Prozeller, D., Simon, J., Mailänder, V., Wurm, F. R., Winzen, S., Landfester, K. (2017) Coating nanoparticles with tunable surfactants facilitates control over the protein corona, *Biomaterials*, 115, 1-8.

# Investigating the Mechanical Properties of Soft Biomaterials Using the Atomic Force Microscopy (AFM)

I. Albaijan<sup>1</sup>, V. Sboros<sup>2,3</sup>, V. Koutsos<sup>1</sup>

<sup>1</sup>Institute for Materials and Processes, School of Engineering, The University of Edinburgh, Sander-son Building, The Kings Buildings, Mayfield Road, Edinburgh EH9 3JL, UK.

<sup>2</sup>Medical Physics, Centre for Cardiovascular Sciences, The University of Edinburgh, Edinburgh, EH16 4SB, UK.

<sup>3</sup>Department of Physics, Institute of Biological Chemistry Biophysics and Bioengineering, Heriot-Watt University, Edinburgh, EH14 4AS UK.

## Abstract:

Biomaterials are used widely in medical applications. They are used in both diagnostic and therapeutic applications. Microbubbles (MBs) are a type of biomaterials which are used in diagnosis as ultrasound contrast agents (UCAs) and in therapy for drug/gene deliveries. They encapsulate an inert gas in very thin monolayer phospholipid shell. The aim of this study was to investigate MBs from the engineering perspective, to assess their mechanical properties and their response under applied forces using the atomic force microscope (AFM) to perform a real direct mechanical test. The AFM was used with a conical-tipped cantilever at constant speed and constant force to investigate the impact of the MBs' size on their mechanical properties. Many mechanical properties were calculated, including plasticity, instability, hysteresis, adhesion forces, Young's modulus and the stiffness. Young's modulus was estimated by three different models, where two of them calculate the elasticity of the shell of the MB while the third model evaluates the elasticity of the whole MB body. A contact mode and a force spectroscopy regime were used with the AFM to acquire the force-deformation curves, as shown in Figure 1. The gradient of the linear part of the force-deformation curves expresses the stiffness of the MB.

**Keywords:** AFM, Microbubbles, Young's modulus, stiffness, Biomaterials, plasticity, instability, hysteresis, adhesion forces.

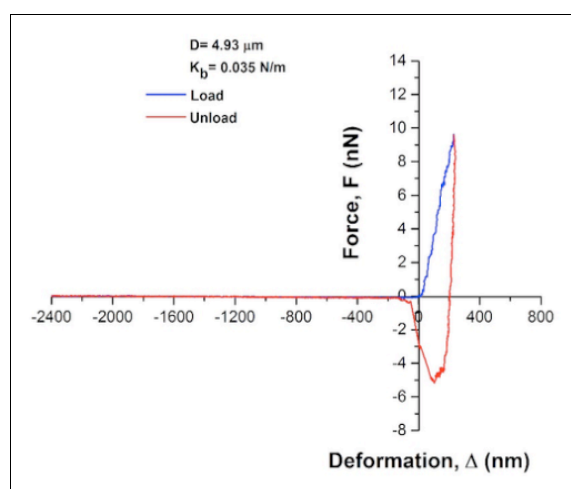


**Figure 1:** Load and unload curves with large hysteresis, where the MB behaves as a pure plastic material ( $\eta=0.95$ ).

## References:

1. E. Buchner Santos, J. K. Morris, E. Glynos, V. Sboros, V. Koutsos. Nanomechanical Properties of Phospholipid Microbubbles. *Langmuir* 2012, 28 (13), 5753–5760.
2. Abou-Saleh, R.H., et al., *Nanomechanics of lipid encapsulated microbubbles with functional coatings*. *Langmuir: the ACS journal of surfaces and colloids*, 2013. 29(12): p. 4096.
3. E. Glynos, V. Koutsos, W. N. McDicken, C. M. Moran, S. D. Pye, J. A. Ross and V. Sboros: 'Nanomechanics of biocompatible hollow thin-shell polymer microspheres', *Langmuir*, 2009, 25, (13), 7514–7522.

# Human Pancreatic Islet Secretory Fingerprint Analysis using a Microfluidic Impedance Spectroscopy Platform

Rafael Francisco Castiello<sup>1</sup>, Khalil Heileman<sup>1</sup>, Maryam Tabrizian<sup>\*1 2</sup>

<sup>1</sup>McGill University, Department of Biomedical Engineering, Montreal, Canada

<sup>2</sup>McGill University, Faculty of Dentistry, Montreal, Canada

## Abstract:

Diabetes mellitus affects 37M adults in the North America and Caribbean region [1]. This disease arises from secretory defects in the pancreatic islets of Langerhans, an endocrine cluster of cells mainly composed of  $\alpha$ ,  $\beta$ ,  $\delta$ , PP, and  $\epsilon$  cells, which cooperate to secrete hormones in response to metabolic changes [2]. Although many research groups are interested in studying the paracrine interactions between islet cells [3] or insulin and glucagon secretion [4], not much works report on monitoring a secretory fingerprint (SF) involving more than two hormones. Advances in microfluidic perfusion systems (MPS) have enabled reproduction of the islet *in vivo* environment and allow different aspects of islet physiology to be studied [5]. In parallel, non-faradaic impedance biosensors have been developed for the detection of insulin in the femto-molar concentration range using a chemically adsorbed zwitterionic polymer with attached monoclonal insulin antibodies [6]. The aim of this work is to develop a microfluidic multiplexed impedance biosensor platform for monitoring different hormones of interest secreted by islets. Interdigitated microelectrodes (IDE) with various geometries were fabricated (Figure 1). To validate the impedance measurement, a surface plasmon resonance imaging biosensor was also employed with the same immobilization strategy as the impedance sensor. To achieve maximum sensitivity, insulin was immobilized on top of a self-assembled monolayer (SAM) of a carboxyl terminated alkyl thiol and a competitive immunoassay was performed. The IDE with a 10x10 micron inter-digit spacing and electrode width led to the largest impedance change and therefore was selected for insulin sensing. Significant changes in impedance spectra between 10 and 50 KHz were observed after flowing hormones and antibodies in the microfluidic device, demonstrating the feasibility of the proposed objective. The ongoing work consists of designing a 3-layer MPS to immobilize pancreatic islets and collect their secretions. This setup allows continuous delivery of secret-

agogues to the islet while avoiding the formation of concentration gradients within the chamber. Our results confirmed that it is possible to sense insulin using impedance spectroscopy in a continuous flow regime. The proposed microfluidic platform with integrated impedance biosensors is promising for real time monitoring of a pancreatic islet SF and could be used to discriminate between healthy and diseased islets.

**Keywords:** Human Pancreatic Islets; Secretory Fingerprint Analysis; Microfluidics, Dielectric Spectroscopy, Diabetes

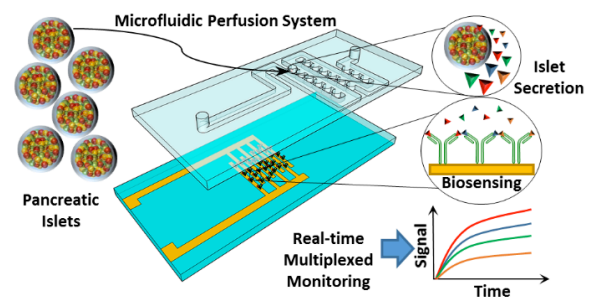


**Figure 1:** Microfluidic perfusion system for pancreatic islet secretion analysis.

**Acknowledgements:** Canadian Institutes for Health Research (CHRP, POP), National Science and Engineering Council of Canada (CHRP, Discovery, Strategic).

## References:

1. Yisahak, S.F., et al. Diabetes Atlas. Diabetes Res Clin Pract, **2013**
2. Hall, J.E.. textbook of medical physiology. Saunders, Philadelphia, **2011**.
3. Caicedo, A. Seminars in Cell & Deve. Biology. **2013**. 24(1): p. 11-21.
4. Li, Y.V. Endocrine. **2014**. 45(2): p. 178-189.
5. Castiello, F.R., K. Heileman, and M. Tabrizian. Lab on a Chip, **2016**. 16(3): p. 409-431.
6. Luo, X., et al. Analytical chemistry, **2013**. 85(8): p. 4129-41.

# Ni ions containing DNA nanowire devices

Chia-Ching Chang<sup>1,2\*</sup>, Chiun-Jye Yuan<sup>1</sup>, Wen-Bin Jian<sup>3</sup>, Yu-Chang Chen<sup>3</sup> and Massimiliano Di Ventra<sup>4</sup>

<sup>1</sup>Department of Biological Science and Technology, National Chiao Tung University, Hsinchu, Taiwan, R.O.C.

<sup>2</sup>Institute of Physics, Academia Sinica, Taipei, Taiwan, R.O.C.

<sup>3</sup>Department of Electrophysics, National Chiao Tung University, Hsinchu, Taiwan, R.O.C.

<sup>4</sup>Department of Physics, University of California, San Diego, 92093 U.S.A.

## Abstract:

DNA is a multifunctional biopolymer which can be used in the field of biomedical clinic or/and researches. Moreover, the usage of DNA has been focus in the field of nanomachines and nanoelectronics, recently, due to nanofabrication and self-assembly technology improvement. DNA exhibits high stability, adjustable conductance, self-organizing capability, programmability and vast information storage. It is an ideal linear material in the applications of nanodevices, nanoelectronics, and molecular computing. By chelating nickel ions within the base-pairs of DNA (Ni-DNA), the conductance of this complex improved dramatically. Further studies showed that nickel ions containing DNA (Ni-DNA) nanowires exhibited characteristics of memristor and memcapacitor making them a potential mass information storage and computing system. In summary, Ni-DNA has promising applications in a variety of fields, including nanoelectronics, biosensors and memcomputing.

**Keywords:** Metal ions, nucleic acid, self-assembled layers, Ni-DNA, nanodevice, nanoelectronics memristor, memcapacitor, redox induced negative resistant, memcomputing.

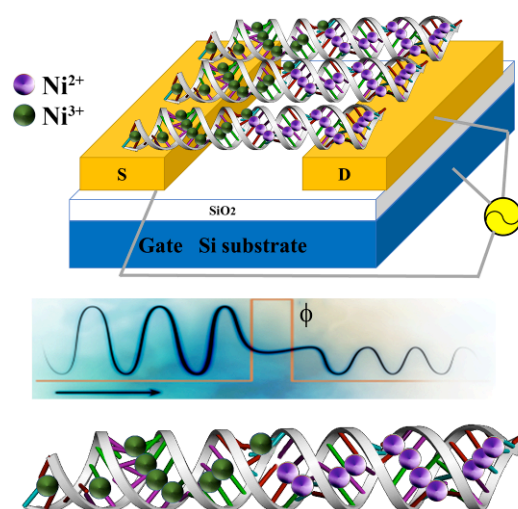


**Figure 1:** Figure illustrating the Ni-DNA devices (upper panel) and the charge transport properties of single based mismatched containing Ni-DNA. In this device the purple spheres denoted  $\text{Ni}^{2+}$  ions and the green spheres denoted  $\text{Ni}^{3+}$  ions. In the single based mismatched containing Ni-DNA device the resistance increase exponentially.

## References:

1. Pandian SRK, Yuan C.-J., Lin C.-C., Wang W.-H., and **Chang C.-C.** \*, DNA-based nanowires and nanodevices (2017) *Advances in Physics: X* 2:1, 22-34
2. Chu, H.-L., Chiu, S.-C., Sung, C.-F., Tseng, W., Chang, Y.-C., Jian, W.-B.\* , Chen, Y.-C.\* , Yuan, C.-J., Li, H.-Y., Gu, F., Di Ventra, M.; **Chang, C.-C.\*** (2014) Programmable redox state of nickel ion chain in DNA, *Nano Letters* 14, 1026-1031.

# Managing industrial accident risks in the Nanomaterials value Chain

B. Debray, A. Vignes, G. Binotto, Y. Ollier, J.M. Lacome, H.D. Le, B. Truchot

INERIS, Verneuil-en-Halatte, France

## Abstract:

Nanomaterials industry is developing, with significant amounts of materials already being produced and transported and many new applications under development. As for any industrial activity, the whole nanomaterials value chain present a series of risks, that include accident risks. Due to specific properties of nanomaterials the management of these risks raises a number of issues that need to be solved in order to ensure a sustainable development of this promising industry and waive concerns that may arise among populations and workers.

The present study was focused on nano powders, which exhibit the highest hazards. For each step of the value chain, a generic risk analysis allows to identify the main accidental scenarios that need to be taken into account : fire, explosion, massive releases and dispersion. For each scenario, it identifies the key aspects that need to be considered in the risk assessment process and the limits of currently available tools. This includes issues relative to the characterization of hazardous properties such as flammability, explosivity, dustiness, toxicity and eco-toxicity. But it also considers the limitations of existing models for air dispersion, fire and explosion modelling. The issues raised by engineering controls that can be implemented to limit risks are also outlined.

A last part of the paper is dedicated to presenting some of the solutions that are presently being developed to overcome these limitations. The first aspect refers to the characterization of physico-chemical hazards for which recent works have lead to a better understanding of the influence of agglomeration processes of the explosion violence<sup>1</sup>. They also resulted into recommendations for testing protocols which are now proposed in dedicated standardization committees.

Recent advances in modelling dispersion of nanoparticles resulting from a breach in a pneumatic transport pipe<sup>2</sup> are also briefly described as an illustration of a more general approach to better estimate the potential consequences of

accidental events involving massive release of nanoparticles.

**Keywords:** nanopowders, accident risk, air dispersion modelling, explosion, fire.

## References:

1. PORCHER, Julien ; VIGNES, Alexis ; DEBRAY, Bruno ; JANES, Agnès ; CARSON, Douglas ; FREJAFON, Emeric ; BOUILLARD, Jacques, CEN/TC 352/WG3/PG3 - Protocols for determining the explosivity and flammability of powders containing nano-objects (for transport, handling and storage), 4. International Conference on Safe Production and Use of Nanomaterials (Nanosafe 2014), 18/11/2014 - 20/11/2014, Grenoble, FRANCE
2. LE, Hong Duc ; LACOME, Jean-Marc ; VIGNES, Alexis ; DEBRAY, Bruno ; TRUCHOT, Benjamin ; FEDE, P., A few fundamental aspects related to the modelling of an accidental massive jet release of nanoparticles, DE RADEMAEKER, Eddy ; SCHMELZER, Peter - Proceedings of the 15th International Symposium on Loss Prevention and Safety Promotion in the Process Industry. Milano : AIDIC, 2016, p. 25-30 (Chemical engineering transactions, 48)

# Probing the size- and charge dependent cytotoxicity of silica nanoparticles and their application in biosensors

Marion Mathelié-Guinlet<sup>a,b</sup>, Laure Beven<sup>c</sup>, Ibtissem Gammoudi<sup>a</sup>, Fabien Moroté<sup>a</sup>, Christine Grauby-Heywang<sup>a</sup>, Marie-Hélène Delville<sup>b</sup>, Touria Cohen-Bouhacina<sup>a</sup>,

<sup>a</sup> LOMA, Université de Bordeaux, UMR CNRS 5798, 351 cours de la Libération, Talence, France

<sup>b</sup> ICMCB, UPR CNRS 9048, Unive. De Bordeaux, 87 avenue du Dr Albert Schweitzer, Pessac, France

<sup>c</sup> INRA, UMR 1332 Biologie du Fruit et Pathologie, Villenave-d'Ornon, France

## Abstract:

Despite the growing enthusiasm for nanotechnologies, nanoparticles (NPs) might put environmental safety and human health at risk, as they can interact with biological systems and affect their behavior. It is therefore essential to know their mechanisms of interactions in order not only to prevent their potential risks but also to benefit from their unique properties, such as in biosensors design. In this context, we study the cytotoxicity of silica NPs, with diverse sizes and charges, on the morphological and nanomechanical properties of *Escherichia coli* (Gram<sup>-</sup>) and *Bacillus subtilis* (Gram<sup>+</sup>) bacteria, by means of atomic force microscopy (AFM) and viability tests. These tests show that negatively charged NPs (NPs<sup>-</sup>) with a diameter  $\phi$  lower than 50-80 nm (critical diameter  $\phi_c$ ) lead to the isolation of bacteria, initially in aggregates, their interactions with cells being stronger than inter-cells ones. Conversely, positively charged NPs (NPs<sup>+</sup>), whatever their diameter, lead to a strong aggregation of the cells, due to the electrostatic interactions with the two bacteria, which are negatively charged. AFM observations specify these phenomena by also showing the antibacterial activity of such NPs. In *E. coli*, NPs<sup>-</sup> with  $\phi < \phi_c$  induce a "spherification" of the cell initially rod shaped, the formation of pore-like lesions in the outer membrane and a reorganization of its structure. All of these damages potentially lead to the cell lysis, a particularly strong one for  $\phi = 4\text{nm}$  (Figure 1A). In *B. subtilis*, although the morphology is unchanged during treatment with such NPs<sup>-</sup>, similar damage to the membrane (peptidoglycan layer) is also observed. For both strains, NPs<sup>-</sup> with a diameter larger than  $\phi_c$  have no effect on population, morphology or bacterial structure. Moreover, independently of this critical diameter, NPs<sup>+</sup> tend to favor the formation of membrane invaginations, not necessarily involving cell lysis. To conclude, we have thus shown that the decrease in diameter and a positive surface charge favor the

antibacterial activity of silica NPs. This fundamental study is currently being used to develop an electrochemical biosensor for bacteria (Figure 1B). NPs involved in such tools offer a fast, high-sensitive and low-cost way of detection. The size and charge of the NPs, previously optimized, will allow not only to detect (harmless NPs) but also to kill (toxic NPs) targeted bacteria.

**Keywords:** cytotoxicity, silica nanoparticles, bacteria, AFM, electrochemistry.

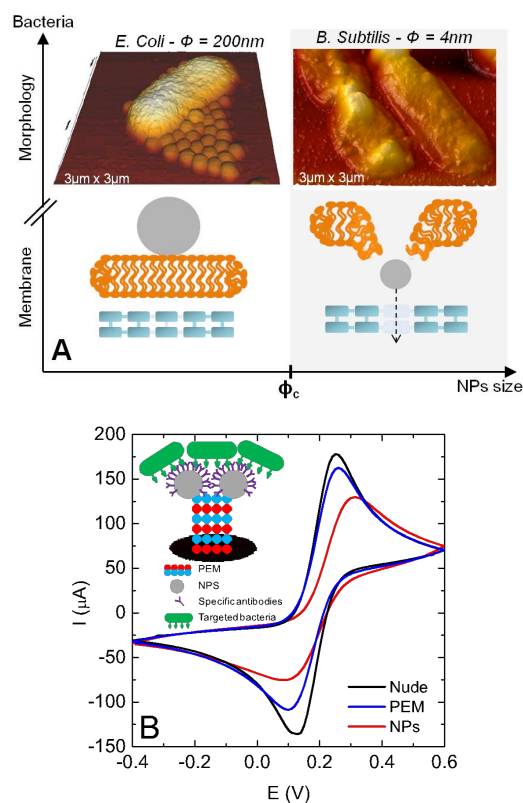


**Figure 1:** Illustration of (A) the potential antibacterial activity of silica NPs depending on their diameter and (B) their potential application in electrochemical biosensors.

# Nanogap Capacitive Biosensor For Label-Free Aptamer-Based Protein Detection

Z. Ghobaei Namhil,<sup>1\*</sup> N.T. Kemp,<sup>1</sup>

<sup>1</sup>School of Mathematics and Physical Sciences, University of Hull, , Hull, UK

## Abstract:

Recent advances in nanotechnology offer a new platform for the label free detection of biomolecules at ultra low concentrations. Nano biosensors are emerging as a powerful method of improving device performance whilst minimizing device size, cost and fabrication times. Nanogap capacitive biosensors are an excellent approach for detecting biomolecular interactions due to the ease of measurement, low cost equipment needed and compatibility with multiplex formats.<sup>1</sup> Initial work in the field was limited to high frequency measurement only, since at low frequency there is large electronic thermal noise ( $\langle V^2 \rangle = 4k_BTR$ ) from the electrical double layer (EDL). This was a significant drawback since this masked most of the important information from biomolecular interactions. A novel approach to remove this parasitic noise is to minimize the EDL impedance by reducing the capacitor electrode separation to less than the EDL thickness.<sup>2</sup> In the case of aptamer functionalized electrodes, this is particularly advantageous since device sensitivity is increased as the dielectric volume is better matched to the size of the biomolecules and their binding to the electrode surface.

In this work we have fabricated a large area vertically oriented capacitive nanogap biosensor with a 40 nm electrode separation between two gold electrodes. A silicon dioxide support layer separates the two electrodes and this is partially etched, leaving an area of the gold electrodes available for thiol-aptamer functionalization. We present results on the electrical characterization of the device as well as its capability for detecting label-free proteins.

**Keywords:** Nanogap capacitive biosensor, label-free detection, Aptamer functionalized surfaces, protein detection.

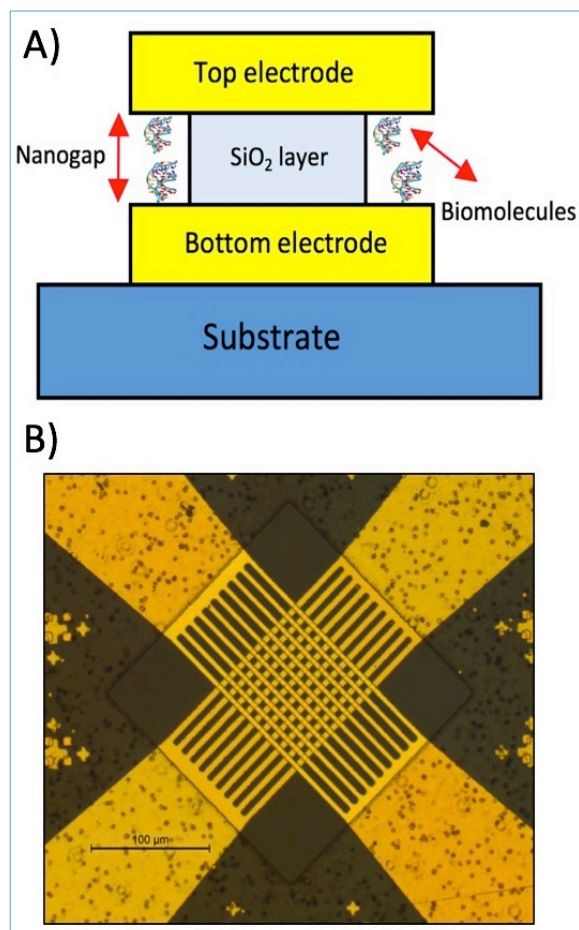


**Figure 1:** Schematic of the nanogap capacitor (A) and image of the final device (B).

## References:

1. Mannoer, M. S.; James, T.; Ivanov, D. V.; Beadling, L.; Braunlin, W. Nanogap Dielectric Spectroscopy for Aptamer-Based Protein Detection. *Biophys. J.* **2010**, *98*, 724–732.
2. Yi, M.; Jeong, K. H.; Lee, L. P. Theoretical and Experimental Study towards a Nanogap Dielectric Biosensor. *Biosens. Bioelectron.* **2005**, *20*, 1320–1326

**Focused Session on  
Nanomedicine for Cancer  
Diagnosis and Therapy**

# Magnetic Nanoparticles for magnetic hyperthermia and cytotoxic action: from the synthesis to their *in vitro* and *in vivo* characterization

Teresa Pellegrino

Drug Discovery and Development Department, Italian Institute of Technology, via Morego 30, 16163, Genoa, Italy  
e-mail: [teresa.pellegrino@iit.it](mailto:teresa.pellegrino@iit.it)

## Abstract:

Chemotherapy together with surgery are the main modalities to treat tumors in clinics. Although there are several FDA approved chemotherapeutic agents, including the most common doxorubicin, cisplatin, paclitaxel etc., they all show together with beneficial actions against tumor cells also various side effects due to their non-specific action against healthy cells.

On the other hand, the use of heat to reduce tumor mass is very ancient. Nowadays, many techniques allow to precisely focalizing the heat in very specific body regions resulting in treatments that are more efficient and minimize side effects. Magnetic nanoparticles can act as heat mediators under oscillating magnetic fields in the so-called “magnetic hyperthermia”. The field of magnetic hyperthermia has received a renewed interest since the development of colloidal preparation by non-hydrolytic methods. These approaches have shown several merits over conventional wet chemical hydrolytic processes as the magnetic nanoparticles obtained by non-hydrolytic methods can achieve a better control in terms of size, size distribution and crystallinity. All these parameters affect structural and magnetic properties of nanomaterials and thus their heat performance. Here, I will first focus on our recent progress on the combination of cubic shaped iron oxide magnetic nanoparticles with thermo-responsive coatings to combine both magnetic hyperthermia and heat-mediated drug delivery. I will cover all topics from the synthesis, to the functionalization and characterization, to the drug loading and *in vitro* characterization, to the *in vivo* long-term study (up to 5 months after hyperthermia treatment) on xenograft tumor murine model. In addition, our bio-distribution studies at the iron

dose needed for hyperthermia have indicated the absence of toxicity of such thermo-responsive iron oxide nanocubes and their *in vivo* degradation over three months.

I will also provide a comparative study of magnetic hyperthermia based on polyethylene glycole stabilized iron oxide nanocubes to another type of nanocubes made of spinel cobalt ferrites ( $\text{Co}_{0.6}\text{Fe}_{2.3}\text{O}_4$  NCs ) providing also in this case the *in vitro* and *in vivo* study. In a murine model, the slow release of cytotoxic cobalt ions together with the heating effects of the  $\text{Co}_{0.6}\text{Fe}_{2.3}\text{O}_4$  NCs under the oscillating magnetic field of clinical use, has brought to a complete tumor regression in case of locoregional treatment of small tumors (less than 1 cm in diameter).

**Keywords:** magnetic nanoparticles, thermo-responsive polymers, drug delivery, magnetic hyperthermia, photoablation

**Acknowledgements:** The author acknowledges the Italian AIRC project (Contract No. 14527), the Cariplo foundation (Contract No. 2013 0865), the EU- Horizon 2020 MSCA RISE call, (COMPASS project – 691185) and the European Research Council (ERC) (starting grant ICARO project, Contract N. 678109) for supporting this research.

# Raspberry-Like Magneto-Fluorescent Nanoassemblies as Versatile Platforms for *In Vitro* and *In Vivo* Diagnostics

J. Boucard,<sup>1</sup> J. Poly,<sup>2</sup> T. Blondy,<sup>3</sup> C. Linot,<sup>3</sup> C. Blanquart,<sup>3</sup> P. Arosio,<sup>4</sup> A. Lascialfari,<sup>4,5</sup> L. Lartigue<sup>1</sup>, E. Ishow<sup>1,2,\*</sup>

<sup>1</sup> CEISAM-UMR CNRS 6230, Université de Nantes, 44322 Nantes, France.

<sup>2</sup> IS2M-UMR CNRS 7361, Université de Haute-Alsace, 68057 Mulhouse, France.

<sup>3</sup> CRCINA, UMR 892 INSERM- UMR CNRS 6299, 44007 Nantes, France

<sup>4</sup> Università di Pavia, 27100 Pavia, Italy.

<sup>5</sup> Department of Physics, Università degli Studi di Milano and INSTM, 20133 Milano, Italy

## Abstract:

Multifunctional nanoassemblies comprising units with complementary properties have emerged as must-have systems in the field of bioimaging for the last decade. In this respect, magneto-fluorescent nanostructures represent attractive multimodal imaging agents that can bridge the gap between *in cellulo* and *in vivo* investigations since they enable high-resolution diagnosis under simple handling and addressing conditions. We have thus designed original high-payload structures comprising a shell of superparamagnetic iron oxide nanoparticles arranged around an organic core of self-assembled fluorophores. The resulting raspberry-like nanostructures *fluo@mag* (~100 nm large) could easily be functionalized with various stabilizing polyelectrolytes and proteins to target specific membrane receptors of tumor cells or bacteria. Proton NMR experiments revealed significantly distinct behaviors as a function of the polyelectrolyte coating, showing that accurate control of the polymer chain using RAFT polymerization brings high benefits. Cell endocytosis studies using ten different cell lines have evidenced strong correlations between their transcriptomic signatures and uptake capabilities as a function of the polyelectrolyte coating. All these results point out the need of a multifold parameter screening before concluding on the efficiency of functional nanomaterials as bioimaging probes.

**Keywords:** multimodal nanomaterials, fluorescent organic nanoparticles, iron oxide nanoparticles, superparamagnetism, bioconjugation, MRI.

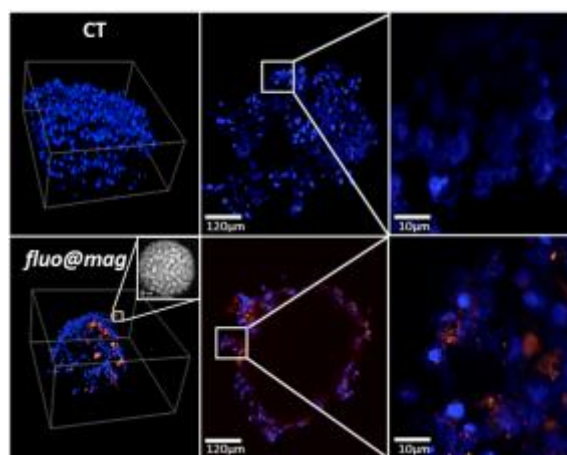


**Figure 1:** Fluorescence confocal imaging of *fluo@mag* nanoassemblies (red spots) internalized in multicellular tumor cell spheroids (DAPI-stained nuclei). Top : control cell (CT). Bottom: *fluo@mag* uptake.

## References:

1. Faucon A. et al (2016) Tuning the architectural integrity of high-performance magneto-fluorescent core-shell nanoassemblies in cancer cells, *J. Coll. Int. Sci.*, 479, 139-149.
2. Faucon A. et al (2015) Long-term fate of fluorescent organic nanoparticles as bioimaging agents in cancer cells and macrophages, *Adv. Health. Mater.*, 4, 2727-2734.

# Nano-modified natural therapeutic agents to target copper homeostasis in Neuroblastoma

O. Vittorio<sup>1,2\*</sup>, M. B. Brandl<sup>1,2</sup>, G. Cirillo<sup>3</sup>, K. Kimpton<sup>1</sup>, E. M. H. Yee<sup>4</sup>, N. Kumar<sup>4</sup>, M. Kavallaris<sup>1,2</sup>

<sup>1</sup>Children's Cancer Institute, Lowy Cancer Research Centre, UNSW Australia, Sydney, Australia; <sup>2</sup>ARC Centre of Excellence in Convergent Bio-Nano Science and Technology, Australian Centre for NanoMedicine, UNSW Australia, NSW, Sydney, Australia; <sup>3</sup>Department of Pharmacy Health and Nutritional Science University of Calabria Arcavacata di Rende, Italy; <sup>4</sup>School of Chemistry, UNSW Australia, Sydney, NSW 2052, Australia;

\*Corresponding author:

Orazio Vittorio PhD, Project Leader, Tumour Biology & Targeting Program, Children's Cancer Institute, Lowy Cancer Research Centre, UNSW Australia, Sydney, Australia; email: ovittorio@ccia.unsw.edu.au

## Abstract

Neuroblastoma is frequently diagnosed at the advanced disease stage and treatment includes high dose chemotherapy and surgery. Despite the use of aggressive therapy, survival rates are poor and children that survive the disease experience long term side effects from their treatment, highlighting the need for effective and less toxic therapies. Catechin is a natural polyphenol with anti-cancer properties and limited side effects, however its mechanism of action is unknown. Here we report that Dextran-Catechin, a conjugated form of catechin that increases serum stability, is preferentially and markedly active against neuroblastoma cells that have high levels of intracellular copper, without affecting non-malignant cells. Copper transporter 1 (CTR1) is the main transporter of copper in mammalian cells and it is upregulated in neuroblastoma. Functional studies showed that depletion of CTR1 expression reduced intracellular copper levels and led to a decrease in neuroblastoma cell sensitivity to Dextran-Catechin, implicating copper in the activity of this compound. Mechanistically, Dextran-Catechin was found to react with copper, inducing oxidative stress and decreasing glutathione levels, an intracellular antioxidant and regulator of copper homeostasis. In vivo, Dextran-Catechin significantly attenuated tumour growth in human xenograft and syngeneic models of neuroblastoma. Thus, Dextran-Catechin targets copper, inhibits tumour growth, and may be valuable in the treatment of aggressive neuroblastoma and other cancers dependent on copper for their growth.

**Keywords:** catechin; copper transporter; copper metabolism; childhood cancer

# Polymer radionuclide conjugates - the selected stories from the Institute of Macromolecular Chemistry AS CR

M. Hrubý\*, J. Kučka, J. Pánek, P. Štěpánek

<sup>1</sup> Institute of Macromolecular Chemistry, Academy of Sciences of the Czech Republic, Heyrovský Sq. 2, 162 06 Prague 6, Czech Republic; \*corresponding author, e-mail: mhruby@centrum.cz.

## Abstract:

For many important research topics in polymer science the use of radionuclides brings significant benefits concerning nanotechnology, polymer drug delivery systems, tissue engineering etc. This contribution describes important achievements of the radionuclide laboratory at the Institute of Macromolecular Chemistry AS CR in the area of polymers for biomedical applications.<sup>1</sup> Particular emphasis will be given to water-soluble polymer carriers of radionuclides such as multistage-targeted delivery system for Auger electron emitters (see Figure 1), thermoresponsive *N*-substituted acrylamide-based and poly(2-alkyl-2-oxazoline)-based polymer radionuclide carriers, thermoresponsive polymers for local brachytherapy including multimodal systems from combined immuno- and radiotherapy and polymer copper chelators for the therapy of Wilson's disease (hereditary disease characterized by copper hyperaccumulation in organism).

The authors acknowledge financial support from the Ministry of Education, Youth and Sports of the Czech Republic (grant # POLYMAT # LO1507), from the Ministry of Health of the Czech Republic (grant # 16-30544A) and from the Czech Science Foundation (grant # 16-03156S).

**Keywords:** water-soluble biocompatible polymers, thermoresponsive polymers, micelles, polymer nanoparticles, drug delivery systems, multimodal probes, noninvasive imaging, radiotherapy, positron emission tomography, single photon emission computed tomography, polymer chelators.

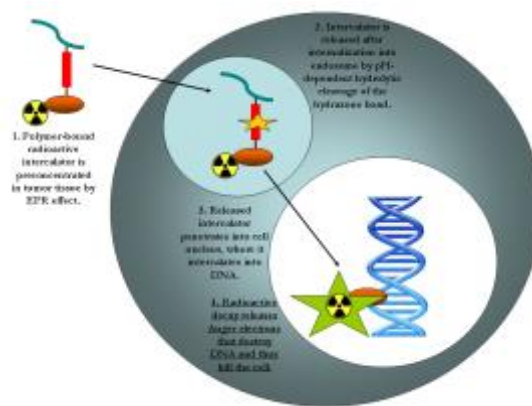


**Figure 1:** Scheme of the multistage-targeted Auger electron emitter delivery.

## References:

1. Pant, K., Sedláček, O., Nadar, R. A., Hrubý, M., Stephan, H. (2017), Radiolabelled polymeric materials for imaging and treatment of cancer: Quo Vadis? *Adv. Healthcare Mater.*, In Press, DOI: 10.1002/adhm.201601115.

# Synthesis and In Vitro Evaluation of a Cancer-Specific Dual-Targeting $^{177}\text{Lu}$ -Nanoradiopharmaceutical

A. González<sup>1,2\*</sup>, E.P. Azorin<sup>2</sup>, C.L. Santos<sup>2</sup>, B.E. Ocampo<sup>2</sup>, N. Jiménez<sup>2</sup>, F.M. Ramírez<sup>2</sup>, K. Isaac<sup>1</sup>, E. Morales<sup>1</sup> and G. Ferro<sup>2</sup>

<sup>1</sup> Universidad Autónoma del Estado de México, Departamento de Física Médica, Toluca, México

<sup>2</sup> Instituto Nacional de Investigaciones Nucleares, ININ, Ocoyoacac, México

## Abstract:

For tumor growth and metastasis, angiogenesis process must be present during the cancer development<sup>1</sup>. The receptors overexpressed on the surface of cancer cells during angiogenesis process represent promising targets for cancer diagnosis or therapy<sup>2</sup>.

The aim of this research was to synthesize and characterize the physicochemical properties of a nanoconjugate labelled with  $^{177}\text{Lu}$  and formed by gold nanoparticles (AuNP), the nuclear localization peptide (NLS), the RGD tripeptide sequence and an aptamer analogous to Pegaptanib. The in vitro potential of this compound ( $^{177}\text{Lu}$ -AuNP-NLS-RGD-Aptamer) as cancer-specific dual targeting probe was also evaluated. The receptors overexpressed on the surface of cancer cells such as  $\alpha(v)\beta(3)$  integrins and the Vascular Endothelial Growth Factor (VEGF), both involved in the angiogenesis process, are the main targets of this theranostic nanoconjugate. RGD sequence specific recognize integrins and the same occurs between the aptamer and the VEGF<sup>3</sup>. These two bonds have also high affinity and stability, being one of the reasons for designing this nanoconjugate. Gold nanoparticles were functionalized with DOTA-GGC, NLS-RGD and the aptamer. In all cases by instant reaction of thiol groups with AuNP surface.  $^{177}\text{Lu}$  was later incorporated into the molecule through DOTA.

The chemical characterization of the DOTA-GGC-AuNP-NLS-RGD-Aptamer nanoconjugate was carried out by UV-Vis, Infrared spectroscopies. The size and size distribution were determined by Dynamic Light Scattering and TEM images. After  $^{177}\text{Lu}$  labelling, the stability in human serum, and in vitro affinity assays (integrins and VEGF molecular targets) were evaluated. In vitro binding studies were carried out in C6 glioblastomas cancer cells. Epifluorescence studies demonstrated the internalization of the radioconjugated into the cell.  $^{177}\text{Lu}$ -AuNP-NLS-RGD-Aptamer may be useful as an imaging agent for cancer tumors

overexpressing integrins and also VEGF as well as targeting radiotherapy.

**Keywords:** Cancer detection and therapy, nuclear medicine, angiogenesis, molecular targeting, Nanoradiopharmaceutical.

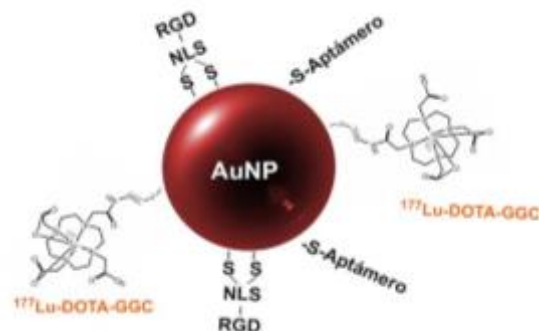


**Figure 1:** Overall scheme of the multifunctional Cancer-Specific Dual-Targeting system of  $^{177}\text{Lu}$ -AuNP-NLS-RGD-Aptamer.

## References:

1. Lopes-Bastos B, Jiang W and Cai J.(2016), Tumour-Endothelial Cell Communications: Important and Indispensable Mediators of Tumour Angiogenesis. *Anticancer research*. 36: 1119-1126.
2. Ferro-Flores G., Ocampo-García B.E., Santos-Cuevas C.L. *et al.* (2015), Theranostic Radiopharmaceuticals Based on Gold Nanoparticles Labeled with  $^{177}\text{Lu}$  and Conjugated to Peptides. *Curr. Radiopharm.* 8, 150-159.
3. Ferrera, N. Gerber, H. P. LeCounter, J. The biology of VEGF and its receptors. *Nature medicine*. **2003**. 9(6): 667-676.
4. Vilchis-Juárez A., Ferro-Flores G., Santos-Cuevas C. *et al.*, (2014) Molecular Targeting Radiotherapy with Cyclo-RGDfK(C) Peptides Conjugated to  $^{177}\text{Lu}$ -Labeled Gold Nanoparticles in Tumor-Bearing Mice. *J. Biomed. Nanotechnol.* 10(3): 393-404.

# Upconverting nanophosphors for bioimaging: Preparation Strategies for Hydrophilic Colloidal Stable Particles

A. Nsubuga, T. Joshi, M. Sgarzi, H. Stephan

Institute of radiopharmaceutical Cancer Research, Helmholtz Zentrum Dresden-Rossendorf, Germany

## Abstract:

Lanthanide doped nanophosphors are capable of converting near-infrared (NIR) radiation into visible light. Biological tissues have an “optical transparency window” in the near-infrared (NIR) range of 650–950 nm which allows a deeper light penetration and reduced photodamage effects, but also offers lower autofluorescence, reduced light scattering, and phototoxicity.<sup>(1)</sup> In this study we have focused on the controllable synthesis of sub-10 nm upconverting nanoparticles that can be excited by 800 nm lasers.

The preparation of ultrasmall, monodisperse and hydrophilic UCNPs that display intense luminescence remains a challenging issue, as smaller UCNPs generally have lower luminescence efficiency. The decrease of the luminescence is due to quenching effects caused by surface defects, ligands and solvents that possess high phonon energy. Only a few examples of ultrasmall and hydrophilic UCNPs have been reported.<sup>[2-4]</sup> In this work we report a convenient and versatile strategy to dramatically enhance the luminescence efficiency of sub-10 nm particles by using organic dyes and functional phospholipids. With this approach, the dye molecules function as antennas, absorbing incident light and transferring their excitation energy to lanthanide ions in the UCNP core (figure 1). The assemblies are all water-soluble and fluorescent in the visible region of the spectrum when excited with 800 nm near-infrared laser.

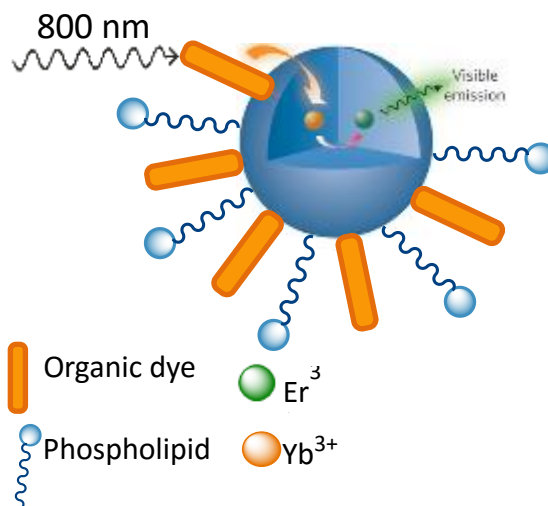
Furthermore the luminescence properties can be tuned by varying the dopants and relative proportions.

The size and shape of the particles will be influenced by controlling the reaction time and temperature. This study will also allow establishing information about the formation of protein corona for ultrasmall UCNPs.

**Keywords:** : Upconversion, lanthanide, Sub 10nm particles, surface functionalization, organic dye

**Figure 1:** Schematic design illustrating energy transfer pathway from the dye to the lanthanide ions<sup>+</sup>

in the core. The  $\text{Er}^{3+}$  ion accepts the energy from the excited  $\text{Yb}^{3+}$  ion, giving rise to upconverted emission



## References:

1. Y. Chen, H. L. Qiu, P. N. Prasad, X. Chen, *Chem. Rev.* **2014**, *114*, 5161-5214.
2. Q. Liu, Y. Sun, T. S. Yang, W. Feng, C. Li, F. Li, *J. Am. Chem. Soc.* **2011**, *133*, 17122-17125.
3. N. J. J. Johnson, W. Oakden, G. J. Stanisz, R. S. Prosser, F. C. J. M. van Veggel, *Chem. Mater.* **2011**, *23*, 3714-3722.
4. W. Wei, G. Chen, A. Baev, G. S. He, W. Shao, J. Damasco, P. N. Prasad, *J. Am. Chem. Soc.* **2016**, *138*, 15130–15133

# Active targeting and *in vivo* multimodal imaging of renally excretable polymer nanoparticles

K. Pant<sup>1</sup>, K. Zarschler<sup>1</sup>, C. Neuber<sup>1</sup>, J. Pufe<sup>1</sup>, J. Pietzsch<sup>1,2</sup>, J. Steinbach<sup>1,2</sup>, R. Haag<sup>3</sup> and H. Stephan<sup>1</sup>

<sup>1</sup>Helmholtz-Zentrum Dresden-Rossendorf, Institute of Radiopharmaceutical Cancer Research, Dresden, Germany

<sup>2</sup>Technische Universität Dresden, Department of Chemistry and Food Chemistry, Dresden, Germany

<sup>3</sup>Freie Universität Berlin, Department of Chemistry and Biochemistry, Berlin, Germany

## Abstract:

Multimodal imaging represents a strategy to integrate multiple modalities on a single carrier molecule so as to increase the detection sensitivity and to obviate the need to administer compounds with different pharmacokinetics. In this regard, dendritic polyglycerols are highly biocompatible nanoscale scaffolds with multiple attachment sites, anti-fouling properties and small size (2-20 nm).<sup>1</sup> The great versatility of the dendritic polyglycerols allows to fine tune physicochemical parameters such as the size, water solubility, surface charge that are relevant for the successful preparation of theranostic systems. Previous experiments showed that the dendritic polyglycerols (>10kDa) show a fast renal clearance with negligible uptake in the mononuclear phagocytic system (MPS) organs such as the liver and spleen.<sup>2-3</sup>

The purpose of this work to design a PET/OI dual modal construct based on dendritic polyglycerols for epidermal growth factor receptor (EGFR) targeting. In this regard, a one-pot strategy was employed for simultaneous attachment of fluorescent labels for optical imaging (cy3/cy7) and macrocyclic chelators based on a 1,4,7-triazacyclononane system for <sup>64</sup>Cu (PET tracer) to thiol anchoring groups of the dPGs. A small camelid single-domain antibody (sdAb) representing a potential recognition agent for EGFR as targeting vector was attached (**1**). In parallel, a probe with similar surface characteristics but an EGFR unspecific sdAb (control) was synthesized (**2**). The conjugates were purified using affinity chromatography, which selectively separates the antibody-conjugated multimodal conjugates. *In vitro* and *in vivo* studies were conducted to assess its diagnostic potential. The *in vitro* results revealed a highly specific receptor mediate uptake of **1** in EGFR expressing A431 and FaDu cell lines using confocal microscopy and radio detection.

Intravenous injection of **1** and **2** on mouse xenografted models studies using PET and optical imaging revealed an overwhelming tumor accumulation of the EGFR-specific **1** in comparison to the EGFR-unspecific **2** and a minimum off-target accumulation of both conjugates. These results unveil the potential of dendritic polyglycerols as

efficient multimodal platforms for theranostic applications.

**Keywords:** dendritic polyglycerols, cancer, biodistribution, radiolabeling, renal clearance, protein corona, biomedical applications.

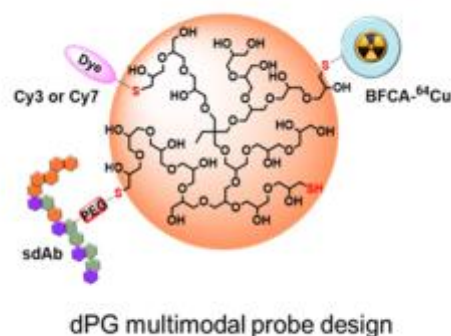


**Figure 1:** Figure illustrating the design of the multifunctional dPG based imaging probe containing macrocyclic chelators for <sup>64</sup>Cu-PET, fluorescence dye for optical imaging and EGFR targeted sdAb or a non-targeted sdAb as a control. Right: Optical imaging of A431 xenograft tumor mice after intravenous injection of the multimodal probes. Ki: Kidneys and Tu: Tumor.

## References:

1. Calderon, M., Quadir, M. A.; Sharma, S. K.; Haag, R. (2010), Dendritic polyglycerols for biomedical applications. *Adv. Mater.*, 22, 190-218.
2. Pant, K.; Gröger, D.; Bergmann, R.; Pietzsch, J.; Steinbach, J.; Graham, B.; Spiccia, L.; Berthon, F.; Czarny, B.; Devel, L.; Dive, V.; Stephan, H.; Haag, R. (2015), Synthesis and biodistribution studies of H-3- and Cu-64-labeled dendritic polyglycerol and dendritic polyglycerol sulfate. *Bioconjugate Chem.*, 26, 906-918.
3. Reichert, S.; Welker, P.; Calderon, M.; Khandare, J.; Mangoldt, D.; Licha, K.; Kainthan, R. K.; Brooks, D. E.; Haag, R. (2011), Size-dependant cellular uptake of dendritic polyglycerol. *Small*, 7, 820-829.

# Mannan conjugates for multimodal imaging

M. Rabyk,<sup>1\*</sup> M. Jiratova,<sup>2</sup> A. Galisova,<sup>2</sup> D. Jirak,<sup>2</sup> M. Hruby<sup>1</sup>

<sup>1</sup> Institute of Macromolecular Chemistry, Academy of Sciences of the Czech Republic, Prague, Czech Republic

<sup>2</sup> Institute for Clinical and Experimental Medicine, Academy of Sciences of the Czech Republic, Prague, Czech Republic

## Abstract:

The aim of this work is development of new hybrid polymer noninvasive multimodal imaging platform based on natural polysaccharide mannan (MN) (Figure 1). Mannan is a biocompatible and biodegradable polysaccharide that could be easily functionalized in order to incorporate imaging moieties with strong self-targeting effect *via* DC-SIGN receptor. Therefore, MN is preferably accumulated in the macrophages and dendritic cells overexpressing the DC-SIGN receptors<sup>1</sup>, what is useful in diagnosis of the sentinel lymph nodes and metastases. The polysaccharide was decorated with functional groups (such as fluorophores and gadolinium complexes for magnetic resonance (MR) imaging) in order to be used as a polymer carrier for solid tumor diagnostics or therapy. Grafting with synthetic polymer decreases the biodegradation rate of polysaccharide and allows easy functionalization of the polymer grafts with active payload. Therefore, mannan was reacted with active poly(2-methyl-2-oxazoline) chains, obtained by ring-opening cationic polymerization in anhydrous acetonitrile, followed with a radical-initiated thiol-click chemistry with cysteamine in order to prepare primary amino group containing mannan-based conjugate. The latter precursor was reacted with NHS ester of IR800CW dye as infrared active fluorescence label and NHS ester of MRI T<sub>1</sub> contrast agent – Gd<sup>3+</sup>-DOTA. The mannan-based conjugates with (MN-Ox) or without oxazoline (MN) were characterized and compared with a commercially available contrast agent (gadoterate meglumine) by <sup>1</sup>H-MR and fluorescence imaging. *In vivo* distribution and accumulation of the probes was examined in animals showing accumulation in sentinel lymph nodes.

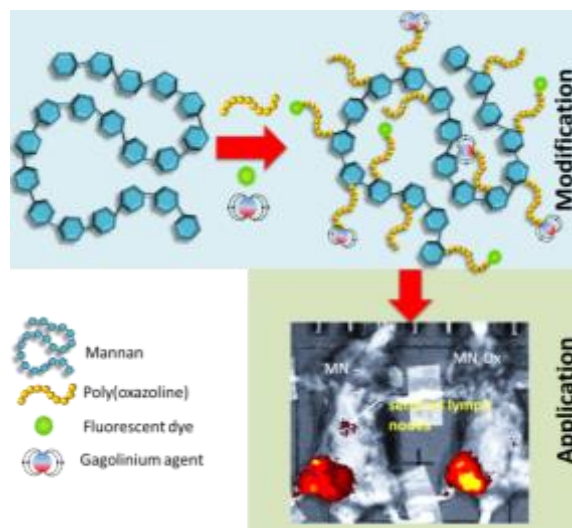


**Figure 1:** Modification and application of mannan-based conjugates as a multi imaging contrast agents.

**Keywords:** polysaccharide modification, mannan, multimodal imaging, biomedical applications.

## References:

1. Cui Z. et al. Drug Dev Ind Pharm, 29(6), 2003.

## Acknowledgment

The authors acknowledge financial support from the Ministry of Education, Youth and Sports of the Czech Republic (grant # LM2015064), from the Ministry of Health of the Czech Republic (grant # 15-25781a) and from the Czech Science Foundation (grant # 16-03156S).

# Biophysical modelisation of gold nanoparticles radiosensitizing effects

F. Poignant<sup>1</sup>, B. Gervais<sup>2</sup>, A. Ipatov<sup>1,\*\*</sup>, C. Monini<sup>1</sup>, M. Cunha<sup>1,\*</sup>, P.J. Lartaud<sup>1</sup>, T. Bacle<sup>1</sup>, E. Testa<sup>1</sup>, M. Beuve<sup>1</sup>

<sup>1</sup> Institut de Physique Nucléaire de Lyon, Lyon, France

<sup>2</sup> CIMAP, Caen, France

\* The author is now at Columbia University, New York, USA

\*\* The author is now at Saint Petersburg Polytechnical University, Saint Petersburg, Russia

## Abstract:

The main challenge of radiotherapy is to focus the irradiation dose in cancer cells while preserving the healthy cells surrounding the tumor. Among the different strategies, the use of radiosensitizers aims to amplify the destructive effects of dose in the tumor<sup>1</sup>. Nanoparticles of heavy metals such as gold and gadolinium, are particularly promising radiosensitizers. If their radiosensitizer effect has been studied for about two decades, the origin of this phenomenon is yet quite unknown and barely quantified.

Litterature suggests that irradiation would generate a physical effect called Auger cascades. This effect would lead to a local increase secondary electrons around the nanoparticle, thus implifying the critical cell damages of direct sensible molecules such as DNA, or through a boost of free radicals. These effects are produced at nanometric scales and at very short time ( $10^{-15}$  to  $10^{-12}$  seconds) but have consequences on the patient scale.

Because this physical and chemical effects are not directly observable, the simulation tool is therefore mendatory to better understand the initial mecanisms. Our goal is to first develop a simulation that enables us to calculate the spatial dose and free radicals distribution around the nanoparticles, and to quantify the induced boost<sup>2,3</sup>. Secondly, we want to inject the results in the model *NanoX*<sup>4</sup>, originally developed in IPNL to calculate the biological dose in hadrontherapy. These two allow us to assess the the quality of our models, and the relevance of the scenarii offered in literature. The final aim is to guide the development of the nanoparticles and, if possible, to help to planify clinical treatment of nanoparticle-based radiotherapy.

**Keywords:** modelisation, nanoparticles, radiosensitizer, nanometric scale

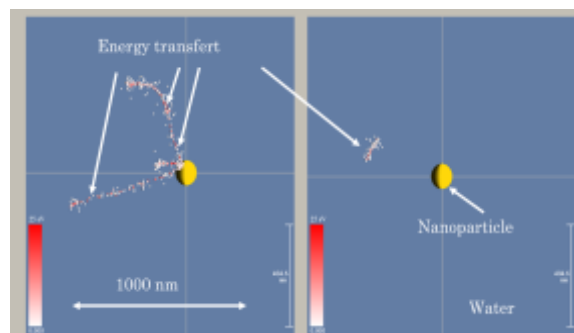


**Figure 1:** Illusatration of the difference between two tracks (energy transfers) when a 20 keV photon originally interacted in the gold nanoparticle (left) through a photoelectric effect or in water (right) through a Compton effect.

## References:

1. J. F Hainfeld et al., 2017, *Nanomedicine*, 1601-1609
2. B. Gervais et al., 2006, *Radiat. Phys. Chem.* **75** 493–513
3. B. Gervais et al., 2005, *Chemical Physics Letters*, **410** 330-334
4. M Cunha et al, 2017, *Phys. Med. Biol.* **62** 1248

# Thermal and biological study of benignly synthesized silver/reduced graphene oxide nanocomposites

Shantilal S. Mehetre, Man Singh,\*

Central University of Gujarat, School of Chemical Sciences, Gandhinagar, Gujarat, India

## Abstract:

Graphene oxide (GO) is a pseudo 2D Nobel material useful for constructing wide variety of graphene-based structures known for innumerable captivating properties. Here, we have benignly synthesized silver adorned reduced graphene oxide (GrO) greenish gray (GG-GrO) and navy blue (NB-GrO) colored nanocomposites by tuning silver nitrate proportions with the extract of an indigenous spice plant *Murraya Koenigii*. The reduction of graphene oxide (GO) and silver nitrate simultaneously accomplished by high contents of extract including polysaccharides as potent reducing agent and other phytoconstituents<sup>4</sup> to produce GG-GrO and NB-GrO nanocomposites. The properties of these nanocomposites were characterized by UV-Vis spectroscopy, SEM-EDS, HRTEM, XRD, FT-IR, TGA, DSC and XPS techniques. These nanocomposites are thermally stable compare to GO and were evaluated for anticancer properties against human lung cancer cell line A549 with adriamycin as the reference drug. A relationship between the amount of silver nanoparticles on the surface of GrO and the anticancer activity of nanoparticles was observed, with an increase in the concentration of silver nanoparticles on the surface of GrO led to enhanced anticancer activity of the nanocomposites. Surprisingly, these nanocomposites were found biocompatible with microbes like *Escherichia coli*, *Staphylococcus aureus*, *Klebsiella pneumoniae*, *Bacillus subtilis*, *Candida albicans*. The combined anticancer and microbial compatibility make these nanocomposites a promising candidate for future health cautions.

**Keywords:** pseudo 2D Nobel material, reduced graphene oxide, spectroscopy, indigenous spice plant extract, anticancer activity of nanoparticles, microbial compatibility.

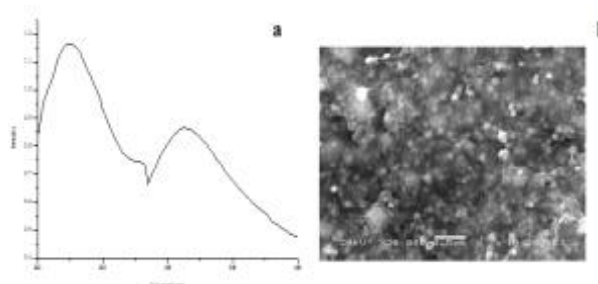


**Figure 1:** Figure (a) NB-GrO nanocomposite illustrating the UV-vis spectra having characteristic peaks at at 250 nm and 420 nm and (b) SEM-EDS image GG-GrO nanocomposite visualising silver nanoparticles embedded in and on GrO sheets of benignly synthesized nanocomposites.

## References:

1. Xianjue Chen, A., Li W., Luo, D., Huang, M., Wu, X., Huang, Y., Hwa Lee S., Chen, X., and. Ruoff Rodney, S. (2017), Controlling the Thickness of Thermally Expanded Films of Graphene Oxide, *ACS Nano*, 11, 665–674.
2. Choi, W., Lahiri, I., Seelaboyina, R., Kang, Y S. (2010), Synthesis of Graphene and Its Applications: A Review, *Crit. Rev. Solid State*, 35, 52-71
3. Huang, X., Qi, X., Boey, F., Zhang, H. (2012), Graphene-based composites, *Chem. Soc. Rev.*, 41, 666-686
4. Philip, D., Unni, C., Aromal, S A., Vidhu, V K. (2011), *Murraya koenigii* leaf-assisted rapid green synthesis of silver and gold nanoparticles, *Spectrochim Acta A Mol Biomol Spectrosc*; 78, 899-904.

**Session V:  
NanoMaterials for Energy**

# Nanofluidic transport in nanotubes and applications to osmotic power

L. Bocquet

Ecole Normale Supérieure, Paris, France

## **Abstract:**

Osmosis describes the flow of water across semi-permeable membranes powered by the chemical free energy contained in salinity gradients. It is a fundamental transport process for water in all living systems, and its applications are countless. While osmosis can be expressed fundamentally in simple terms via the van't Hoff ideal gas formula for the osmotic pressure, it is a subtle phenomenon taking its roots in the interactions occurring at the scale of the membrane nanopores.

In this talk, I will discuss some molecular views of osmosis, which will be used in various contexts in order to harvest this powerful transport phenomenon. I will explore in particular the phenomenon of diffusio-osmosis, which is an interfacially driven transport phenomenon allowing for osmotic flow without the need of semi-permeable membranes.

I will illustrate these concepts on the basis of various experiments using individual nanopores and nanotubes made of carbon and boron-nitride materials. I will in particular highlight applications to osmotic energy harvesting using various materials.

# Nanofluids the New Revolution in Thermal Science and Engineering

Muataz Hussien<sup>1&2</sup>

<sup>1</sup>College of Science and Engineering, Hamad bin Khalifa University (HBKU), Qatar Foundation, PO Box 5825, Doha, Qatar

<sup>2</sup>Qatar Environment and Energy Research Institute (QEERI), Hamad bin Khalifa University (HBKU), Qatar Foundation, PO Box 5825, Doha, Qatar

## Abstract:

Heat transfer is an important area of study in thermal engineering. Selection of a suitable heat transfer fluid for heat dissipation is an important consideration in the thermal design of heat exchangers. Heat transfer fluid is one of the critical parameters, which affects the cost, and size of heat exchanger systems. Conventional fluids like water and oils have limited heat transfer potentialities. Different research groups around the world sense the need for development of new classes of fluids with enhanced heat transfer capabilities. The advances in nanotechnology have made it possible to manufacture metal and metal oxide particles on a Nano-dimensional scale. Nano particles are considered to be new generation material having potential applications in the heat transfer area.

Any host liquid, which contains nanoparticles in a suspended state, is known as a nanofluid. Nanofluids are two-phase fluids of solid-liquid mixtures and are considered to be new generation heat transfer fluids. In the recent past nanofluids have emerged as promising thermo fluids for heat transfer applications. The thermal conductivity property of nanofluids is expected to be greater than that of the base liquids. Nanofluids, on the other hand, offer many advantages over single-phase pure fluids and suspensions with micro particles. Nanofluids are considered to be an alternate and new generation of liquids for heat energy transport and can be employed as heat transfer fluids in heat exchangers in place of pure single-phase fluids. The applications of nanofluids for heat transfer include radiators in automobiles, components in chemical engineering and process industries, solar water heaters, refrigeration units, and in the cooling of electronics devices. The main objective of obtaining heat transfer enhancement-using nanofluids is to accommodate high heat fluxes and, hence, to

reduce the cost and size of heat exchangers which, in turn, results in the conservation of energy and material.

Over the last several years, considerable research has been carried out in order to develop heat transfer enhancement methods. Generally, many additives have been used to increase the heat transfer features of base fluids. Therefore, nanofluids may be perfectly suited in actual applications as their use may have little increases in pressure drop, and may positively change the heat transfer characteristics and transport properties of the fluid. Due to the fine nature of these Nano-particles, nanofluids behave as a single phase rather than as a solid-liquid mixture, multiphase (figure 1).

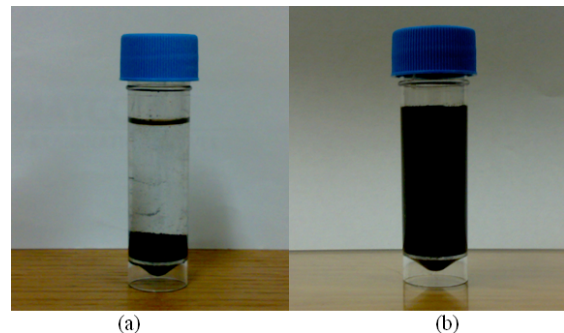


Figure 1: Figure **Error! No text of specified style in document.**2: In (a) CNTs rapidly settle without surfactant, whereas in (b) CNTs are well dispersed in water with surfactant.

# The role of the base fluid arrangement to enhance heat transfer of Ag-Nanofluid used for concentrating solar power plants

Elisa I. Martín,<sup>1,\*</sup> Antonio Sánchez-Coronilla,<sup>2</sup> Javier Navas,<sup>3</sup> Roberto Gómez-Villarejo,<sup>3</sup> Teresa Aguilar,<sup>3</sup> Juan Jesús Gallardo,<sup>3</sup> Rodrigo Alcántara,<sup>3</sup> Desireé De los Santos,<sup>3</sup> Iván Carrillo-Berdugo,<sup>3</sup> Concha Fernández-Lorenzo<sup>3</sup>

<sup>1</sup>Seville University, Department of Chemical Engineering, Seville, Spain

<sup>2</sup>Seville University, Department of Physical Chemistry, Seville, Spain

<sup>3</sup>Cádiz University, Department of Physical Chemistry, Cádiz, Spain

## Abstract:

Concentrating solar power is one of the most interesting alternatives to conventional energy sources nowadays. Improving the thermophysical properties of the fluids used is of particular interest for enhancing the heat transfer processes that take place. In these plants as this should result in an increase in their overall efficiency. In this sense, the use of nanofluids has been shown to be an interesting option for enhancing the thermal properties of base fluids. In this work, nanofluids based on a eutectic mixture of diphenyl oxide and biphenyl as the base fluid were prepared varying Ag nanoparticle concentrations, and their physical and chemical stability, viscosity, isobaric specific heat and thermal conductivity were characterized. According to the experimental system, molecular dynamic calculations were performed to reach a better understanding of the nanofluid system at a molecular level. The isobaric specific heat and thermal conductivity values followed the same experimental tendency, which validates the methodology proposed. An analysis of the radial distribution functions (RDFs) and spatial distribution functions (SDFs) shows that there is a first layer of base fluid molecules around the metal in which the oxygens play an important role. This first layer encourages the directionality of the movement in the heart of the nanofluid, which leads to enhanced thermal properties.

**Keywords:** nanofluids, nanoparticles Concentrating Solar Power, heat transfer fluid, specific heat, thermal conductivity, Dynamic Molecular, radial distribution functions, spatial distribution functions.

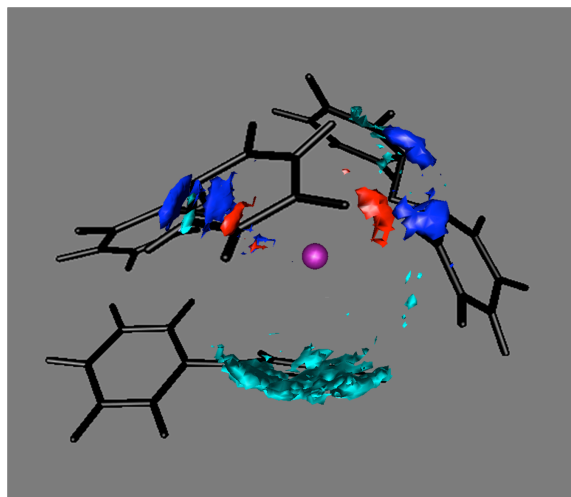


**Figure 1:** SDF for the Ag-nanofluid system in a radius of 4 Å with the Ag in the centre (purple colour). The red coloured spatial distribution is assigned to O atoms, the blue coloured spatial distribution corresponds to the C atoms linked to the O atoms of the diphenyl oxide, and the sky-blue correspond to the ring C atoms, from the benzene rings of diphenyl oxide and biphenyl.

## References:

1. Yoo, D. H., Hong, K. S., Yang, H. S. (2007) Study of thermal conductivity of nanofluids for the application of heat transfer fluids, *Thermochim. Acta*, 455,66-69.
2. Singh, D., Timofeeva, E. V., Moravek, M. Cingarapu, S. R., Yu, W. H., Fischer, T., Mathur, S. (2014) Use of the metallic nanoparticles to improve the thermophysical properties of the organic heat transfer fluids used in concentrated solar power, *Sol. Energy*, 105, 468-478.

# Topology optimized nanoparticles for near-infrared enhanced photon upconversion

Joakim Vester-Petersen<sup>1</sup>, Rasmus E. Christiansen<sup>2</sup>, Brian Julsgaard<sup>3</sup>, Peter Balling<sup>3</sup>  
Ole Sigmund<sup>2</sup>, Søren P. Madsen<sup>1</sup>

<sup>1</sup>Department of Mechanical Engineering, Aarhus University, Inge Lehmanns Gade 10,  
8000 Aarhus C., Denmark

<sup>2</sup>Department of Mechanical Engineering, Technical University of Denmark, Nils Koppels Allé,  
Building 404, 2800 Kgs. Lyngby, Denmark

<sup>3</sup>Department of Physics and Astronomy, Aarhus University, Ny Munkegade 120,  
DK-8000 Aarhus C, Denmark

## Abstract:

This work is a part of the SunTune project which addresses efficiency improvements of solar modules by manipulating the spectrum of sunlight to better match the range of efficient current generation in silicon solar cells. Photons with energies below the band gap energy of silicon ( $<1.1eV$ ) are (up)converted into photons with higher energies through absorption in rare earth ions ( $Er^{3+}$ ) followed by radiative decay. This process converts otherwise non-absorbed long wavelength photos to shorter wavelength photons able to bridge the band gap energy and contribute to the energy generation of the solar modules.

The upconversion process is naturally inefficient, and without any enhancement of the incident light, the process is negligible. The probability for upconversion can be increased by focusing the incident light into areas doped with  $Er^{3+}$  ions, using optimized nanoparticles placed into or near these areas. Studies have shown that the intensity of the upconverted light is proportional to the intensity of the incident light raised to some power,  $n$ , [1]. Experimentally  $n$  is found to be 1.5 and the light intensity is proportional to the square of the electric field norm,  $|E|^2$ .

We aim to enhance the incident light using topology optimized nanoparticles. Here, the distribution of nanoparticle material is optimized to enhance  $|E|^3$  in a thin  $Er^{3+}$  doped  $TiO_2$  film. Topology optimization has previously proven successful for optimizing wave propagation in acoustics [2] and electromagnetics [3,4]. The governing physics is modeled classically using Maxwell equations in the frequency domain. The model is excited by an incoming plane wave with a wavelength, within the near-infrared absorption band of  $Er^{3+}$  (1480nm - 1560nm).

**Keywords:** Topology optimization, nanooptics, photovoltaics, plasmonics, light enhancement

## References:

1. M. Pollnau et al. "Power dependence of up-conversion luminescence in lanthanide and transition-metal-ion systems". In: *Phys. Rev. B* 61.5 (2000)
2. Rasmus E. Christiansen et al. "Creating geometrically robust designs for highly sensitive problems using topology optimization: Acoustic cavity design". In: *Struct. Multidiscip. Optim.* 52.4 (2015)
3. Maria B. Dühning et al. "Plasmonic versus dielectric enhancement in thin-film solar cells". In: *Appl. Phys. Lett.* 100.21 (2012)
4. Jacob Andkjær et al. "Topology optimization of grating couplers for the efficient excitation of surface plasmons". In: *J. Opt. Soc. Am. B* 27.9 (Sept. 2010)

# Photovoltaic Performance and Excited State Properties of AgInS<sub>2</sub>-ZnS Quantum Dots

Steven M. Kobosko<sup>1,2</sup>, Danilo H. Jara<sup>1,3</sup>, Prashant V. Kamat<sup>1,2,3</sup>

<sup>1</sup>University of Notre Dame, Radiation Laboratory, Notre Dame, USA

<sup>2</sup>University of Notre Dame, Chemical and Biomolecular Engineering, Notre Dame, USA

<sup>3</sup>University of Notre Dame, Chemistry and Biochemistry, Notre Dame, USA

## Abstract:

Quantum dots are extremely small semiconductor nanoparticles which exhibit different properties from the bulk material. The ability to tune properties such as absorption and emission by changing size and shape make them good candidates for numerous applications ranging from bioimaging to photocatalysis to photovoltaics.<sup>1</sup> Binary chalcogenide quantum dots such as PbS and CdSe are two of the most studied materials for quantum dot photovoltaics due to their favorable material properties, but suffer from the fact that they contain the highly toxic elements Pb and Cd.<sup>2,3</sup> Ternary and quaternary quantum dots such as AgInS<sub>2</sub> and AgInS<sub>2</sub>-ZnS offer an alternative to these binary chalcogenides, possessing many of the advantageous properties while offering increased flexibility to tune properties. The optical and electronic properties of these multinary semiconductors can be modified not only with particle size, but also with composition.<sup>4</sup> In this study, AgInS<sub>2</sub>-ZnS quantum dots were employed as sensitizers in liquid-junction solar cells to evaluate their viability for photovoltaics. The devices were tested periodically over 7 weeks to assess the stability of the solar cells over time. A power conversion efficiency of 2.25% was achieved by our champion cell 1 month after its fabrication.<sup>5</sup> In order to increase the efficiency of quantum dots solar cells further, it is important to establish their excited state properties. The excited state interaction between AgInS<sub>2</sub>-ZnS and TiO<sub>2</sub> was investigated by photoluminescence emission spectroscopy and femtosecond transient absorption spectroscopy in order to gain a greater understanding of the mechanisms which affect photovoltaic performance. An electron transfer rate constant of  $1.8 \times 10^{10} \text{ s}^{-1}$  was determined by transient absorption spectroscopy. The limitations of AgInS<sub>2</sub>-ZnS quantum dots in achieving greater photovoltaic efficiency are discussed.

**Keywords:** AgInS<sub>2</sub>, solar cells, electron transfer, transient absorption spectroscopy, emission quenching, quantum dots

## References:

1. Bera, D., Qian, L., Tseng, T.-K., Holloway, P. H. (2010), Quantum Dots and Their Multimodal Applications: A Review, *Materials*, 3 (4), 2260–2345.
2. Chuang, C.-H. M., Brown, P. R., Bulović, V., Bawendi, M. G. (2014), Improved Performance and Stability in Quantum Dot Solar Cells through Band Alignment Engineering, *Nat. Mater.*, 13 (8), 796–801.
3. Kim, G.-H., García de Arquer, F. P., Yoon, Y. J., Lan, X., Liu, M., Voznyy, O., Yang, Z., Fan, F., Ip, A. H., Kanjanaboos, P., Hoogland, S., Kim, J. Y., Sargent, E. H. (2015), High-Efficiency Colloidal Quantum Dot Photovoltaics via Robust Self-Assembled Monolayers, *Nano Lett.*, 15 (11), 7691–7696.
4. Dai, M., Ogawa, S., Kameyama, T., Okazaki, K., Kudo, A., Kuwabata, S., Tsuboi, Y., Torimoto, T. (2012), Tunable Photoluminescence from the Visible to near-Infrared Wavelength Region of Non-Stoichiometric AgInS<sub>2</sub> Nanoparticles, *J. Mater. Chem.*, 22 (25), 12851–12858.
5. Kobosko, S. M., Jara, D. H., Kamat, P. V. (2017), AgInS<sub>2</sub>-ZnS Quantum Dots. Excited State Interactions with TiO<sub>2</sub> and Photovoltaic Performance, *ACS Appl. Mater. Interfaces*, DOI: 10.1021/acsami.6b14604

# An Effect of Fullerenes C60 Additives on Thermophysical Properties of Refrigerant/Mineral Oil Solutions and Efficiency of Vapor Compression Machine

A. Nikulin,<sup>1\*</sup> O. Khliyeva,<sup>2</sup> S. Moroz,<sup>2</sup> M. Lukianov,<sup>2</sup> V. Zhelezny,<sup>2</sup> A. L. N. Moreira,<sup>1</sup>

<sup>1</sup> Instituto Superior Técnico, University of Lisbon, Center for Innovation, Technology and Policy Research, IN+, Lisboa, Portugal

<sup>2</sup> Odessa National Academy of Food Technologies, Department of Thermophysics and Applied Ecology, Odessa, Ukraine

## Abstract:

The addition of nanoparticles to a base fluid allows artificially and purposefully regulate its thermophysical properties, thus opening a wide potential to create working fluids with specially designed properties, suitable for new types of energy equipment.

In recent years, the influence of nanoparticle additives on the thermal conductivity and viscosity of various base fluids have been investigated. However, their impact on vapor pressure and surface tension remains poorly examined, although these properties largely determine the heat transfer characteristics during phase change, as well as the efficiency of vapor compression machines.

This paper reports the results of an experimental study of the influence of the fullerenes C60 additives on the vapor pressure, surface tension and viscosity of the refrigerant R600a/compressor oil solutions.

The stability of the fullerenes C60/compressor oil nanofluid is evaluated based on measurement of the light absorption coefficient made with a spectrophotometer in the wavelength range 360–800 nm. The results show an excellent stability of the prepared nanofluid samples for as long as two months.

Measurements of the investigated thermophysical properties show that the fullerenes C60 additives also reduce the viscosity and surface tension of the refrigerant/oil solution. Furthermore, these results show good agreement with predictions made with the SP-QSPR model described by Zhelezny et al. (2014) in a wide range of conditions.

Experiments were also conducted to measure the efficiency of the vapor compression machine in the range of coolant mass flow from  $0.202 \cdot 10^{-3}$  to  $0.404 \cdot 10^{-3}$  kg/s at the boiling and condensation temperatures of refrigerant 255 K and 301 K respectively.

Results show that the addition of fullerenes C60 in mass fraction 0.5 wt.% to the compressor oil, reduces the power consumption by an average of 4%.

**Keywords:** nanofluid, refrigerant/oil solution, viscosity, saturated vapor pressure, surface tension.

## References:

1. Godson, L. Raja, B., Lal, D. M., Wongwises, S. (2010). Enhancement of heat transfer using nanofluids - an overview. *Renewable and sustainable energy reviews.*, 14, 629–641.
2. Zhelezny, V. Sechenyh V. Nikulina A. (2014). A New Scaling Principles–Quantitative Structure Property Relationship Model (SP-QSPR) for Predicting the Physicochemical Properties of Substances at the Saturation Line. *J. Chem. Eng. Data.*, 59 (2), 485–493.
3. Zhelezny, V., Lukianov, N., Khliyeva, O., Nikulina, A., Melnyk, A (2017). A complex investigation of the nanofluids R600a-mineral oil- $\text{Al}_2\text{O}_3$  and R600a-mineral oil- $\text{TiO}_2$ . Thermophysical properties. *International Journal of Refrigeration.*, 74, 486–502.

# A Comparative Study on loading RGo Nanosheet in Fe<sub>2</sub>O<sub>3</sub> and MoSe<sub>2</sub> Nanocomposites, using Watersplitting

P.Sangpour<sup>1</sup>, M. Nasiri<sup>1</sup>, Z.Khajehsaeidi<sup>1</sup>, M.Bagheri<sup>1</sup>

<sup>1</sup>Material and Energy Research Center, Department of Nanotechnology and Advanced Materials, P.O. Box 31787-316, Karaj, Iran

## Abstract:

H<sub>2</sub> evolution by photocatalytic watersplitting has attracted a lot attention as a clean and renewable solar H<sub>2</sub> generation system. Despite tremendous efforts, the present great challenge in materials science is to develop highly active photocatalysts for splitting of water at low cost. Graphene, a single layer of graphite, has been reported to be an efficient catalyst for photocatalytic H<sub>2</sub> evolution because of its high specific surface area and superior electron mobility. Inside using graphene, metal oxide nanoparticle has wide attention due to high electron-hole production under solar irradiated. One of the best candidate for photocatalytic under solar irradiation is Fe<sub>2</sub>O<sub>3</sub> nanoparticle and MoSe<sub>2</sub> nanosheets, which has been improve by adding graphene nanosheet. So, here we report a comparative study between Fe<sub>2</sub>O<sub>3</sub>/rGO and MoSe<sub>2</sub>/rGO nanocomposite. The photocatalytic water oxidation activity of hematite ( $\alpha$ -Fe<sub>2</sub>O<sub>3</sub>) has been greatly enhanced by incorporating hematite nanoparticles on the reduced graphene oxide (rGO) nanosheets. Photoelectrochemical measurement results show that coupling the hematite nanoparticles with the rGO greatly increases the photocurrent and reduces the charge recombination rate. A three-dimensional (3D) hybrid of rosebud-like MoSe<sub>2</sub> nanostructures supported on reduced graphene oxide (rGO) nanosheets was successfully synthesized through a facile hydrothermal strategy. The prepared MoSe<sub>2</sub>/rGO hybrid nanostructure showed enhanced electrocatalytic activity for watersplitting. In comparison with rGO/Fe<sub>2</sub>O<sub>3</sub> nanocomposite due to synergic effect of two dimensional of MoSe<sub>2</sub> and graphene nanosheets.

**Keywords:** reduce graphene oxide, Fe<sub>2</sub>O<sub>3</sub>, RGo-Fe<sub>2</sub>O<sub>3</sub>, MoSe<sub>2</sub>, RGo-MoSe<sub>2</sub>, photocatalysts, photoelectrochemical, watersplitting.

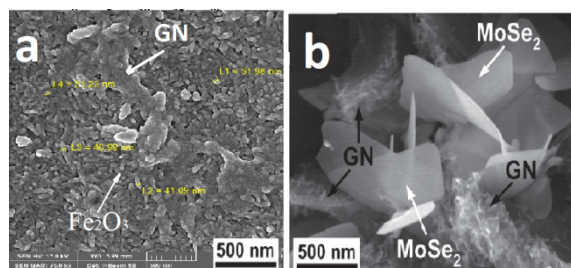


**Figure 1:** an illustrated FESEM Fe<sub>2</sub>O<sub>3</sub>. b illustrated FESEM MoSe<sub>2</sub>

## References:

1. Tang, H., Dou, K.P., Kaun, C.C., Kuang, Q., Yang, S.H. (2014) MoSe<sub>2</sub> nanosheets and their graphene hybrids: synthesis, characterization and hydrogen evolution reaction studies, *J. Mater. Chem A.*, 360–364.
2. Yuan, Y., Jianga, W., Wanaga, Y., Shena, P., Lia, F., Lia, P., Zhaob, F., Gao, H. (2014) Hydrothermal preparation of Fe<sub>2</sub>O<sub>3</sub>/graphene nanocomposite and its enhanced catalytic activity on thermal decomposition of ammonium perchlorate, *Applied Surface Science.*, 303.

# Nanocrystalline $\text{Li}_4\text{Ti}_5\text{O}_{12}$ spinel as an anode material for Na-ion batteries

M. Zukalova, B. Pitna Laskova and L. Kavan

J. Heyrovský Institute of Physical Chemistry, v.v.i., Academy of Sciences of the Czech Republic,  
Dolejškova 3, CZ-182 23 Prague 8, Czech Republic

## Abstract:

Lithium titanate spinel ( $\text{Li}_4\text{Ti}_5\text{O}_{12}$ , LTO), used as the negative electrode material in Li-ion batteries, has also been examined for the Na-ion battery recently. LTO is known as a “zero-strain” and “high potential” negative electrode material with a formal potential of 1.55 V vs.  $\text{Li}/\text{Li}^+$ . Na insertion in  $\text{Li}_4\text{Ti}_5\text{O}_{12}$  is accompanied with development of extra phase with an about 4-5% larger unit cell volume which co-exists with LTO in a single particle and is identified as a Na-substituted LTO phase.

In our work Na insertion into sol-gel made nanocrystalline spinel,  $\text{Li}_4\text{Ti}_5\text{O}_{12}$  (nano LTS) and reference commercial spinel (Aldrich LTS) was studied by cyclic voltammetry and galvanostatic chronopotentiometry at 1C and 2C charging/discharging rates. Nanocrystalline LTS exhibited the best performance for Na storage, its charge capacities reach  $156 \text{ mAhg}^{-1}$  and were twice as high as those of reference Aldrich LTS. A capacity drop of nano LTS taking place during galvanostatic cycling was ascribed to irreversible structural changes induced by Na accommodation in the  $\text{Li}_4\text{Ti}_5\text{O}_{12}$  lattice. Raman spectroscopy of nano LTS after Na insertion revealed a formation of orthorhombic  $\text{Li}_{0.5}\text{TiO}_2$  phase in originally phase pure  $\text{Li}_4\text{Ti}_5\text{O}_{12}$ . The occurrence of this phase, which is commonly formed during Li insertion into anatase, is discussed in terms of induced Li redistribution and its accommodation in amorphous-like nanocrystals exhibiting just short-range ordering in nano LTS grain boundaries or defects sites.

**Acknowledgement:** This work was supported by the Grant Agency of the Czech Republic (contract No. 15-06511S).

**Keywords:** Na-ion batteries, Na insertion,  $\text{Li}_4\text{Ti}_5\text{O}_{12}$ , spinel, nanocrystalline, Raman spectroscopy

## References:

1. Kitta, M., Kuratani, K., Tabuchi, M., Takeichi, N., Akita, T., Kiyobayashi, T., Kohyama, M. (2014) Irreversible structural change of a spinel  $\text{Li}_4\text{Ti}_5\text{O}_{12}$  particle via Na insertion-extraction cycles of a sodium-ion battery, *Electrochimica Acta* 148 175-179.
2. Sun, Y., Zhao, L., Pan, H., Lu, X., Gu, L., Hu, Y.S., Li, H., Armand, M., Ikuhara, Y., Chen, L., Huang, X. (2013) Direct atomic-scale confirmation of three-phase storage mechanism in  $\text{Li}_4\text{Ti}_5\text{O}_{12}$  anodes for room-temperature sodium-ion batteries, *Nat Commun* 4 1870.
3. Kavan, L., Graetzel, M. (2002) Facile synthesis of nanocrystalline  $\text{Li}_4\text{Ti}_5\text{O}_{12}$  (spinel) exhibiting fast Li insertion, *Electrochemical and Solid State Letters* 5 A39-A42.
4. Kavan, L., Prochazka, J., Spitler, T.M., Kalbac, M., Zukalova, M., Drenzen, T., Graetzel, M. (2003) Li insertion into  $\text{Li}_4\text{Ti}_5\text{O}_{12}$  p(Spinel) - Charge capability vs. particle size in thin-film electrodes, *Journal of the Electrochemical Society* 150 A1000-A1007.
5. Zukalova, M., Pitna Laskova, B., and Kavan, L. (2017) Na insertion into nanocrystalline  $\text{Li}_4\text{Ti}_5\text{O}_{12}$  spinel: An electrochemical study, *Electrochimica Acta*, submitted

# Increasing the hydrogen storage capacity of IRMOF-1 via applied electric fields

Liviu P. Zarbo, Marius A. Oancea, Daniel I. Bilc

Department Molecular and Biomolecular Physics, INCDTIM Cluj-Napoca, Romania

## Abstract:

Adsorption of hydrogen in nanoporous materials promises to offer the ideal storage solution for the excess energy currently produced from renewable sources. Hydrogen is the ideal energy carrier as it burns cleanly releasing three times more energy per unit of mass than gasoline. Soon after the discovery of metal-organic frameworks (MOFs), it became apparent that these crystalline hybrid materials, could represent the ideal media for high density hydrogen storage. These inorganic-organic hybrid materials with tunable pores and large surface areas ( $\sim 10^3$ - $10^4$  m<sup>2</sup>/g) could adsorb reversibly a large enough quantity hydrogen to compete with traditional compressed hydrogen systems which store hydrogen at 700 bar. But, owing to the fact that hydrogen binds only weakly (3-7kJ/mol) via van der Waals interactions to the atoms of MOFs, the enthalpy of adsorption for hydrogen is too small, which leads to poor adsorption performance at room temperature. Various modifications in the MOF structures succeeded to increase these binding energies, but not enough to improve dramatically the room temperature performance of MOFs.

In a recent work [1], it was suggested to apply an external polarizing electric field on the storage material. The induced dipole-dipole interaction between hydrogen and MOF's atoms could increase the binding energies in a controllable way, leading to a better adsorption performance. We selected IRMOF-1 as our test system and used a multiscale approach we adapted for including polarization effects to evaluate the adsorption capacity of this material in electric fields. Our calculated adsorption isotherms for hydrogen at 300K and 77K show a 5% and 20% improvement in the excess uptake, respectively. These are consistent with the increases in the binding energies of hydrogen adsorbed on the atoms in the crystalline cell of IRMOF-1. Despite these increases in the binding energies, we are still far from achieving the optimal values of 15-20kJ/mol. Moreover, the applied electric field is of the order of GeV/m, similar to the values chosen in the previous theoretical studies. These fields are much larger than the fields that could be conceivably used in a practical device.

This research suggests that standard hydrogen storage in standard MOFs is not going to be improved significantly by applying electric fields, and it is necessary to look for more polarizable porous materials.

## References

- [1] J. Zhou, Q. Wang, Q. Sun, P. Jena, and X. S. Chen, "Electric field enhanced hydrogen storage on polarizable materials substrates," *Proceedings of the National Academy of Sciences*, vol. 107, no. 7, pp. 2801–2806, 2010.

# Hydrothermal Reaction Combined with a Post Anion-Exchange Reaction of Hierarchically Nanostructured NiCo<sub>2</sub>S<sub>4</sub> for High-Performance QDSSCs and Supercapacitors

S. Srinivasa Rao, Ikkurthi Kanaka Durga, Nagabhushanam Kundakarla, Dinah Punnoose, Chandu V.V.M. Gopi, Araveeti Eswar Reddy, and Hee-Je Kim,\*

School of Electrical Engineering, Pusan National University, Busandaehak-ro 63beon-gil, Geumjeong-gu, Busan, 46241, Rep. of KOREA

## Abstract:

This paper proposes a novel and facile strategy to synthesize hierarchical nanostructured NiCo<sub>2</sub>S<sub>4</sub> on Ni foam by a simple hydrothermal reaction combined with a post anion-exchange reaction that was used directly as an electrode in supercapacitors and quantum-dot sensitized solar cells (QDSSCs). By applying the appropriate material concentration, deposition temperature, and time, the NiCo<sub>2</sub>S<sub>4</sub> were densely deposited over the entire surface of the Ni foam with good adhesion. The phase structure and morphology of the NiCo<sub>2</sub>O<sub>4</sub>, NiCo<sub>2</sub>S<sub>4</sub>, and NiCo<sub>2</sub>Se were characterized by X-ray diffraction, X-ray photoelectron spectroscopy, and scanning electron microscopy. The hierarchical nanostructure of the NiCo<sub>2</sub>S<sub>4</sub> electrode exhibited outstanding electrochemical performance in supercapacitors and QDSSCs with a high specific capacitance of 1612.95 F/g, energy density of 56 Wh kg<sup>-1</sup> at 5 A/g, good cycling stability (only 3% loss after 1000 cycles at 6 A/g), power conversion efficiency of 3.94%, and J<sub>sc</sub> of 12.27 mA/cm<sup>2</sup>. The NiCo<sub>2</sub>S<sub>4</sub> electrode exhibited almost double the output values than that of NiCo<sub>2</sub>O<sub>4</sub> (693.6 F/g at 6.66 A/g and PCE of 1.81%) and NiCo<sub>2</sub>Se (1401.4 F/g at 10 A/g and PCE of 3.86%), resulting from the excellent electrochemical performance of the NiCo<sub>2</sub>S<sub>4</sub>. This study shows that the NiCo<sub>2</sub>S<sub>4</sub> hierarchical nanostructure can be applied not only in high energy density fields, but also in high power density (energy storage, flexible electronics and electric vehicles) and energy harvesting applications.

**Keywords:** quantum-dot sensitized solar cell, counter electrode, supercapacitor, charge transfer resistance, stability test.

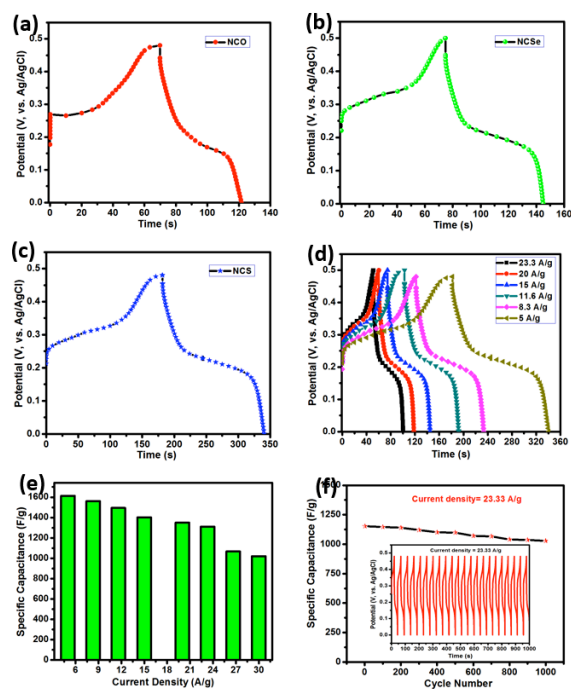


**Figure 6:** Galvanostatic charge-discharge curves of the (a) NCO, (b) NCSe, and (c) NCS at current density of 6.66 A/g. (d) GCD curves of NCS nanotube arrays on Ni foam with different current density. (e) Specific capacitance (F/g) as a function of the different current density of 5, 8, 11.6, 15, 20, 23.3, 26.5, and 30 A/g. (f) Cyclic performance of NCS electrode at a current density of 23.33 A/g.

## Acknowledgments:

This research was supported by Basic Research Laboratory through the National Research Foundations of Korea funded by the Ministry of Science, ICT and Future Planning (NRF-2015R1A4A1041584). We also thank KBSI for HR-SEM, EDX, XRD and XPS measurements.

# Laser-induced graphenization of polymeric surface as powerful method for flexible supercapacitor fabrication

A. Lamberti<sup>1,2\*</sup>, F. Perrucci<sup>1</sup>, M. Fontana<sup>1,2</sup>, G. Ferraro<sup>1,2</sup>, S. Bocchini<sup>2</sup>, M. Serrapede<sup>1</sup>, S. Bianco<sup>1,2</sup>, S. Ferrero<sup>1</sup>, L. Scaltrito<sup>1</sup>, A. Chiolerio<sup>2</sup>, E. Tresso<sup>1</sup>, C. F. Pirri<sup>1,2</sup>

<sup>1</sup> Politecnico di Torino, Dipartimento di Scienza Applicata e Tecnologia (DISAT), Corso Duca Degli Abruzzi, 24, 10129 Torino, Italy. \*corresponding author: [andrea.lamberti@polito.it](mailto:andrea.lamberti@polito.it)

<sup>2</sup> Istituto Italiano di Tecnologia, Center for Sustainable Future Technologies, Corso Trento, 21, 10129 Torino, Italy

## Abstract:

Graphene and graphene-like materials have been intensively studied in the field of electrochemical energy storage, and in the last three years the research focus has been broadened on new layered 2D-materials, such as MoS<sub>2</sub> and other transition metal dichalcogenides. Recently, laser-induced graphene (LIG) has been proposed as an efficient active material for flexible supercapacitor (SC) electrodes (Fig. 1a). This material consists of a 3D network of multilayer graphene (Fig. 1b) obtained by a laser writing process on polymer surface during which the sp<sup>3</sup>-carbon atoms in the polymer are photothermally converted to sp<sup>2</sup>-carbon atoms. Herein we report a rapid one-pot synthesis of MoS<sub>2</sub>-decorated laser induced graphene by direct writing of polyimide and S-PEEK foils. By covering the polymer surface with a layer of MoS<sub>2</sub> dispersion before processing, we have been able to obtain an in-situ decoration of porous graphene network during laser writing (Fig. 1c), enabling both electric double layer and pseudo-capacitance behavior [1]. A deep investigation of the material properties has been performed to understand the chemical-physical characteristics of the hybrid MoS<sub>2</sub>-graphene-like material. Additionally a simple method to transfer the LIG porous layer obtained onto polyimide sheet to a transparent and elastomeric substrate (PDMS) is proposed [2]. The elastomeric nature of the host matrix allows high deformation-tolerance of the supercapacitors (Fig. 1d) that demonstrate great potential for the development of stretchable and wearable energy storage devices highly desired in applications such as artificial skin and other conformal electronic systems.

**Keywords:** Laser-induced graphene, flexible, supercapacitor, MoS<sub>2</sub>, PDMS, Polyimide

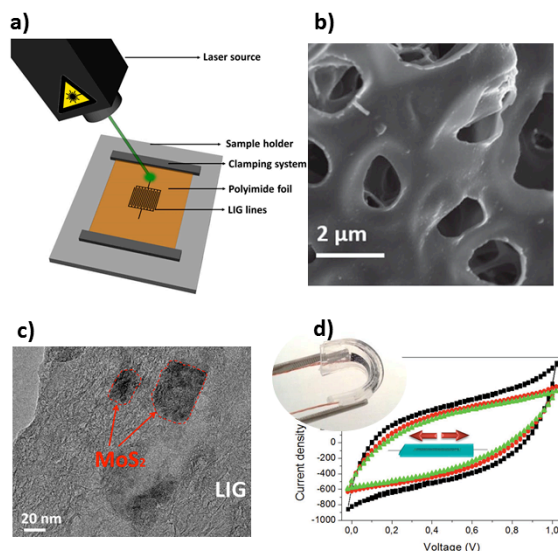


**Figure 1:** 3D scheme of the LIG process (a); FESEM image of the LIG morphology (b); TEM image of the intercalated MoS<sub>2</sub> flakes into LIG structure (c) and cyclic voltammeteries of LIG/PDMS-based supercapacitor under different stretching condition (d) – a digital photograph showing the flexible device is reported in the inset.

## References:

1. F. Clerici et al., ACS applied materials & interfaces 8, 10459 (2016).
2. A. Lamberti et al., Advanced Energy Materials 6, 1600050 (2016).

# Carbon coated MoS<sub>2</sub> flakes as anode for lithium-ion batteries

Duc Anh Dinh<sup>1,2</sup>, Haiyan Sun<sup>1</sup>, Leyla Najafi<sup>1,2</sup>, Carlo Di Giovanni<sup>1</sup>, Antonio Esau Del Rio Castillo<sup>1</sup>, Alberto Ansaldo<sup>1</sup>, Zhiya Dang<sup>1</sup>, Vittorio Pellegrini<sup>1</sup>, and Francesco Bonaccorso<sup>1</sup>

<sup>1</sup>Istituto Italiano di Tecnologia, Graphene Labs, Via Morego 30, Genoa, 16163, Italy

<sup>2</sup>Università di Genova, Dipartimento di Chimica e Chimica Industriale, via Dodecaneso 31, 16164 Genoa, Italy

## Abstract:

Currently, lithium-ion batteries (LIBs),<sup>1</sup> displaying energy densities of ~120–150 Wh kg<sup>-1</sup>, are dominating the ever-increasing market for portable electronic devices. Commercial LIBs are based on graphite anode, which exhibits a low specific capacity value of 372 mAh g<sup>-1</sup>,<sup>2</sup> thus being unable to meet the requirement of high energy applications (e.g. electric vehicles or electrical storage system in renewable wind/solar plants).<sup>3</sup> In the quest for high capacity and energy density LIB electrodes, various anode materials have been proposed e.g., metal, metal oxide (Si, Sn, SnO<sub>2</sub>, etc.) and layered materials (few-, multi-layer graphene and transition metal dichalcogenide).<sup>4</sup> However, most of the proposed materials suffer capacity fading due to their large volume change during lithiation and de-lithiation. Amongst them, molybdenum disulfide (MoS<sub>2</sub>), having a theoretical specific capacity of 670 mAh g<sup>-1</sup> and a large spacing layer (0.62 nm) which is favorable for Li<sup>+</sup> intercalation with respect to graphite (0.34 nm),<sup>5,6</sup> has attracted great attention as a promising material for LIB anode.<sup>5</sup> However, MoS<sub>2</sub> as stand-alone anode is limited by its low conductivity and electrode pulverization.<sup>6</sup> These issues can be overcome by decreasing the lateral size and thickness of MoS<sub>2</sub> flakes to obtain short Li<sup>+</sup> diffusion lengths, and by integrating MoS<sub>2</sub> with carbon material to accommodate the volume change as well as improve the electrical conductivity.<sup>7</sup> Current approaches to produce MoS<sub>2</sub> flakes, e.g., hydrothermal, solvothermal, or template assisted techniques<sup>6</sup> require multi-steps synthesis and toxic precursors (ammonium thiomolybdate).<sup>6</sup> Thus, we propose a simple approach to fabricate MoS<sub>2</sub> nanoflakes by liquid phase exfoliation of bulk MoS<sub>2</sub> in an environmentally friendly solvent. A thermal decomposition of carbon sources (polyacrylic acid) is exploited for the coating of the MoS<sub>2</sub> flakes. The as-prepared MoS<sub>2</sub>/C with three different C ratios (10%, 16% and 30%) are coated onto copper substrated as anode and tested in half cell configurations, to investigate the effect of various carbon content on electrochemical properties of MoS<sub>2</sub>. As shown in HR-SEM images (Fig. 1), in case of MoS<sub>2</sub> electrode, the flake morphology of MoS<sub>2</sub> are clearly observed with sharp edges. However, with the increase in carbon content, this feature diminishes due to the integration of carbon with MoS<sub>2</sub> flakes. The MoS<sub>2</sub>/C-16% (16 wt% of C) electrode exhibits a specific capacity of 521 mAh g<sup>-1</sup> after 100 cycles (Fig. 2a), as well as the

lowest value (30 Ω) of charge transfer resistance (R<sub>ct</sub>) with respect to the other electrodes (Fig. 2b). Our study demonstrates the optimization of the (electro)chemical properties of MoS<sub>2</sub>/C electrode by a simple carbon coating. Moreover, the carbon coating provides the mechanical stability of the electrode, avoiding its pulverization upon cycling (Fig. 2a).

**Keywords:** liquid phase exfoliation, Li-ion batteries, MoS<sub>2</sub>, anode, carbon coating, stability.

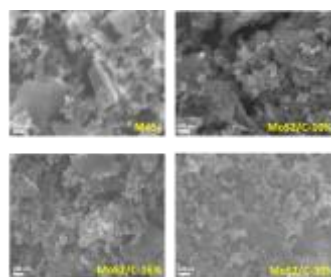


**Figure 1:** HR-SEM images of MoS<sub>2</sub>/C electrodes with different wt% C.

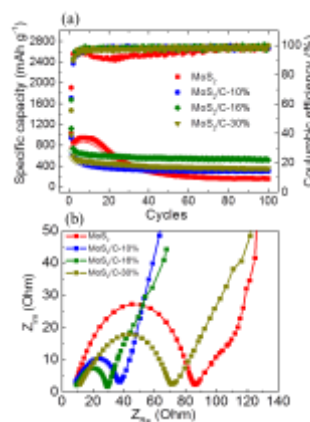


**Figure 2:** a) Specific capacity and coulombic efficiency over charge/discharge galvanostatic cycles and b) impedance spectroscopy of MoS<sub>2</sub>/C electrodes with different wt% C.

## References:

1. Hassoun, J., et. al. (2014), Nano Lett., 14, 4901–4906
2. Tarascon, J. M., Armand, M. (2001) Nature, 414, 359-367
3. Armand, M.; Tarascon, J. M. (2008) Nature, 451, 652–657
4. Mahmood, N., Tang, T., Hou, Y. (2016) Adv. Energy Mater., 257, 6, 1600374
5. Du, G., et. al. (2010) Chem. Commun., 46, 1106–1108
6. T. Stephenson, T., et al. (2014) Energ Environ Sci, 7, 209-231.

7. Li, H., Zhou, H. (2012) *Chem. Commun.*, 48, 1201–1217

# Oxygen reduction reaction on anisotropic silver nanoparticles in alkaline media for fuel cell application

M.Malviya\*, Rajeev Kumar Gupta, A.D. Verma, I Sinha

Department of Chemistry, IIT (BHU) Varanasi, Varanasi UP-221005

## Abstract:

The development of catalysts for oxygen reduction reaction (ORR) is essential for using fuel cell as an alternative source of the renewable energy. In general, ORR is catalyzed by noble metal catalysts like Pt and Pd making it an expensive alternative, consequently these metals are being gradually replaced by cheaper and easily available non Pt group of metal and their alloy. In the present work, electrocatalytic activity of anisotropic Ag nanoparticles formed by using Cu salt as an etchant was investigated. three types of Ag nanoparticles were prepared in presence of different amounts of Cu salt as etchant. Thus, in  $\text{Ag}_{100}(\text{Cu salt})_0$ ,  $\text{Ag}_{50}(\text{Cu salt})_{50}$  and  $\text{Ag}_{67}(\text{Cu salt})_{33}$  nanoparticles. These different types of anisotropic Ag nanoparticles were then used for investigating the ORR in KOH electrolyte. The synthesized materials were characterized by transmission electron microscopy (TEM) and X-ray diffraction (XRD). The effect of Ag nanoparticle anisotropy (due to the different amount of Cu salt etching) with respect to electrocatalytic performance was investigated by using techniques, such as cyclic voltammetry (CV), and linear sweep voltammograms (LSV). The study showed that the effect of Cu salt on Ag nanoparticles increased the electrochemically active area as well as apparent electrocatalytic activity showing maximum for  $\text{Ag}_{67}(\text{Cu salt})_{33}$ . According to Linear sweep voltammograms, the reduction peak position and the intensity of silver oxide is at lower applied potential for the  $\text{Ag}_{67}(\text{Cu salt})_{33}$  compared to  $\text{Ag}_{100}(\text{Cu salt})_0$ ,  $\text{Ag}_{50}(\text{Cu salt})_{50}$  nanoparticle. This phenomenon indicates a stronger adsorbed-oxygen interaction with the Ag etched by Cu salt than that in  $\text{Ag}_{100}(\text{Cu salt})_0$  nanoparticle prepared without etchant. This stronger interaction between oxygen and silver facilitates the splitting of O-O bond thus increasing the ORR kinetics.

**Keywords:** Anisotropic AgNPs; Oxygen reduction reaction (ORR); Electrocatalysis; Cyclic voltammetry; Linear sweep voltammetry.

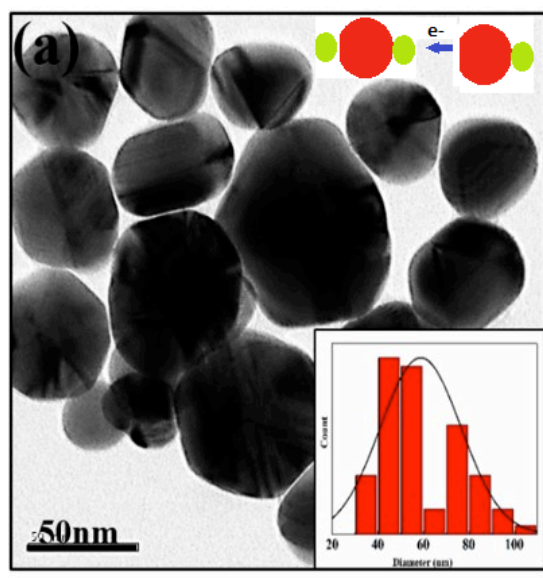


**Figure:** Figure illustrating the fundamental reduction of oxygen to water molecule on the as synthesized anisotropic Ag nanoparticles in KOH solution.

## References:

- (1) A.D. Verma, R. Mandal, I. Sinha, , *Rsc Adv* 6(105) (2016) 103471-103477.
- (2) H. Qin, L. Jiang, Y. He, J. Liu, K. Cao, J. Wang, Y. He, H. Ni, H. Chi, Z. Ji, *J Mater Chem A* 1(48) (2013) 15323-15328.
- (3) M. Malviya , R.N. Singh and P. Chartier, *J. New Materials for Electrochem. Syst.*, 10 (2007) 181-186.

**Session VI:  
NanoMaterials for Environmental  
applications**

# Photocatalysis of Doped ZnO nanomaterials: Importance of the Location of Dopants

T. Tsuzuki,<sup>1\*</sup> R. He<sup>2</sup>

<sup>1</sup>Australian National University, Research School of Engineering, Canberra, Australia

<sup>2</sup>Deakin University, Institute for Frontier Materials, Geelong, Australia

**Abstract:** ZnO is one of the most investigated wide-bandgap semiconductor materials for photocatalytic applications. Doping of impurity elements in ZnO is frequently studied to enhance or reduce the photocatalytic activity. However, many conflicting results have been reported on the effects of dopants. For example, by doping Co in ZnO nanoparticles, Xu et al. reported increased photoactivity,<sup>1</sup> whereas Nair et al. found reduced photoactivity.<sup>2</sup> The effects of dopants on other properties such as bandgap energy and cathodoluminescence emission wavelength also showed conflicting results.<sup>3</sup> The uncertainty in the doping effects is largely due to the insufficient characterisation of doping states, in particular, the location of dopant ions. This paper gives such examples in Co and Mn doped ZnO nanomaterials and discusses how the location of dopants affects photocatalytic activities.<sup>4</sup>

Mn-doped and Co-doped ZnO nanomaterials were synthesised using three techniques: mechanochemical processing, hydrothermal methods and wet-chemical co-precipitation methods. Dopant concentration was varied from 0 to 5 at%. UV-vis study showed reduced bandgap energy in both Co-doped and Mn-doped samples. X-ray diffraction (XRD) pattern showed only peaks associated with ZnO for both Co-doped and Mn-doped samples. The XRD pattern also indicated that the lattice constants shifted to higher and lower values by Mn-doping and Co-doping, respectively. These results are normally considered sufficient to argue that crystal-doping was successful. However, zeta potential measurements and X-ray absorption spectroscopy (XAS) indicated the precipitation of Mn<sub>3</sub>O<sub>4</sub> phase on the particle surface in Mn-doped ZnO. In contrast, zeta potential and XAS study on Co-doped ZnO indicated substitution of Zn-ions with Co-ions. Photocatalytic activity of Mn-doped ZnO as a function of dopant level showed a trend similar to that of ZnO with Mn<sub>3</sub>O<sub>4</sub> coating, whilst that of Co-doped ZnO showed a response to the amount of Co different from that of Co-decorated ZnO. This example demonstrates the importance of in-depth analysis in the location of dopants using a combination of many techniques, which is often overlooked in the photocatalysis research.

**Keywords:** ZnO nanoparticle, doping, photocatalysis.

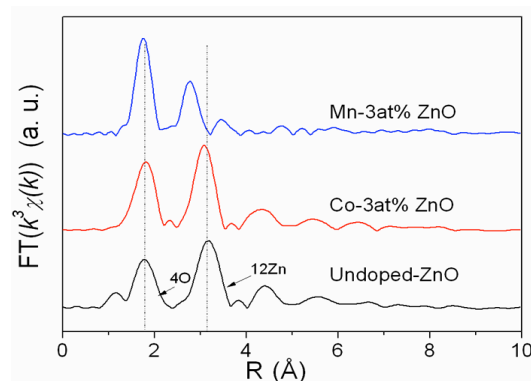


**Figure 1:** Fourier transform of Mn, Co and Zn K-edge EXAFS  $k^3\chi(k)$  spectra for Mn-doped, Co-doped and undoped ZnO, respectively.

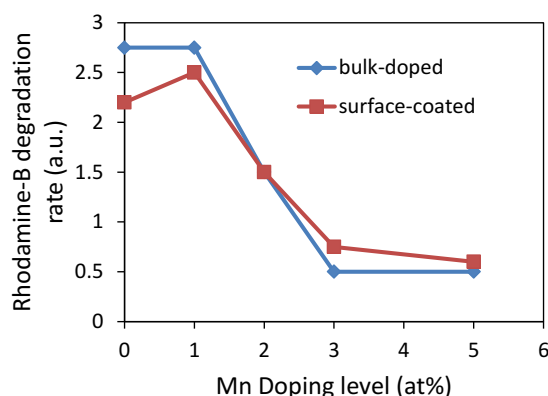


**Figure 2:** Rhodamine-B degradation rates of (a) mechanochemically synthesised Co-doped and Mn-doped ZnO nanoparticles.

## References:

- Xu, C., Cao, L., Su, G., Liu, W., Qu, X., Yu, Y. (2010) Preparation, characterization and photocatalytic activity of Co-doped ZnO Powders, *J. Alloy. Compounds*, 497, 373–376..
- Nair, M.G., Nirmala, M., Rekha, K., Anukalini, A. (2011) Structural, optical, photocatalytic and antibacterial activity of ZnO and Co doped ZnO nanoparticles, *Mater. Lett.* 65, 1797–1800.
- He, R., Tang, b., Ton-That, C., Phillips, M., Tsuzuki, T. (2013) Physical structure and optical properties of Co-doped ZnO nanoparticles prepared by co-precipitation, *J. Nanopart. Res.*, 15, article 2030.

# Metal Oxide Nanocomposites for Enhanced Performance of Supercapacitors and Photocatalysts

Jae-Jin Shim,\* Sumanta Sahoo, Nhu Minh Tue Le, Nguyen Van Quang

School of Chemical Engineering, Yeungnam University, Gyeongsan, S. Korea

## Abstract:

Metal oxide nanocomposites have been developed for energy storage (supercapacitor) and photocatalysis applications. For getting a higher performance, various synthetic methods have been developed. Modifying the metal oxide nano structures with graphene, graphene oxide, or reduced graphene oxide have shown successful results owing to their large surface area and high electrical conductivity. Using a mixed-metal oxides instead of single metal oxide also resulted in a higher performance due to the synergistic effect of each metal component. Replacing oxygen by sulfur also produced a promising results. Doping of graphene with nitrogen was also proven to be another method for improving the properties fo nanocomposites. Nickel foam has been getting tremendous attention as it provide a large surface area and large pores, together with the high conductivity, that enables electrolytes and charges penetrates freely.

In this study, various methods of preparing highly active materials for energy storage, photocatalysts, and sensors have been investigated and discussed. In the synthesis of these materials, a cleaner technology has been employed. These nanocomposites with high surface areas, high conductivities, and remarkable electrochemical properties are necessary for developing high-performance next-generation energy storage supercapacitors and photocatalysts.

**Keywords:** metal sulfide, nanocomposite, energy storage, supercapacitor, graphene

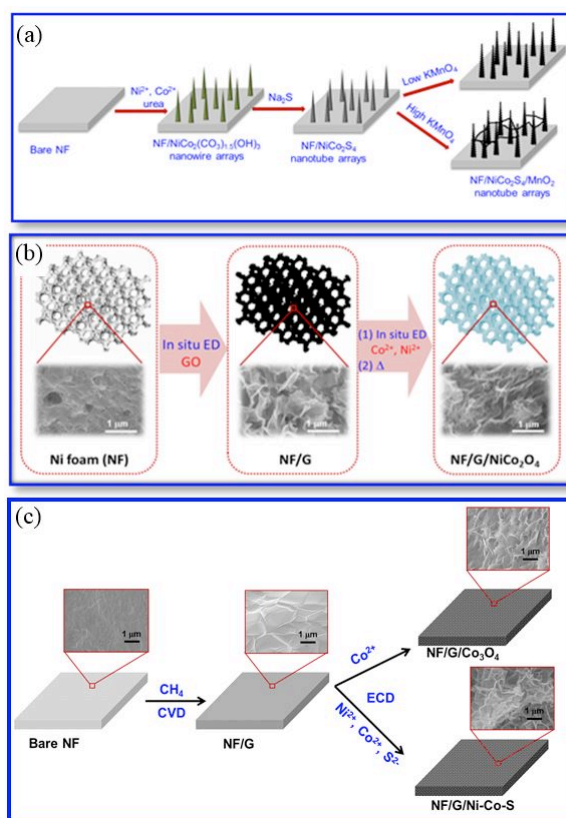


**Figure 1:** Synthetic routes of mixed-metal oxide nanocomposite: (a) hydrothermal deposition and growth, (b) electrochemical deposition, and (c) chemical vapor deposition/electrochemical deposition.

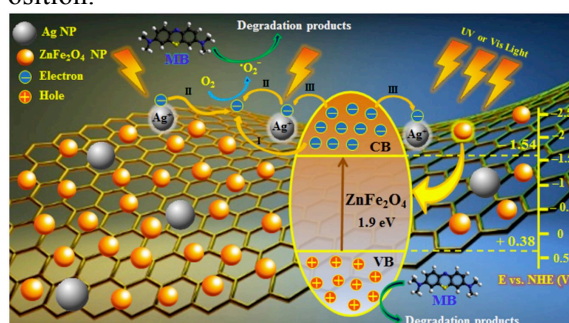


**Figure 2:** Schematic diagram of the MB degradation on Ag-ZnFe<sub>2</sub>O<sub>4</sub>@rGO under UV and vis irradiation.

## References:

1. Mady AH, Baynosa ML, Tuma D, Shim J-J (2017) Facile microwave-assisted green synthesis of Ag-ZnFe<sub>2</sub>O<sub>4</sub>@rGO nanocomposites for efficient removal of organic dyes under UV- and visible-light irradiation. *Appl. Cat. B.* 203: 416-427.

2. Sahoo S, Shim J-J (2017) Facile synthesis of three-dimensional ternary ZnCo<sub>2</sub>O<sub>4</sub>/reduced graphene oxide/NiO composite film on nickel foam for next generation supercapacitor electrodes. ACS Sust. Chem. Eng. 5: 241-251.
3. Lamiel C, Nguyen VH, Roh C, Kang CK, Shim J-J (2016) Synthesis of mesoporous RGO@(Co,Mn)<sub>3</sub>O<sub>4</sub> nanocomposite by microwave-assisted method for supercapacitor application. Electrochim. Acta. 210: 240-250.
4. Nguyen VH, Shim J-J (2015) Three-dimensional nickel foam/graphene/NiCo<sub>2</sub>O<sub>4</sub> as high-performance electrodes for supercapacitors. J. Power Sources. 273: 110-117.

# Nanoclays for adsorption of industrial contaminants: A sustainable application

C. del Hoyo Martínez, S. Monreal Pascual, M. S. Lozano García, V. Sánchez Escribano and M. Villa García

Departamento de Química Inorgánica. USAL

## Abstract:

Removal of dyes effluent is one of the most significant and difficult to treat environmental problems since many of the dyes are of synthetic origin and a complex molecular structure, making them more stable and difficult to biodegrade. Drinking water is an increasingly scarce commodity, especially in the countries with the lowest human development index, where millions of people do not have any access to sources of clean water to meet their basic needs and often becomes vehicle diseases. That is why water pollution is an issue of vital importance to be solved. Sorption techniques produce high quality treated effluent and sorption processes have been investigated as a method of removing dyes wastewater. Amaranth is a typical synthetic, watersoluble anionic dye. The amaranth dye has been banned in the United States since 1974 because it is suspected carcinogen. This substance appears to cause the most allergic and intolerances reactions of all the azo dyes, particularly among asthmatics and those with aspirin intolerance. Consequently, the wastewater containing amaranth with various concentrations should be treated before.

The adsorption of amaranth by attapulgite is studied in this work. Results show a strong interaction between clays and the colorants because of the hydrogen bonds between the amaranth and the adsorbent when the adsorption takes place.

**Keywords:** Adsorption, clays, ultrasound technique, amaranth

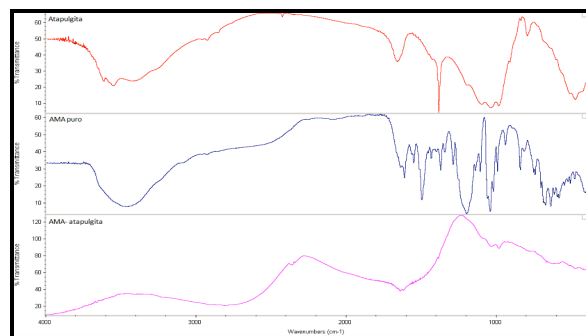


**Figure 1:** FT-IR Spectra: Systems Amaranth-attapulgite obtained by aqueous adsorption

## References:

1. C. del Hoyo Martínez, J. Cuéllar Antequera, V. Sánchez Escribano, M. S. Lozano García, R. Cutillas Díez, “Clays and Clay minerals and their environmental application in Food Technology”, *Geophysical Research Abstract. EGU. Vol 15, 13726-13728. 2013.*
2. C. del Hoyo Martínez, M. S. Lozano García, V. Sánchez Escribano, J. Cuéllar Antequera, “Modified Nanoclays for an Environmental Application”. *Phantoms Foundation Imagenano Vol. 3, 8-10. 2015.*
3. Lozano García, M. S. “Study of nanoclays adsorbents for a sustainable application”. *PhD Thesis. University of Salamanca. 2016.*
4. M. S. Lozano García, C. del Hoyo Martínez, J. Cuéllar Antequera V. Sánchez Escribano, “Technique for adsorption of contaminants by nano clays”. *Phantoms Foundation Imagenano Vol. 3, 17-19. 2015.*
5. O. Korkut, E. Sayan, O. Lacin, B. Bayrak. “Investigation of adsorption and ultrasound assisted desorption of lead (II) and copper (II) on local bentonite: A modelling study” *Desalination Vol. 259, pp 243-248. 2010.*
6. V.K. Gupta, Suhas. “Application of low-cost adsorbents for dye removal. A review” *Journal of Environmental Management Vol. 90, pp 2313-2342. 2009.*

# Photocatalytic Removal of Some Emerging Micropollutants From Raw Hospital Wastewater Using TiO<sub>2</sub> Nanoparticles

G. Guney,<sup>1\*</sup> D.T. Sponza,<sup>1</sup>

<sup>1</sup>Dokuz Eylul University, Engineering Faculty, Environmental Engineering Department, Tinaztepe Campus, 35160, Buca, Izmir, TURKEY

## Abstract:

Emerging micropollutants have potential hazards to the ecosystem because of their incomplete removal during wastewater treatment (Petrie et al., 2014). Legal regulations check macropollutant concentrations in the effluents of the treatment plants such as BOD<sub>5</sub>, COD, nitrogen, phosphorus, suspended solids and heavy metals. For this reason wastewater treatment plants are not designed to treat emerging micropollutants efficiently. Hospitals are one of the main sources of emerging micropollutants and hospital wastewaters are almost untreated before being discharged into municipal wastewater treatment plants via sewage systems (Frédéric et al., 2014). Hospital wastewaters are not treated and directly discharged to the sewage systems in Turkey. Therefore, novelty of this study is to treat some emerging micropollutants (2,3,4,5,6-Penta bromoethyl benzene; PBT, ibuprofen; IBU and N-nitrosodimethylamine; NDMA) in a raw hospital wastewater by photocatalytic processes in laboratory conditions choosing optimum experimental condition considering economy and time limitations for the first time in Turkey. The aim of the study was investigating the photocatalytic removal of 2,3,4,5,6-Penta bromoethyl benzene (PBT; flame retardant), ibuprofen (IBU; anti-inflammatory) and N-nitrosodimethylamine (NDMA; disinfection byproduct) in a raw hospital wastewater using titanium (IV) oxide (nano-TiO<sub>2</sub>) because their presence in lower concentrations (ng L<sup>-1</sup> to µg L<sup>-1</sup>) have been associated with respiratory tract irritation, toxicity to blood, respiratory and nervous system and possible carcinogenicity, respectively. Nano-TiO<sub>2</sub> was selected because of photostable, reusable, inexpensive and photoreactive properties. Two parallel experiments were carried out under sunlight at outdoor conditions and with UV lamps in laboratory conditions. Effects of nano-TiO<sub>2</sub> concentrations (0.25; 0.50; 1.00; 1.50 gr L<sup>-1</sup>), irradiation times (15; 30; 45; 60; 90 min) and UV lamp powers (120; 210; 300 W) on micropollutant yields were investigated while only sunlight power was constant (80 W) at a pH of 7.00 and at a

temperature of 25 °C for all conducted experiments. Optimum experimental conditions were obtained with 1.00 gr L<sup>-1</sup> nano TiO<sub>2</sub> concentration after 45 min irradiation time at 25 °C at a pH of 7.00 under 210 W UV light power. As a result of this study, photocatalytic process with nano-TiO<sub>2</sub> enables the photodegradation of PBT (93%), IBU (85%) and NDMA (80%) with the help of the hydroxyl radicals (OH<sup>•</sup>) occurred via photocatalytic reactions in raw hospital wastewater efficiently, quickly and economically. The photocatalytic first order reactions showed that the PBT was removed with high reaction rate (k=16.99 day<sup>-1</sup>) following by NDMA (k= 7.49 day<sup>-1</sup>) and IBU (k=3.74 day<sup>-1</sup>). Furthermore, the photocatalytic metabolites of PBT, IBU and NDMA will be discussed.

**Keywords:** emerging micropollutants, hospital wastewater, photocatalytic process, TiO<sub>2</sub> nanoparticle.

## References:

1. Petrie, B., McAdam, E.J., Lester, J.N., Cartmell, E. (2014) Obtaining process mass balances of pharmaceuticals and triclosan to determine their fate during wastewater treatment, *Science of the Total Environment*, 497-498, 553-560.
2. Frédéric, O. and Yves, P. (2014), Pharmaceuticals in hospital wastewater: their ecotoxicity and contribution to the environmental hazard of the effluent, *Chemosphere*, 115, 31-39.

# Synthesis of Ag- TiO<sub>2</sub>- Reduced Graphene Oxide Hybrid Composites as Photocatalyst for Degradation of Petrochemical Contaminated Waste Water

Dhanesh Tiwary<sup>1\*</sup>, Pardeep Singh<sup>1</sup>, Ankita Ojha<sup>1</sup> P.K Mishra<sup>2</sup>

<sup>1</sup>Department of Chemistry, Indian Institute of Technology (Banaras Hindu University) Varanasi, India

<sup>2</sup>Department of Chemical Engineering and technology Indian Institute of Technology (Banaras Hindu University) Varanasi, India

Presenter Contact Details (Email: dtiwari.apc@itbhu.ac.in, Mob Number: +91-9415992174)

## Abstract:

In present study Ag-TiO<sub>2</sub>-Reduced graphene oxide (Ag-TiO<sub>2</sub>-rGO) hybrid composites were synthesized by aqueous solution method with different loading of Ag and graphene oxide. The resulting hybrid catalysts were characterized by X-ray diffractometry (XRD), transmission electron microscopy (TEM), scanning electron microscope (SEM), energy-dispersive X-ray (EDX), Fourier transform infrared spectroscopy (FT-IR), Raman spectroscopy and UV-vis spectroscopy. The Photocatalytic efficiencies of the synthesized hybrid composites were determined by the degradation of petrochemical contaminated waste water (Benzene, Toluene and phenolic compound) under UV and visible irradiation in photochemical reactor under ambient conditions. It is found that the photocatalytic efficiency by Ag-TiO<sub>2</sub>-rGO is much higher than the bare TiO<sub>2</sub>, rGO-TiO<sub>2</sub> under visible and UV irradiation. Degradation of petrochemical contaminant in water was estimated by gas chromatography (GC). This approach can be further used for degradation of wide range of organic pollutants even with the visible light irradiation.

**Keywords:** Ag-TiO<sub>2</sub>-Reduced graphene oxide (Ag-TiO<sub>2</sub>-rGO) hybrid composites, photocatalyst, degradation, petrochemical contaminated waste water

# Photocatalytic Titanium-Carbon Nanotube Hybrid Material for Water Remediation

S. Shaw<sup>1</sup> S. Kang<sup>2</sup> C. Johnson<sup>3</sup> H. Harrison<sup>3</sup> K. Kumar<sup>3</sup> T. Lim<sup>4</sup>, J. Bang<sup>3,5\*</sup>

<sup>1</sup> Joint School of Nanoscience and Nanoengineering, Dept. of Nanoengineering, Greenboro, NC USA

<sup>2</sup> Kyonggi University, Dept. of Material Engineering, Suwon, S. Korea

<sup>3</sup> North Carolina Central University, EEGS, Durham, NC USA

<sup>4</sup> Nanyang Technological University, School of Civil and Environmental Engineering, Singapore

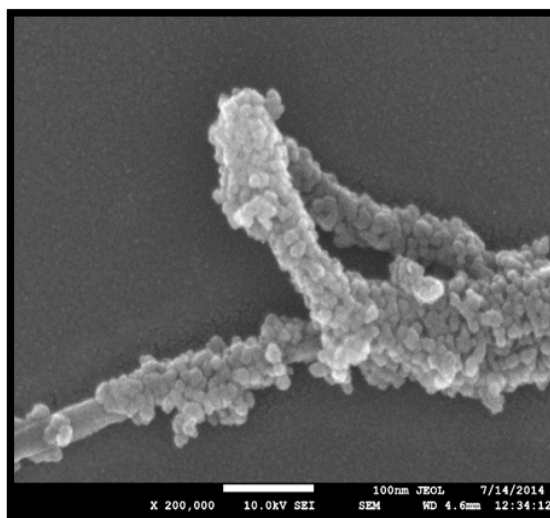
<sup>5</sup> North Carolina Central University, Pharmaceutical Sciences, Durham, NC USA

## Abstract:

Pollution of water by chemicals and microbes in various types of water has threatened not only human health but also our ecological systems. Titanium has shown its potential as photocatalytic remediator in fluidal environment. Carbon nanotubes (CNTs), on the other hand, has shown its unique electrochemical properties including large surface to volume (and mass) ratio that can prolong the duration of electron separation for facilitation of free radical formation which, in turn, can increase the efficiency of chemical and microbial removal from contaminated water. This study investigated the potential role of photocatalytic titanium-CNT hybrid generated by Sol-Gel method in the removal of chemicals (Fig. 1). Methylene blue (MB) was used as a representative chemical for our preliminary testing in neutral pH condition with one solar unit equivalent UV exposure condition. The mixing ratio between titanium (in the form of TTIP) and multiwall carbon nanotubes was changed between 10:1 to 50:1 for finding an optimal condition. The same hybrid material was also used to test its efficiency with different saline condition upto 3.5% to simulate ballast water condition. Results indicated that titanium-CNT hybrid photocatalytic material removed over 95% of MB within 3 hours of one solar unit equivalent UV exposure. The hybrid material also showed a potential for its efficiency under visible light range in addition to UV range although its response rate was slower under visible light exposure condition.

**Keywords:** Titanium-carbon nanotube hybrid, photocatalysis, electrochemical property, sol-gel method, fresh water, ballast water, UV and Visible light.

**Figure 1:** Figure illustrating how titanium particles used (in the form of TTIP) through sol-gel method evenly distributed and dopes on the surface of multiwall CNT. Size bar is 100nm size.



## References:

1. Bruggen, Bart Van Der. "The Separation Power of Nanotubes in Membranes: A Review." *ISRN Nanotechnology 2012* (2012): 1-17
2. Chong, Meng Nan, Bo Jin, Christopher W.k. Chow, and Chris Saint. "Recent Developments in Photocatalytic Water Treatment Technology: A Review." *Water Research* 44.10 (2010): 2997-3027.
3. Jassby, David; Budarz, Jeffrey; Wiesner, Mark; "Impact of Aggregate Size and Structure on the Photocatalytic Properties of TiO<sub>2</sub> and ZnO Nanoparticles"; *Environmental Science and Technology*, (2012); 6934.

# Simultaneous Recovery of Clean Water and Energy Using Nano-Structured Pt Catalysts Deposited on the Surface of Microfiltration Polymeric Hollow Fibers

K. Katuri,<sup>1</sup> N. Bettahalli,<sup>1</sup> X. Wang,<sup>1</sup> G. Matar,<sup>1</sup> S. Chisca,<sup>1</sup> S. Nunes,<sup>1</sup> P. Saikaly<sup>1,\*</sup>

<sup>1</sup> King Abdullah University of Science and Technology, Biological and Environmental Sciences and Engineering Division, Thuwal, Saudi Arabia

## Abstract:

Providing adequate supply of clean fresh water and energy as the world's population increases is one of the grand challenges facing society in the current century. One possible solution to address both challenges is to recover clean water for reuse and energy from wastewater by integrating micro- or ultra-filtration membrane cathodes with microbial electrolysis cells (MECs) in what is referred to as electrochemical membrane bioreactor (EMBR). The porous cathodes serve the dual function as the cathode for hydrogen evolution reaction (HER) and membrane for the filtration of treated water. Here, we demonstrated for the first time the development of a novel electro-catalytic and microfiltration polymeric hollow fibers by combining the fabrication of porous polymeric hollow fibers made of fluorinated polyoxadiazole (POD) by phase inversion, followed by deposition of a very thin layer of nano-platinum (Pt) catalyst on the outer surface (Figure 1) by atomic layer deposition (ALD) to make the porous POD hollow fibers electro-catalytic. High resolution transmission electron microscope image of the Pt film confirms that the catalyst layer on the POD hollow fiber membrane surface is assembled by nano-sized Pt particles. The electro-catalytic and filtration efficacy of the porous hollow fiber cathodes were tested in EMBR using acetate or real wastewater as fuel source. Despite significantly lower Pt loading, the electrochemical performance of the porous hollow fiber cathode was comparable to the benchmark Pt-carbon cloth cathode. The ALD technique facilitated the uniform coverage of the porous hollow fibers with low Pt loading, which minimizes the costs associated with the use of noble-metal catalysts. Platinum was used here as a model catalyst because of its high electrochemical activity towards HER and to demonstrate the feasibility of this new approach. In the future, one may explore lower-cost materials for current collection and catalysis. By using ALD method, we were able to fine tune the pore size of the porous hol-

low fibers resulting in high quality water (turbidity <0.1 nephelometric turbidity units) enabling reclamation of treated effluent. The superior performance of the porous hollow fiber cathode for membrane fouling mitigation was attributed to the in-situ cleaning by hydrogen bubble formation and other factors associated with HER activity.

**Keywords:** atomic layer deposition, porous hollow fiber cathode, biofouling, resource recovery, membrane bioreactor, nano-platinum.

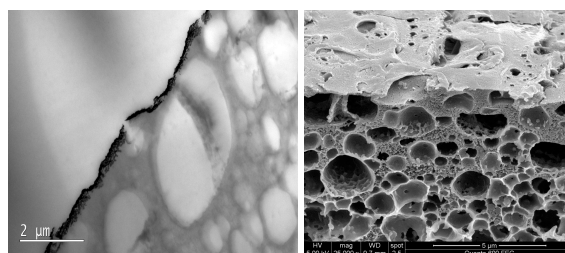


**Figure 1:** (A) Transmission electron microscope image showing a close up view of the deposited Pt layer on the surface of the porous hollow fiber cathode. (B) Scanning electron microscope image showing the deposited Pt layer on the surface of the porous hollow fiber cathode

## References:

1. Katuri, K., Bettahalli, N.M.S., Wang, X., Matar, G., Chisca, S., Nunes, P.S., and Saikaly, P.E. (2016), A microfiltration polymer-based hollow fiber cathode as a promising advanced material for simultaneous recovery of energy and water, *Adv. Mater.*, 28, 9504-9511.

# Two-Dimensional Carbon Nanomaterials for Next Generation Water Treatment Technologies

Khaled A. Mahmoud<sup>1\*</sup> Kashif Rasool<sup>1</sup> and Yury Gogotsi<sup>2</sup>

<sup>1</sup>Qatar Environment and Energy Research Institute (QEERI), Hamad Bin Khalifa University (HBKU), Qatar Foundation, , Doha, Qatar.

<sup>2</sup>Department of Materials Science and Engineering and A.J. Drexel Nanomaterials Institute, Drexel University, Philadelphia, PA, USA

## Abstract:

Membrane processes including reverse osmosis (RO), forward osmosis (FO), membrane distillation (MD), and pretreatment membranes (UF/NF) are rapidly expanding as economic and efficient desalination and water purification technologies. Conventional polymeric materials often cannot tolerate high temperatures, corrosive media, and membrane fouling, which are challenges major challenges facing membrane based water treatment processes. This talk will be discussing our recent development of advanced membranes that enable ultrafast water permeation while maintaining good mechanical properties is very important for the water purification and desalination technologies.

Graphene oxide (GO) emerged recently as an alternative for manufacturing ultrathin, high-flux and energy-efficient sieving membranes because of its unique two-dimensional (2D) and atomically thin structure, outstanding mechanical strength, good flexibility, as well as possibility of facile solution processing. In our lab we have used other low-dimensional materials and developing composite membranes containing GO which helped to achieve efficient water flux and ions sieving through size-selective nanochannels, but does not solve all problems. More recently, we have presented two-dimensional  $Ti_3C_2T_x$  (MXene) as novel water desalination/purification membranes. MXenes are a new family of atomically thin, two-dimensional (2D) transition metal carbides and carbonitrides that can challenge graphene and other well-studied 2D materials due to a unique combination of properties and a large diversity of composi-

tions. MXenes show metallic conductivity combined with a negative surface charge and hydrophilicity which adds a possibility to control ion flux and biofouling by applying a small potential to the membrane.  $Ti_3C_2T_x$  shows a much higher antibacterial efficiency toward both Gram-negative and Gram-positive bacteria. Consequently MXene membranes showed high resistant to bio-fouling and offer bactericidal properties to the new UF/NF membranes. We used density functional theory (DFT) calculations to understand the mechanisms of charge-selective ionic transport through MXene membranes. We confirmed the charge selectivity originates from the charged nature of the MXene layers.

We introduced new class of 2D carbon membranes and membrane coatings for water treatment, which may also find applications in other separation/filtration processes in liquids and gases.

**Keywords:** MXene, Graphene, membranes, water treatment, nanoparticles

## References:

1. KA Mahmoud, B Mansoor, A Mansour, M Khraisheh *Desalination*, **2015**, 356, 208-225.
2. CE Ren, KB Hatzell, M Alhabeab, Z Ling, KA Mahmoud, Y Gogotsi *J. Phys. Chem. Lett.*, 2015, 6, 4026-4031.
3. K Rasool, M Helal, A Ali, CE Ren, Y Gogotsi, KA Mahmoud "Antibacterial Activity of  $Ti_3C_2T_x$  MXene" *ACS Nano* **2016**, 10, 3674-3684.
4. GR Berdiyrov, ME Madjet, KA Mahmoud *Appl. Phys. Lett.*, **2016**, 108, 113110.

# Noninvasive Relaxometry Evidence of Linear Pore Size Dependence of Water Diffusion in Nanoconfinement

H. Chemmi<sup>1</sup>, D. Petit<sup>1,2,\*</sup>, P. Levitz<sup>3</sup>, R. Denoyel<sup>4</sup>, A. Galarneau<sup>5</sup>, J.-P. Korb<sup>1</sup>

<sup>1</sup>Physique de la Matière Condensée, CNRS/Ecole Polytechnique, 91128 Palaiseau, France

<sup>2</sup>Laboratoire Charles Coulomb, CNRS/Université de Montpellier, Montpellier, France

<sup>3</sup>Physicochimie des Electrolytes et Nanosystèmes Interfaciaux, UPMC, Paris, France

<sup>4</sup>MADIREL, Université Aix-Marseille, Centre de St Jérôme, Marseille, France

<sup>5</sup>Institut Charles Gerhardt Montpellier, UMR 5253 CNRS-UM-ENSCM, Montpellier, France

## Abstract:

We propose an original experimental method based on NMR at variable magnetic fields experiments (NMRD) and a theoretical analysis of the data that allows probing the spatial dependence of the diffusion coefficient of liquids specifically at proximity to pore surfaces. One of the key results found from these experiments is the linear relationship between average parallel diffusion coefficients and pore radii<sup>1</sup>. Another result is the robustness of the frequency scaling<sup>1, 2, 3, 4</sup> of the master curve approach able to take into account the complexity of the water dynamics at pore surface for samples of different geometries. This approach has proven useful for evaluating the efficiency of the coupling between liquid layers within nanopore by extracting gradients of diffusion coefficients. The application of this method to water confined in synthesized calibrated nanopores like MCM-41 for cylindrical geometry<sup>5</sup> and SEOS for spherical geometry<sup>6</sup> has been successful to deal with several dynamical processes on pore surface for different materials. This shows the ability of the proposed method to discriminate between the influence of the geometrical confinement on intrapore dynamics and the chemistry of the interface induced by different synthesis of the materials. For instance, the frequency selectivity of NMRD profiles has been able to separate the different couplings coming from the spatial heterogeneities on the pore surfaces<sup>1, 2</sup>. This frequency selectivity of NMRD has also allowed discriminating several steps of a complex dynamics process composed by both loops in water and surface diffusion during adsorption events<sup>7, 8, 9</sup>. Based on our experimental and theoretical results, we believe that the proposed noninvasive method allows exploring the interplay between molecular and continuous description of fluid dynamics relevant in physical and biological confinements.

**Keywords:** Calibrated nanoporous silicates, Dynamics of confined water. Noninvasive method.

**Figure 1:** <sup>1</sup>H NMRD profiles of MCM-41 saturated samples with 3.3 nm (diamond) and 11.8 nm (square) pore diameters (main figure). In inset, the master curve obtained by scaling both relaxation rate and frequency by the factors  $f_{R1} = 1.6$  and  $f_{\text{freq}} = 3.3/11.8$ , respectively is superposed to the MCM-41 of 11.8 nm pore diameter.

## References:

1. H. Chemmi, D. Petit, P. Levitz, R. Denoyel, A. Galarneau, J.-P. Korb, *J. Phys. Chem. Lett.* 7 (2016) 393–398.
2. H. Chemmi, PhD thesis, Ecole Polytechnique, Fr., 2011 <pastel-00671390v1>.
3. H. Chemmi, D. Petit, J.-P. Korb, R. Denoyel, P. Levitz, *Micro. and Meso. Mater.* 178 (2013) 104–107.
4. H. Chemmi, D. Petit, V. Tariel, J.-P. Korb, R. Denoyel, R. Bouchet, P. Levitz, *Eur. Phys. J. Special Topics* 224 (2015) 1749.
5. B. Coasne, A. Galarneau, F. Di Renzo, R. J. M. Pellenq, *Langmuir* 22 (2006) 11097.
6. E. Bloch, T. Phan, D. Bertin, P. Llewellyn, V. Hornebecq, *Micro. and Meso. Mater.* 112 (2008) 612.
7. P. Levitz, J.-P. Korb, D. Petit, *Eur. Phys. J. E* 12, 1 (2003) 29.
8. P. Levitz, J.-P. Korb, *Europhys. Lett.* 70, 5 (2005) 684.
9. J.-P. Korb, P.E. Levitz, *AIP Conf. Proc.* 1081 (2008) 55.

# Composite Membranes Modified with Polyelectrolyte Nanolayers: Characterization and Antifouling Potential

V.Kochkodan\*, D. Johnson, M. Hussein

Qatar Environment and Energy Research Institute, Hamad Bin Khalifa University, Doha, Qatar

## Abstract:

The main problem arising upon water treatment and desalination using pressure driven membrane processes such as microfiltration, ultrafiltration, nanofiltration and reverse osmosis is membrane fouling that seriously hampers the application of the membrane technologies [1]. One of the main approaches to mitigate membrane fouling is to minimize adhesion interactions between a foulant and a membrane [2]. Surface coating of the membranes with polyelectrolytes seems to be a simple and flexible technique to improve the membrane fouling resistance [3].

In this study composite polyamide membranes NF-90, NF-270 and BW-30 were modified using electrostatic deposition of polyelectrolyte nanolayers made from various polycationic and polyanionic polymers of different molecular weights. Different anionic polyelectrolytes such as: poly(sodium 4-styrene sulfonate), poly(vinylsulfonic acid, sodium salt), poly(4-styrene sulfonic acid-co-maleic acid) sodium salt, poly(acrylic acid) sodium salt (PA) and cationic polyelectrolytes such as poly(diallyldimethylammonium chloride), poly(ethylenimine) and poly(hexamethylene biguanide) were used for membrane modification.

An effect of deposition time and a number of polyelectrolyte layers on the membrane modification has been evaluated. The surface morphology of the prepared composite membranes were studied using atomic force microscopy. It was shown that the surface membrane roughness decreases significantly as a number of the polyelectrolyte layers on the membrane surface increases. This smoothing of the membrane surface might contribute to the reduction of membrane fouling as lower roughness most often associated with a decrease in surface fouling. It was shown that the surface charge of the membranes modified with polyelectrolytes can be switched between positive and negative after coating with a cationic or an anionic polyelectrolyte. On the other hand the water contact angle was strongly affected when the outermost polyelectrolyte layer was changed.

Finally, a distinct difference in the performance of the noncoated membranes and the polyelectrolyte modified membranes was found during treatment of seawater in the non-continuous regime. A possible mechanism of the higher fouling resistance of the modified membranes has been discussed.

**Keywords:** surface modification, polyelectrolytes, membrane fouling, atomic force microscopy

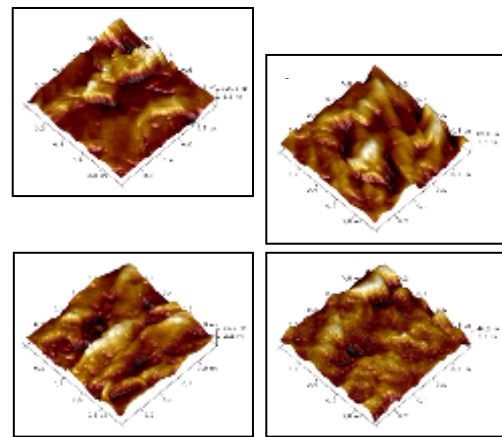


**Figure:** AFM images of initial NF90 membrane (a) and modified samples with a different number of polyelectrolyte nanolayers: (b) – 2; (c) – 4; (d) – 8 layers.

## References:

1. Baker, R.W. (2004) Membrane Technology and Applications, John Wiley & Sons, NY.
2. Kochkodan, V., Hilal, N. (2015) A comprehensive review on surface modified polymer membranes for biofouling mitigation, *Desalination*, 356, 187-207.
3. Ng, L.Y., Mohammad, A.W., Ng, C.Y. (2013) A review on nanofiltration membrane fabrication and modification using polyelectrolytes: Effective ways to develop membrane selective barriers and rejection capability, *Adv. Colloid Interface Sci.*, 197-198, 85-107.

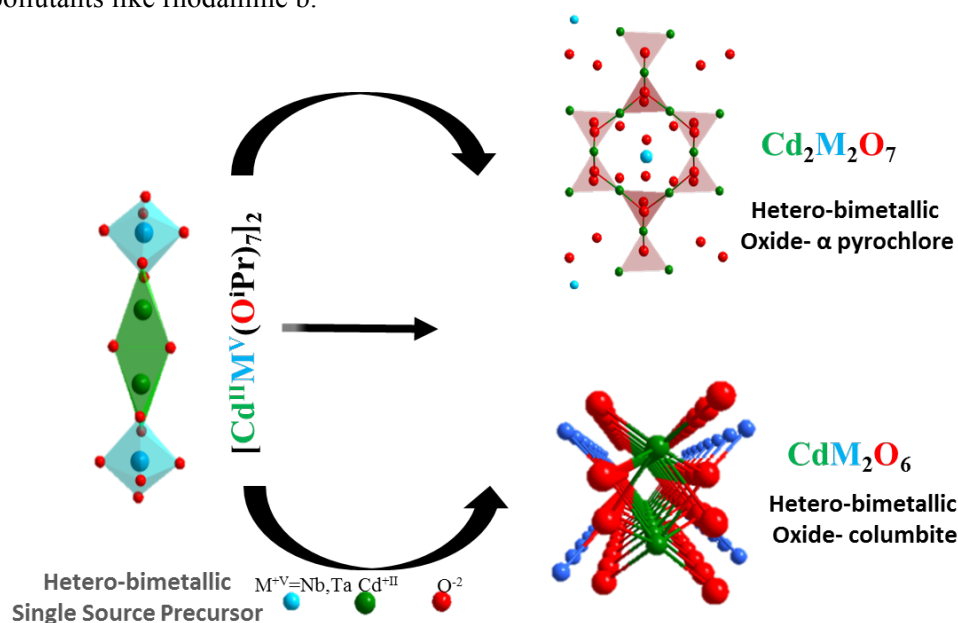
# New Hetero-bimetallic Alkoxides $[\text{Cd}^{\text{II}}\text{M}^{\text{V}}(\text{O}^i\text{Pr})_7]_2$ (M = Nb, Ta) as Potential Precursors to selective oxide phase and photocatalysis

Rishabh Garg, Corinna Hegemann, and Sanjay Mathur \*

Institute of Inorganic Chemistry, University of Cologne, GreinstraÙe 6, D-50939 Cologne, Germany

## Abstract:

The prime focus for the controlled synthesis is the quest for new hetero-bimetallic single source precursor compounds for new materials. Therefore, series of novel hetero-bimetallic single source precursors (SSP) with a formula  $[\text{Cd}^{\text{II}}\text{M}^{\text{V}}(\text{O}^i\text{Pr})_7]_2$  (M = Nb(1), Ta(2)) to result in direct selective decomposition to pyrochlore  $\text{Cd}_2\text{M}_2\text{O}_7$  metal oxides has been developed. The synthetic strategy exploits the Lewis acidic nature of cadmium alkoxide resulting in successful isolation of bimetallic complexes. These compounds have been thoroughly characterized by spectroscopic methods and single crystal XRD. Spray Pyrolysis and TG-DTA analysis showed that complex 1 and 2 undergo clean facile thermal decomposition at 600°C to give the respective ternary phase. Temperature variable X-ray diffraction analysis of 1 additionally proved the possible formation of crystalline  $\text{Cd}_2\text{Nb}_2\text{O}_7$  phase. The oxide ion conducting phases have been produced by direct pyrolysis of the precursor molecules to achieve the desired pyrochlore structure to utilize its unique photocatalytic properties towards degradation of organic pollutants like rhodamine b.



## Keywords:

Hetero-bimetallic complexes, cadmium, single source, pyrochlore, photocatalysis,  $\text{TiO}_2$ , columbite, microwave,

## References:

1. Veith, M.; Mathur, S.; Mathur, C. *Polyhedron* **1998**, *17*, 1005.
2. Buixaderas, E.; Kamba, S.; Petzelt, J.; Savinov, M.; Kolpakova, N.N. *Eur. Phys. J. B* **2001**, *19*, 9.
3. Ronconi, C. M.; Gonçaves, D.; Suvorova, N.; Alves, O. L.; Irene, E. A. *J. Phys. Chem. Solids* **2009**, *70*, 234.
4. Łukaszewicz, K.; Pietraszko, A.; Stepień-Damm, J.; Kolpakova, N. N. *Materials Research Bulletin* **1994**, *9*, 987.
5. Dasa, D.; Ganguli, A.K. *RSC Adv.*, **2013**, *3*, 21697.
6. Veith, M.; Mathur, S.; Huch, V. *J. Am. Chem. Soc.* **1996**, *118*, 903.
7. Veith, M.; Mathur, S.; Huch, V. *Inorg. Chem.* **1996**, *35*, 7295.

# Synthesis of Pd-Ag Bimetallic Alloy Decorated Nitrogen Doped Graphene and Their Catalytic Study for Selective Hydrogenation in Excess Ethylene

Firozeh Mansourkhani<sup>1\*</sup>, A. Badiei<sup>1</sup>, A.M Rashidi<sup>2</sup>, S. Khajehmandali<sup>3</sup>

<sup>1</sup>University of Tehran, Department of chemistry, Tehran, Iran

<sup>2</sup>Research Institute of Petroleum Industry, Tehran, Iran

<sup>3</sup>Research and Development Department, Shazand Petrochemical Company, Arak, Iran

## Abstract:

The presence of small amounts of acetylene in ethylene obtained from thermal cracking of oil compounds is considered as an impurity in the ethylene-based polymerization reactions. Conventionally, hydrogenation reaction is proposed as a major method for ethylene purification [1]. In this work, Pd-Ag bimetallic alloy decorated over a nitrogen doped graphene support by polyol reduction process, then applied for selective hydrogenation of acetylene in an ethylene-rich flow stream. Nitrogen doping of graphene can influence the growth kinetics of metal nanoparticles that lead to their small particle size, uniform dispersion, and different morphology. Also, nitrogen doping of the support materials can give better chemical binding between support and metal nanoparticles resulting enhanced stability [2]. TEM image of Pd-Ag/NG in Figure 1 shows that Pd-Ag nanoparticles are uniformly dispersed over nitrogen doped graphene with high dispersion and narrow size distribution (5-6 nm). Performance tests of Pd-Ag/NG nanocatalyst were conducted for selective hydrogenation of acetylene from the ethylene rich stream (contains 80, 17.6, 1.4, 1 Vol % for ethylene, ethane, hydrogen and acetylene, respectively) at 40–200 °C. Pd-Ag/NG nanocatalyst showed excellent ethylene conversion and selectivity and also, its selectivity increased with both temperature and acetylene conversion. Figure 2 shows the acetylene conversion and ethylene selectivity versus temperature during the reaction for Pd-Ag/NG catalyst with 1:1 molar ratio of Pd to Ag. Catalytic behavior of Ag-promoted Pd catalysts is affected by geometric and electronic factors which are more pronounced in the case of Ag/Pd=1. Ag played significant role along with Pd as a hydrogenation reaction catalyst, enhancing simultaneously acetylene conversion and ethylene selectivity.

**Keywords:** Hydrogenation catalyst, Nitrogen doped graphene, Pd-Ag alloy, Selective acetylene hydrogenation.

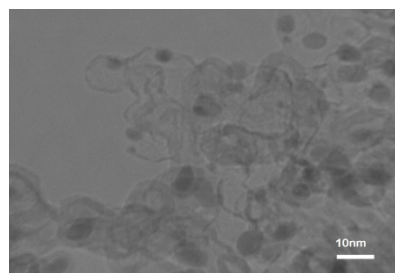


**Figure 1:** TEM image of Pd-Ag/NG

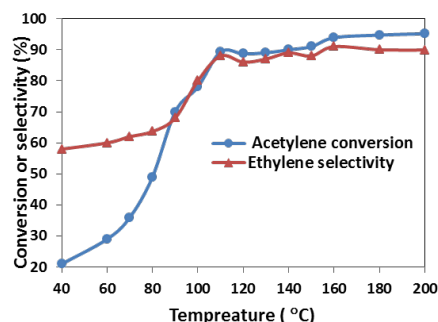


**Figure 2:** Acetylene conversion and ethylene selectivity for Pd-Ag(1:1)/NG catalyst

## References:

1. Panpranot, J., Kontapakdee, K., Praserttham, P. (2006), Selective hydrogenation of acetylene in excess ethylene on micron-sized and nanocrystalline TiO<sub>2</sub> supported Pd catalysts, *Applied Catalysis A: General.*, 314, 128-133
2. Geng, D., Chen, Y., Chen, Y., Li, Y., Li, R., Sun, X., et al. (2011), High oxygen-reduction activity and durability of nitrogen doped graphene, *Energy & Environmental Science.* 4, 760-764.

# APTES functionalized of cocoa shell (CS) surfaces obtained from biomass and its application in CO<sub>2</sub> adsorption

R. Bargougui<sup>a</sup>, N. Bouazizi<sup>a</sup>, P. Fotsing<sup>b</sup>, O. Thoumire<sup>c</sup>, G. Ladam<sup>c</sup>, N. Brun<sup>d</sup>, E. Djoufac Woumfo<sup>b</sup>, J. Vieillard<sup>a</sup>, N. Mofaddel<sup>a</sup>, F. Le Derf<sup>a</sup>

<sup>a</sup> Normandie Univ, UNIROUEN, INSA Rouen, CNRS, COBRA (UMR 6014), 76000 Rouen, France.

<sup>b</sup> Laboratoire de Physico-Chimie des Matériaux Minéraux, Département de Chimie Inorganique, Faculté des Sciences, Université de Yaoundé I, B.P. 812 Yaoundé, Cameroun.

<sup>c</sup> Laboratoire de Biophysique et Biomateriaux (La2B - MERCI EA 3829), Université de Rouen, Centre Universitaire d'Evreux, 1 Rue Du 7ème Chasseurs, Evreux Cedex, 27002, France.

<sup>d</sup> Institut Charles Gerhardt, ENSCM, 34296 Montpellier Cedex 5, France.

## Abstract

The aim of this research is to investigate how the covalent grafting of APTES at the surface of cocoa shell (CS) may improve its activity for the adsorption of CO<sub>2</sub> at 20°C. Pure cocoa shells (CS) are agricultural by-products, usually inexpensive and abundantly available. They were functionalized by covalent grafting of (3-aminopropyl) triethoxysilane (APTES) and subsequent immobilization of cobalt nanoparticles (Co-NPs) by insertion in mixed solvent (ethanol/water 75/25 v/v) at 80°C. Physical and thermal properties of the adsorbents like analysis stability, surface charge and morphology were investigated by FTIR, SEM, EDX, BET, DSC and zeta potentiometry techniques. The mechanism for the CO<sub>2</sub> capture by the CS- APTES-Co was investigated by FTIR and EDX, and the results indicated a high CO<sub>2</sub> capture capacity. The favorable adsorption of the as-prepared materials was mainly attributed to their original structure (i.e., surface area, functional groups, and the Co-NPs). The adsorption capacity was also remarkably increased from 0.018 mmol CO<sub>2</sub>.g<sup>-1</sup> for the raw material to 0.24 mmol CO<sub>2</sub>.g<sup>-1</sup> after surface modification. This work should open up a new pathway to slow down the atmospheric CO<sub>2</sub> as well as resolve the pollution of waste biomass.

**Keywords:** APTES; cocoa shell; cobalt NPs; functionalization; CO<sub>2</sub> capture.

# Impact of Nitro Phosphate-ZnO Nanoparticle Composites on Spinach Growth and Nutrient Use Efficiency

Archana P. Kale,<sup>1</sup> Satyavikas N. Gawade<sup>2</sup>

<sup>1,2</sup>Research and Development Department (Bio-agro research)  
Rashtriya Chemicals and Fertilizers Limited, A Government of India Undertaking,  
Chembur, Mumbai, Maharashtra state, India, 400074

## Abstract:

Application of nanoparticle viz. Zn, Fe, Cu etc. in agriculture have shown increase in crop yield and Nutrient Use Efficiency (NUE). Due to increase in activity related to high surface to mass ratio, such particles can be used as a tool for faster entry in the stomata, cuticle, root tips, rhizodermis, root junctions and wounding of the plant. After entry in to the plant, they trigger the enzymes during the transportation. In the present study, the Nitrophosphate (NPK complex fertilizer-Suphala)-ZnO nanoparticle composite enters in to the plant system and change the spinach (*Spinacia Oleracea* L.) plant metabolism. As a result the NUE improved to the tune of eight times against the recommended dose of fertilizer (RDF) of the crop. It has also improved the vegetative growth hence the yield of the crop. There was a gradual increase in the yield with decrease in the RDF by keeping ZnONP at constant rate. The reduction in the yield was noticed after 12.5% RDF which explains optimization of RDF-ZnONP combination (figure 1). The decrease in concentration of NPK nutrient particles facilitates easy access to nanoparticles and thus the interaction between them increases. Due to this, efficiency of the nutrient particle has shown remarkable response. The minute quantity of ZnONP i.e.1246 mg/Ha has influenced the activity of NPK bulk particles such that NUE has increased as much as eight times. This has initiated the idea of designing new nanofertilizer composition. The reduction in the dose of fertilizer will decrease 1) losses due to mineralization 2) environmental pollution, 3) sustainable use of non-renewable resources, 4) decrease in stress on logistics 5) a great step towards sustainable agriculture and hence 6) food security. The study also shows new direction for application of nanoparticles in the formulations of nanofertilizer with increased NUE as well as food security.

**Keywords:** Nanoparticles, recommended dose of fertilizers, nutrient use efficiency, Nitrophosphate, Suphala.

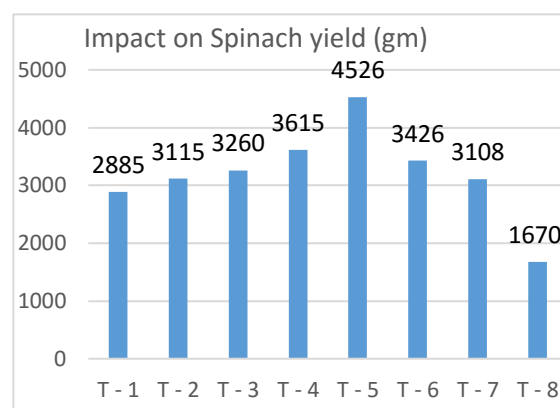


**Figure 1:** Influence of ZnONP in increasing the yield of Spinach crop by decrease in % fertilizer recommended dose. Where T-1, T-2, T-3, T-4, T-5, T-6, T-7, and T-8 are 100% RDF (control), 100% RDF+ ZnONP, 50% RDF+ ZnONP, 25% RDF+ ZnONP, 12.5%+ ZnO NP, 6.25% RDF+ ZnONP, 5% RDF+ ZnONP, and No fertilizer respectively.

## References

1. Giraldo J.P., Landry M.P., Faltermeier S.M., McNicholas T.P., Iverson N.M., Boghossian A.A., Reuel N.F., Hilmer A.J., Sen F., Brew J.A., Strano M.S. (2014) Plant nanobionics approach to augment photosynthesis and biochemical sensing. *Nat Mater.* doi:10.1038/nmat 3890.
2. Prasad, T.N.V., Sudhakar P., Sreenivasanlu Y., Latha P., Munaswami V., Raja R.K., Sreeprasad T. S., Sajanalal P.R., Pradeep T. (2012) Effect of nano scale zinc oxide. Particles on the germination, growth and yield of peanut. *J Plant Nutr.* **35**:905 - 927.

# Novel ionic liquid bonded magnetic nanoparticle decorated zeolite nanocomposite for excellent catalytic reduction of dyes

A. Vasanthakumar,<sup>1\*</sup> R. M. Gengan,<sup>1</sup> G. G. Redhi<sup>1</sup>

<sup>1</sup> Durban University of Technology, Department of Chemistry, Durban, South Africa

## Abstract:

Novel 2,3-epoxypropyl-n-methyl pyrrolidinium salicylate [EPpyr]<sup>+</sup>[Sal]<sup>-</sup> ionic liquid bonded iron oxide (Fe<sub>3</sub>O<sub>4</sub>)magnetic nanoparticle modified zeolite nanocomposite (Fe<sub>3</sub>O<sub>4</sub>/IL/Zeolite) was synthesized via facile chemical method and characterized by fourier transform infrared spectroscopy, scanning electron microscope, energy dispersive X-ray spectrometry, transmission electron microscopy and thermogravimetry and differential scanning calorimetry to evaluate their functional groups, physical, chemical, surface morphology and thermal stability nature of the material. In this case, ionic liquid and iron oxide magnetic nanoparticles were synthesized and characterized. Both these compounds contribute enhancing binding, efficacy and thermostability of the nanomaterial. Researchers were established zeolite based nanocomposite with graphene oxide or ionic liquids for application of dyes reduction and separation of CO<sub>2</sub>.<sup>1,2</sup> The new nanocomposite acts as an excellent catalyst for reduction of different dyes such as methylene blue, allura red and methyl orange and it can be monitor by UV-Visible spectroscopy. Furthermore, the catalyst was removed after completion of reaction, purified and recycled for several times with negligible loss of activity. In addition, the reduction reaction could occur in aqueous solution making this is an economical, eco-friendly and effective prptocol.

**Keywords:** Epoxypropyl pyrrolidinium, Magnetic nanoparticles, Zeolite, Ionic liquid, Nanocomposite.

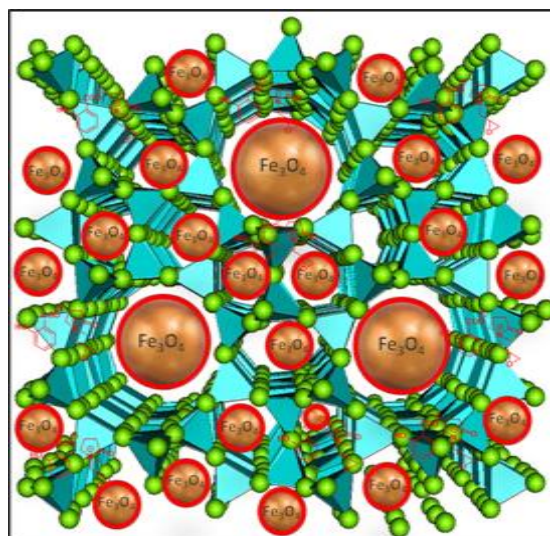


**Figure 1:** Ionic liquid bonded Fe<sub>3</sub>O<sub>4</sub> decorated Zeolite nanocomposite (Fe<sub>3</sub>O<sub>4</sub>/IL/Zeolite).

## References:

1. Tang, M., Li, X., Gao, C., Li, X., Qiu, H. (2017) Adsorption performance of CuFe<sub>2</sub>O<sub>4</sub>/rGO nanocomposites towards organic dye, *Mat. Chem. Phy.*, 185, 114-121
2. Hudiono, Y. C., Carlisle, T. K., Bara, J. E., Zhang, Y., Gina, D. L., Noble, R. D. (2010) A three-component mixed-matrix membrane with enhanced CO<sub>2</sub> separation properties based on zeolites and ionic liquid materials. *J. Memb Sci.*, 350 (1-2) 117-123

# EFFECT OF NANO-ZnO-SiO<sub>2</sub> ON THE PHOTODEGRADATION OF OLIVE MILL EFFLUENT, RECOVERIES OF NANO-ZnO-SiO<sub>2</sub>, POLYPHENOLS AND UTILISABILITY OF TREATED WASTEWATER AS IRRIGATION PURPOSE

Ç. Ulusoy<sup>1</sup>, D.T. Sponza<sup>2</sup>

<sup>1,2</sup>, Dokuz Eylül University, Engineering Faculty, Environmental Engineering Department, 35160, İzmir; TURKEY

## Abstract:

Olive oil mill wastewater contains high concentration of organic matter, acidic pH values, suspended solids and high content of phenols and polyphenols which are toxic substances. In this study, Nano-ZnO-SiO<sub>2</sub> e was used to treat the pollutants from the olive mill industry wastewaters by photo-degradation. ZnO is an n-type semiconductor with a wide direct bandgap of 3.37 eV. ZnO microcrystal showed also good photocatalytic activity for wastewater containing phenol. One of the most promising methods to increase the photocatalytic efficiency is surface modification of ZnO, this can be achieved by metal such as SiO<sub>2</sub> doping into the ZnO catalyst. Dopant can act as a sink to collect photogenerated electrons from the conduction band of the semiconductor. Thus, it hinders the recombination of photogenerated electrons and holes through increasing the charge separation. The aim of this study is to remove of COD, total phenol, total solid (TS), total nitrogen, total phosphorus. Furthermore the recovery studies of polyphenols (gallic acid, para coumaric acid, t-para coumaric acid) were studied from the OMW by nano-ZnO-SiO<sub>2</sub> composite with adsorption and photocatalytic treatment (UV and sunlight). The optimum treatment conditions were determined to remove the pollutants. The maximum removal efficiencies were obtained with UV treatment. The maximum yields of COD (78%), total phenol (86%), TS (77%) and total nitrogen (100%) were obtained with 1 g/L nano-ZnO-SiO<sub>2</sub> composite excluding total phosphorous (5 g/L). The maximum yields of COD, total phenol, TS and total nitrogen were obtained after 15 min excluding total phenol (90 min) and total nitrogen (60 min). The maximum removal efficiencies of COD, total phenol and TS were obtained at original pH of OMW (4.01) excluding total nitrogen (pH 7), total phosphorous (pH 10). In the treatment of OMW with sunlight 3 g/L Nano-ZnO-SiO<sub>2</sub> composite is

required for maximum yields of COD (77%), total phenol (73%), TS (64%) and total nitrogen (96%) excluding total phosphorous (5 g/L). The maximum yields of COD, total phenol and TS were obtained at original pH of OMW (4.01). The maximum yields of total nitrogen and total phosphorous (80%) were obtained at pH 7 and 10, respectively. In the reusability studies of the Nano-ZnO-SiO<sub>2</sub> composite it was found that the same nano-composite can be used again six sequential times for treatment of OMW throughout photocatalytic treatment with UV. 1 euro was spent for 20 UV lamps, while the chemical cost, electricity consumption and nanocomposite cost were only 0.3 euro for the treatment of liter of OMW. Treated OMW was also examined for the irrigation purpose according to limits of irrigation criteria in Turkey. Gallic acid, para coumaric acid and t-para coumaric acid were recovered with yields varying between 85% and 93%

**Keywords:** Nano-ZnO-SiO<sub>2</sub>, Photocatalytic degradation, Polyphenols, Olive mill Wastewater, Recovery, Reuse UV Irradiation, Irrigation.

**Acknowledgment:** The authors would like to express appreciation for the support of the sponsors; (TUBITAK PROJECT NUMBER: TOV 1130558 and Dokuz Eylül University Scientific Research Project (KB.FEN.020)).

# Characterization and Behavior of SiO<sub>2</sub> and Fluoride Nanoparticles in Aqueous Systems : Influence of pH and Commercial Polymers

M.O. Fatehah,<sup>1\*</sup> M.Z. Noor Aina,<sup>1</sup> J.Y. Sin,<sup>1</sup>

<sup>1</sup>Universiti Sains Malaysia, School of Civil Engineering, Nibong Tebal, Malaysia

## Abstract:

For the past few decades, semiconductor industry has well developed sector in Malaysia and many other countries around the world. In the next few years, this industry is expected to expand its growth to a wider prospect (Ahmed et al., 2011). The electric and electronic industry has assumed the role of a prime mover in the Malaysian economy securing foreign investment and creating employment. According to the Malaysia Investment Performance Report 2015, exports of electrical and electronic products accounted for RM277.9 billion and contributed 44.4 percent of total manufacturing goods in 2015 (Growth, 2015).

The semiconductors are used in various types of equipment such as computer devices, telecommunication devices, consumer electronic products, electronic control devices, scientific and also in medical test equipment. Water is fundamental to the manufacture of semiconductors. The semiconductors produced must be rinsed after produced, which require massive amount of water. According to (GWI 2009), industry statistics indicate that creating an integrated circuit on a 300 mm wafer requires approximately 2200 gallons of water in total, of which 1500 gallons is ultra-pure water. Ultra-pure water which is defined as water of utmost purity and without presence of microorganisms, minerals, or trace organic or nonorganic chemicals (Lee & Choi, 2012). It is widely used in polishing the semiconductors (Hernon, Zhang, Siwak, & Schoepke, 2010) and hence large amount of wastewater is produced from the effluents of semiconductor industry.

**Keywords:** silica dioxide, zinc oxide, metal oxide, engineered nanoparticles, dynamic light

scattering, zeta potential, particle size, aggregation, disaggregation, potable water.

## References:

1. Ahmed et. al 2011
2. Growth, 2015
3. GWI 2009
4. Lee & Choi, 2012)
5. (Hernon, Zhang, Siwak, & Schoepke, 2010)

**Session VII:  
NanoElectronics / NanoPhotonics**

# The Study of Emerging Materials in Nano-electronic Devices and Their Corresponding Electrical Performances

Hui-Lin Chang,<sup>1,2,\*</sup> Chi-Tso Chang,<sup>1</sup>

<sup>1</sup> Department of Material Science and Engineering, National Chiao Tung University, HsinChu, Taiwan, 30050

<sup>2</sup> Advanced Device Technology, Globalfoundires, Malta, New York, USA, 12020

## Abstract:

The sustaining of Moore's law requires continual transistor scaling. Therefore, the adoption of emerging materials will surely prove extremely valuable for future nano-electronic applications. Several emerging devices such as Si nanowire, carbon nanotube, III-V compounds field effect transistors (FETs) all hold promise to be potential candidates to extend Moore's law. Presented here is a systematic work of random oriented SiCN tubes, nanowire/conical rod and 2-D graphite/seaweed structures including a design of an integration of nano-electronic device flow. The electronics performances of emerging materials are considered in detail. The integration of nanostructure materials into Si-based metal-oxide semiconductor field effect transistors (MOSFETs) was adopted by selective patterning processes. In this study, we employed two methods to make horizontally aligned nanotube field effect transistors (HFET) and vertical aligned nanotube field effect transistors (VFET). The  $\text{CoSi}_2$  catalysts, used to enhance nanotube growth, were patterned in the trench or holes to control the growth directions vertically. The  $\text{NiSi}_2$  was patterned in the parallel plate to grow nanotubes horizontally. It is clear that field alignment, using applied direct current bias (-200V), effectively direct nanotube growth perpendicularly to the substrate. Moreover, the catalyst density is also important in determining nanotube growth direction. Likewise, gaseous sources play crucial role in controlling nanotube growth orientations. When the flow of gas is guided horizontally with respect to the substrate, nanotubes will grow in the same direction. Two catalysts plates produce horizontal nanotube growth while separate catalyst islands lead to horizontal nanotube formation. The current density-electric field (J-E) curves of SiCN crystal and tubes, vertical nanotubes and horizontal nanotubes are compared. The current density-electric field (J-E) curves of SiCN tubes and SiCN crystals at  $1\text{mA}/\text{cm}^2$  is obtained at 2.56 and 7.98V/ $\mu\text{m}$ , with a turn-on electric field (Eturn-on) of 1.57 and 4.32 V/ $\mu\text{m}$  for horizontal

nanotubes and vertical nanotubes at a current density of  $1\text{mA}/\text{cm}^2$ , respectively. The current density of  $1\text{mA}/\text{cm}^2$  for nanotubes at trenches and holes is obtained at 3.97 and 6.30 V/ $\mu\text{m}$ . On account of Moore's law, which relies on constant transistor scaling, emerging materials, such as Si nanowires, carbon nanotubes and III-V semiconductor FETs, are expected to transform future nano-electronics applications validating this theory. This study demonstrates how deposition methods for selective nanotubes will lead to vertically and horizontally oriented growth. The development of nanostructure materials with unique electrical properties may therefore expand nano-electronic device applications.

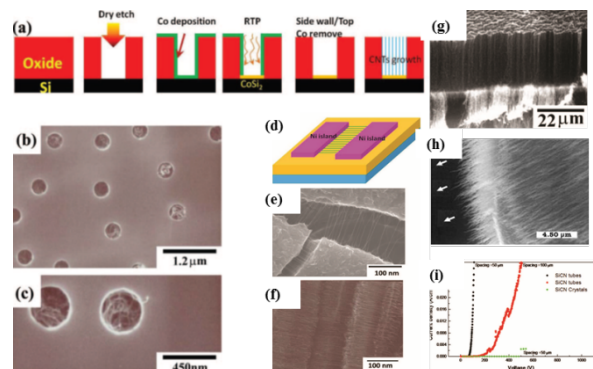


Fig (a) Selective nanotube growth in designed hole arrays (b) Top-views SEM image of tubes, (c) Zoom in image of (b), (d) Selective horizontal nanotube deposition on parallel Ni plates, (e) (f) Zoom in TEM images of horizontal nanotube images, (g) Vertical nanotube deposition (h) Horizontal nanotube deposition (f) J-E curves of Si-C-N tubes and crystals.

**Keywords:** nanotube, CMOS, electronic device, FET, catalyst, semiconductor, nanotechnology

## References:

1. Chang, H. L., Chang, C. T., and Kuo, C. T. ECS Journal of Solid State Science and Technology, 3 (10) M64-M70 (2014)
2. Chang, H. L., Chang, C. T., and Kuo, C. T. ECS Journal of Solid State Science and Technology, 2 (11) N217-M221 (2013)

# Hybrid graphene – colloidal quantum dot phototransistor for IR-imaging applications

I. Nikitskiy,<sup>1\*</sup> Stijn Goossens,<sup>1</sup> D. Kufer,<sup>1</sup> T. Lasanta,<sup>1</sup> G. Navickaite,<sup>1</sup> G. Konstantatos,<sup>1</sup> F. Koppens.<sup>1</sup>

<sup>1</sup>ICFO - The Institute of Photonic Sciences, Barcelona, Spain

## Abstract:

Graphene is an appealing material for optoelectronics applications. It has various extraordinary properties, including ultrahigh mobility at room temperature, which enables fast response times. Colloidal quantum dots (QDs) exhibit unique optical properties of spectral tunability and high absorption coefficients. We combine the favourable electronic properties of graphene with the optical characteristics of QDs to realize a novel hybrid graphene-QD phototransistor for light detection in visible and infrared ranges. The unique electronic properties of graphene enable us to tune the sensitivity and operating speed of the detector. The implementation of nanoscale local gates enables a locally tunable photoresponse, which is useful for pixelated imaging applications. We exploit gate-tunability of the phototransistor to maximize the responsivity, gain and external quantum efficiency (EQE) of the detector or to fully reduce them to zero. We also demonstrate our novel approach to fully suppress dark currents in graphene-based photodetectors and increase operation speed of our devices. Our single and multipixel photodetectors can be fabricated on various substrate, including the flexible ones, and operate at up to 90 frames-per-second rate. Most recently, we have demonstrated a monolithic integration of the hybrid detectors with CMOS read-out electronics to create a broadband 388×288 pixel image sensor array. The resulting technology is extremely promising for visible and, more importantly, short-wave infrared (SWIR) imaging applications. Sensing and imaging in SWIR range lies at the heart of safety and security applications in civil and military surveillance, night vision applications, automotive vision systems for driver safety, environmental monitoring and food inspection.

**Keywords:** photodetectors, sensors, CMOS, graphene, colloids, quantum dots, nanocrystals, nanomaterials, infrared imaging, surveillance, food inspection, flexible electronics.

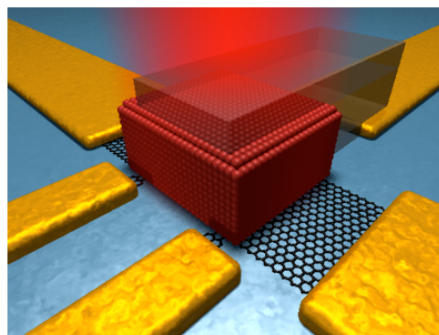


**Figure 1:** Schematic of the hybrid graphene – QD photodetector.

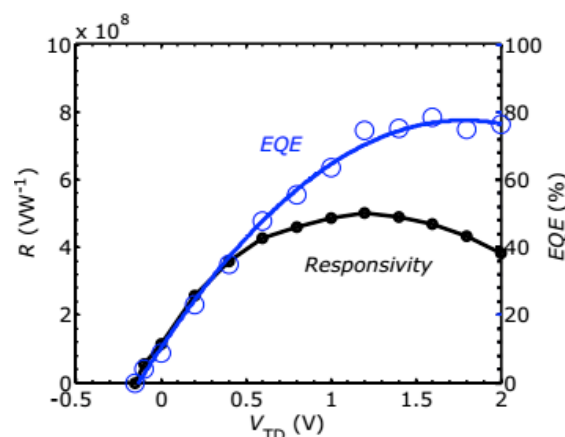


**Figure 2:** Responsivity and EQE of the integrated devices as a function of gate voltage

## References:

1. Konstantatos et al. (2012) Hybrid graphene–quantum dot phototransistors with ultrahigh gain. *Nature Nano.*, 7, 363–368.
2. Nikitskiy et al. (2016) Integrating an electrically active colloidal quantum dot photodiode with a graphene phototransistor. *Nature Commun.*, 7, 11954
3. Goossens et al. (2017) Broadband image sensor array based on graphene-CMOS integration. *Nature Photonics*, Accepted.

# Tuning the properties of graphene nanomesh for high-performance supercapacitors

Yan Zhong,<sup>1,2</sup> Tielin Shi<sup>1,2</sup>, Zirong Tang<sup>1,2</sup>

<sup>1</sup> State Key Laboratory of Digital Manufacturing Equipment and Technology, Huazhong University of Science and Technology, Wuhan 430074, People's Republic of China

<sup>2</sup> Wuhan National Laboratory for Optoelectronics, Huazhong University of Science and Technology, Wuhan 430074, People's Republic of China

## Abstract:

Graphene, due to its superior electrochemical performance, is widely used as energy storage material, especially in the area of supercapacitors. However, ion transport is limited due to its large lateral size. How to improve the utilization of the graphene material as well as enhance the energy storage capacity is still under a long way. Recently, more studies are focused on graphene nanomesh, which can prevent the restack of graphene and facilitate the 3D transport of ion. In this regard, our recent studies focus on tuning the nanomesh size and density of graphene by controlling the concentration of the stannous chloride solution and the time of high-temperature catalysis. First, hydrothermal method is used to prepare the reduced graphene hydrogel. Then ion absorption is completed in stannous chloride solution. Finally, high temperature catalysis are utilized to induce nanomesh. By this method, preliminary results are obtained. As shown in Fig. 1(a), stannous chloride is absorbed on the the hydrogel, showing a rough surface. Fig. 1(b) shows a enlarged SEM picture, depicting stannous chloride evenly distributed on the graphene. It proves that the prepared electrode exhibits rapid charge and discharge performance, even at the scan rate up to 1V/s. The GCD testing curves are highly linear and symmetrical, demonstrating excellent capacitive performance, where the capacity is up to 234.79 mF/cm<sup>2</sup> at the current density of 0.5 mA/cm<sup>2</sup>. A 88.3% retention is kept at 3 mA/cm<sup>2</sup>, exhibiting excellent rate performance. The good performance is mainly due to: (1) the high conductivity of the graphene; (2) sufficient mesopores on the graphene layer; (3) 3D ion transport of electrolyte. Different size and density of graphene nanomesh will be further tuned in our future work.

**Keywords:** graphene nanomesh, rate performance, 3D ion transport, conductivity, supercapacitor, high temperature catalysis.

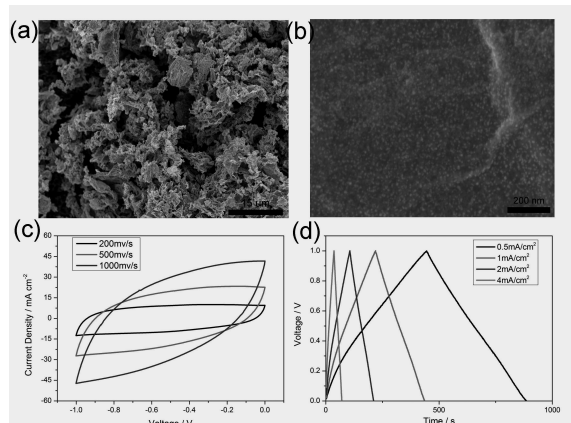


**Figure 1:** (a) The SEM picture after ion absorption; (b) The enlarged SEM picture after high-temperature calcinations; (c) CV testing at a scan rate from 200 mV/s to 1000 mV/s; (d) GCD testing at a current density from 0.5 mA/cm<sup>2</sup> to 4mA/cm<sup>2</sup>

## References:

1. Kim H K, Bak S M, Lee S W, et al. Scalable fabrication of micron-scale graphene nanomeshes for high-performance supercapacitor applications. *Energy & Environmental Science*, 2016, 9(4): 1270-1281.
2. Jiang L, Fan Z. Design of advanced porous graphene materials: from graphene nanomesh to 3D architectures. *Nanoscale*, 2014, 6(4): 1922-1945.

# Threshold Voltage Adjustment on MoS<sub>2</sub> Field Effect Transistor (FET) by Dielectric Capping Layer

June Park<sup>1</sup>, Seung-Hwan Kim<sup>2</sup>, Sun-Woo Kim<sup>1</sup>, and Hyun-Yong Yu<sup>2</sup>

<sup>1</sup>Department of Nano-Semiconductor, Korea University, Seoul 136-713, Korea

<sup>2</sup>School of Electrical Engineering, Korea University, Seoul 136-713, Korea

## Abstract:

The two-dimensional (2-D) layered transition-metal dichalcogenides (TMDCs) has received great attention due to their fascinating properties. For optimizing device performance, suitable threshold voltage adjustment techniques for TMDCs are necessary. However, unlike conventional CMOS, general ion implantation is not appropriate technique for TMDCs because it can induce fatal damage to the crystal structure of TMDCs. Recently, some researches suggested new techniques for threshold voltage adjustment on TMDCs. They used dielectric capping layer for making operation change on several TMDCs. However, those studies have limit that showing negative threshold voltage shift only.

In this study, we have suggested two materials (Al<sub>2</sub>O<sub>3</sub> and SiO<sub>2</sub>) as dielectric capping layer for producing both of negative and positive threshold voltage shift. By choosing proper dielectric layer material on the device, we can control operation of the device easily. We used MoS<sub>2</sub> (molybdenum disulfide) as channel material. Furthermore, we proceeded experiments that deposit two dielectric layer in a row. We observed similar threshold voltage shift regardless of order. By using combination of two dielectric capping layer, we can obtain advanced controllability of MoS<sub>2</sub>-FET. Also, we established model of threshold voltage adjustment by dielectric capping layers. Due to defect charges in dielectric capping layer, band bending is induced and operation of the device changed. Our research can help to control threshold voltage on TMDCs-based devices and further understanding about dielectric layer on TMDCs.

**Keywords:** TMDCs, MoS<sub>2</sub>, threshold voltage,

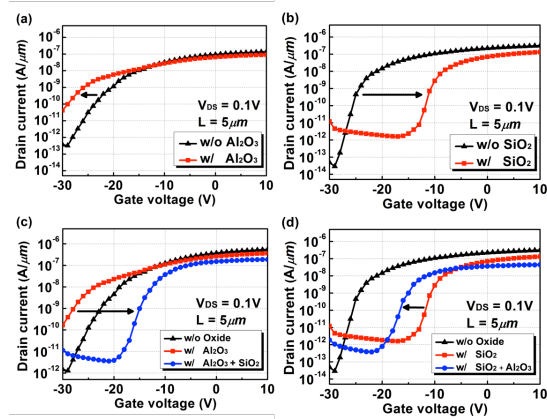


**Figure 1:** (a), (b) The  $I_d$ - $V_g$  characteristics of a back-gated MoS<sub>2</sub> FET without/with single dielectric capping layer. The negative threshold voltage change with Al<sub>2</sub>O<sub>3</sub> layer is observed while the positive threshold voltage change with SiO<sub>2</sub> layer. (c), (d) The  $I_d$ - $V_g$  characteristics of a back-gated MoS<sub>2</sub> FET with combination of two dielectric capping layers.

## References:

1. B. Radisavljevic et al., "Single-layer MoS<sub>2</sub> transistors," *Nature Nanotechnol.*, vol. 6, no. 3, pp. 147–150, 2011.
2. H. Liu et al., "The Effect of Dielectric Capping on Few-Layer Phosphorene Transistors: Tuning the Schottky Barrier Heights" *IEEE Electron Device Lett.*, vol. 35, no. 7, pp. 795-797, 2014.
3. H. M. Li et al., "Metal-Semiconductor Barrier Modulation for High Photoresponse in Transition Metal Dichalcogenide Field Effect Transistors" *Sci. Rep.* 4, 4041, 2014.

# Spirobifluorene in the STM junction: a molecular toggle switch

L. Gerhard<sup>1</sup>, K. Edlmann<sup>1,2</sup>, J. Homberg<sup>1</sup>, M. Valášek<sup>1</sup>, S. G. Bahoosh<sup>3</sup>, M. Lukas<sup>1</sup>, F. Pauly<sup>3</sup>, M. Mayor<sup>1,4</sup>, W. Wulfhekel<sup>1,2</sup>

<sup>1</sup>Karlsruhe Institute of Technology, Institute of Nanotechnology, Karlsruhe, Germany

<sup>2</sup>Karlsruhe Institute of Technology, Physikalisches Institut, Karlsruhe, Germany

<sup>3</sup>University of Konstanz, Department of Physics, Konstanz, Germany

<sup>4</sup>University of Basel, Department of Chemistry, Basel, Switzerland

## Abstract:

With regard to possible applications of molecular junctions as electrical switches or even memory devices, they have to be addressed in a controlled and reproducible manner by external stimuli such as mechanical forces, electric fields, currents or light. In this respect, the combination of functional molecular groups and specifically designed carrier platforms into a single molecule is a promising alternative to the deposition of functional molecules onto thin insulating films.

Here we present a low-temperature scanning tunneling microscope (STM) study of such self-decoupled molecules, namely spirobifluorene platforms with a benzonitrile head group deposited on a Au(111) surface [1]. By systematic variation of the tunneling parameters, we show that the dipole moment of the benzonitrile allows us to exert forces on the molecule by applying electric fields in the STM junction. The resulting deformation of the molecule leads to the formation or the rupture of a coordinative bond between the nitrile group and the gold tip, depending on the applied bias voltage. This hysteretic switching between two stable states of the conductance is highly reproducible and deterministic. Several thousand contacting measurements were performed by both approaching the tip mechanically and by application of a bias voltage. By variation of the applied bias, which leads to an electrostatic force on the dipole moment of the nitrile, we can bring the two states close in energy so that we observe thermally induced random switching. This allows us to study the energies that are involved in the formation of the molecular junction. In particular, we derive the force that is needed to pull apart the molecular junction. We confirmed our model by DFT calculations and reproduced our experiments on a second variant of the molecule.

**Keywords:** scanning tunneling microscope, molecular switch, approach-retract curve, 2D conductance histogram, tripodal molecules.

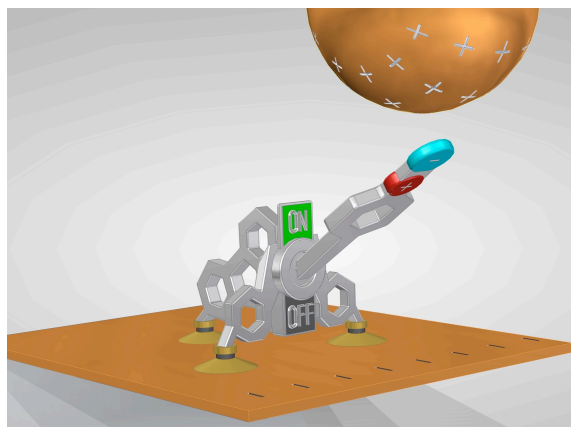


**Figure 1:** Illustration of the molecular toggle switch which can be actuated both mechanically by approaching the tip and electrostatically by application of a bias voltage.

## References:

1. Gerhard, L., Edlmann, K., Homberg, J., Valášek, M., Bahoosh, S., Lukas, M., Pauly, F., Mayor, M., Wulfhekel, W. (2017) An electrically actuated molecular toggle switch, *Nat. Nanotech.*, In Press.
2. Valášek, M., Edlmann, K., Gerhard, L., Fuhr, O., Lukas, M., Mayor, M. (2014) Synthesis of Molecular Tripods Based on a Rigid 9,9'-Spirobifluorene Scaffold, *J. Org. Chem.* 79, 7342-7357.

# Thermally Stable Metal-Interlayer-Semiconductor Structure for Source/Drain Contact of Germanium n-channel Transistors

Gwang-Sik Kim<sup>1</sup> and Hyun-Yong Yu<sup>1,\*</sup>

<sup>1</sup>Korea University, School of Electrical Engineering, Seoul, Korea

## Abstract:

Germanium (Ge) is a good candidate as a novel channel materials which can substitute conventional silicon (Si) in complementary metal-oxide-semiconductor (CMOS) technology due to its higher carrier mobilities and a good process compatibility with the Si process. However, high source/drain (S/D) contact resistance, which is caused by severe Fermi-level pinning in metal/Ge contact, is a bottleneck in the development of Ge n-channel transistors. A metal-interlayer-semiconductor (M-I-S) structure has been researched to reduce the S/D contact resistance because the structure can reduce the Schottky barrier height (SBH) of metal/n-Ge contact by alleviating Fermi-level pinning problem. A TiO<sub>2</sub> layer has been adopted as an interlayer between metal and n-Ge because it can minimize the tunneling resistance of the interlayer due to its low conduction band offset (CBO) with Ge.<sup>1,2</sup> The reduced SBH of the M-I-S structure should be maintained after subsequent thermal annealing process because transistors would experience the thermal process during some other post annealing processes.<sup>3</sup> However, the Ti/TiO<sub>2</sub>/n-Ge structure that is a typical structure of the M-I-S structure for n-Ge cannot maintain its SBH reduction effect after thermal annealing due to thermal instability of Ti and TiO<sub>2</sub> both. In this work, TaN and Al-doped ZnO (AZO) are introduced into the M-I-S structure as the contact metal and the interlayer, respectively, to enhance its thermal stability. The TaN is more thermally stable than the Ti, thus the it is less likely to react with the interlayer or Ge substrate through a diffusion process. Also the AZO interlayer can play a role as a diffusion barrier to block the interdiffusion process between metal and Ge during thermal annealing while the TiO<sub>2</sub> interlayer cannot. As shown in **Fig. 1**, the TaN/AZO/n-Ge structure can maintain the reduced SBH after thermal annealing at 500°C in vacuum while the Ti/TiO<sub>2</sub>/n-Ge shows severe degradation in the reverse current density. Therefore, the proposed TaN/AZO/n-Ge structure can be very promising contact structure in Ge to incorporate the M-I-S structure into practical CMOS process due to its better thermal stability.

**Keywords:** metal-interlayer-semiconductor, thermal stability, germanium, tantalum nitride, Al-doped zinc oxide

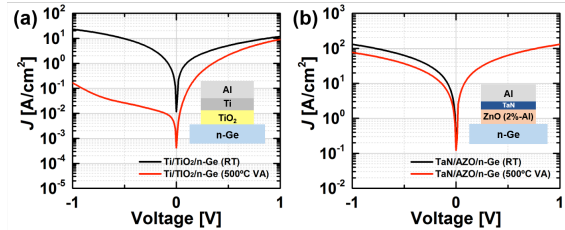


**Figure 1:**  $J$ - $V$  characteristics of (a) Ti/TiO<sub>2</sub>/n-Ge and (b) TaN/AZO/n-Ge structures before and after 500°C vacuum annealing for 30 min.

## References:

1. Lin, J.-Y. J., Roy, A. M., Saraswat, K. C. (2012) Reduction in specific contact resistivity to Ge using interfacial layer, *IEEE Electron Device Lett.*, 33(11), 1541-1543.
2. Kim, G.-S., Kim, J.-K., Kim, S.-H., Jo, J., Shin, C., Park, J.-H., Saraswat, K. C., Yu, H.-Y. (2014) Specific contact resistivity reduction through Ar plasma-treated TiO<sub>2-x</sub> interfacial layer to metal/Ge contact, *IEEE Electron Device Lett.*, 35(11), 1076-1078.
3. Biswas, D., Biswas, J., Ghosh, S., Wood, B., Lodha, S. (2017) Enhanced thermal stability of Ti/TiO<sub>2</sub>/n-Ge contacts through plasma nitridation of TiO<sub>2</sub> interfacial layer, *Appl. Phys. Lett.*, 110, 052104

# Permanent Excimer Superstructures By Supramolecular Networking of Metal Quantum Clusters

Beatriz Santiago-Gonzalez,<sup>1</sup> Angelo Monguzzi,<sup>1</sup> Jon Mikel Azpiroz,<sup>2,3</sup> Mirko Prato,<sup>4</sup>  
Silvia Erratico,<sup>5</sup> Marcello Campione,<sup>6</sup> Roberto Lorenzi,<sup>1</sup> Jacopo Pedrini,<sup>1</sup>  
Carlo Santambrogio,<sup>7</sup> Yvan Torrente,<sup>5</sup> Filippo De Angelis,<sup>2,4</sup>  
Francesco Meinardi,<sup>1</sup> Sergio Brovelli<sup>1\*</sup>  
[sergio.brovelli@mater.unimib.it](mailto:sergio.brovelli@mater.unimib.it)

<sup>1</sup> Dipartimento di Scienza dei Materiali, Università degli Studi di Milano-Bicocca, via Roberto Cozzi 55, I-20125 Milano, Italy

<sup>2</sup> Computational Laboratory for Hybrid and Organic Photovoltaics, National Research Council–Institute of Molecular Science and Technologies (CNR-ISTM), Via Elce di Sotto 8, Perugia, Italy.

<sup>3</sup> Kimika Fakultatea, Euskal Herriko Unibertsitatea (UPV/EHU), and Donostia International Physics Center, 20080 Donostia, Euskadi, Spain.

<sup>4</sup> Istituto Italiano di Tecnologia, Via Morego 30, 16163 Genova, Italy.

<sup>5</sup> Dipartimento di Fisiopatologia Medico-Chirurgica e dei Trapianti, Università degli Studi di Milano, Fondazione IRCCS (Istituto di Ricovero e Cura a Carattere Scientifico) Cá Granda Ospedale Maggiore Policlinico, Centro Dino Ferrari, Via Francesco Sforza 35, 20122 Milano, Italy.

<sup>6</sup> Dipartimento di Scienze dell'Ambiente e del Territorio e di Scienze della Terra, Università degli Studi Milano-Bicocca, Piazza della Scienza, 20125 Milano, Italy

<sup>7</sup> Dipartimento di Biotecnologie e Bioscienze, Università degli Studi Milano-Bicocca, Piazza della Scienza, 2, 20126 Milano, Italy.

## Abstract:

Metal quantum clusters are an important class of functional nanomaterials with growing applicative potential as size-tunable biocompatible luminescent probes for molecular theranostics and optoelectronic technologies. Here, we demonstrate for the first time that the optical properties of gold clusters ( $\text{Au}_8$ ), and in particular the energy separation between the emission and absorption spectra (Stokes shift), can be tuned by control of the inter-particle distance imposed by the capping ligands leading to the formation of inter-cluster excimers. Based on this newfound motif, we demonstrate a strategy for overcoming the intrinsic limitation to the use of molecular excimers in single-particle applications, that is, their nearly zero collisional formation probability in ultra-diluted solutions. To this aim, we use  $\text{Au}_8$  clusters as building blocks for fabricating permanent excimer-like colloidal superstructures ( $\text{Au}_8\text{-pX}$ ) held together by a network of hydrogen bonds between the capping ligands. In the ground state, unexcited clusters behave as individual photophysical entities, whilst optical excitation results in the formation of inter-cluster excimers featuring long-lived Stokes-shifted luminescence with no corresponding excitation transition. The obtained supramolecular architectures effectively represent a new aggregation state of matter conveying the photophysics of excimers into self

standing individual particles that find their natural application as non-resonant emitters in cellular imaging and integrated photonic nanotechnologies. Importantly, in vitro confocal imaging experiments reveal the strong ability of  $\text{Au}_8\text{-pXs}$  in scavenging cytotoxic reactive oxygen species responsible of premature cellular death, thereby further enhancing their potential for bio-medical applications.

**Keywords:** clusters, superstructures, luminescent probes, building blocks.

## References:

1. B. Santiago-González, A. Monguzzi, J. M. Azpiroz, M. Prato, S. Erratico, M. Campione, R. Lorenzi, J. Pedrini, C. Santambrogio, Y. Torrente, F. De Angelis, F. Meinardi, S. Brovelli. *Science*, 353, 571-575 (2016)

# Gallium nitride nano-wire based flexible piezoelectric sensor: design, fabrication and electrical performances.

A. El Kacimi,<sup>1</sup> E. Pauliac-Vaujour,<sup>1</sup> J. Eymery,<sup>2</sup>

<sup>1</sup>University Grenoble Alpes, CEA, LETI, MINATEC Campus, F-38054, Grenoble, France

<sup>2</sup>University Grenoble Alpes, CEA, INAC-MEM, Nanostructures and Synchrotron Radiation Laboratory, F-38000 Grenoble, France

## Abstract:

Gallium Nitride (GaN) wire-based flexible piezoelectric sensor have been demonstrated as an original solution for mechanical sensing applications thanks to their outstanding physical properties in terms crystalline quality, robustness and long life-time[1]. GaN wires are grown by Metal Organic Vapor Phase Epitaxy on c-sapphire substrate with in-situ injection of silane during the growth. This process provide N-polar wires with a hexagonal cross-section and a slight conical shape with an angle varying in the 0.2° - 3° range. The wire geometry in terms of length can be tuned by growth conditions (temperature, pressure, growth time) and it varies from 10 to 700 μm [2]. These wires are vertically integrated into a flexible PDMS matrix through a straightforward process to make flexible piezoelectric membranes used as sensors. The PDMS is first spread over the surface of a donor substrate with vertically aligned wires issued from the growth, and annealed for 30 min at 120° C. The membrane containing the GaN wires is then peeled off and contacted with electrodes to make capacitive structure. This process was also demonstrated to fabricate Light Emitting Diodes (LEDs) based on short GaN wires[3], [4].

In this work, we will be presenting the electrical performances of such devices. Variants of this sensors with different dimensions and GaN wire geometries are fabricated and characterized under a compression constraint using an automated mechanical bench. The sensor's output signal is studied as function of the wire length and PDMS thickness in view of optimizing the device design. The sensor sensitivity is also investigated by exploring the evolution of the device response to the variations of the applied force.

The electrical characterization results show that sensors with long GaN wires (> 100 μm) provide higher output signal and are more sensitive to the variation of the mechanical excitation. Moreover, a small PDMS to wire length ratio around 1.2 to 1.5 is demonstrated to be optimal for conversion efficiency enhancement. These

results are also confirmed through finite element modelling simulations that has been conducted and that will be shown along with the characterization results.

**Keywords:** GaN, nanowires, piezoelectric, flexible, sensor

## References:

1. S. Salomon, J. Eymery, and E. Pauliac-Vaujour, "GaN wire-based Langmuir-Blodgett films for self-powered flexible strain sensors.," *Nanotechnology*, vol. 25, no. 37, p. 375502, Sep. 2014.
2. J. Eymery, X. Chen, C. Durand, M. Kolb, and G. Richter, "Self-organized and self-catalyst growth of semiconductor and metal wires by vapour phase epitaxy: GaN rods versus Cu whiskers.," *Comptes Rendus Physique*, vol. 14, no. 2–3, pp. 221–227, Feb. 2013.
3. X. Dai, A. Messanvi, H. Zhang, C. Durand, J. Eymery, C. Bougerol, F. H. Julien, and M. Tchernycheva, "Flexible Light-Emitting Diodes Based on Vertical Nitride Nanowires.," *Nano letters*, vol. 15, no. 10, pp. 6958–64, Oct. 2015.
4. N. Guan, X. Dai, A. Messanvi, H. Zhang, J. Yan, E. Gautier, C. Bougerol, F. H. Julien, C. Durand, J. Eymery, and M. Tchernycheva, "Flexible White Light Emitting Diodes Based on Nitride Nanowires and Nanophosphors.," *ACS photonics*, vol. 3, no. 4, pp. 597–603, Apr. 2016.

# ZnO nanorod-based piezoelectric stress sensor embedded within carbon fiber composite

M. Culiolo,<sup>1,\*</sup> M. Villani,<sup>1</sup> D. Delmonte,<sup>1</sup> D. Calestani,<sup>1</sup> N. Coppedè,<sup>1</sup> M. Solzi,<sup>2</sup> L. Marchini,<sup>3</sup> R. Bercella,<sup>3</sup> A. Zappettini,<sup>1</sup> T.Y. Kim,<sup>4</sup> S.W. Kim<sup>4,5</sup>

<sup>1</sup> IMEM-CNR, Parco Area delle Scienze 37/A, Parma, Italy

<sup>2</sup> Dipartimento di Fisica e CNISM, Università di Parma, Via G.P. Usberti 7/A, Parma, Italy

<sup>3</sup> Bercella s.r.l., Via Enzo Ferrari 10, Varano de' Melegari (PR), Italy

<sup>4</sup> SKKU Advanced Institute of Nanotechnology (SAINT), Sungkyunkwan University (SKKU), Suwon 440-746, Republic of Korea

<sup>5</sup> School of Advanced Materials Science and Engineering (AMSE), Sungkyunkwan University (SKKU), Suwon 440-746, Republic of Korea

## Abstract:

Carbon fiber composites (CFC) are a fundamental class of materials in applications where both high mechanical resistance and light weight are requested (automotive, civil engineering, aerospace, etc.). Thanks to the latter feature, the use of these materials in transportation leads to significant reduction of CO<sub>2</sub>, NO<sub>x</sub> and noise. Mentioning the aviation field, an aircraft composed of 53% CFC by weight such as Airbus 350XWB can save up to 25% fuel. A life-cycle CO<sub>2</sub> emissions analysis shows a reduction up to 2700 tons of CO<sub>2</sub> per aircraft every year (Boeing 787 Dreamliner, 50% CFC by weight).

Nevertheless, due to their intrinsic structure strongly dependent on carbon fiber (CF) fabric and resin arrangement, a precise predictive deformation and failure behavior is hard to model, which is one of the main causes limiting the use of these materials in aerospace technologies. Hence, on account of the very heavy loads the CFC structures are subject to, it is important to carry out real-time monitoring of deformations and vibrations.

Nowadays' stress sensors in CFC, mainly based on piezoelectric PZT and optical fibers (Fiber Bragg Grating, FBG), present some drawback such as large size (compared to CF's) and weight addition. The use of zinc oxide (ZnO) piezoelectric nanostructures can overcome these issues and lead to a real-time stress sensor completely embedded within CFC

In this work low cost, low temperature and low environmental impact synthesis of ZnO nanorods on CF is carried out, as well as piezoelectric characterization of such micro-composite sensor.

**Keywords:** piezoelectric, zinc oxide, carbon fiber, integration, composites, stress, vibrations, deformation, sensor.

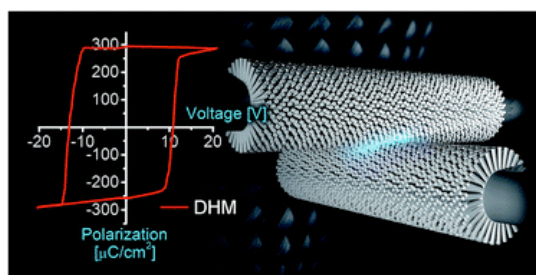


**Figure 1:** Structure and piezoelectric behavior of the CF/ZnO sensor.

## References:

1. S. Chand (2000), Review Carbon fibers for composites, *J. Mater. Sci.*, 35, 1303–1313.
2. S. W. Tsai and J. D. D. Melo (2016) A unit circle failure criterion for carbon fiber reinforced polymer composites, *Compos. Sci. Technol.*, 123, 71–78.
3. V. Giurgiutiu (2016) Fatigue Damage Monitoring, in Structural Health Monitoring of Aerospace Composites, ed. V. Giurgiutiu, *Academic Press*, pp. 409–432, ISBN 978-0-12-409605-9.
4. R. Di Sante (2015) Fibre Optic Sensors for Structural Health Monitoring of Aircraft Composite Structures: Recent Advances and Applications, *Sensors*, 15, 18666–18713.
5. Tariq Chady (2013) Airbus versus Boeing - Composite materials: The sky's the limit..., *lemauricien.com*, <http://www.lemauricien.com/article/airbus-versus-boeing-composite-materials-sky-s-limit>
6. Toray, Using Advanced Materials to Reduce CO<sub>2</sub> Emissions, [http://www.toray.com/csr/special/link1/lin\\_001.html](http://www.toray.com/csr/special/link1/lin_001.html)

# Effects of electrical breakdown on the photocurrent generation in thin-film single-walled carbon nanotubes

W. Dumnernpanich,<sup>1\*</sup> M. Spankaew,<sup>1</sup> J. Jantawong,<sup>2</sup> N. Penpondee,<sup>2</sup> C. Hruanun,<sup>2</sup> Y. Jompol,<sup>1</sup>

<sup>1</sup> Mahidol University, Department of Physics, Bangkok, Thailand

<sup>2</sup> Thai Microelectronic Center, Chachoengsao, Thailand

## Abstract:

We have observed the reduction in the photocurrent measurement after an electrical breakdown of a thin-film semiconducting single-walled carbon nanotube (s-SWCNT) field-effect transistor (FET). The photocurrent ( $I_{ph}$ ) is defined as the excess currents between light and dark conditions and studied under ambient temperature with different light intensities. Before the electrical breakdown, the measured current-voltage (I-V) characteristic exhibits non-linear behaviour upon changing wavelength and light intensity suggesting that electrons tunnel across Schottky barriers of metal-SWCNTs junctions. In contrast to the dark current, the photocurrent before the electrical breakdown was found  $I_{ph}^{Before} \approx 2.51 \mu\text{A}$ . After the electrical breakdown (by passing a large current up to 0.14 mA through drain electrode in order to improve contact series resistance), the I-V characteristic becomes linear, but we have seen almost no change in the measured current when increasing light intensities, which results in  $I_{ph}^{After} \approx 0.17 \mu\text{A}$ .

This observation indicates that charge-carrier transport is governed by electron diffusion through the Schottky barriers. Our results also suggest that the photocurrent generation in SWCNTs depends strongly on charge-carrier separation by the Schottky barriers and inter-tube junctions. Further verification of charge-carrier separation in such devices can be demonstrated by electrical noise measurements.

**Keywords:** thin-film single-walled carbon nanotubes, photocurrent generation, Schottky barriers, electrical breakdown, charge-carrier transports

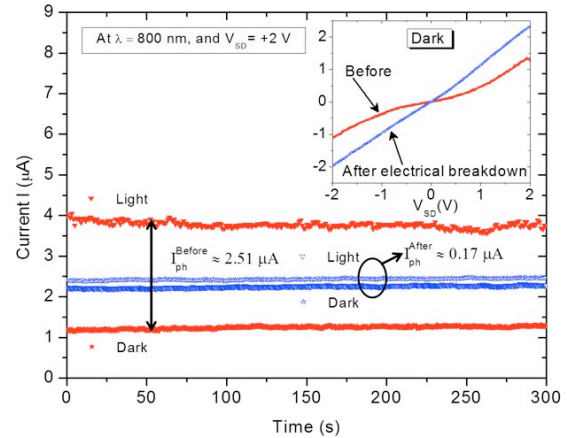


**Figure 1:** Measured currents at a fixed source-drain voltage,  $V_{SD} = +2 \text{ V}$ , as a function of time obtained by illuminating monochromatic light of  $\lambda = 800 \text{ nm}$  (red and blue downtriangle), compared with the measured currents in the dark (square and star symbols). Inset graph shows I-V characteristics before and after electrical breakdown in the dark condition.

## References:

1. T. Toda et al., "Thin-Film Transistors Using Uniform and Well-Aligned Single-Walled Carbon Nanotubes Channels by Dielectrophoretic Assembly", *J. Appl. Phys.*, **52**, 03BB09(2013).
2. Qingsheng Zeng et al., "Carbon nanotube arrays based high-performance infrared photodetector", *Optical materials express* **2**, 847(2012).
3. E. S. Snow et al., "Random networks of carbon nanotubes as an electronic material", *Appl. Phys. Lett.*, **82**, 2145 (2003).
4. M. Freitag et al., "Photoconductivity of single carbon nanotube", *Nanoletters* **3**, 1067(2003).
5. M. A. El Khakani et al., "Photocurrent generation in random networks of multiwall-carbon-nanotubes grow by an "all-laser" process", *Applied Physics Letters* **95**, 083114 (2009).

**Session IV-2:  
NanoBioMedecine / Nanosafety**

# Nanopores: Transistors for Ions in Solution

Jiandong, Feng<sup>1\*</sup>

<sup>1</sup>Laboratory of Nanoscale Biology, Institute of Bioengineering, School of Engineering, EPFL, 1015 Lausanne, Switzerland  
[jiandong.feng@epfl.ch](mailto:jiandong.feng@epfl.ch)

## Abstract:

Nanopore-based measurements enable to probe the physics of biology at ultrahigh precision. This precision relies on the dimension of the nanopore and our single-layer MoS<sub>2</sub> nanopores could offer sub-nanometer resolution due to its well-defined geometry at the atomic scale(1). The key driving force in nanopore research is single molecule DNA sequencing where the sequence of DNA can be extracted based on the modulation of ionic current through the pore caused by individual nucleotides(2). In essence, nanopores play a role in ion transport as significant as the role of transistors in electron transport and can also be applied to probe various physical processes beyond sequencing(3, 4). In this talk, I will demonstrate the ability of using nanopores for probing physics and biology at the single molecule level with tunable resolutions: from identification of single nucleotides to fundamental ion transport physics and energy conversion.

**Keywords:** nanopores, DNA sequencing, ion transport, Coulomb blockade, osmotic power generation

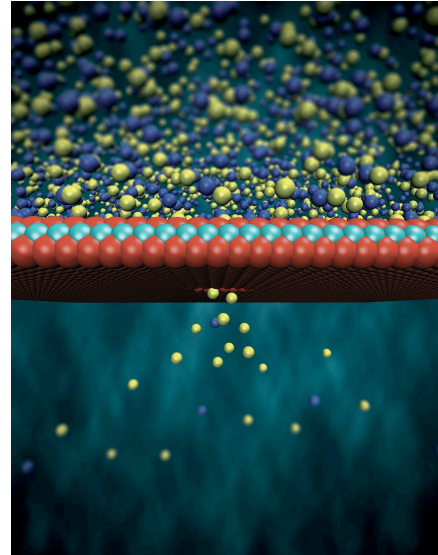


**Figure 1:** Figure illustrating ion transport through nanopores.

Image credit: Steven Duensing at the National Center for Supercomputing Applications at the University of Illinois at Urbana-Champaign.

## References:

1. J. Feng *et al.*, Electrochemical Reaction in Single Layer MoS<sub>2</sub>: Nanopores Opened Atom by Atom. *Nano letters* **15**, 3431 (2015).
2. J. Feng *et al.*, Identification of single nucleotides in MoS<sub>2</sub> nanopores. *Nature nanotechnology* **10**, 1070 (2015).
3. J. Feng *et al.*, Observation of ionic Coulomb blockade in nanopores. *Nature materials* **15**, 850 (2016).
4. J. Feng *et al.*, Single-layer MoS<sub>2</sub> nanopores as nanopower generators. *Nature* **536**, 197 (2016).

# Innovative materials for active food packaging: antimicrobial release from inorganic carrier embedded into biodegradable composites

M. Stanzione<sup>1</sup>, F. Tescione<sup>1</sup>, P. Cerruti<sup>2</sup>, M. Lavorgna<sup>1</sup>, G.G. Buonocore<sup>1</sup>

<sup>1</sup> Institute of Polymers, Composites and Biomaterials – CNR, P.le E. Fermi 1, 80055 Portici (Naples), Italy

<sup>2</sup> Institute of Polymers, Composites and Biomaterials – CNR, Via Campi Flegrei, 3480128 Pozzuoli (Naples), Italy

## Abstract:

Inorganic materials have been long recognized as very promising materials with a wide range of possible applications. Among these, many investigation efforts focused on the exploitation of the porous network provided by such materials as a reservoir for the accommodation of drug molecules. In fact, the well-known opportunity to chemically functionalize the surface of siliceous mesostructures with different organic moieties constitutes a route for controlling the drug release by diffusion under specific conditions. Drug release from mesoporous materials is generally controlled by diffusion. Nevertheless, when the interactions between desorbing molecules and silica pore walls are significantly strong and/or show some kind of specificity, the release also depends by the stability of the complex between the functional groups of the drug and those of the substrate. This phenomenon allows then to fine tune the release of specific molecules from a given mesostructure by simply changing the functional groups that are attached to its pore walls during the synthesis process. In addition to the production of smart drug delivery systems, such approach can be also used in the field of food packaging due to the increasing interest in the concept of “active packaging” materials as compounds which, interacting with the packaged foodstuff, are able to control quality as well as to increase shelf-life.

The aim of the present work is the study and the comparison of the release from active polymeric films of various active compounds embedded or supported into/onto various inorganic carriers i.e. SBA (Santa Barbara Amorphous), Montmorillonite and Halloysite. Migration tests were performed at 25 °C, using 96% v/v ethanol and water as food simulant, from polymer films obtained by embedding active inorganic carriers into biodegradable and polyolefinic matrices. Obtained results show the influence of functionalization of the inorganic carriers on the diffu-

sion of active compounds and thus on their release kinetics into the liquid media.

**Keywords:** inorganic carrier, chemical functionalization, active compound release.

## References:

1. J. Brockgreitens and A. Abbas. Responsive Food Packaging: Recent Progress and Technological Prospects. *Comprehensive Reviews in Food Science and Food Safety*, 15, (2016) 3-15.
2. M. Stanzione. Peculiarities Of Vanillin Release From Amino-Functionalized Mesoporous Silica Embedded Into Biodegradable Composites. *European Polymer Journal*. 89, (2017) 88-100.

# Colloidal characterization of surface modified CuO nanosuspensions in media relevant for nano (eco) toxicology

Simona Ortelli<sup>1</sup>, Magda Blosi<sup>1</sup>, Ilaria Zanoni<sup>1</sup>, Carlo Baldisserri<sup>1</sup>, Anna Luisa Costa<sup>1</sup>

<sup>1</sup> CNR-ISTEC, Institute of Science and Technology for Ceramics, National Research Council, Faenza, Italy

## Abstract:

The relationships between the physicochemical properties of engineered nanoparticles and their adverse health and environmental effects are still unclear. In order to identify key properties that drive nano-bio/eco interactions and to convert this knowledge into “Safety by Design” (S<sub>byD</sub>) strategies, it is essential to study the colloidal properties of ENMs in media relevant to nano (eco) toxicology (1). This work investigates the dispersion stability of copper oxide NPs modified by means of four non-hazardous modifying agents [i.e. polyethylenimine (PEI), sodium ascorbate (ASC), sodium citrate (CIT), and polyvinylpyrrolidone (PVP)]. The modifiers were added to CuO NP suspensions for promoting the in situ coating of particles and compare four design alternatives, achieving positive (PEI), negative (ASC, CIT), and neutral (PVP) surface charging on the NPs. The effects of these four stabilizers on the CuO NPs' physicochemical properties were investigated in different biological and environmental media by combining Dynamic and Electrophoretic Light Scattering (DLS and ELS) with Inductively Coupled Plasma Optical Emission Spectroscopy (ICP-OES). Results showed improved dispersion stability for CuO-CIT, CuO-ASC and CuO-PEI in both MilliQ and Phosphate Buffered Saline (PBS) as compared to CuO-pristine and CuO-PVP. Higher ionic strength in artificial fresh (AFW) and marine (AMW) water strongly destabilized all CuO NP suspensions, except for CuO-PEI dispersed in AFW. The presence of proteins and amino acids in the biological test media had a strong influence on the colloidal stability of all dispersions. Characterization of colloidal properties showed the correlation between NP aggregates size and  $\zeta$ -pot, confirming that coupling DLS with ELS provides an effective tool for colloidal stability evaluation (2). The obtained results in support to (eco) toxicological outputs are highly relevant for hypothesizing early effects of toxicological pathway and deriving criteria and guiding principles for grouping and read-across.

**Keywords:** CuO nanoparticles; colloidal stability; nano-bio interaction; biological and environmental media.

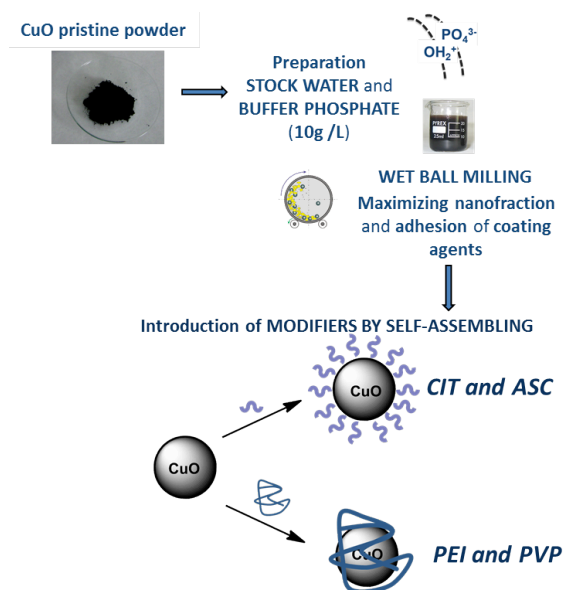


**Figure 1:** Schematic representation of S<sub>byD</sub> strategy applied: introduction of modifying agents (i.e. CIT, ASC, PEI and PVP) by self-assembling.

## References:

1. Mudunkotuwa, I.A.; Grassian, V.H. (2015) Biological and environmental media control oxide nanoparticle surface composition: the roles of biological components (proteins and amino acids), inorganic oxyanions and humic acid, *Environ Sci: Nano*, 2, 429-439.
2. Ortelli, S., Costa, A.L., et al. (2017) Colloidal characterization of CuO nanoparticles in biological and environmental media, *Environ Sci: Nano*, accepted.

# Gold nanoparticles induce mitochondrial dysfunction in monocytic THP.1 cells: a combined transcriptomics and proteomics approach

A. Gallud,<sup>1</sup> S. Katayama,<sup>2</sup> A.J. Ytterberg,<sup>3,4</sup> T. Skoog,<sup>2</sup> N.K. Tarasova,<sup>3</sup> V. Gogvadze,<sup>5</sup> S. Moya,<sup>6</sup> J. Ruiz,<sup>7</sup> D. Astruc,<sup>7</sup> R.A. Zubarev,<sup>3</sup> J. Kere,<sup>2</sup> B. Fadeel<sup>1</sup>

<sup>1</sup> Nanosafety & Nanomedicine Laboratory, Division of Molecular Toxicology, Institute of Environmental Medicine, Karolinska Institutet, Stockholm, Sweden; <sup>2</sup> Department of Biosciences and Nutrition, Karolinska Institutet, Huddinge, Sweden; <sup>3</sup> Department of Medical Biochemistry and Biophysics, Karolinska Institutet, Stockholm, Sweden; <sup>4</sup> Division of Physiological Chemistry I, Department of Medical Biochemistry and Biophysics; <sup>4</sup> Rheumatology Unit, Department of Medicine, Karolinska Institutet, Solna, 17177 Stockholm, Sweden; <sup>5</sup> Division of Toxicology, Institute of Environmental Medicine, Karolinska Institutet, Stockholm, Sweden; <sup>6</sup> CIC biomaGUNE, Paseo Miramon 182, Edif C, 20009 San Sebastian, Spain; <sup>7</sup> ISM, Université de Bordeaux, UMR CNRS 5255, Talence, France

## Abstract:

Systems biology is increasingly being applied in the field of nanosafety research for observing and predicting the biological perturbations inflicted by exposure to engineered nanoparticles (NPs). In the present study, we used a combined transcriptomics and proteomics approach to assess the effects on monocytic THP.1 cells of AuNPs of 5 or 20 nm in diameter. The role of surface functional groups was addressed by synthesizing alkylammonium bromide-, alkyl sodium carboxylate- or poly(ethylene glycol) (PEG)-terminated thiolate-AuNPs. These AuNPs were characterized using transmission electron microscopy (TEM), UV-vis. spectroscopy, dynamic light scattering and zeta potential measurements. We also ensured that all the AuNPs were endotoxin-free. Then, we performed a cytotoxicity screening of THP.1 cells exposed to the AuNPs for 24 h at doses up to 100 µg/mL, using the Alamar Blue assay. Cytotoxicity effects were observed only for the ammonium-terminated AuNPs, while no cell death was obtained after exposure to carboxylated or PEGylated AuNPs, regardless of the AuNP size. Using TEM we observed that the ammonium-modified AuNPs were partly located into mitochondrial compartments and that they induced high impact on the cell morphology with appearance of large vacuoles (Figure 1). Next, we performed transcriptomics analysis using highly sensitive Single-cell Tagged Reverse Transcription (STRT)-RNA sequencing in parallel with label-free quantitative mass spectrometry based

proteomics analysis, followed by pathway enrichment analysis. The importance of the nanomaterials surface modification, rather than the diameter size, was demonstrated using these approaches. Notably, ammonium-modified AuNPs were found to have the most pronounced effects on the monocytic THP.1 cells with a significant impact on mitochondrial functions. Taken together, these studies have disclosed specific cytotoxic effects of AuNPs as a function of the particle surface properties, in human immune cells.

**Keywords:** Au nanoparticles; THP.1 cells; STRT-RNA sequencing; label-free quantitative proteomics, mitochondrial dysfunction.

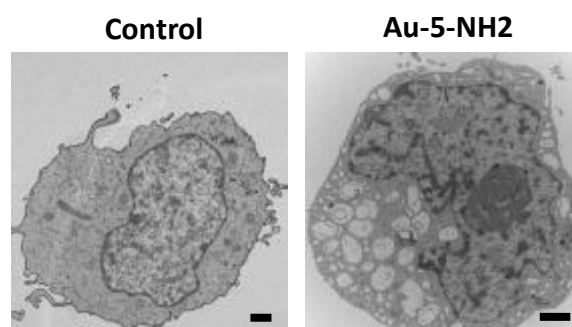


**Figure 1:** Transmission electron microscopy of THP.1 cells exposed for 4 h to Au-5-NMe<sub>3</sub><sup>+</sup> Br<sup>-</sup> nanoparticles at 50 µg/mL. Cytoplasmic vacuolization is noted in NP-exposed cells. Scale bars: 1 µm.

# Fabrication of hieratically porous calcium carbonate scaffolds for bone tissue engineering

**Sudhir Kumar Sharma**<sup>1</sup>, Abiy D. Woldetsadik<sup>2</sup>, Mazin Magzoub<sup>2</sup> and Ramesh Jagannathan<sup>1</sup>

<sup>1</sup>Engineering Division, New York University Abu Dhabi, Abu Dhabi, UAE.

<sup>2</sup>Biology Program, Division of Science, New York University Abu Dhabi, Abu Dhabi, UAE

## Abstract

We report a versatile method for the fabrication of hierarchically porous CaCO<sub>3</sub> scaffolds on silicon substrate via a supercritical carbon dioxide nebulization process. This process consists of evaporation of CO<sub>2</sub>-enriched water micro-droplets (diameter ~3 μm) deposited from an aerosol onto heated silicon substrates. A variety of porous CaCO<sub>3</sub> scaffolds with micron-sized pores (1-3 μm) were fabricated by altering the deposition conditions. Post-deposition sintering of the scaffolds resulted in the generation of nano-sized pores around the walls of the porous scaffolds with a dual arrangement of typical pore sizes (~50 nm and 1–3 μm). We observed that our scaffolds formation and micro-droplets evaporations follows typical coffee-ring effect mechanism. Furthermore, CaCO<sub>3</sub> scaffolds were exposed to monocytic THP-1 cells. These scaffolds yielded negligible levels of tumor necrosis factor-alpha (TNF-α) and further confirmed the lack of immunogenicity of the scaffolds. These scaffolds were also treated against extracellular matrix (ECM) proteins such as fibronectin (FN), vitronectin (VN) and collagen (CL), respectively. ECM treatment on to CaCO<sub>3</sub> scaffolds showed enhanced adsorption in the order of FN > VN > CL as compared to the standard control. Moreover, these investigations demonstrate that our porous CaCO<sub>3</sub> scaffolds promoted ECM production and calcium mineralization (which is an important biomarker), in turn beneficial for bone tissue engineering.

**Keywords:** Supercritical CO<sub>2</sub>, CaCO<sub>3</sub> scaffolds, Coffee-ring effect and extracellular matrix (ECM) proteins,

# Biocompatible scaffolds for tissue regeneration

G. Panella<sup>1</sup>, A.C. Dhez<sup>1</sup>, F. Giansanti<sup>1</sup>, G. Fioravanti<sup>2</sup>, L. Ottaviano<sup>2</sup>, F. Angelucci<sup>1</sup>, L. Di Leandro<sup>1</sup>, L. Cristiano<sup>1</sup>, A. Cimini<sup>1</sup>, R. Ippoliti<sup>1</sup>

<sup>1</sup>Department of Health, Life and Environmental Sciences, University of L'Aquila, L'Aquila I-67100, Italy; <sup>2</sup>Department of Physics and Chemistry, University of L'Aquila, L'Aquila I-67100  
gloria.panella86@gmail

## Abstract:

The design of scaffolds based on biocompatible materials is a great goal to support tissue regeneration. On this basis, we worked with protein-based and graphene oxide (GO)-based scaffolds to test their properties as supports for neural tissue regeneration. We considered several type of materials (GO, bovine pericardium and alginate) as bases for the development of biocompatible scaffolds, and tested their applicability for growing SHSY5Y cells, as in vitro models of neuronal differentiation.

Our group has previously demonstrated that a protein-based scaffold (1) can be obtained by growing a mutant of the protein Prx (peroxiredoxin from *S. mansoni*) as an array of protein nanotubes. This material can be used to induce the growth and differentiation of SHSY5Y cells in vitro, and can furthermore sustain the growth and development of rat cortical neurons.

We are also studying the ring-shaped monomer (wtPrx) and the mutant Prx, as a polymerization agents to induce graphene oxide gelation into a 3D porous material, to be used as a support for the growth and differentiation of SHSY5Y cells. Cells grow on our scaffold based on graphene-oxide with or without the presence of the wild-type or a mutant protein(2).

To check the growth and the degree of differentiation we analyzed the surface interaction with SEM and immunofluorescence analysis. We have shown that the GO-based scaffold is biocompatible, in fact the SHSY5Y cells colonize the surface preserving their morphology.

We also know that the mutated protein Prx can induce cell differentiation as well as, a structural reorganization of the GO to get a 3D assembly with more space between the sheets that allows cell growing inside the scaffold.

The goal is to obtain a biocompatible system for 3D neuronal regeneration that allows to culture and manipulate cells in order to study their physiology and characteristics for the possible re-implantation in patients.

We also obtained a decellularized bovine pericardium, a biological tissue widely used as a biomaterial for tissue engineering applications, including the construction of a variety of bioprostheses to repair complex anatomical defects of several tissues such as cardiac defects, abdominal wall defects, and to strengthen the suture line during general surgical procedures and, more frequently, heart valves(3), with good features as a biomaterial that finds application as device adjuvating tissue regeneration after several type of surgery.

In summary, the coating of the scaffolds with GO linked to Prx provide a strong recellularization of these scaffolds. Furthermore the mutated protein can trigger the differentiation of the SHSY5Y cells on all scaffolds and 3D system is very interesting perspective for future purposes.

**Keywords:** biomaterial, Graphene-oxide, biocompatible scaffolds, Bovine pericardium, Alginate, Prx.

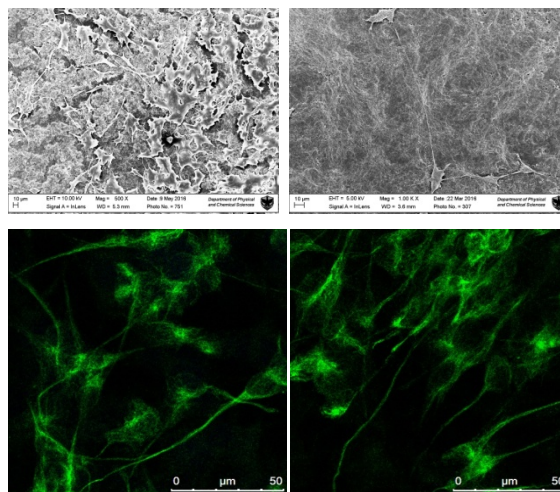


**Figure 1:** Figure illustrates the differentiation of cells grew on the surface of GO+Prx mutant. On the top is shown SEM investigation of the surface and below IF confocal images stained with N200 antibody.

## References:

1. Switching between the Alternative Structures and Functions of a 2-Cys Peroxiredoxin, by Site-Directed Mutagenesis F. Angelucci, F. Saccoccia, M. Ardini , G. Boumis, M. Brunori , L. Di Leandro, R. Ippoliti , A.E. Miele, G. Natoli , S. Scotti and A. Bellelli. *J. Mol. Biol.* (2013) 425, 4556–4568
2. A Peroxiredoxin-based proteinaceous scaffold for growth and differentiation of neuronal cells and tumor stem cells in the absence of pro-differentiation agents. Cimini Annamaria, Ardini Matteo, Gentile Roberta, Giansanti Francesco, Benedetti Elisabetta, Cristiano Loredana, Fidamore Alessia, Scotti Stefano, Panella Gloria, Angelucci Francesco, Ippoliti Rodolfo University of L'Aquila, Life, Health And Environmental Sciences *Journal of Tissue Engineering and Regenerative Medicine* 2015
3. Biomimetic acellular detoxified glutaraldehyde cross-linked bovine pericardium for tissue engineering Santosh Mathapati Dillip Kumar Bishi, Soma Guhathakurta, Kotturathu Mammen Cherian, Jayarama Reddy Venugopal , Seeram Ramakrishna c, Rama Shanker Verma *Materials Science and Engineering C* 33 (2013) 1561–1572

# Creating a discovery solution for nanotechnology – Challenges & Prospects

A. Gheisi,<sup>1</sup> W. Chiuman,<sup>2</sup> P. Roy<sup>3</sup>, J. Xiao<sup>4</sup>

<sup>1</sup> Database Research Group, Department of Nanoscience & Technology, Springer Nature, Heidelberg

<sup>2</sup> Database Research Group, Department of Nanoscience & Technology, Springer Nature, HongKong

<sup>3</sup> Database Research Group, Department of Nanoscience & Technology, Springer Nature, New York

<sup>4</sup> Database Research Group, Department of Nanoscience & Technology, Springer Nature, Shanghai

## Abstract:

Vast amount of information and data related to nanotechnology are scattered throughout different journals and patents. Moreover, the lack of standardized nomenclature for nanomaterials and nanostructures is a big challenge which makes the finding and transfer of scientific results a difficult task for researchers. In this work a solution under nano.nature.com will be illustrated and will be explained how these issues can be addressed. The presented solution provides highly indexed and structured information related to nanomaterials derived from peer-reviewed journals and patents. These include composition, synthesis, properties, characterization methods and application information.

Our solution aims to provide nanotechnology research communities fast and precise insight into this multi- and interdisciplinary field, and to help them keep up to date with new discoveries and developments. By collecting information from research articles and patents, it follows the definition of nanomaterials and nanodevices used by the community.<sup>1</sup>

1. What is Nano?, Nature Nanotechnology 11, 575, 2016

**Keywords:** nanotechnology research solution, precise data search, nanomaterials & nanodevices data

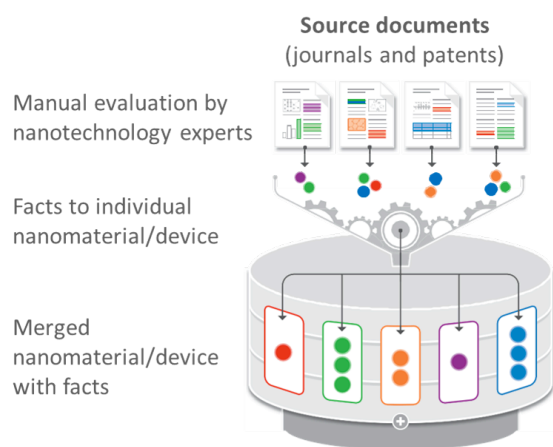


**Figure 1:** Figure illustrating the creation of curated profiles of nanomaterials/devices

## References:

**Posters Session I:  
Nanomaterials synthesis,  
characterization/Nanometrology  
and properties**

# Light-Matter Strong Coupling in Liquid Fabry-Perot Nanocavities

H. Bashoun, A. Thomas, T. Chervy, K. Börjesson†, J. George, E. Devaux, C. Genet, J. Hutchison\*, T.W. Ebbesen\*

University of Strasbourg, CNRS, ISIS, 8 allée G. Monge, 67000 Strasbourg, France

† University of Gothenburg, Department of Chemistry and Molecular Biology, 41296 Gothenburg, Sweden

## Abstract:

Interactions between light and matter can be profoundly altered by the presence of an optical cavity. For the resonance case, rapid energy exchange between the cavity photonic mode and a transition dipole of the material brings the system into the strong coupling regime generating two new light-matter hybrid states. Many studies have shown that these hybrid states have modified properties compared to their original constituents. In the visible spectral range, strong coupling of light with nanomaterials can be achieved using Fabry-Perot (FP) cavities with nanoscale dimensions. While all-solid nanoscale FP cavities are relatively simple to fabricate, liquid phase FP nanocavities are far more challenging. Herein, we report a facile method we developed for the fabrication of metallic nano-fluidic FP cavities tunable over a wide range of wavelengths in the visible spectrum (Figure 1). Our nano-fluidic cavities have been fully characterized and put to use to achieve the strong coupling of various dyes in solution phases. Particularly we show modifications to the photo-physical properties of a dissolved dye, chlorin e6 upon its strong coupling to the optical modes of our cavities.

**Keywords:** Light-matter hybrid states, strong coupling, fluidic Fabry-Perot nano-cavities, nano fabrication, spectroscopy, photo physical properties.

ties of varying thicknesses, with the corresponding dispersion of the confined light mode.

## References:

1. Thomas W. Ebbesen, Hybrid Light-Matter States in a Molecular and Material Science Perspective, *Acc. Chem. Res.* 2016, 49, 2403–2412
2. Shaojun Wang, Thibault Chervy, Jino George, James A. Hutchison, Cyriaque Genet, and Thomas W. Ebbesen, Quantum Yield of Polariton Emission from Hybrid Light-Matter States, *J. Phys. Chem. Lett.* 2014, 5, 1433–1439

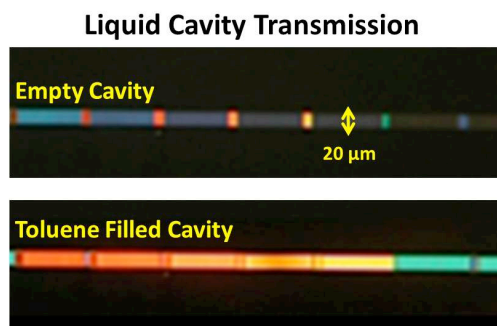


**Figure 1:** Optical micrographs showing white light transmission through our nanofluidic FP cavities before and after filling them with toluene. The colored rectangles represent FP cavi-

# The effect of Al<sub>2</sub>O<sub>3</sub> addition on ZrO<sub>2</sub>-Al<sub>2</sub>O<sub>3</sub> nanoceramics formation and their properties

I. Koltsov<sup>1</sup>, **M. Malysa**<sup>1</sup>, J. Wojnarowicz<sup>1</sup>, A. Rogowska<sup>1</sup>, G. Kimmel<sup>2</sup>, W. Łojkowski<sup>1</sup>

<sup>1</sup>Institute of High Pressure Physics PAS, Sokolowska 29/37, 01-142 Warsaw, Poland

<sup>2</sup>Ben-Gurion University of the Negev, Beer Sheva, 8410501, Israel

## Abstract:

Zirconia in metastable, high-temperature tetragonal phase (t-ZrO<sub>2</sub>) is important for applications where materials with high hardness and high melting point are needed. In order to stabilize the tetragonal phase at room temperature various stabilizers are used. The most common of them is Ytria (Y<sub>2</sub>O<sub>3</sub>). On the other hand, for grain sizes less than 30 nm, the tetragonal phase is stable at room temperature without any stabilizers. Since alumina (Al<sub>2</sub>O<sub>3</sub>) - zirconia (ZrO<sub>2</sub>) solid solution forms only when zirconia is in t-ZrO<sub>2</sub>, it opens a way to produce ZrO<sub>2</sub>-Al<sub>2</sub>O<sub>3</sub> ceramics where the particle size remains in the nano-range. Alumina as a stabilizer of the t-ZrO<sub>2</sub> is less expensive, than the conventionally used yttria and other rare earth ions.

The aim of this work was to choose the most efficient synthesis method and its parameters in order to obtain ZrO<sub>2</sub>-Al<sub>2</sub>O<sub>3</sub> nanopowders in whole composition range (from 1 to 99 mol.% of Al<sub>2</sub>O<sub>3</sub>). Complementary characterization methods allowed to find composition where ZrO<sub>2</sub>-Al<sub>2</sub>O<sub>3</sub> solid solution is created.

In this work we present results obtained for ZrO<sub>2</sub>-Al<sub>2</sub>O<sub>3</sub> nanopowders, where two different synthesis methods were applied: sol-gel method and Microwave Hydrothermal Synthesis (MHS). The synthesized materials were further characterized by X-Ray Diffraction, Scanning Electron Microscopy (SEM), Transmission Electron Microscopy (TEM), Specific Surface Area (SSA-BET) [1], pycnometric density [2], and zeta potential ( $\zeta$ ). The grain size examination was undertaken by investigating the broadening of diffraction lines (XRD) and by BET method. Materials chemical composition was confirmed using Energy-Dispersive X-Ray Spectroscopy (SEM-EDS) [3] and Inductively Coupled Plasma Spectroscopy (ICP-OES) methods.

We found that samples obtained in MHS reaction show faster crystallization kinetics than materials produced in sol-gel synthesis. Solid solution of ZrO<sub>2</sub>-Al<sup>3+</sup> exists in composition range from 1 to 25 mol.% of Al<sub>2</sub>O<sub>3</sub> addition.

Samples density and zeta potential values were used to confirm quality of synthesized composi-

tion. In addition, BET, XRD and SEM-EDS results show linear trends and interdependence of molar % addition of Al<sub>2</sub>O<sub>3</sub> to ZrO<sub>2</sub>.

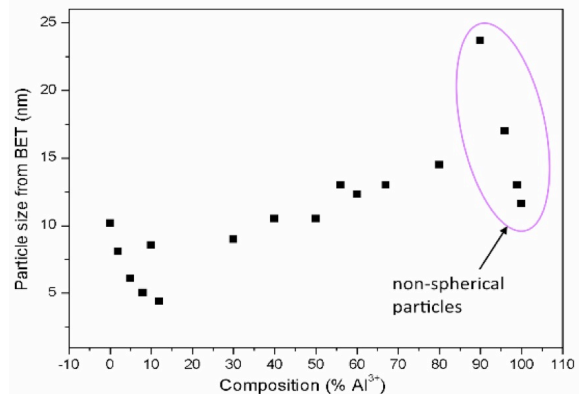


**Figure 1** Particle size obtained from SSA<sub>BET</sub> for ZrO<sub>2</sub> with different Al<sup>3+</sup> content in the function of composition

**Keywords:** microwave hydrothermal synthesis, stabilized zirconia (t-ZrO<sub>2</sub>), alumina-zirconia solid solution, nanomaterials

## Acknowledgments:

Authors are grateful to the Polish National Science Centre for financial support under contract No. UMO-2013/11/D/ST8/03429 - "Sonata 6".

## References:

1. ISO 9277, second edition 2010
2. ISO 12154, first edition 2014
3. ISO 22309, second edition 2011

# Synthesis of core-shell structured Tungsten micropowder/Copper nanoparticle by inductively coupled thermal plasma process

Kyou-Hyun Kim<sup>1\*</sup>, Hanshin Choi<sup>1</sup>, Chulwoong Han<sup>1</sup>

<sup>1</sup>Advanced Materials R&D Group, Incheon Regional Division, Korea Institute of Industrial Technology, Incheon 406-840, South Korea

## Abstract:

Tungsten (W)-Copper (Cu) composite materials are widely used in electronic components for thermal/electrical management because W has a low coefficient of thermal expansion while Cu has high thermal/electrical conductivity [1]. The physical properties of W-Cu composites can be tailored by optimizing the phase composition and microstructure. The challenges in fabricating W-Cu composites, however, come from the mutual insolubility of W and Cu due to high positive heat of mixing. Also, the quite different thermophysical properties such as density and melting temperature (W: 3410 °C, Cu: 1080 °C) make it difficult to fabricate W-Cu composites.

A large body of study has been carried out to develop processing methods to fabricate W-Cu composites. W-Cu composites can be fabricated by Cu infiltration sintering [2-4] or by liquid phase sintering of blended W and Cu powders [5-7]. The Cu infiltration method produces the W-Cu composite by a process in which molten Cu is poured into the sintered W porous structure. The infiltration process, however, requires high sintering temperature of 1200~1400 °C and even results in microstructural inhomogeneity. On the other hand, the process of liquid phase sintering with blends of W and Cu powder utilizes the selective melting of low melting point Cu and the redistribution of molten Cu to fabricate W-Cu composite materials. However, the W-Cu binary system shows densification behaviors different from those of the W-Ni [8, 9] and WC-Co systems [10-12]. W and Cu have no mutual solubility, and so W is not dissolved into molten Cu, which affects the microstructure of the sintered W-Cu composites.

The homogeneity of component phases in the W-Cu composite is critical to determine the physical properties. In liquid phase sintering, the densification of W-Cu composites is achieved mainly by rearrangement of W particles due to the capillary force and surface tension of molten Cu particles [13]. The microstructure of the W-Cu composite is thus dependent largely on the characteristics of the feedstock powder, such as the morphology and size [6, 7, 14, 15]. In con-

sequence, extremely fine particles are considered to form the homogeneous microstructure in the W-Cu composite. The mechanical alloying of elemental W and Cu powders has attracted much research interest because the particle size can be effectively reduced to mere nanometers in diameter [16]. On the other hand, Cu-coated W powders are produced by the electroless coating technique [17-19]. Ibrahim and coworkers reported that Cu-coated W powder is beneficial for compaction [17]. In addition, Cu-coated W powders improve the dispersion of the low melting point component of Cu during sintering, leading to a homogeneous microstructure with improved thermal conductivity and thermal expansion coefficient. Considering earlier studies, therefore, W/Cu core/shell structured powder can be regarded as having an ideal morphology for the achievement of high relative sintered density and homogeneous microstructure for W-Cu composites. Nevertheless, the irregular morphology of W powders, the high melting temperature component, can induce microstructural inhomogeneities in such areas as pore size and size distribution of pores. In addition, the apparent viscosity of a semisolid system is larger for irregular solid particles than for spherical particles at the same volume fraction in terms of rheology [20]. The reduced inter-particle friction between spherical powders is helpful for the rearrangement of spherical solid particles, which, in turn, improves the density of the liquid/solid mixture during liquid phase sintering. It is therefore determined that the replacement of conventional agglomerated W micropowder with spherical W powder is beneficial for manufacturing the low Cu content composite.

Based on the above, the spherical W-micropowder/Cu-nanoparticle core/shell structured composite powder was designed using in-situ reactive RF thermal plasma. Both the high energy density and the chemical reactivity of the thermal plasma were manipulated to prepare Cu nanoparticle coated spherical W micropowder.

In this study, we synthesized a Cu nanoparticle attached spheroidized W micropowder using in-situ reactive radio-frequency (RF) thermal

plasma with a blended feedstock of tungsten and cupric oxide micropowder. The spherical W micropowder improves the packing density and uniformity of the compacted body. On the other hand, the Cu nanoparticles allow the spherical W powders to be compacted by rigid die compaction at 400 MPa. Moreover, homogeneous sintering in both solid state and liquid state takes place even at low Cu contents of 5wt.% due to the uniform distribution of Cu.

**Keywords:** radio-frequency (RF) thermal plasma, Cu nano-particle, W spheroidized powder, core/shell structured composite powder, compaction, sintering.

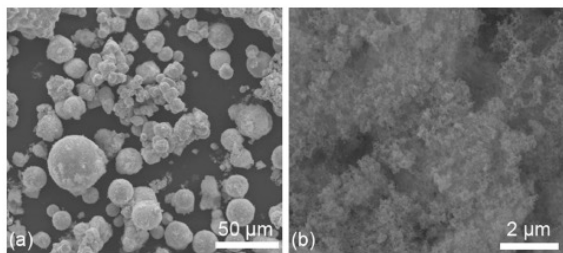


**Figure 3:** SEM images recorded from the as-synthesized W/Cu composite powder. (a) The low magnification image shows the overall morphology of spherical W/Cu composite powder, and (b) the magnified images show the surface morphology of the W/Cu composite powder.

#### Acknowledgement:

This study has been published online in *Metallurgical and Materials Transactions A* (2016) and was financially supported by the Korea Institute of Industrial Technology.

#### References:

1. R.M. German, K.F. Hens, J.L. Johnson, *Int. J. Powder. Metal.* 30 (1994) 205-215.
2. A.K. Bhalla, J.D. Williams, *Powder Metal.* 19 (1976) 31-37.
3. P.W. Ho, Q.F. Li, J.Y.H. Fuh, *Mater. Sci. Eng. A* 485 (2008) 657-663.
4. L. Duan, W. Lin, J. Wang, G. Yang, *Int. J. Refract. Met. H.* 46 (2014) 96-100.
5. J.L. Johnson, R.M. German, *Metall. Trans. A* 24 (1993) 2369-2377.
6. J.-C. Kim, S.-S. Ryu, Y.-D. Kim, I.H. Moon, *Scripta Mater.* 39 (1998) 669-676.
7. J.-C. Kim, I.-H. Moon, *Nanostruct. Mater.* 10 (1998) 283-290.
8. D.N. Yoon, W.J. Huppmann, *Acta Metall.* 27 (1979) 693-698.
9. H. Riegger, (2010).
10. Z. Fang, P. Maheshwari, X. Wang, H.Y. Sohn, A. Griffo, R. Riley, *Int. J. Refract. Met. H.* 23 (2005) 249-257.
11. Z.Z. Fang, X. Wang, T. Ryu, K.S. Hwang, H.Y. Sohn, *Int. J. Refract. Met. H.* 27 (2009) 288-299.
12. R. Bao, J. Yi, *Int. J. Refract. Met. H.* 43 (2014) 269-275.
13. J. Johnson, J. Brezovsky, R. German, *Metall. Mat. Trans. A* 36 (2005) 1557-1565.
14. J.L. Johnson, J.J. Brezovsky, R.M. German, *Metall. Mater. Trans. A* 36a (2005) 2807-2814.
15. H. Wang, Z.Z. Fang, K.S. Hwang, H. Zhang, D. Siddle, *Int. J. Refract. Met. H.* 28 (2010) 312-316.
16. J.-S. Lee, T.-H. Kim, *Nanostruct. Mater.* 6 (1995) 691-694.
17. A. Ibrahim, M. Abdallah, S.F. Mostafa, A.A. Hegazy, *Mater. Design* 30 (2009) 1398-1403.
18. S.L. Liu, K. Yu, Q. Shen, M.J. Li, W.S. Chen, G.Q. Luo, L.M. Zhang, J. Wuhan. *Univ. Technol.* 28 (2013) 829-833.
19. L.M. Zhang, W.S. Chen, G.Q. Luo, P.G. Chen, Q. Shen, C.B. Wang, *J. Alloy. Compd.* 588 (2014) 49-52.
20. Z. Fan, *Int. Mater. Rev.* 47 (2002) 49-85.

# Fabrication of Single-Walled Carbon Nanotube/Graphene Hybrid structure using Alcohol Catalytic Chemical Vapor Deposition

T. Maruyama,<sup>1,\*</sup> R. Ghosh,<sup>1</sup> Y. Iwashige,<sup>1</sup> S. Ogawa,<sup>2</sup> T. Saida,<sup>1</sup> S. Naritsuka,<sup>2</sup> S. Iijima<sup>3</sup>

<sup>1</sup>Meijo University, Department of Applied Chemistry, Nagoya, Japan

<sup>2</sup>Meijo University, Department of Materials Science and Engineering, Nagoya, Japan

<sup>3</sup>Meijo University, Faculty of Science and Technology, Nagoya, Japan

## Abstract:

Single-walled carbon nanotubes (SWCNTs)/graphene hybrid structures have been anticipated for various applications such as supercapacitors and electrode materials for rechargeable battery. However, it has been difficult to grow SWCNTs directly on graphene, although previous studies reported multi-walled CNT growth on graphene layers. In this study, we attempted to grow SWCNTs directly on graphene by chemical vapor deposition (CVD).

After acid treatments for graphite substrates, Pt catalysts were deposited on them by a pulsed arc plasma gun. Then, SWCNTs were grown on them at 700°C using alcohol catalytic CVD [1]. We also carried out SWCNT growth on graphene oxide. The grown SWCNTs/graphene hybrid structures were characterized by SEM, TEM, Raman spectroscopy and X-ray photoelectron spectroscopy (XPS).

Figure 1(a) shows a SEM image of SWCNTs grown on graphene layers, which were exfoliated from the graphite surface. SWCNTs were seen only on the exfoliated graphene layers. TEM and Raman measurements showed that most SWCNTs grown on the graphene layers were semiconducting and that their diameters were less than 1.1 nm (Fig. 1(b)) with a narrow distribution [2]. In addition, the SWCNTs were attached to the graphene surface. C 1s core level XPS spectra showed that graphite surface was oxidized at first, but, after SWCNT growth, the graphite oxide was reduced. On the other hand, when graphene oxides were used as substrates, SWCNTs were grown on a portion of the surface. However, using the Al<sub>2</sub>O<sub>3</sub> support layers, high-density web-like SWCNTs were grown on all over the surface of graphene oxides. These results showed that SWCNTs/graphene hybrid structures were formed by direct growth of SWCNTs on acid treated graphite and graphite oxide.

**Keywords:** Single-walled carbon nanotube (SWCNT), graphene, CVD, Raman spectroscopy, SEM.

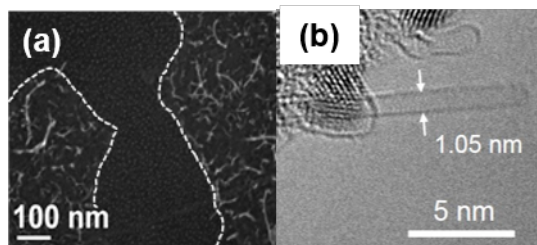


**Figure 1:** (a) SEM image of SWCNTs on graphene (the white dashed lines indicate the edges of graphene layer). (b) TEM image of SWCNTs grown on graphene layers.

## References:

1. Maruyama, T., Kondo, H., Ghosh, R., Kozawa, A., Naritsuka, S., Iizumi, Y., Okazaki, T., Iijima, S. (2016) Single-walled carbon nanotube synthesis using Pt catalysts under low ethanol pressure via cold-wall chemical vapor deposition in high vacuum, *Carbon* 96, 6-13.
2. Ghosh, R., Maruyama, T., Kondo, H., Kimoto, K., Nagai, T., Iijima, S. (2015) Synthesis of single-walled carbon nanotubes on graphene layers, *Chem. Commun.* 51, 8974-8977.

# Correlation between property and an electric field-induced network of graphene nanoplatelets in poly (lactic acid)

O. Kwon<sup>1</sup>, H. Watanabe<sup>2,\*</sup>, K.Ahn<sup>1,\*</sup>, S.Lee<sup>1</sup>

<sup>1</sup> School of Chemical and Biological Engineering, Institute of Chemical Processes, Seoul National University, Seoul, Korea

<sup>2</sup> Institute for Chemical Research, Kyoto University, Kyoto, Japan

## Abstract:

For melt-compounded poly (lactic acid) composites comprising graphene nanoplatelets (GNPs) at dilute concentrations,  $\phi_{\text{GNP}} \leq 0.34$  vol%, this research focused on interrelation between composite properties and a higher order structure of GNPs induced by a strong alternating current (AC) electric field. Optical microscopy, transmission electron microscopy and X-ray diffraction measurements evidently suggest that randomly-aligned GNPs in the as-prepared composites are oriented and formed into a chain-like structure in the field direction. This electric field-induced chain-like structure bridged the plates (or electrodes) when  $\phi_{\text{GNP}}$  was above a threshold concentration,  $\phi_{\text{GNP}}^* \geq 0.17$  vol%. Regarding this field-induced structural change, the liquid-like rheological behavior of the as-prepared composites, characterized by the storage modulus  $G'$  being almost proportional to  $\omega^2$  at low angular frequencies  $\omega$ , changed into the solid-like behavior, where  $G'$  is nearly frequency-independent at low  $\omega$  (for the composites with  $\phi_{\text{GNP}} \geq \phi_{\text{GNP}}^*$ ), after application of the field. On the other hand, the loss modulus  $G''$  was rarely affected by application of the electric field and remained nearly proportional to  $\omega$  at low  $\omega$ , suggesting that the electric field-induced structure elastically bridged between the electrodes (no viscoelastic loss). This bridge was also performed as an electrically conducting path for free electrons to travel, thereby resulting in an insulator-conductor transition when the composites with  $\phi_{\text{GNP}} \geq \phi_{\text{GNP}}^*$  were subjected to the strong electric field. Quantitative analysis of the equilibrium storage modulus and static electrical conductivity of the composites suggested that the field-induced columnar structure was not a rigid single slab but comprised of interjunctions which were mechanically softer and electrically more resistive than the single body of GNP. Besides, analysis of the  $\phi_{\text{GNP}}$  dependence of the equilibrium storage modulus and static electrical conductivity after the transition (for  $\phi_{\text{GNP}} \geq \phi_{\text{GNP}}^*$ ) suggested that an elastically inert secondary structure was formed by the left-over GNP stacks remaining out of the columnar structure (primary structure) and this secondary

structure was appear to be in *soft* contact with the primary structure to provide an extra conductive path to enhance the conductivity without too much affecting the modulus.

**Keywords:** graphene nanoplatelets, biodegradable polymer, electric field, melt rheology, dielectric properties

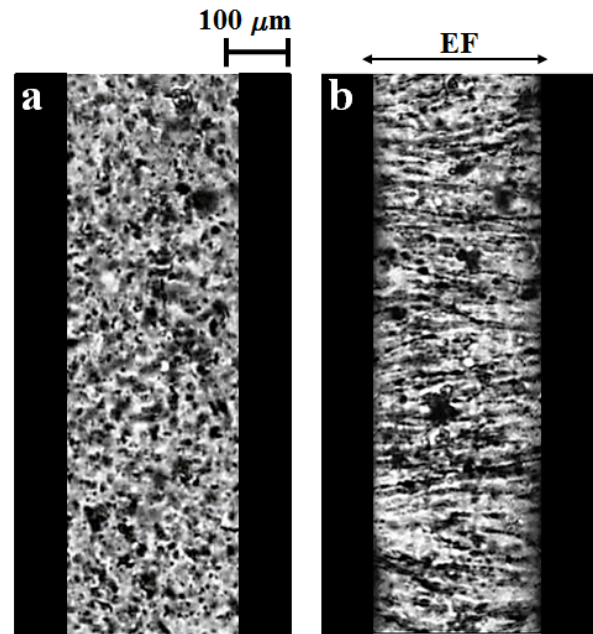


**Figure 1:** Figure illustrating optical micrographs (OM) of GNP composite with a very low  $\phi_{\text{GNP}} = 0.028$  vol% (a) before and (b) after application of the electric field (2.5 kV/mm,  $f = 60$  Hz) for 75 min at 190 °C.

## References:

1. Kwon, O., Watanabe, H., Ahn, K., Lee, S. (2017), Interplay between structure and property of graphene nanoplatelet networks formed by an electric field in a poly (lactic acid) matrix, *J. Rheology.*, 61, 291-303

# Structural and Thermal Characteristics of Graphites Treated in Alkaline or Acidic Solution

Weontae Oh

Dong-Eui University, Division of Advanced Materials Engineering, Busan, KOREA

## Abstract:

Structural characteristics and (thermal / electrical) conductivity of the natural, artificial, and expandable graphites were analyzed after treatment in alkaline or acidic aqueous solution. In order to investigate the elimination of the oxidized groups and impurities on the graphite surfaces after NaOH treatment, the graphite samples were structurally characterized by using XRD, XPS, Raman, FE-SEM. The thermal and electrical conductivity of the graphite samples were significantly improved after NaOH treatment (Figure 1). These results were caused by the structural rehabilitation. Natural and expandable graphites were chemically treated in the acidic aqueous solutions such as acetic acid or mixture of acetic acid and nitric acid. Structures and thermal conductivity of the as-treated graphites were characterized in detail. Both graphites were significantly oxidized in the mixed acidic solution of  $H_2SO_4$  and  $HNO_3$ , of which condition was generally used for the oxidation of carbon nanotubes. This considerable oxidation of graphites caused to depress their thermal conductivity. The structural characteristics obtained by XRD and XPS show that the graphites treated in the relatively weak acidic conditions (acetic acid or mixture of acetic acid and nitric acid) were quite similar to the untreated graphites. However, the thermal conductivities of both acidic-treated graphites remarkably were increased (Figure 2).

**Keywords:** thermal conductivity, electrical conductivity, alkali, acid, graphite.

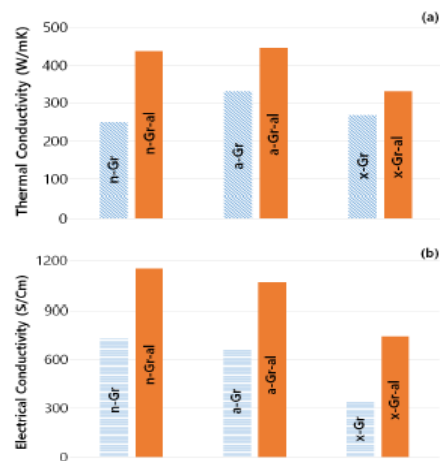


**Figure 1:** Comparisons of (a) thermal conductivity and (b) electrical conductivity obtained from graphites.

**Figure 2:** Thermal conductivity of natural (n) and expanded (x-) graphites and their analogues treated in acidic solutions.

## References:

1. Song, S. W., Min, E. H., Kim, Lee, D. W., J., Nam, D.-G., Oh, W. (2016) Thermal/Electrical Conductivities of Graphites Treated in Aqueous NaOH Solution, *J. Korean Inst. Electr. Electron. Mater. Eng.*, 29, 659-664.
2. Song, S. W., Min, E. H., Lee, D. W., Kim, J., Oh, W. Structural and Thermal Characteristics of Graphites treated in Acidic Solutions, *Korean J. Mater. Res.*, In Press.

# Aligned graphene nanosheets for highly efficient flexible field emitters

Ho Young Kim<sup>1,2</sup>, Seung Yol Jeong<sup>1</sup>, Joong Tark Han<sup>1</sup>, Geon-Woong Lee<sup>1</sup>, Mun Seok Jeong<sup>2</sup>, and Hee Jin Jeong<sup>1,\*</sup>

<sup>1</sup>Nanocarbon Material Research Group, Korea Electrotechnology Research Institute (KERI), Changwon 642-120, Korea

<sup>2</sup>IBS center for Integrated Nanostructure Physics, Institute for Basic Science, Sungkyunkwan University, Suwon 440-746, Korea  
(\*wavicle11@keri.re.kr)

## Abstract:

One of critical issues for the application of flexible field emitters using graphene nanosheets is to realize graphene nanosheets to be vertically aligned to the substrate. The recent progress in the fabrication of field emitters based on graphene nanosheets, their morphological and electrical properties, which affect their degree of field enhancement as well as the electron tunnelling barrier height, should be controlled to allow for better field-emission properties. Here we report method that fabrication of graphene field emitters using a thermal welding, filtration-transfer technique, self-assembly by breath figure, and freeze-drying methods. As a result, the graphene edges were vertically aligned as shown in Fig. 1. In addition to the high field enhancement factor, we controlled the work function of graphene field emitters via chemical doping. The resulting field-emission characteristics of the resulting emitters are discussed. The synthesized graphene emitters were highly flexible, maintaining their field-emission properties even when bent at large angles. This is attributed to the high crystallinity and emitter density and good chemical stability of the graphene emitters, as well as to the strong interactions between the graphene emitters and the substrate.

**Keywords:** graphene, field emission, flexible, vertically align, thermal welding, chemical doping, breath figure.

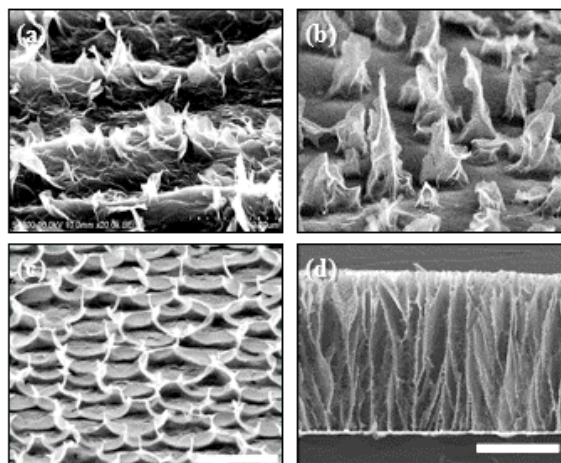


**Figure 1:** SEM images of aligned graphene nanosheet fabricated by a) thermal welding, b) filtration-transfer, c) self-assembly via breath figure, and d) freeze-drying

## References:

1. H. J. Jeong, H. D. Jeong, H. Y. Kim, S. H. Kim, J. S. Kim, S. Y. Jeong, J. T. Han, G.-W. Lee, **Small**, 8, 272 (2012)
2. S. Y. Jeong, S. H. Kim, J. T. Han, H. J. Jeong, S. Yang, G.-W. Lee, **ACS Nano**, 5, 870 (2011).
3. H. J. Jeong, H. Y. Kim, H. D. Jeong, S. Y. Jeong, J. T. Han, G.-W. Lee, **J. Mater. Chem.** 22, 11277 (2012)..
4. H. J. Jeong, H. D. Jeong, H. Y. Kim, S. Y. Jeong, J. T. Han, G.-W. Lee, **Small**, 9, 2182 (2013)
5. H. Y. Kim, S. Y. Jeong, S. Y. Jeong, K. J. Baeg, J. T. Han, M. S. Jeong, G. W. Lee, H. J. Jeong, **Nanoscale**, 7, 5495 (2015)

# Microwave-induced ultrafast heating for intrinsic properties of graphene on plastic substrates

Hee Jin Jeong<sup>1,\*</sup>, Jae-Won Lee<sup>1,2</sup>, Ho-Soon Yang<sup>2</sup>, Seung Yol Jeong<sup>1</sup>, Joong Tark Han<sup>1</sup>, Geon-Woong Lee<sup>1</sup>

<sup>1</sup>Nanocarbon Material Research Group, Korea Electrotechnology Research Institute (KERI), Changwon 642-120, Korea

<sup>2</sup>Department of Physics, Pusan National University, Busan 609-735, Korea.

(\*[wavicle11@keri.re.kr](mailto:wavicle11@keri.re.kr))

## Abstract:

Despite recent progress in producing flexible and stretchable electronics based on graphene sheets, their intrinsic properties are often degraded by the presence of polymeric residues that remain attached to the graphene surfaces following fabrication. Further breakthroughs are therefore keenly awaited to obtain clean graphene surfaces compatible with flexible applications. Here we report a method that allows the graphene to be intrinsically integrated onto flexible substrates. The method involves thermal decomposition of polymeric residues by microwave-induced selective heating of the graphene surface without affecting the underlying flexible substrate as shown in Fig. 1. Mapping the C=O stretching mode by Fourier-transform infrared spectroscopy in combination with atomic force microscopy confirms the elimination of the polymeric residues from the graphene surface. Flexible devices prepared using microwave-cleaned graphene sheets show enhanced electrical, optoelectrical, and electrothermal performances. This simple technique is applicable to a wide range of graphene-based materials and represents an important advance in the field of flexible devices

**Keywords:** graphene, 2D nanomaterial, microwave, flexible ultrafast nanheating, selective heating, flexible device.

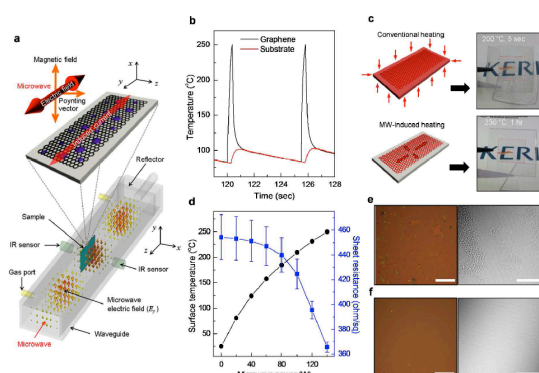


**Figure 1:** Schematic illustration of the experimental setup for microwave-induced selective heating of the graphene sheet and photographs of graphene films transferred onto PC substrates following homogeneous heating in a conventional oven or selective heating by microwave irradiation.

## References:

1. Kim, K. S., Zhao, Y., Jang, H., Lee, S. Y., Kim, J. M., Kim, K. S., Ahn, J.-H., Kim, P., Choi, J.-Y., Hong, B. H. (2009) Large-Scale Pattern Growth of Graphene Films for Stretchable Transparent Electrodes, *Nature*, 457, 706–710.
2. Jeong, H. J.; Kim, H. Y.; Jeong, H.; Han, J. T.; Jeong, S. Y.; Baeg, K.-J.; Jeong, M. S.; Lee, G.-W. (2014) One-Step Transfer and Integration of Multifunctionality in CVD Graphene by TiO<sub>2</sub>/Graphene Oxide Hybrid Layer, *Small*, 10, 2057–2066

# Luminescence of $\text{K}_2\text{SiF}_6:\text{Mn}^{4+}$ prepared by redox precipitation

Min Hyuk Im, Young Jin Kim\*

Department of Advanced Materials Engineering, Kyonggi University, Suwon 16227, Korea

## Abstract:

Nitride powders are prevalingly used as red phosphors for use in white light emitting diodes pumped by blue chips. Recently,  $\text{K}_2\text{SiF}_6:\text{Mn}^{4+}$  powders have been intensively investigated as an alternative red phosphor, because it has advantages over luminous efficiency and color rendering index of white light emitting diodes compared with nitride phosphors. In this study, we synthesized  $\text{K}_2\text{SiF}_6:\text{Mn}^{4+}$  powders by redox precipitation using mixed solutions.  $\text{H}_2\text{SiF}_6$  and  $\text{K}_2\text{MnF}_6$  solutions were prepared by dissolving  $\text{SiO}_2$  and  $\text{KMnO}_4/\text{KF}$  in dilute HF, respectively, and then they were mixed together, adding  $\text{H}_2\text{O}_2$ . As a result, yellow precipitates were produced. Finally,  $\text{K}_2\text{SiF}_6:\text{Mn}^{4+}$  powders were obtained via washing, centrifugation, filtering, and drying process. The photoluminescence excitation and emission spectra of synthesized powders are shown in Figure 1. Strong excitation peak was observed at 467 nm, which was assigned to the  ${}^4\text{A}_2 \rightarrow {}^4\text{T}_1$  transition of the  $\text{Mn}^{4+}$  ions. Corresponding emission spectra exhibited sharp emission peaks in the red region assigned to the  ${}^2\text{E} \rightarrow {}^4\text{A}_2$  transition of the  $\text{Mn}^{4+}$  ions; the 632 nm peak appeared as the strongest one. The emission intensity was affected by preparation conditions including the concentration of  $\text{KMnO}_4$  and HF, washing solutions, and temperatures.

**Keywords:**  $\text{K}_2\text{SiF}_6$ , phosphors, luminescence, redox precipitation.

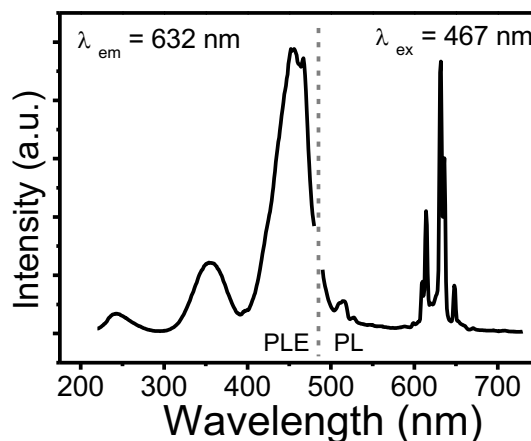


**Figure 1:** PLE and PL spectra of  $\text{K}_2\text{SiF}_6:\text{Mn}^{4+}$  powders.

## References:

1. Liao, C., Cao, R., Ma, Z., Li, Y., Dong, G., Sharafudeen, K. N., Qiu, J. (2013) Synthesis of  $\text{K}_2\text{SiF}_6:\text{Mn}^{4+}$  phosphor from  $\text{SiO}_2$  powders via redox reaction in HF/ $\text{KMnO}_4$  solution and their application in warm-white LED, *J. Am. Ceram. Soc.* 96, 3552–3556.
2. Yeo, B. E., Cho, Y. S., Huh, Y. D. (2016) Synthesis and photoluminescence properties of a red-emitting phosphor,  $\text{K}_2\text{SiF}_6:\text{Mn}^{4+}$ , for use in three-band white LED applications, *Opt. Mater.* 51, 50–55.

# Influence of Au nanoparticles on the performance of green quantum dot light emitting diodes (QLEDs)

Jae Min Kim, Hyung In Lee and Jiwan Kim\*

Department of Advanced Materials Engineering, Kyonggi University, Suwon 443-760, Korea

## Abstract:

Colloidal quantum dots (QDs) emit vivid light with narrow full width half maximum and their wavelength is tunable due to quantum confinement effect. From these unique optical/electrical properties, various display applications using QDs, therefore, have been spotlighted as a post OLED display technology. One of advantages of quantum dot light-emitting diodes (QLEDs) is a low fabrication cost, because it is based on a solution process. However, the lower current efficiency compared to OLED is still a weakness. Many researchers have been constantly tried various materials for efficient charge transport within device, at last, they came to agreement the use of inorganic nanoparticles (NPs) as an electron transport layer to improve the performance of QLEDs.

The light extraction technology is one of the well-known technologies to increase the optical efficiency of the light emitting devices. Among them, localized surface plasmon resonance (LSPR) is a technology that can improve the luminance by controlling refraction and scattering of light using metal NPs in the device. Here, we investigated the LSPR effect on the device performance by dispersing the Au NPs in the hole transport layer (HTL) and hole injection layer (HIL) (Figure 1). The result indicates that the optical enhancement of the QLEDs is attributed to strong resonance coupling between excitons in the QDs and LSP in the Au NPs in the HTL. Further optimization using Au NPs will help make highly efficient QLEDs for future display application.

**Keywords:** quantum dots, gold nanoparticles, localized surface plasmon resonance, inorganic material, quantum dot light emitting diodes.

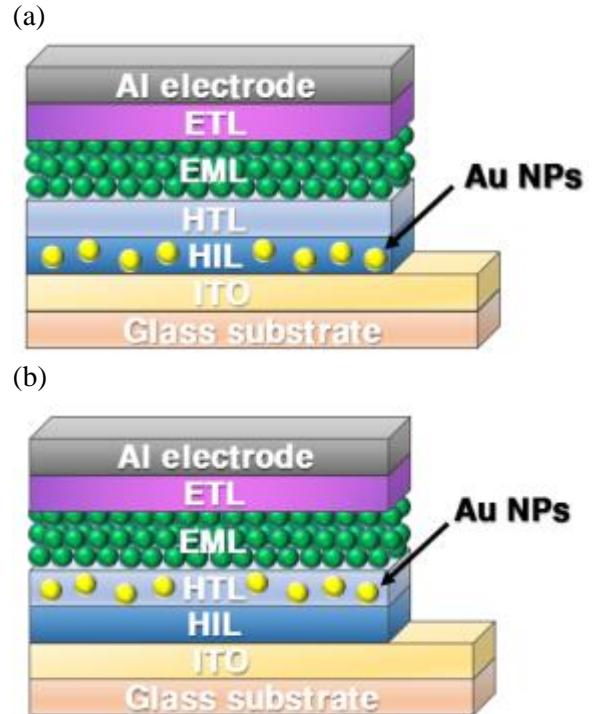


**Figure 1:** Schematic device structures of QLEDs with (a) Au NPs in HIL and (b) Au NPs in HTL

## References:

1. Y. Xiao, J. P. Yang, P. P. Cheng, J. J. Zhu, Z. Q. Xu, Y. H. Deng, S. T. Lee, Y. Q. Li, and J. X. Tang. (2012) Surface plasmon-enhanced electroluminescence in organic light-emitting diodes incorporating Au nanoparticles, *App. Phys. Lett.*, **100**, 013308.

# Tuning the Optical Response of Hybrid Colloidal Plasmonic-Photonic Crystals via Colloidal Etching

Cristian Alexandru Țîra<sup>1,3</sup>, Simion Aștilean<sup>1,3</sup>, Renaud A. L. Vallee<sup>2</sup>, Cosmin Farcau<sup>3</sup>

<sup>1</sup> Babeș-Bolyai University, No. 1 Mihail Kogălniceanu, RO-400084 Cluj-Napoca, Romania

<sup>2</sup> CNRS, University of Bordeaux, CRPP, UPR8641, 115 avenue Schweitzer, 33600 Pessac, France

<sup>3</sup> Institute for Interdisciplinary Research in Bio-Nano-Sciences, Babeș-Bolyai University, Cluj-Napoca, Romania

## Abstract:

Hybrid colloidal plasmonic-photonic crystals (HPPC) [1], i.e. metal-coated arrays of dielectric colloids, are known for their fundamentally relevant and tunable optical properties [2]. Their main attractive feature consists in the possibility to adjust the wavelength of the plasmon-enhanced transmission bands by the diameter of the colloids [3]. Here, we explore the transmission characteristics of close and non-close packed HPPC obtained through a gradual etching of the polymer spheres in an oxygen plasma.

In order to modify the morphology of the initial close packed colloidal crystal (CC), we reduced the spheres' diameter by plasma etching. By controlling the oxygen flow inside the etching chamber, power of the generator and etching time, the diameter of the polystyrene microspheres was altered, while maintaining the lattice period (500 nm in this study). These samples were then coated by a gold film (45-50 nm) in order to obtain the close and non-close packed HPPC. The structural modifications were analyzed by Scanning Electron Microscopy and Atomic Force Microscopy, while the optical properties were analyzed by micro-spectroscopy.

Finite-difference time-domain simulations were also employed, and provided input for the understanding of the correlations between the optical/plasmonic (Figure 2) and the morphological properties. The effects of reducing the sphere size and simultaneous increase of the nanoparticles formed on the substrate (see Figure 1), could be thus pinpointed. Interestingly, by this approach of colloidal etching, the plasmonic landscape including both gold caps on the spheres and nanostructures below the spheres could be altered.

By corroborating SEM, AFM, experimental and simulated optical spectra, this study shows how the optical/plasmonic response of HPPC can be tuned in a controlled way and contributes to the current understanding of the photonic/plasmonic interactions in these plasmonic nanostructures.

**Acknowledgement.** This work was supported by a grant of the Romanian National Authority for Scientific Research and Innovation, CNCS-UEFISCDI, project number PN-II-RU-TE-2014-4-2639.

**Keywords:** hybrid plasmonic-photonic crystals, colloidal self-assembly, FDTD, surface plasmons

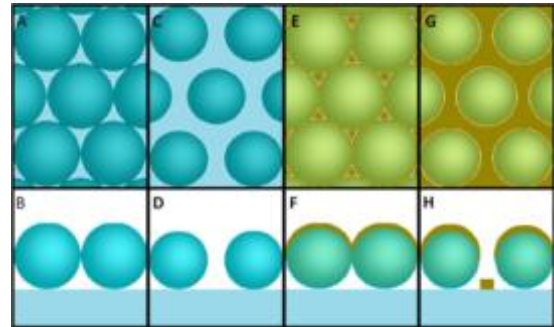


**Figure 1:** Scheme depicting a top view (first row) and a cross-section view (second row) of colloidal crystals (CC) (A and B), NC-CC (C and D), HPPC (E and F) and NC-HPPC (G and H).

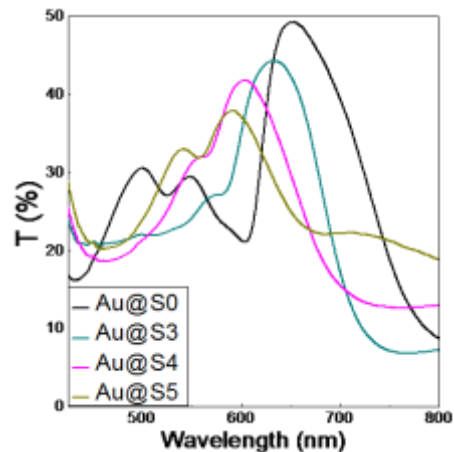


**Figure 2** Transmission experimental spectra of the HPPC (S0) and NC-HPPC(S3-S5)

## References:

1. S. G. Romanov, A. V. Korovin, A. Regensburger, and U. Peschel, "Hybrid Colloidal Plasmonic-Photonic Crystals," *Adv. Mater.* 23, 2515–2533 (2011)
2. V. Saracut, M. Giloan, M. Gabor, S. Astilean, and C. Farcau, "Polarization-sensitive linear plasmonic nanostructures via colloidal lithography with uniaxial colloidal arrays" *ACS Appl. Mater. Interfaces* 5, 1362–1369 (2013)
3. C. Farcau, M. Giloan, E. Vinteler, and S. Astilean, "Understanding plasmon resonances of metal-coated colloidal crystal monolayers," *Appl. Phys. B* 106, 849–856 (2012)

# Fabrication of Novel Nanointerfaces on a Gold Thin Film and Their Applications for Gas Biosensor

Jina Kim<sup>1</sup>, Youngbo Choi<sup>2</sup>, Surin Hong<sup>1,\*</sup>

<sup>1</sup>CHA University, Department of Biotechnology, Gyeonggi, Korea

<sup>2</sup>Chungbuk National University, Safety Engineering, Chungbuk, Korea

## Abstract:

As in many different technological fields, nanomaterials have developed appropriate use for biosensing applications. The intelligent use of such nanomaterials or nanostructures led to enhanced performances with increased sensitivities and lowered detection limits for target analytes. In this study, the fabrication method of novel nanointerfaces on a gold thin film for gas biosensor was developed. The method and sensing principle are based on the sensitive and specific interaction between the ligand-modified TiO<sub>2</sub> nanocomposite and gas molecules, and the effect of this on changes in the surface plasmon resonance (SPR) profiles of the gold thin film. The ligand plays a role as a specific receptor for target gas molecules, which results in a sensitive detection and a lower detection limit. In addition, due to the surface properties of TiO<sub>2</sub> nanocomposite as a dielectric spacing layer, it allows the sensing signal to be more enhanced. As a proof of concept test, the formaldehyde, as known to be a breast cancer biomarker in human exhalation, is selected for the development of diagnostic biosensor. The SPR properties of the resulting selectively formed complexes are altered, leading to significant changes in SPR reflectance near the SPR angle. The working range of this sensing system is under ppm level, therefore, it would be applicable for use in biological monitoring and diagnosis.

**Keywords:** gas biosensor, TiO<sub>2</sub> nanomaterial, nanostructure, gold thin film, surface plasmon resonance measurements.

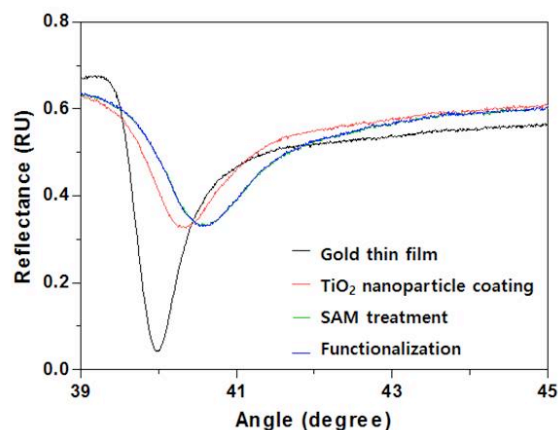


**Figure 1:** SPR profiles for fabrication procedure of TiO<sub>2</sub> nanostructure on a gold thin film that we are tempting to utilize gas biosensor.

## References:

1. Choi, Y., Kwak, H., Hong, S. (2014) Quantification of arsenic(III) in aqueous media using a novel hybrid platform comprised of radially porous silica particles and a gold thin film, *Anal. Methods*, 6, 7054-7061.
2. Choi, Y. Shin, S.H., Hong, S. Kim, Y. (2016), A combined top-down/bottom-up approach to structuring multi-sensing zones on a thin an the application to SPR sensors, *Nanotechnology*, 27, 1-6.

# Multifunctional Supramolecular Nanoplatfoms for Sensory and Delivery Applications

Jeonghun Lee, Chulhee Kim,

Inha University, Department of Polymer Science and Technology, Incheon, Korea

## Abstract:

Nanotubes have been a subject of great interests due to their innovative properties and potential applications in a variety of areas of nanoscience. In particular, for organic nanotubes, the precise functionalization and interconnection of the building blocks provided a vision that they could exhibit not only unprecedented architectures but also valuable functions for applications such as electronics and biomedicine. We report the construction of unique supramolecular fluorescent organic nanotubes derived from self-assembly and inclusion complexation of dendrons with cyclodextrins (CDs) or cucurbituriles (CBs). In particular, their biosensory and delivery characteristics will be discussed. The organic nanotubes with unique fluorescence characteristics were fabricated by a hierarchical self-assembly process derived from a host-guest complexation between the amide dendrons with the focal pyrene moiety and CDs and CBs. The supramolecular approach provided a facile synthetic route to organic nanotubes with highly complex and precise structures with specific function. The unique structural aspect of the nanotubes is that the surface of the nanotubes is covered with CDs or CBs. Therefore, the functional group on the surface of the nanotube is precisely controlled by modifying the functionality of CDs. In addition, the fluorescent properties of the nanotubes are highly dependent on the exterior environment of the nanotube. The facile functionalization of the nanotube with specific peptide epitope provides high selectivity as a sensory vehicle. Therefore, this type of supramolecular nanotubes exhibited unique biosensory function for proteins, sugars, and ions. In addition, the nanotube is a useful carrier vehicle for biomolecules. The supramolecular approach by employing functionalized building blocks provided an opportunity for fine tuning of the surface of the nanotubes for diverse application as biosensory or target delivery vehicle. The unique strategic concept of the CD-covered organic nanotubes were extended towards the CD-covered nanoparticles for stimuli-responsive delivery vehicle. Further, the specificity of responsiveness of peptides were introduced to the nanoobjects to de-

monstrate their effective function as smart sensory vehicles. In particular, for the first time, we demonstrate the stimuli-responsive conformational conversion of peptides on the surface nanoobjects could be utilized as a key motif for smart bio-responsive delivery vehicles.

**Keywords:** self-assembled nanotubes, mesoporous nanoparticles, sensory platform, stimuli-responsive surfaces, conformational conversion of peptides, bio-responsive delivery nanovehicle.

## References:

1. J. Lee, E.-T. Oh, H. Yoon, H. Kim, H. J. Park, C. Kim, *Nanoscale*, 2016, 8, 8070.
2. J. Lee, H. Kim, S. Han, E. Hong, K.-H. Lee, and C. Kim, *J. Am. Chem. Soc.*, 2014, 136, 12880.
3. C. Park, J. Lee, C. Kim, *Chem. Commun.*, 2011, 47, 12042.
4. C. Park, M. S. Im, S. Lee, J. Lim, C. Kim, *Angew. Chem. Int. Ed.* 2008, 47, 9922.

# Characterization of large-scale self-organization in novel semi-conducting polythiazoles

M. Urdanpilleta<sup>1\*</sup>, J. Jäger<sup>2</sup>, N. T. Yimga<sup>3,4</sup>, E. von Hauff<sup>4</sup>, F. Pammer<sup>2</sup>

<sup>1</sup>Dept. of Applied Physics I, University of the Basque Country (UPV/EHU), San Sebastián, Spain

<sup>2</sup>Institute of Organic Chemistry II and Advanced Materials, University of Ulm, Ulm, Germany

<sup>3</sup>Institute of Physics, Carl von Ossietzky University of Oldenburg, Oldenburg, Germany

<sup>4</sup>Department of Physics and Astronomy, Vrije Universiteit Amsterdam, Amsterdam, Netherlands

## Abstract:

The field of polymeric semiconductors has made great progress in the last decades, and this allows developing conjugated polymers that can be tailored for many applications in organic electronics, such as organic field effect transistors, organic light-emitting diodes, and organic photovoltaic cells. Nevertheless, the prediction of the final performance of a semiconducting material is in general not possible, as it is affected not only by its intrinsic electronic (optical and electrochemical) properties, but also by the morphology of the active layer of the device [1,2]. This morphology depends on fabrication conditions, and also on the interplay of the given material with other components forming the active layer. In general, an ordered structure and a high degree of crystallinity favor charge-transport in polymer semiconductors.

In this work, we study the bulk morphology of three new head-to-tail regioregular poly(4-alkylthiazole)s (PTzTHX, PTzTNB and PTzTIB) through Atomic Force Microscopy (AFM), Scanning Electron Microscopy (SEM) and Grazing Incidence X-ray Diffraction (GIXD). We find that morphological characteristics vary drastically depending on the nature of the conjugated side-chain introduced to modify the electronic properties of the polymer [3]. The complementary electrical characterization demonstrates a correlation between the charge carrier mobility and the highly ordered crystalline morphology (see Figure 1) of the polymer films [3].

**Keywords:** polymeric semiconductor, morphology, atomic force microscopy, scanning electron microscopy, grazing-incidence X-ray diffraction, carrier mobility, electrical characterization

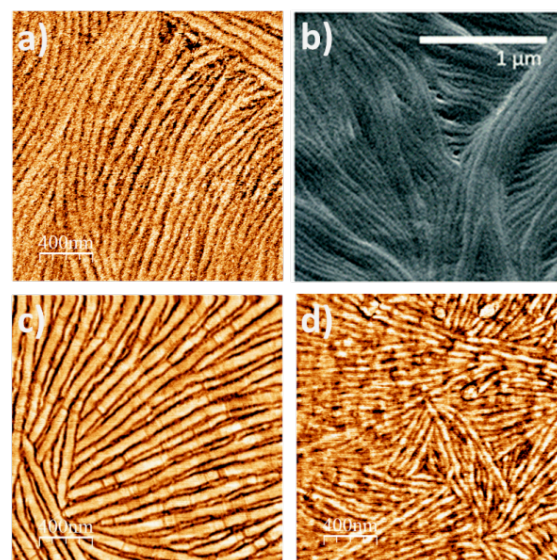


**Figure 1:** Images of three batches of PTzTHX with different number-average molecular weight,  $M_n$ . (a) AFM and (b) SEM,  $M_n = 59.8$  kDa (c) AFM,  $M_n = 39.5$  kDa, (d) AFM,  $M_n = 20.0$  kDa. Films deposited by spin-coating on ITO/PEDOT:PSS.

## References:

1. Heinze, J., Frontana-Urbe, B. A., Ludwigs, S. (2010), Electrochemistry of Conducting Polymers-Persistent Models and New Concepts, *Chem. Rev.*, 110, 4724-4771.
2. Huang, Y., Kramer, E. J., Heeger, A. J., Bazan, G. C. (2014) Bulk heterojunction solar cells: morphology and performance relationships, *Chem. Rev.*, 114, 7006-7043.
3. Jäger, J., Yimga, N. T., Urdanpilleta, M., von Hauff, E., Pammer, F. (2016) Toward n-type analogues to poly(3-alkylthiophene)s: influence of side-chain variation on bulk-morphology and electron transport characteristics of head-to-tail regioregular poly(4-alkylthiazole)s, *J. Mater. Chem. C* 4 (13), 2587-2597

# Using magnetosomes nanoparticles from magnetotactic bacteria as a therapeutic substance for magnetic hyperthermia treatment against brain tumors

C. Mandawala<sup>1,2\*</sup>, I. Chebbi<sup>1</sup>, M. Durand-Dubief<sup>1</sup>, R. Le Fevre<sup>1</sup>, Y. Hamdous<sup>1</sup>, F. Guyot<sup>2</sup>, E. Alphandéry<sup>1,2</sup>

<sup>1</sup>Nanobacterie SARL, Paris, France.

<sup>2</sup>Muséum National d'Histoire Naturelle and University Pierre et Marie Curie, CNRS. Sorbonne Universités. Institut de minéralogie et de physique des Matériaux et de Cosmochimie (IMPMC), Paris, France.

## Abstract:

Magnetic hyperthermia, alone or in combination with other conventional cancer therapies, using magnetic nanoparticles subjected to an alternating magnetic field (AMF), may increase patients' life expectancy, especially in glioblastoma<sup>1</sup>.

In this study<sup>2</sup>, we report the fabrication of iron oxide magnetosome minerals isolated from magnetotactic bacteria, which are magnetic nanoparticles with better characteristics than chemical nanoparticles. For the first time, our purification process using chemicals results in nanoparticles without pyrogenic components of bacterial origin. Then, these nanoparticles, are stabilized with different biodegradable, biocompatible coating agents or transfecting agent. Several methods of physico-chemical analysis such as transmission electron microscopy (TEM), Fourier transform infrared spectroscopy (FT-IR), CHNS analysis and zeta potential measurements are used to verify the presence of a coating surrounding the crystallized core of maghemite, to determine the surface charge, stability of these nanoparticles in suspension as well as their organization, in chains. Using a *Limulus Amebocyte* Lysozyme test (LAL) assay, we determined a low endotoxin concentration (~160 EU/ mL/ mg in iron) in these nanoparticle suspensions, similar to that of chemically synthesized nanoparticles BNF-Starch currently used for magnetic hyperthermia<sup>3</sup>.

*In vitro* studies are carried out to measure a half maximal inhibitory concentrations (IC<sub>50</sub>), of these nanoparticles in the presence of healthy 3T3 cells, which is larger than IC<sub>50</sub> values of most common cytotoxic anticancer drugs. When biological nanoparticles are incubated with cancerous glioblastoma GL-261 cells and exposed to an AMF of frequency 198 kHz and average strength of 34 mT, the average specific absorption rates (SAR), are higher for coated magnetosomes than for BNF-Starch. The percentage of cell destruction due to the AMF application is between 10 ± 3% and 43 ± 3%, depending on the coating agent surrounding these biological nanoparticles.

*In vivo* antitumor efficacy is studied on C57BL/6 mice bearing subcutaneous GL-261 glioblastoma tumors. And these treatments led to a higher percentage of mice with full tumor disappearance of 50% for coated magnetosomes compared with 20% for BNF-Starch, respectively. These promising results indicate that purified and then coated magnetosome minerals are good candidates to carry out the magnetic hyperthermia treatment of tumors.

**Keywords:** magnetosomes, magnetotactic bacteria, magnetosome minerals, magnetic hyperthermia, alternating magnetic field.

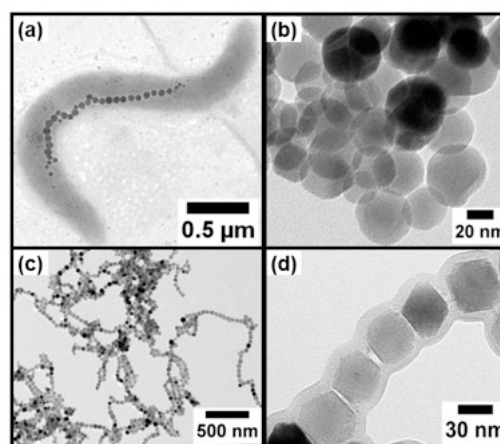


**Figure 1:** TEM images of, (a), magnetosomes contained inside magnetotactic bacteria, (b), magnetosomes extracted from these bacteria and purified yielding “naked” magnetosome mineral cores, (c) and (d), coated magnetosome mineral cores usable as therapeutic substance for magnetic hyperthermia treatment of tumors.

## References:

1. Maier-Hauff, K., Rothe, R., Scholz, R., Gneveckow, U., Wust, P., Thiesen, B., & al., (2007), Intracranial Thermotherapy using Magnetic Nanoparticles Combined with External Beam Radiotherapy: Results of a Feasibility Study on Patients with Glioblastoma Multiforme. *Journal of Neuro-Oncology*.

2. Mandawala, C., Chebbi, I., Durand-Dubief, M., Le Fèvre, R., Guyot, F., Alphandéry, E., (2017), Biocompatible and stable magnetosome minerals coated with poly-L-lysine, citric acid, oleic acid, and carboxy-methyl-dextran, for application in the magnetic hyperthermia treatment of tumors, *Journal of Materials Chemistry B*, Submitted .
3. Zadnik, PL., Molina, CA., Sarabia-Estrada, R., Groves, ML., Wabler, M., Mihalic, J., & al., (2014), Characterization of intratumor magnetic nanoparticle distribution and heating in a rat model of metastatic spine disease: Laboratory investigation, *Journal of Neurosurgery*.

# Insect repellent nanocapsules with improved thermal and mechanical properties

M.M. Sánchez-Navarro\*, M.A. Martínez-Sánchez, F. Arán-Aís  
INESCOP. Centre for Technology and Innovation. Elda (Alicante), Spain; [\\*msanchez@inescop.es](mailto:msanchez@inescop.es)

## Abstract:

The need for the development of insect repellent materials arises from the fact that mosquitoes are vectors of multiple viruses, becoming one of the major carriers of infectious diseases to humans. In fact, mosquitoes are the cause of diseases widely spread in certain areas of population, such as malaria, Japanese encephalitis, dengue, etc.

It is known, that there are a high number of substances with anti-mosquito/insect repellent activity, however the vast majority of them are thermolabile substances. Many natural compounds and extracts are not compatible with the high requirements in manufacturing and curing processes employed in the industries. In this sense, microencapsulation technology presents a great potential to the industry due to its capability to protect the active substances from external agents responsible of their degradation.

Microencapsulation could be defined as a substance coating process with an inert shell, generally of a polymeric nature, which protects or isolates an active compound from external agents and allows its controlled release. However, not all the shell materials employed in microencapsulation technology can bear the severe industrial footwear processes, plastic extrusion and food production processes, which require high demands of pressure and heat that may produce the rupture of microcapsules with the subsequent degradation of the active ingredients incorporated into the material or into the final product; a premature release may also cause the loss of the desired functionality. Generally, polymers, synthetic or natural, are the common shell materials used. However, one of the main drawbacks that arise with the use of different natural and synthetic polymers is its low thermal and mechanical resistance, which difficult their use in microcapsules to be valid to functionalize certain industrial products (Figure 1).

As an alternative, to solve the above mentioned inconveniences, this study presents the use of inorganic nature compounds as microcapsule shell. Materials such as carbonates, silicas and other metal oxides, are capable of withstanding

high temperatures and with a great mechanical resistance.

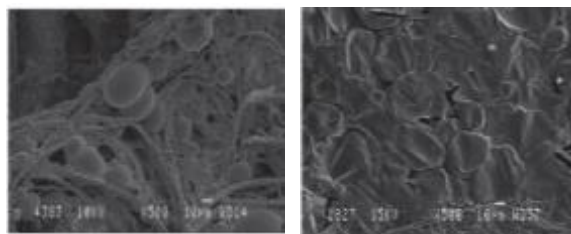


**Figure 1:** Image of leather with natural polymer microcapsules, before and after fabrication process.

The results of this study will help food, packaging, plastic and footwear industries, among others, to improve their current manufacturing processes and the final quality of their products, making them more sustainable and healthier for the final consumer.

**Keywords:** functional materials, controlled release, silica microcapsules, SEM, TGA, GC-MS.

Authors thank the partial financial support to the by IVACE (the Valencian Centre of Business Competitiveness) and ERDF Funds through the project (Ref. IMDECA 2016/66).

## References:

1. Insect Repellents: Principles, Methods, and Uses. Mustapha Debboun, Stephen P. Frances and Daniel Strickman (Eds). CRC Press, 2007.
2. Sánchez-Navarro, M.M.; Pérez-Limiñana, M.A.; Arán-Ais, F.; Orgilés-Barceló, C. (2015). Scent properties by natural fragrance microencapsulation for footwear applications. *Polym. Int.*, 64, 1458-1464.
3. Hoffmann F, Cornelius M, Morell J, Foroba M. (2006). Silica based mesoporous organic-inorganic hybrid materials. *Angew Chem Int Ed* 45:3216-3251.

# Corrosion Resistance of Mg-Al LDH Nanocontainer-Equipped Mg(OH)<sub>2</sub> Film Formed on Magnesium Alloys by Steam Coating

A. Serizawa,<sup>1,\*</sup> Y. Hirai,<sup>2</sup> T. Kim,<sup>2</sup> T. Ishizaki,<sup>1</sup>

<sup>1</sup> Shibaura Institute of Technology, Department of Materials Science and Engineering, Tokyo, Japan

<sup>2</sup> Shibaura Institute of Technology, Graduate School of Engineering and Science, Tokyo, Japan

## Abstract:

Magnesium and its alloys have been used as advanced structural and functional materials in aerospace, automobile and railway industries because of their excellent physical and mechanical properties such as low density, good electromagnetic shielding and high specific strength. Their low corrosion resistance, however, has hindered their use on a larger scale. To improve the corrosion resistance of the magnesium alloys, the development of a novel coating technology has been required. In this presentation, we report a novel preparation method of an anticorrosive Mg-Al layered double hydroxide/oriented magnesium hydroxide composite film on magnesium alloys by steam coating [1]. The corrosion resistance of the composite film was also investigated.

Magnesium alloys AZ31 and AZX 612 were used as a substrate. The cleaned substrates were set in the autoclave. The autoclave was saturated with water vapor by introducing steam at 140 to 180 °C for 0.5 to 2 h, resulting in the formation of anticorrosive films on magnesium alloys. Figure 1 shows XRD patterns of the film formed on AZ31 at 180 °C (1), 140 °C (2) and 160 °C (3), and on AZX 612 at 150 °C (4) and 160 °C (5). XRD patterns revealed that all the films were composed of crystalline Mg(OH)<sub>2</sub>. The film formed at 180 °C had a peak assigned to Mg-Al LDH at  $2\theta = 11.4^\circ$ . O1s XPS spectrum of the film formed at 180 °C also showed the presence of MgO. However, no peak attributable to MgO can be observed in the XRD pattern. Thus, the films could be composed of amorphous MgO, crystalline Mg(OH)<sub>2</sub> and Mg-Al LDH. The corrosion resistances of the composite films formed on magnesium alloys were investigated by CCT test and electrochemical measurements. The films formed on magnesium alloys showed higher corrosion resistance than untreated magnesium alloys.

**Keywords:** Magnesium alloy, layered double hydroxide, steam coating, corrosion resistance, surface modification.

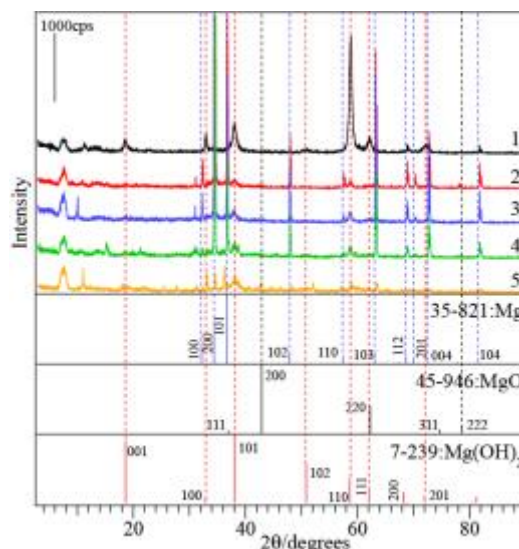


**Figure 1:** XRD patterns of samples subjected to steam coating under different conditions.

## Acknowledgement:

This research was partially supported by Japan Science and Technology Agency (JST), Adaptable and Seamless Technology Transfer Program through Target-driven R&D (A-step: No. AS2815047S).

## References:

1. Ishizaki, T., Kamiyama, N., Watanabe, K., Serizawa, A. (2015), Corrosion resistance of Mg(OH)<sub>2</sub>/Mg-Al layered double hydroxide composite film formed directly on combustion-resistant magnesium alloy AMCa602 by steam coating, *Corros. Sci.*, 92, 76-84.

# Dynamic Response of Ti-based Metallic Glasses under Brazilian Disc Test Conditions

Ping Hong Lin<sup>1</sup>, Liren Tsai<sup>1\*</sup>, Shih-Han Wang<sup>2</sup>

<sup>1</sup>National Kaohsiung University of Applied Sciences, Department of Mechanical Engineering, Taiwan

<sup>2</sup>National Yunlin University of Science and Technology, Department of Chemical Engineering, Taiwan

## Abstract:

Bone losses often happens in aging population. Serious bone losses could resulted in various complicated damages, and orthopedic implant becomes inevitably. Metal materials were commonly used in artificial substitutes and human body assembly parts. Although currently many metal materials have clinical success for implant, there are many factors for the reliability of implants which includes wear, fatigue failure and corrosion. Careful selection of alloying additions when design new alloys for biomedicine can improve properties of corrosion, increased strength and wear resistance, decreased Young's modulus, etc. In this research, Ti-based metallic glasses were studied. The materials were melted then passed through a mold Rod size of about 3 ~ 6 mm were produced. The surface morphology and lattice structure of the alloying elements were observed by X-ray diffractometer and scanning electron microscopy. Dynamic tensile and static mechanical properties of Ti-based bulk metallic glass materials were investigated by means of a Brazilian disc method (BD) using a material testing system and a Split Hopkinson Pressure Bar, respectively. The mechanical and mechanical properties of the materials were mainly tensile strength and strain and stress. Dynamic and static fracture process of the Ti-based bulk metallic glasses at various loading rates was measured. Ti-based metal glass has a lower Young's modulus than human bone and high strength properties and good corrosion resistance; it has great potential as human bone implant material.

**Keywords:** Spilt Hopkinson Pressure Bar, Brazilian Disc, Ti-based bulk metallic glass

# Water droplet behavior on surfaces covered with two types of organic silane molecules with different alkyl-chain length

T. Ishizaki,<sup>1,\*</sup> S. Hisada,<sup>2</sup> A. Takada,<sup>2</sup>

<sup>1</sup>Department of Materials Science and Engineering, College of Engineering, Shibaura Institute of Technology, Tokyo 135-8548, Japan

<sup>2</sup>Graduate School of Materials Science and Engineering, Faculty of Engineering, Shibaura Institute of Technology, Tokyo 135-8548, Japan

## Abstract:

Development of surface treatment technology for control of water droplet behavior is essential for various applications such as  $\mu$ -TAS, automobile, and so on, because the technology holds the promise for considerably reducing energy consumption in their industries. Superhydrophobic surface with a water contact angle of more than  $150^\circ$  is known as a surface to repel extremely water. [1,2] The superhydrophobicity is created by two factors, i.e., low surface energy and nanostructure. The nanostructure is easily damaged by physical contact, resulting in the decrease in the water contact angle. Thus, it is required to create a novel surface that can control wetting behavior of water droplet after physical contact. Hydrophobic surface with a low contact angle hysteresis is considered to be an alternative surface to respond to the request, because the surface can control wetting behavior of water droplet. In addition, the surface does not have nanostructure, so it is hardly affected by the physical damage. Thus, it is very important to develop a technology for creating hydrophobic surface with a low contact angle hysteresis. In this study, we aimed to prepare dewetting surface showing a low contact angle hysteresis by a simple and easy process.

Si wafer was used as substrate. Hydrophobic surface was prepared on the cleaned substrate using mixed raw materials composed of trimethoxy(methyl)silane (TTMS), dodecyltrimethoxysilane (DDS) or hexyltrimethoxysilane (HXS) and octadecyltrimethoxysilane (ODS) by a chemical vapor deposition at 373 K for 24 h.

Fig 1 shows water contact angle hysteresis values as a function of ODS amounts in raw materials. The water contact angle hysteresis on the surface covered with HXS and ODS, and DDS and ODS were decreased with an increase in ODS amounts in raw materials. The contact angle hysteresis of the samples were approximately kept constant at  $10^\circ$ . The surface covered with HXS and ODS became water contact angle hysteresis of less than  $10^\circ$ , showing the lowest water contact angle hysteresis. On the other hand,

water contact angle hysteresis of the surface covered with TTS and ODS were approximately kept constant at  $20^\circ$ . These results indicate that the difference in the alkyl chain length of the raw material affects the contact angle hysteresis.

**Keywords:** Wettability, contact angle hysteresis, dynamic behavior of water droplet, CVD.

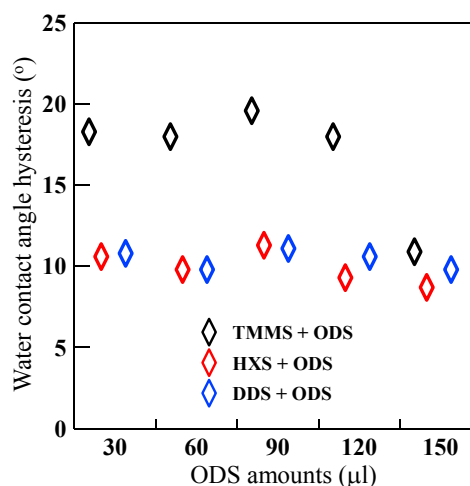


**Figure 1:** Water contact angle hysteresis values as a function of ODS amounts in raw materials.

## References:

1. X. Feng, J. Zhai, L. Jiang, *Angew. Chem. Int. Ed.* 2005, 44, 5115.
2. Y. Zhu, J. Zhang, Y. Zheng, Z. Huang, L. Feng, L. Jiang, *Adv. Func. Mater.* 2006, 16, 568.

**Acknowledgment:** This work was partly supported by Grant-in-Aid for Scientific Research (A) (No. 16H02400) from Japan Society for the Promotion of Science.

# Supercritical Water Synthesized Polyaniline/reduced Graphene Oxide-Based Composites for Room Temperature ppb-Level Ammonia Gas Sensing

Shih-Han Wang<sup>1\*</sup>, Jing-Huei Wang<sup>2</sup> and Liren Tsai<sup>3</sup>,

<sup>1</sup>Department of Chemical and Materials Engineering, National Yunlin University of Science and Technology, Yunlin, Taiwan

<sup>2</sup>Department of Chemical Engineering, I-Shou University, Kaohsiung, Taiwan

<sup>3</sup>Department of Mechanical Engineering, National Kaohsiung University of Applied Science, Kaohsiung, Taiwan

<sup>4</sup>Department of Chemistry and Material Engineering, National Defense University, Taoyuan, Taiwan

## Abstract:

Ammonia is a harmful environmental pollutant, and it is also an important breath biomarker of kidney and liver diseases. The ammonia level for human breath and ambient environment is in the range of hundreds ppm to several ppb. However, it is difficult to detect low-level ammonia using single sensor at room temperature. Polyaniline [1] is also a kind of ammonia sensitive material, however, it showed relatively poor mechanical properties and selectivity. In the previous study, some metallic nanoparticles, such as Au NP, Cu NP and Pt NP [2], were doped to improve the sensing performance. The easily functionalized and excellent electrical properties of reduced graphene (rGO) was exploited to be the composite matrix in this study. In this study, a polyaniline/ reduced graphene oxide nanocomposite was synthesized in a one-pot system. Aniline monomer introduced into the rGO surface between layer-by-layer was enhanced in high pressure system.

In order to eliminate the surface tension and enhance the uniformity, supercritical water was utilized to synthesis copper nanoparticle decorated composite. The copper nanoparticle was deposited onto rGO surface uniformly in supercritical water to form the PANI/MNP/rGO. PANI/MNP/rGO catalyzed the oxidation reaction of ammonia. The surface morphology and microstructure of the sensing layers were analyzed by scanning electron microscopy and transmission electron microscopy. The chemical structure of the sensing materials was characterized by Fourier transform infrared spectroscopy (FTIR) and X-ray photoelectron spectroscopy (XPS). This chemiresistor ammonia sensor was operated at room temperature. The resistance of the sensing layer increased as the monotonic function of ammonia concentration. This sensor showed a highly sensitivity in a wide range of 250 ppm to 25 ppb. The experimental results

suggested that our PANI/rGO-based sensor was successfully developed for ppb-level ammonia sensing for environment and biomedical applications.

**Keywords:** ammonia gas sensor, reduced graphene oxide, polyaniline, supercritical water

## Acknowledgement

Authors like to thank the financial support from Ministry of Science and Technology, R.O.C. (no. 105-2221-E-224 -065 -).

## References:

1. Fratoddi, I., Venditti, I., Cametti, C., Russo, M.V.(2015) Chemiresistive polyaniline-based gas sensors: A mini review, *Sensors and Actuators B: Chemical*, 220, 534-548.
2. Patil, U.V., Ramgira, N.S., Karmakar, N., Bhogale, A., Debnath, A.K., Aswal, D.K., Gupta, S.K., Kothari, D.C. (2015) Room temperature ammonia sensor based on copper nanoparticle intercalated polyaniline nanocomposite thin films, *Applied Surface Science.*, 8, 69-74.

# FeNi Electrodeposited on Meso and Macroporous Silicon

S. Ouir,<sup>1,2,\*</sup> G. Fortas,<sup>2</sup> S. Sam<sup>2</sup>, N. Gabouze<sup>2</sup>

<sup>1</sup> University Blida1, B.P. 270, route de Soumaa, Blida, Algeria

<sup>2</sup> CRTSE, 02, Bd. Frantz Fanon, B.P. 399 Alger-Gare, Algiers, Algeria.

## Abstract:

In this present work, we report on the electrodeposition of FeNi into porous silicon (PS) formed on n-type Si with different resistivity.

Mesopore and macropores silicon layers were formed at constant current density in HF-based electrolyte. FeNi films were electrodeposited by applying a constant bias potential. The electrodeposited thin films were characterized by scanning electron microscopy (SEM) and energy dispersive (EDS) and X-ray diffraction.

The results show that the FeNi growth on PS surfaces is predetermined by the pore Si morphology and follows the pore silicon shape. In the case of macroporous layers, the FeNi grains decorate the inner of pore and grow in a cylindrical-like or tubular-like form perpendicular to the substrate surface – However, for a FeNi deposition into mesoporous Si layers, the FeNi grains first penetrate deep into the pore and agglomerate at the entry of the pore due to its obstruction by the FeNi particles. The deposition occurs on the entire surface. In addition, the results clearly confirm that the plating parameters (deposition procedure: fixed or sweep potential, pore morphology, etc) have a strong influence on morphology and composition of the FeNi films.

Finally, the obtained results are discussed and a grow mechanism for each case is proposed.

**Keywords:** Alloys, Chemical synthesis, Iron-Nickel, Porous silicon.

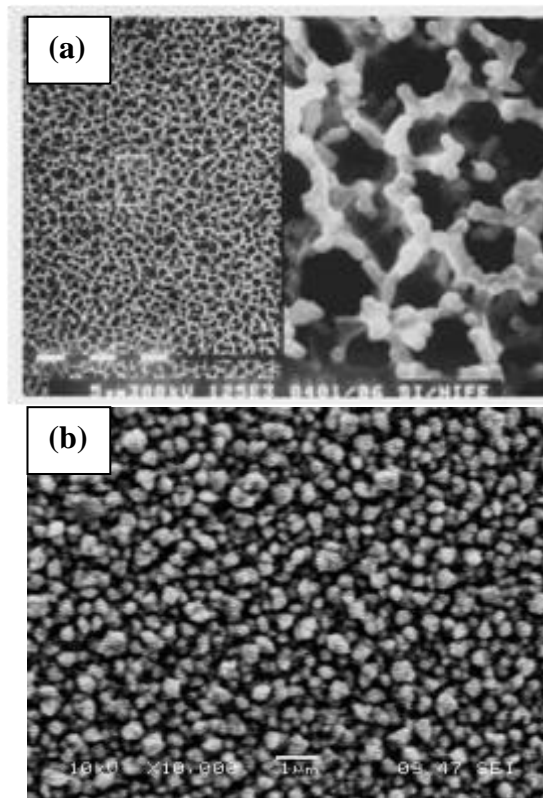


**Figure 1:** Figure illustrating Plan view SEM images after deposition of a FeNi film on macro porous Si substrate(a) and mesoporous Si (b).

## References:

1. F. Ronkel, J. W. Schultze and R. Arens Fisher, *Thin Solid Films*, 276, 40 (1996).
2. C. Renaux, V. Scheuren and D. Flandre, *Microelectron. Reliab.* 40,877 (2000).
3. F. Hamadache, J.- L. Duvail, V. Scheuren, L. Pinaux, C. Poleunes, P. Bertrand an M. S. Belkaid *J. Mater. Res.*, Vol. 17, N<sup>o</sup>.5 (2002) 1075.
4. P.Gorostiza, M. A. Kulandainathan, R. Diaz, F. Sanz, P. Allongue and J. R. Morane, *J. Electrochem. Soc.* 147 (2000) 1026.

**Posters Session II:  
NanoBioMedecine / Nanosafety**

# Biodegradable Polymer Nanosheets Incorporated with Nano-Containers as Dressing for Burn Wound Healing

S.A. Kulinich,<sup>1,\*</sup> M.H.Q. bin Ishak,<sup>2</sup> Y. Okamura,<sup>1</sup> S. Iwamori <sup>2</sup>

<sup>1</sup> Tokai University, Institute of Innovative Science and Technology, Hiratsuka, Japan

<sup>2</sup> Tokai University, Department of Mechanical Engineering, Hiratsuka, Japan

## Abstract:

Resently, much attention has been payed to development of highly efficient new dressing materials for burn wounds with faster healing time. As a unique dressing material, nanosheets made from poly L-lactic acid (PLLA) showed numerous attractive properties such as high adhesion and flexibility on skin, biocompatibility, biodegradability and so on. They also demonstrated efficiency *in vivo*, holding gastric incision area and accelerating wound healing, thus showing promise as a good alternative to conventional suture/ligation materials [1].

Microelements such as zinc, iron, copper and magnesium have been reported as essential for wound healing [2]. Therefore, it is believed that incorporating such elements (nanocontainers leaching Zn, Fe, Cu and Mg ions) into PLLA nanosheets will enhance their healing performance as wound dressing, leading to the development of next-generation biomedical materials.

This work deals with PLLA nanosheets (see Figure 1) incorporated with nanoparticles that serve as nanocontainers releasing metal ions. We mainly focused on Zn-containing nanoparticles which were prepared by the laser ablation in liquid method (a convenient and easy-to-use laboratory technique) [3]. PLLA nanosheets were incorporated by ZnCl<sub>2</sub> and ZnO nanoparticles (see Figure 1), and the dynamics of Zn<sup>2+</sup> release into physiological solution at 37 °C was evaluated. As a next step, *in vivo* experiments on animals are planned in order to study how the use of such Zn-incorporated nanosheets influences wound healing.

**Keywords:** wound healing, dressings, burn wound, polymer nanosheets incorporated with nanoparticles, Zn-containing nanoparticles, biomedical marerials.

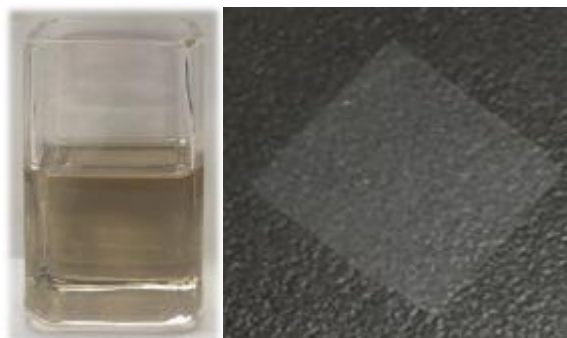


**Figure 1:** Cuvette with colloidal solution of ZnCl<sub>2</sub> nanoparticles prepared via laser ablation in liquid (left) and free-standing PLLA nanosheet incorporated with such nanoparticles (right), floating on water. The nanosheet is about 3x3 cm<sup>2</sup> and about 50 nm thick, which provides superior flexibility and adhesion on any surface.

## References:

1. Okamura, Y., Kabata, K., Kinoshita, M., Saitoh, D., Takeoka, S. (2009), Free-standing biodegradable poly(lactic acid) nanosheet for sealing operations in surgery, *Adv. Mater.*, 21, 4388-4392.
2. Arnold, M., Barbul, A. (2006), Nutrition and wound healing, *Plastic Reconstr. Surg.*, 117, 42s-58s.
3. Zheng, H.B., Du, X.W., Singh, S.C., Kulinich, S.A., Yang, S.K., He, J.P., Cai, W.P. (2012) Nanomaterials via laser ablation /irradiation in liquid: A review, *Adv. Funct. Mater.*, 22, 1333-1353.

# Surface Charge-Switchable Theranostic Nanoparticles Capable of Active Penetration into Deep Tumor Tissues for Photothermal/Chemo Combinational Therapy

H.C. Chiu and W.H. Chiang

National Tsing Hua University, Department of Biomedical Engineering and Environmental Sciences, Hsinchu, Taiwan

## Abstract:

In order to promote antitumor efficacy by the imaging-guided photothermal/chemo combined therapy, a practical approach was developed herein to prepare tumor pH-responsive surface charge-switchable nanoparticles capable of co-delivering a photothermal agent, indocyanine green (ICG), and a chemotherapy drug, doxorubicin (DOX, free base form) for enhanced tumor uptake and penetration. The drug-loaded nanoparticles (NPs) were obtained from the co-assembly of the hydrophobic chemodrug (doxorubicin), the phototherapeutic agent (ICG) and the biodegradable copolymer, poly(lactic-co-glycolic acid) (PLGA), followed by implementing the NP surface with a layer of N-acetyl histidine modified D- $\alpha$ -tocopheryl polyethylene glycol succinate (His-TPGS) via hydrophobic association to improve the colloidal stability both in vitro and in vivo. The obtained NPs in this work exhibits a mean hydrodynamic diameter of ca 50 nm and negatively charged surface in aqueous solution at pH 7.4. Through the small size along with the increase in surface positive charges due to the pH-triggered protonation of histidine residues, the payload-carrying NPs show a rapid accumulation in murine prostate TRAMP-C1 and human breast MCF-7 cancer cells as well as murine macrophage-like RAW 264.7 cells in vitro under weak acidic conditions. This is caused in part by their enhanced attraction with the negatively-charged cell membrane surfaces, due to the increased positive charges on particle surfaces. The in vivo and ex vivo biodistribution studies demonstrated the substantial accumulation of the theranostic nanoparticles in tumor of tumor (Tramp-C1)-bearing mice after intravenous injection. The immunohistochemical examination of tumor sections confirmed the enhanced tumor uptake and penetration of therapeutic nanoparticles decorated with His-TPGS. The prominent imaging-guided photothermal therapy of ICG/DOX-loaded nanoparticles after tumor accumulation induced extensive tumor tissue ablation, which further promoted their extravasation

and DOX permeation, thus effectively suppressing tumor growth.

**Keywords:** tumor accumulation, deep tumor penetration, charge transition, chemotherapy, photothermal therapy, tumor hypoxia.

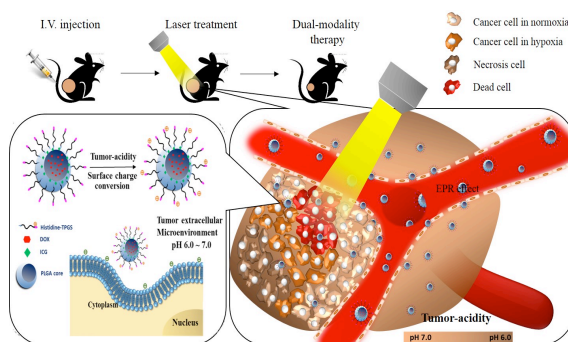


**Figure 1:** Illustration of active tumor penetration and uptake of therapeutics-loaded nanoparticles with tumor environmental pH-triggered surface charge transition for the imaging-guided photothermal/chemo combinational therapy.

## References:

1. Gratton, S. E., Ropp, P. A., Pohlhaus, P. D., Luft, J. C., Madden, V.J., Napier, M. E., DeSimone, J. M. (2008) The effect of particle design on cellular internalization pathways. *Proc. Natl. Acad. Sci. USA.*, 105, 11613-11618.
2. Lee, E. S., Shin, H. J., Na, K., Bae, YH. (2003) Poly(L-histidine)-PEG block copolymer micelles and pH-induced destabilization. *J. Controlled Release.*, 90, 363-374.

# Gel Formulations Containing Chitosan-Silver Sulfadiazine Polymeric Micelles: Preparation, Characterization and *In Vitro* Drug Release Studies

S. Gürçan<sup>1</sup>, M. Arıcı<sup>1</sup>, M.C. Bonferoni<sup>2</sup>, B. Eraç<sup>3</sup>, Ö. Özer<sup>1</sup>

<sup>1</sup>Ege University, Department of Pharmaceutical Technology, Izmir, Turkey

<sup>2</sup>University of Pavia, Department of Drug Sciences, Pavia, Italy

<sup>3</sup>Ege University, Department of Pharmaceutical Microbiology, Izmir, Turkey

## Abstract:

Chitosan (CS) is the second most abundant amino polysaccharide and is estimated to be produced annually almost as much as cellulose (1). Chitosan basically is obtained from waste seafood (prawn/crab shells) after deacetylation process of chitin (2). Silver sulfadiazine (AgSD) has wide antibacterial spectrum as long as using present limitations due to poor solubility and cytotoxicity (3). It has a primary significance to prevent infections (4). Therefore, it has anti-infective effect as a topical formulation (3). Polymeric micelles are generated for its structure and properties of the amphiphilic block copolymers that form stable polymeric micelles, having high loading capacity towards poorly soluble pharmaceuticals (5-6).

In this study, gel formulations containing silver sulfadiazine or chitosan-silver sulfadiazine polymeric micelles were prepared with hydroxypropyl methylcellulose (HPMC) as gelling agent. Formulations were characterized by rheological property, *in vitro* drug release and antibacterial activity studies.

**Keywords:** silver sulfadiazine, chitosan, polymeric micelles, gel formulation, hydroxypropyl methylcellulose (HPMC)

## Preparation of HPMC Gel Formulations

HPMC gel was prepared by solubilization of 4% hydroxypropyl methylcellulose in hot water (70°C). Gel formulations was obtained by adding AgSD or polymeric micelles equivalent to 1% AgSD, into 4% HPMC gel.

## Characterization Studies on HPMC Gel Formulations

AgSD content of HPMC gel formulations was determined by an HPLC system consisting of Thermo Scientific Dionex Ultimate 3000 pump, autosampler (maintained at 25 °C), column oven and UV absorbance detector (set at 254 nm) and a ACE C<sub>18</sub>, 5 µm, 4.6 mm × 250 mm column.

The rheological properties of gel formulations were determined by using rheometer (Haake Mars Thermo Modular System). PP20Ti con

plate was used at 25°C, where the viscosity of the gels was determined under a constant increase in the shear rate. Then, the viscosity was plotted against the shear rate and the rheological properties were evaluated.

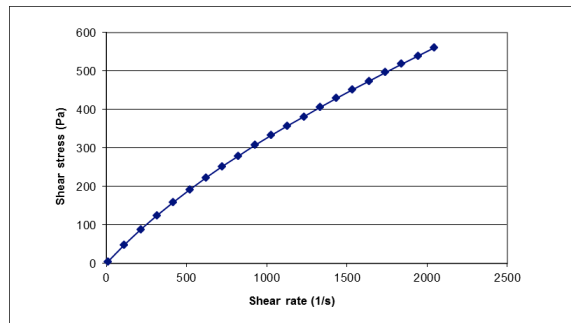
*In vitro* drug release studies were conducted in Franz type diffusion cells with 7 mm diameter range (Logan FDC-6 Transdermal Testing System, Logan Instruments Corp., NJ, USA).

Antibacterial activities of gel formulations were determined by the agar well diffusion method (7). Standard suspensions of *Escherichia coli* ATCC 25923, *Pseudomonas aeruginosa* ATCC 27853 and *Staphylococcus aureus* ATCC 25922 strains were spread on Mueller-Hinton Agar (MHA, Oxoid) plates. Gel formulations were put aseptically into the wells made in the plates and incubated at 35°C for 16-18 h. Inhibition zone diameters formed around the formulations were measured.

## Results

AgSD content of HPMC gel formulations was found between 1.2-1.7%.

The flow curves of different HPMC gels showed non-Newtonian flow behaviour (Figure 1-4). When gel formulations compared to each other, while plain gel was showing pseudoplastic flow the other one showed plastic flow behaviour.



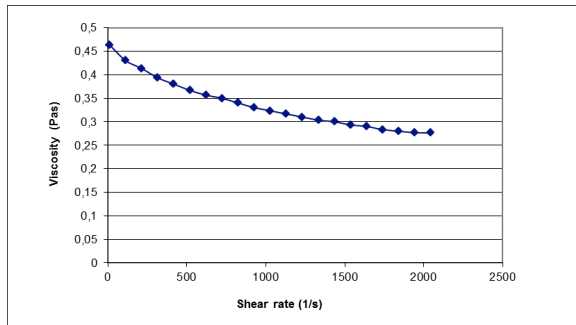


**Figure 2:** Viscosity vs. shear rate curve of plain gel formulation.

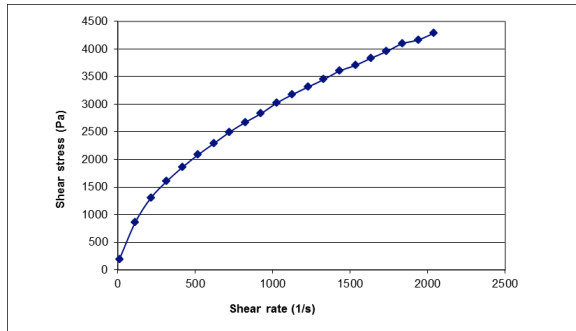


**Figure 3:** Shear stress vs. shear rate curve of gel formulation with polymeric micelles.

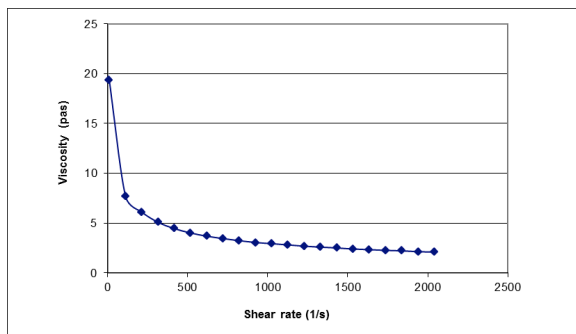


**Figure 4:** Viscosity vs. shear rate curve of gel formulation with polymeric micelles.

- Drug release of gel formulations with polymeric micelles was obtained slower than plain gel formulation. It has shown that polymeric micelles structure has a considerable effect on AgSD release (Figure 5).

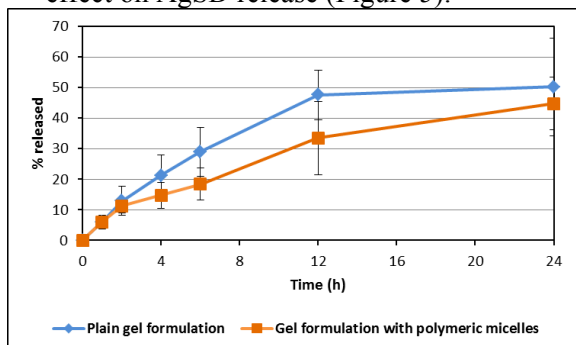


**Figure 5:** *In vitro* silver sulfadiazine release profiles from gel formulations.

- In accordance with drug release studies, antibacterial effect obtained by gel formulation with polymeric micelles was lower than plain gel formulation (Figure 6).

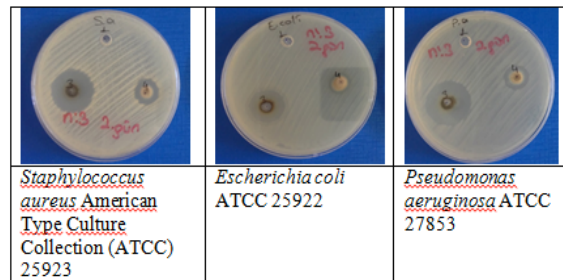


**Figure 6:** Inhibition zone diameters of 4% HPMC gel (1), plain gel formulation (3) and gel formulation with polymeric micelles (4) against *Staphylococcus aureus* American Type Culture Collection (ATCC) 25923, *Escherichia coli* ATCC 25922 and *Pseudomonas aeruginosa* ATCC 27853 standard strains.

### Conclusion

HPMC based silver sulfadiazine gel formulations were prepared successfully with chitosan polymeric micelles.

### References:

1. Özcan İ, Şenyiğit T, Gökçe EH, Özer Ö. Current Status of Chitosan on Dermal/Transdermal Drug Delivery Systems. New York, USA: Nova Science Publishers Inc.; 2010.
2. Demir A, Seventekin N. Kitin, Kitosan ve Genel Kullanım Alanları. Tekstil Teknolojileri Elektronik Dergisi 2009;3(2):92-103.
3. Üstünes L, Ed. RxMediaPharma İnteraktif İlaç Bilgi Kaynağı, İzmir, GEMAŞ, 2016.
4. Dellera E, Bonferoni MC, Sandri G, Rossi S, Ferrari F, Del Fante C et al.. Development of chitosan oleate ionic micelles loaded with silver sulphadiazine to be associated with platelet lysate for application in wound healing. Eur J Pharm Biopharm 2014;88(3):643-50.
5. Sezgin Z, Yüksel N, Baykara T. Preparation and characterization of polymeric micelles as drug carrier system. J Fac Pharm Ankara 2003;32(2):125-142.
6. Gürcan S, Arıcı M, Bonferoni MC, Özer Ö. Chitosan-Silver Sulfadiazine Polymeric Micelles: Preparation and Characterization Studies. 18<sup>th</sup> International Pharmaceutical Technology Symposium (IPTS), Antalya, Turkey, 18-21 Sep 2016, pp. 253-256.
7. Rençber S, Karavana SY, Şenyiğit ZA, Eraç B, Limoncu MH, Baloğlu E. Mucoadhesive in situ gel formulation for vaginal delivery of clotrimazole: formulation, preparation, and in vitro/in vivo evaluation. Pharm Dev Technol. 2016 Apr 7:1-11.

### Acknowledgments

This present study was supported by Ege University Research Foundation (15/ECZ/009). The authors would like to thank The Pharmaceutical Sciences Research Centre (FABAL) of Ege University, Faculty of Pharmacy for equipmental support and some analysis.

# DNA and proteins binding and dispersion activities of titanium dioxide and cerium dioxide nanoparticles

P. Łabuz,<sup>1</sup> W. Macyk,<sup>1</sup> G. Stochel<sup>1</sup>

<sup>1</sup>Jagiellonian University, Department of Inorganic Chemistry, Kraków, Poland

## Abstract:

Over the years colloidal semiconductor nanoparticles have attracted considerable attention owing to their unique size-dependent optical and electronic

properties. Lately, a new direction has emerged in potential biotechnological applications such as luminescence tagging, immunoassay, drug delivery and cellular imaging. Their photoactivity is also the reason for considering them as photo-drugs.

A wide range of biological and biochemical effects of nanomaterials might be resulted from the direct or indirect interaction with biological targets such as DNA or proteins. Nanoparticles have the ability to bind and interact with biological matter changing the surface characteristics depending on the environment they are present, resulting in an increased concern over its potential effect on human body. Thus the characterization of nanoparticles in contact with the biological systems becomes even more complex. Little is known about evidence for interaction of nanocrystalline oxides such as TiO<sub>2</sub> or CeO<sub>2</sub> with its targets *in vivo* and particularly the their effect on the DNA structure and cell apoptosis *in vivo*. In addition, when irradiated by light of appropriate energy, the semiconductor nanoparticles are known to be source of reactive oxygen species i. e. hydroxyl radical, superoxide, etc. This study presents the results of investigation of various interactions between nanoparticles and biomolecules, including binding of nanoparticles to DNA and proteins, their effects on structure and integrity of biomolecules both in the dark and under irradiation.

The financial support from the SONATA program 'Mechanisms of toxicity and phototoxicity of photoactive oxide nanomaterials' awarded by the National Science Centre is gratefully acknowledged (2016/21/D/NZ7/00611)

# DNA-binding drug screening by novel palladium nano thinfilm electrodes

Chia-Yu Chang<sup>1</sup>, Wei Chen<sup>1</sup>, Chien-Hao Su<sup>2</sup>, Guo-Cheng Hsu<sup>2</sup>, Chia-Ching Chang<sup>1,3\*</sup>

<sup>1</sup>Department of Biological Science and Technology, National Chiao Tung University, Hsinchu, Taiwan, R.O.C.

<sup>2</sup>Cheeshin Technology Co, Jhunan, Taiwan, R. O. C.

<sup>3</sup>Institute of Physics, Academia Sinica, Nankang, Taipei, Taiwan, R. O. C.

\*: Corresponding author: Chia-Ching Chang, E-mail: ccchang01@faculty.nctu.edu.tw

## Abstract:

Electrochemical spectroscopy is provided the method to detect the bio-molecular interaction sensitively and selectively. Although the Gold electrode has the excellent charge transfer property that has been widely used in electrochemical analysis. But, the cost of such gold electrode is high. Moreover, it spends a lot of time and it is complicated to regenerate active gold electrode. Of this reason, a ready-to-use electrode is highly desired for electrochemical analysis. In our study, we were successful to develop a novel nanocrystalline thin film palladium (Pd) film electrode which is deposited on flexible polyethylene terephthalate (PET) by sputtering.

Recently, we used the novel nanocrystalline palladium (Pd) film electrode to detect the interaction between DNA and small molecule interaction. This technique using electrochemistry impedance spectroscopy (EIS) to detect drugs and DNA interaction are both usability and sensitivity increased.

As a result, we demonstrated a Pd nano-thin film electrode was used in anticancer drugs and DNA interaction detection. And the sensitivity is as sensitive as sub nano-gram level. The nanocrystalline palladium (Pd) film electrode has the potential in DNA binding drug screening.

**Keywords:** Electrochemical spectroscopy, Nano crystalline electrode, DNA structure, Impedance, DNA-drug interaction.

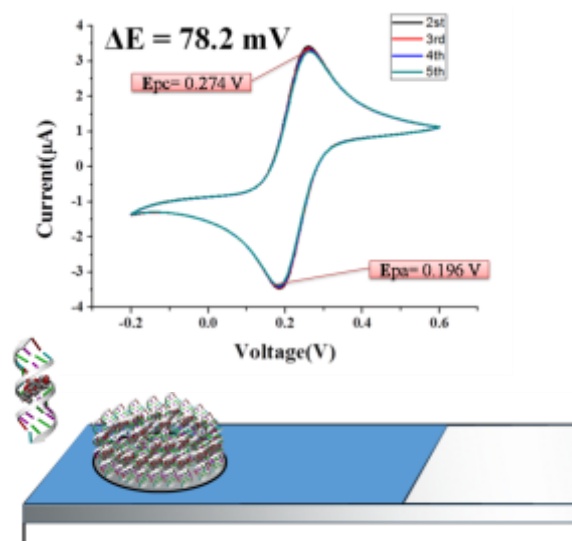


**Figure 1:** Figure illustrating the cyclic voltammogram profile of bare Pd nano thin film electrode (upper panel) and the structure of Pd nano thin film electrode with drug bound DNA SAM (lower panel). The performance of bare Pd nano thin film is as good as conventional gold electrodes. The sensitivity of our Pd thin film electrode is as sensitive as sub nano-gram level.  $E_{pa}$  is the potential of oxidation stage,  $E_{pc}$  is the potential of reduction stage of  $\text{Fe}(\text{CN})_6^{3+/4+}$  electrolyte. The inset in left denoted the drug-DNA complex. The gray area is Pd thin film with the thickness around 20 nm. The substrate below the Pd film is plastic polymer. The blue area on the electrode is insulating layer.

# *Echinococcus granulosus* antigens encapsulation for the development of a nanovaccine.

C. Silvarrey<sup>1</sup>, U. Benavides<sup>2</sup>, E. Almouazen<sup>3</sup>, S. Briañon<sup>3</sup>, A. Esteves<sup>1</sup>.

<sup>1</sup> Republic University of Uruguay, Faculty of Science, Montevideo, Uruguay

<sup>2</sup> Republic University of Uruguay, Faculty of Veterinary, Montevideo, Uruguay

<sup>3</sup> Claude Bernard University Lyon 1, Faculty of Pharmacie and Medicine, Lyon, France

## Abstract:

Cystic echinococcosis caused by the flatworm parasite *Echinococcus granulosus*, is a serious health and economic problem in several countries, including Uruguay, Argentina, Chile, Perú and Brasil. This disease affects both humans and livestock. Diagnosis of the disease is performed using imaging and immunological techniques. However, once the hydatid cyst is detected the most effective treatment is surgery, with the risk of rupture of the cyst and larvae reseeding. An effective way to eliminate this disease is through the development of vaccines to prevent infection in the definitive host, the dog. This approach is less expensive and more effective than a vaccine designed for intermediate host (sheep and cattle). It is possible to achieve high levels of complex and reliable protection against metazoan parasites using recombinant antigens. We have selected EgVAL1 and EgVAL2 proteins belonging to the CAP superfamily of proteins. Promising results have been obtained using nematodes proteins of this superfamily as vaccine candidates. EgVALs were encapsulated in polylactic acid nanoparticles coated with chitosan by the double emulsion with solvent evaporation method, obtaining the adequate parameters (Fig.1). In addition, the encapsulated antigens were well preserved when submitted to gastrointestinal conditions. Using nanoparticulate system offers a great possibility to enhance antigen delivery to intestinal presenting cells and hence the immune protection against *Echinococcus granulosus*. Future trials are needed to assess the effectiveness of these antigens in generating a vaccine to be administered orally to dogs.

**Keywords:** Hydatid disease, recombinant protein, encapsulation, double emulsion method, polymeric nanoparticles, vaccine, nanomedicine, mucosal immunity.

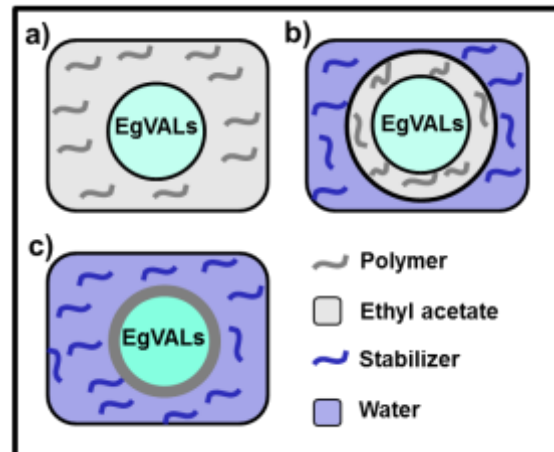


**Figure 1:** EgVALs encapsulation in polymeric nanoparticles by double emulsion with solvent evaporation method. a) and b) sequential emulsions, c) ethyl acetate evaporation.

## References:

1. des Rieux A, Fievez V, Garinot M, Schneider YJ, Pr at V. Nanoparticles as potential oral delivery systems of proteins and vaccines: a mechanistic approach. *J Control Release*. 2006 Nov;116(1):1-27.
2. Silvarrey MC, Echeverr a S, Cost bile A, Castillo E, Paulino M, Esteves A. Identification of novel CAP superfamily protein members of *Echinococcus granulosus* protoscoleces. *Acta Trop*. 2016 Jun;158:59-67.
3. Zhao, L., Seth, A., Wibowo, N., Zhao, C.-X., Mitter, N., Yu, C., Middelberg, A.P.J., Nanoparticle vaccines. *Vaccine*, 2014. 32, 327–337.

# Real-time investigation of nanoparticle circulation in bloodstream of living animals using magnetometry

I.V. Zelepukin,<sup>1,2\*</sup> M.P. Nikitin,<sup>1,2,3\*</sup> P.I. Nikitin,<sup>3</sup> Deyev S.M.<sup>1</sup>

<sup>1</sup> Shemyakin-Ovchinnikov Institute of Bioorganic Chemistry RAS, Moscow, Russia

<sup>2</sup> Moscow Institute of Physics and Technology (State University), Dolgoprudny, Russia

<sup>3</sup> Prokhorov General Physics Institute RAS, GPI RAS, Moscow, Russia

## Abstract:

Nanoparticles (NP) are promising vehicles for drug delivery because of their capacity to transport considerable amounts of drugs, possibility for active targeting, etc. Nevertheless, many types of nanocarriers show rather limited efficiency *in vivo* due to rapid elimination by macrophages of the mononuclear phagocytic system after intravenous administration [1]. Here, we report thorough investigation of factors, which affect NP blood circulation dynamics and other pharmacokinetic properties.

In this study, for registering nanoparticle blood circulation dynamics, we used highly sensitive magnetic particle quantification (MPQ) technique [2,3], which offers convenient and accurate non-invasive detection of magnetic nanoparticles in real time *in vivo*. The method is based on non-linear magnetization of magnetic materials in the ac field generated at two frequencies and measuring the response at the combinatorial frequency.

We have investigated the circulation parameters for many types of magnetic nanoparticles with different sizes, shape, coatings, as well as for many particle administration parameters such as doses, etc. For the majority of particles, their circulation can be fitted by the monoexponential dependence (see example in Fig. 1). We have found that reducing size and increasing dose of the injected particles significantly prolongs their circulation in blood. Moreover, we investigated the influence of two types of nanoparticles on each other's pharmacokinetics when they are injected in series or in parallel.

The developed methodology along with the obtained results is attractive for rational design of drug nanocarriers and other *in vivo* applications of nanoparticles.

**Keywords:** nanoparticles, pharmacokinetics, blood circulation, magnetic detection, drug delivery vehicles.

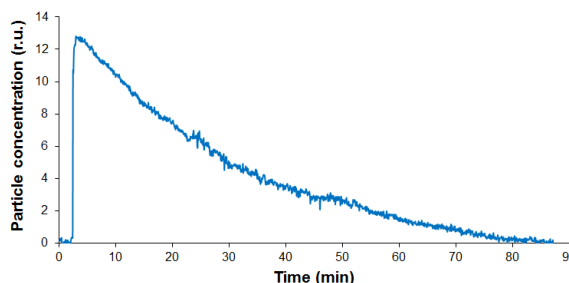


**Figure 1:** The standart behavior of NP circulation in blood measured with the MPQ method. Arrow shows moment of nanoparticle administration.

## References:

1. Yoo, J. W., Chambers, E., & Mitragotri, S. (2010), Factors that control the circulation time of nanoparticles in blood: challenges, solutions and future prospects. *Curr. Pharm. Des.*, 16(21), 2298-2307
2. Nikitin, P. I. & Vetoshko, P. M. Meter of magnetic susceptibility. Russian patent no. RU2177611 (2000).
3. Nikitin, M.P., Vetoshko, P.M., Brusentsov, N.A., Nikitin, P.I. (2009), Highly sensitive room-temperature method of non-invasive *in vivo* detection of magnetic nanoparticles, *J. Magn. Magn. Mater.*, 321, 1658-1661.

# Therapeutic Potential of A Cell Penetrating Peptide (CPP, NP1) Mediated siRNA Delivery: Evidence in 3D Spheroids of Colon Cancer Cells

K. Al-Husaini, X. Han, A. Elkamel, P. Chen\*

Department of Chemical Engineering and Waterloo Institute for Nanotechnology, University of Waterloo, Waterloo, Ontario, Canada

## Abstract:

At the forefront of revolutionizing medicine, RNA interference (RNAi) holds great potential as a therapeutic route. Since the most preclinical drug screening *in vitro* was carried out in a monolayer cell culture, it is not physiologically relevant to the *in vivo* conditions, where three-dimensional tissues are the objects. Thus, development of more biologically relevant models for early drug screening is greatly needed. Here, the aim of the present study was to develop 3D spheroids and evaluate effectiveness of NP1, a novel CPP (STR-H16R8) developed in our group, to deliver anticancer siRNAs. 3D spheroid of human colon cancer cells- HCT 116 cells was generated and its morphology was characterized. It revealed that the cells can form compact spheroid within 3 days with three distinct layers of proliferating, dormant and necrotic cells. As well, spheroid showed large cohesive cells with apparent epithelial phenotype and large atypical nuclei with occasional prominent nucleoli, which closely mimic the features of tumors *in vivo*. Furthermore, NP1 in complex with siRNA elicited a high cellular uptake of siRNA in both 2D and 3D cell culture followed by potent knockdown efficiencies of Bcl-2- and VEGF-1a- siRNA with 53% and 51% of reductions in Bcl-2 and VEGF-1a mRNA expressions respectively. In addition, 3D spheroids demonstrated apoptosis resistance compared to 2D cells. Taken together, 3D spheroids provide an improved model for testing siRNA delivery *in vitro*, NP1 as a siRNA carrier can effectively protect and deliver siRNAs and maintain high silencing efficiency.

**Keywords:** 3D spheroids, Bcl-2-siRNA, VEGF-1a-siRNA, cell penetrating peptide, cellular uptake, knockdown efficiency, apoptosis.

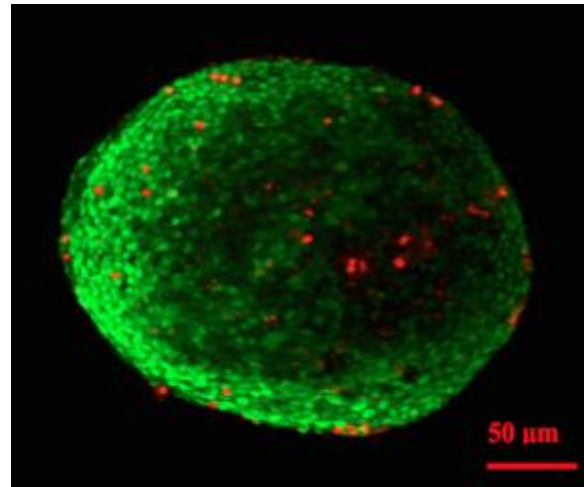


**Figure 1:** Figure 1 displaying zonal characteristics of 3D cell biology under confocal laser microscope. Spheroid was stained with dyes (calcein AM and ethidium homodimer (EthD-1)) to detect live and dead cells (live/dead assay). It shows clearly that cells within the spheroids are divided into three distinct layers namely the outer rim of live and proliferative cells emitting green fluorescence, the middle layer of cells not emitting any fluorescence, known as quiescent cells and the inner center cells emitting red fluorescence, known as necrotic core.

## References:

1. Ambesajir, A., Kaushik, A., Kaushik, J. J. & Petros, S. T. RNA interference: A futuristic tool and its therapeutic applications. *Saudi J Biol Sci* **19**, 395–403 (2012).
2. Haycock, J. W. 3D cell culture: a review of current approaches and techniques. *Methods Mol. Biol.* **695**, 1–15 (2011).

# Photodynamic Inactivation of *Plasmodium falciparum* from erythrocytes by Photo-induced Reactive Oxygen Species

K. K. Wang,\* Y. R. Kim

Yonsei University, Department of Chemistry, Seoul, Rep. of Korea

## Abstract:

Malaria is a mosquito-borne disease caused by *Plasmodium malariae*, which annually induces 800,000 deaths worldwide. Malaria epidemics is mediated by the *Plasmodium*-infected mosquitoes where malaria protozoans parasitize in erythrocytes and reproduce through self-replication. Malignant malaria, *P. falciparum*, shows lack of persistent immune response when it is infected to human. Various antimalarial drugs of quinolones and anti folates have been developed for the treatments. Also, recently, a few researchers showed that photodynamic therapy could be used for the treatment of various tropical diseases including malaria.

In this study, we investigated the antimalarial effect of photodynamic inactivation (PDI) coupled with magnetic nanoparticles (MNPs) as a potential strategy to combat the emergence of drug-resistant malaria and resurgence of malaria after treatment. Because the malarial parasite proliferates within erythrocytes, PDI agents need to be taken up by erythrocytes to eradicate the parasite. We used photofunctional MNPs as the PDI agent because nanosized particles were selectively taken up by *Plasmodium*-infected erythrocytes and remained within the intracellular space due to the enhanced permeability and retention effect. Photofunctionality was provided by a photosensitizer (PS), which generates reactive oxygen species (ROS) under irradiation. PSs were covalently bonded to the surface of the MNPs. The morphology and structural characteristics of the MNPs were investigated by scanning electron microscopy and X-ray diffraction (XRD). And the photophysical properties of the PFNs were studied with various spectroscopic method. Generation of singlet oxygen, one of the ROS, was directly confirmed with time-resolved phosphorescence spectroscopy. In order to evaluate the ability of PFNs to kill malarial parasites, the PDI effect of PFNs was evaluated within the infected erythrocytes. Furthermore, malarial parasites were completely eradicated from the erythrocytes after PDI treatment using PFNs on the basis of an 8 day erythrocyte culture test.

**Keywords:** singlet oxygen, magnetic nanoparticles, eradication, plasmodium malaria, photodynamic inactivation

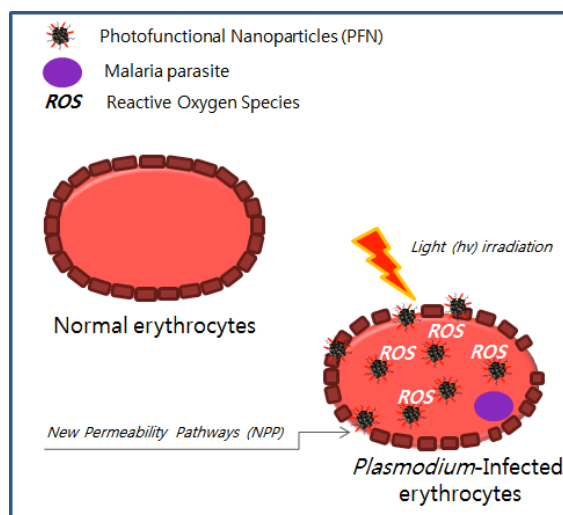


**Figure 1:** Schematic of photodynamic inactivation of *Plasmodium falciparum* in erythrocytes by Photofunctional nanoparticles

## References:

1. LeBlanc, D., Story, R., Gross, E. (2012) Laser-Induced Inactivation of Plasmodium Falciparum. *Malar. J.*, 11, 1-7.
2. Zhao, X. J., Lustigman, S., Kenney, M. E., BenHur, E. (1997) Structure-Activity and Mechanism Studies on Silicon Phthalocyanines with Plasmodium Falciparum in the Dark and under Red Light. *Photochem. Photobiol.*, 66, 282-287.

# Nanoparticles for bioseparation and detection with application in cell electroporation

Oana Nedelcu,<sup>1,\*</sup> Otilia Cinteza,<sup>2</sup> Dana Stan,<sup>3</sup> Mona Mihailescu<sup>4</sup>,  
Bogdan Bită<sup>1</sup>, Eugenia Vasile<sup>4</sup>, Roxana Radu,<sup>5</sup>

<sup>1</sup> National Institute for Research and Development - IMT Bucharest, Romania

<sup>2</sup> Faculty of Chemistry, University of Bucharest, Romania

<sup>3</sup> SC DDS Diagnostic SRL, Romania

<sup>4</sup> Faculty of Applied Sciences, University Politehnica of Bucharest, Romania

<sup>5</sup> SC Spital LOTUS SRL, Ploiesti, Romania

## Abstract:

The advances in nanoparticles synthesis and functionalization led to a large area of biomedical applications as labelling, targeting drug carriers, thermoablation or magnetic resonance imaging [1]. The diagnostic devices for cells analysis that use electroporation to permeabilize cell membrane for transfection or lysis can benefit from physical properties of magnetic nanoparticles through cell labelling for detection and improved sensing based on modified electrical system parameters. In this work we investigated the properties of nanoparticles related to their influence on cell separation by dielectrophoresis (DEP) and contribution to electric properties of labelled cells that can improve the selective manipulation of electroporated and unaffected biological samples in a micro-electro-fluidic system. The system integrates a fluidic component with microchannels and inlet/outlet chambers and an electric part with microelectrodes aligned to flow path. The cells in buffer are separated in the region of high electric field by positive DEP and subjected to high field pulses to induce membrane permeabilization; they are further transported through two exit channels by separating the unaffected and electroporated cells using frequency that induces opposite (positive/negative) mobility. Cell labelling using magnetic nanoparticles modifies their DEP mobility via conductivity and permittivity as illustrated in figure 1 for cervical cells and it allows selective and more precise handling and separation. Fe<sub>3</sub>O<sub>4</sub> nanoparticles were synthesized by co-precipitation procedure [2] modified in our laboratory, coated with gold to obtain “raspberry-like” nanoparticles, and functionalized with specific cellular antibodies for cells caption and detection. The nanoparticles were investigated by microphysical characterization techniques as SEM (Figure 2), TEM, XRD, FTIR and UV-VIS spectroscopy.

**Keywords:** magnetic nanoparticles, cell labelling, dielectrophoretic separation, cell electroporation.

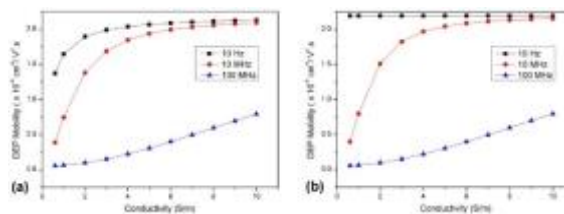


**Figure 1:** Variation of DEP mobility as function of labelled cell conductivity at low and high frequency for two values of buffer conductivity.

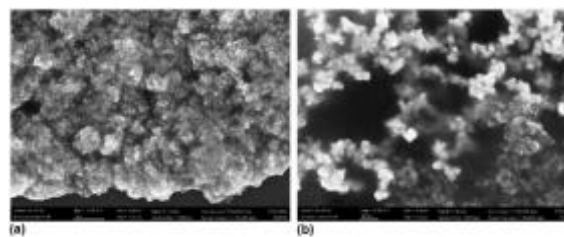


**Figure 2:** SEM Images of nanoparticles: (a) Fe<sub>3</sub>O<sub>4</sub>; (b) Fe<sub>3</sub>O<sub>4</sub>@Au

**Acknowledgements:** This work was supported by PN-II-PT-PCCA National Programme, Contract no. 30/2014.

## References:

1. Hao, R., Xing, R., Xu, Z., Hou, Y.,\* Gao, S., and Sun, S., (2010), Synthesis, Functionalization, and Biomedical Applications of Multifunctional Magnetic Nanoparticles, *Adv. Mater.*, 22, 2729-2742.
2. Dassler, K., Roohi, Lohrke, J., Ide, A., Schuetz, G., Dassler, K., (2012), Studying the effect of particle size and coating type on the blood kinetics of superparamagnetic iron oxide nanoparticles, *Int J Nanomedicine.*, 7, 4447-4458.

# Capsular- and Planar-Scaffold for Clustering and Oriented Immobilization of Sensing Molecules

M. Iijima,<sup>1,\*</sup> S. Kuroda,<sup>1</sup>

<sup>1</sup>Osaka University, The Institute of Scientific and Industrial Research (ISIR-Sanken), Osaka, Japan

## Abstract:

For increasing the sensitivity and analyte-binding capacity of biosensors, sensing molecules (*e.g.*, IgGs, receptors) on solid phase should be clustered and fixed in an oriented immobilization manner<sup>1</sup>. Here, we present a novel ~30-nm scaffold ZZ-bionanocapsule (ZZ-BNC; Figure 1A), consisting of hepatitis B virus envelope L protein fused with the protein A-derived IgG Fc-binding Z domains (ZZ-L protein), that serves for both clustering and oriented immobilization of Fc-containing sensing molecules<sup>1-4</sup>.

In QCM and SPR equipped with IgGs or Fc-fused receptors as immobilized sensing molecules, ZZ-BNC could adsorb onto the gold surface of sensor chips firmly, and thereby markedly enhance the sensitivity, analyte-binding capacity, and affinity of sensors<sup>2,3</sup>. High-speed atomic force microscopy (HS-AFM) of the sensors revealed that IgGs underwent rotational Brownian motion on ZZ-BNCs with the Fc region serving as the supporting point<sup>4</sup>. Furthermore, we succeeded in the disassembly of ZZ-BNC to ZZ-L micelles by surfactants. By mixing with liposomes on biosensor surface, they could transform into planar ZZ-L membrane spontaneously, allowing us to control the density of ZZ-L proteins. The planar ZZ-L membrane is more applicable to various biosensors than capsular ZZ-BNC for enhancing the sensitivity and analyte-binding capacity (unpublished).

**Keywords:** bio-nanocapsules, scaffolds, clustering, oriented immobilization, sensing molecules, biosensor surface.

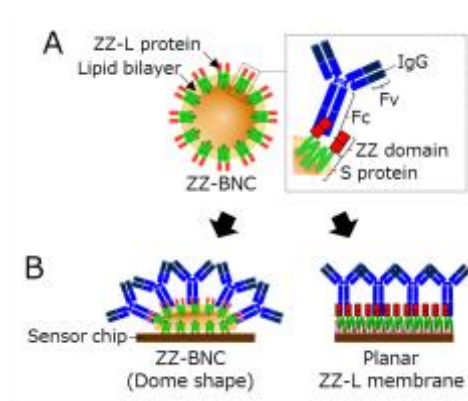


**Figure 1:** (A) Structure of ZZ-BNC. (B) ZZ-BNC- and planar ZZ-L membrane-scaffold for clustering and oriented immobilization of sensing molecules on biosensor surfaces.

## References:

1. Iijima, M., Kuroda, S. (2017) Scaffolds for oriented and close-packed immobilization of immunoglobulins, *Biosens. Bioelectron.*, 89, 810-821.
2. Iijima, M., Kadoya, H., Hatahira, S., Hiramatsu, S., Jung, G., Martin, A., Quinn, J., Jeong, S.Y., Choi, E.K., Arakawa, T., Hinako, F., Kusunoki, M., Yoshimoto, N., Niimi, T., Tanizawa, K., Kuroda, S. (2011) Nanocapsules incorporating IgG Fc-binding domain derived from *Staphylococcus aureus* protein-A for displaying IgGs on immunosensor chips, *Biomaterials*, 32, 1455-1464.
3. Iijima, M., Yoshimoto, N., Niimi, T., Maturana, A.D., Kuroda, S. (2016) Bio-nanocapsule-based scaffold improves the sensitivity and ligand-binding capacity of mammalian receptors on the sensor chip, *Biotechnol. J.*, 11, 805-813.
4. Iijima, M., Somiya, M., Yoshimoto, N., Niimi, T., Kuroda, S. (2012) Nano-visualization of oriented-immobilized IgGs on immunosensors by high-speed atomic force microscopy, *Sci. Rep.*, 2, 790.

# Nano Composite Chiral Hydrogel For Cell-Cell Separation

Andisheh Motealleh, Nermin Seda Kehr

Physikalisches Institut and CeNTech, Universität Münster, Münster (Germany)

## Abstract:

The chemical functionalization of nanomaterials with bioactive molecules have been used as an effective tool to mimic extracellular matrix and study the cell material interaction in tissue engineering [1]. In this respect, periodic mesoporous organosilica (PMO) nanoparticles were functionalized with different enantiomers D(L)-penicillamine (PEN) and a D(L)-mannose derivative (MAN) embedded in a 3 Dimensional (3D) alginate (Alg) hydrogel to control the affinity of cells to the hydrogel surfaces, and enrich one cell type from a mixture of healthy and cancerogenous ones (Fibroblast [F] and Colo 818 [C]). The results showed that the affinity of cells to the respective hydrogel scaffolds affected by the enantiomers was more pronounced in D(L)-PEN-Alg and F cells could enrich 3 times more than C cells (Fig.1). This new advanced nanocomposite hydrogel can be utilized in drug delivery system, cell-cell separation and especially in cancer therapy.

**Keywords:** nanomaterials, periodic mesoporous organosilica (PMO), enantiomers, nanocomposite hydrogel, cell-cell separation, healthy and cancerogenous cell.

## References:

1. N. S. Kehr, Enantiomorphous, Biomacromolecules. 17(3), 1117 (2016)

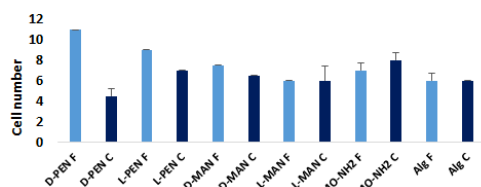
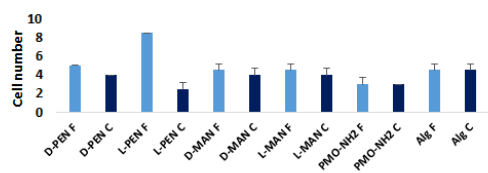


**Figure 1:** Fig.1 Quantitative numbers of live ( $10^3$ ) F and C cells in D-PEN, L-PEN, D-MAN, L-MAN, PMO-NH2 Alginate scaffold and just alginate hydrogel after 1 day and 3 days incubation (at  $37^\circ\text{C}$ ).

# Studying the effects of pattern size and protein type on *staphylococcus aureus* adhesion

H. Khateb,<sup>1</sup> D. Sutherland,<sup>2</sup>

<sup>1,2</sup>Aarhus University, Interdisciplinary Nano Centre, Aarhus, Denmark

## Abstract:

The effects pattern size on bacteria adhesion, spreading, and focal adhesion development are studied.

Fibronectin patterns from 0.1 to 1 $\mu$ m produced by colloidal lithography reveal important differences in how cells adhere to and bridge focal adhesions across protein nanopatterns versus micropatterns. The differences in patterns size are implicated as important factors in bacterial adhesion development.

**Keywords:** Protein patterns, cell adhesion, fibronectin

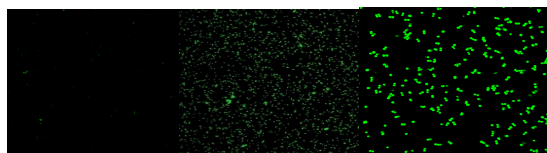


**Figure 1:** Confocal Laser Microscopy 20 $\times$  image of the *Staphylococcus aureus* adhesion and colonization on (100,300,800) Sio<sub>2</sub> nano-holes.

## References:

1. Malmstrom, J.; Kristensen, S.; and Sutherland, D. *Nano Lett.* 2011, 11, 2264–2271.

# New Design on Denim Garment with the Synthesis of Nano-copper

D. Zarbaf<sup>1</sup>, M. Montazer<sup>2</sup>, A. Sadeghian Maryan<sup>3</sup>

<sup>1</sup>Islamic Azad University, South Tehran Branch, Department of Textile Engineering, Tehran, Iran

<sup>2</sup>Amirkabir University of Technology, Department of Textile Engineering, Tehran, Iran

<sup>3</sup>Islamic Azad University, Ardabil Branch, Department of Chemistry, Ardabil, Iran

## Abstract:

In this study, a variety of denim color shades was achieved along with antibacterial properties in a single step process. On site synthesis of nano-copper was carried out by chemical reduction method of copper(II) sulfate with the presence and absence of glucose acting as a reducing agent resulting in the two forms of copper(II) and copper(I) oxides with different colors and effects on denim garment. Copper nanoparticles were characterized by UV-visible spectrometer of the remaining solution after the treatment. The antibacterial properties of the treated denim samples showed significant growth reduction in *E. coli* and *S. aureus* bacteria. XRD and EDX analyses of the treated denim garment confirmed the synthesis of copper(II) and copper(I) oxides on the fabric. Also, the particle shape, size and distribution of nano-copper was observed by SEM and MAPPING analysis (Figure 1).

**Keywords:** Nano-copper, Antibacterial, Denim Garment, Denim design, Color changes

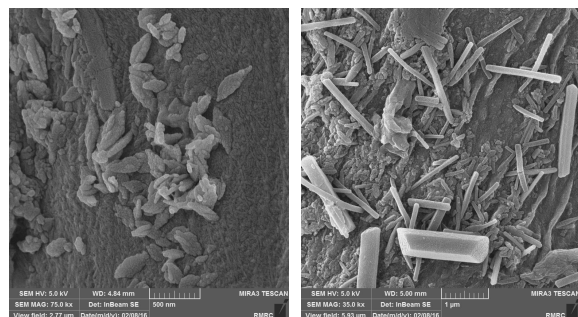


**Figure 1:** SEM images of the synthesized copper nanoparticles on denim garment (a) copper(II) oxide and (b) copper(I) oxide

## References:

1. Paul, R., (2015) Denim: Manufacturing, Finishing and Applications, Elsevier Science, 1-11
2. Perelshtein, R., Lipovsky, A., Perkas, N., Gedanken, A., Moschini, E., Mantecca, P., (2015) The influence of the crystalline na-

ture on nano-metal oxides on their antibacterial and toxicity properties, Nano Research, 34:695-707

3. Sedighi, A., Montazer, M., (2016) Tunable shaped N-doped CuO nanoparticles on cotton fabric through processing conditions: synthesis, antibacterial behavior and mechanical properties, Cellulose, 23:2229-2243

# Microscale Thermophoresis to Diagnose alpha1-Antitrypsin Deficiency Disorder in Plasma

E.V. Edeleva<sup>1,3</sup>, T. Dau<sup>2</sup>, A.I.S. Seidel<sup>1</sup>, D. Jenne<sup>2</sup>, and D. Braun<sup>1,3</sup>

<sup>1</sup> Systems Biophysics, Ludwig Maximilians University München, Amalienstrasse 54, 80799 Munich, Germany

<sup>2</sup> Comprehensive Pneumology Center, Ludwig Maximilians University, and Helmholtz Zentrum München, Max-Lebsche-Platz 31, 81377 Munich, Germany

<sup>3</sup> Graduate School of Quantitative Biosciences (QBM), Ludwig-Maximilians-University, Feodor-Lynenstraße 25, 81377 Munich, Germany

## Abstract:

Conventional diagnostics of deficiency disorders is often limited to the measurement of concentration, not the affinity of the deficient component. In case of alpha1-antitrypsin (AAT) deficiency disorder, AAT plasma level is low in patients due to the genetic mutation. However, measured concentration of AAT does not correlate with the manifestation of symptoms. We hypothesized that its affinity to its target neutrophil elastase is different in plasma of different patients.

We developed a competition assay based on the physical phenomenon of thermophoresis [1]. Our assay assesses the affinity of AAT in addition to its concentration. The measurement is performed directly in the natural milieu of blood plasma. The three-body binding problem is used to fit the experimental data.

The amplitude of thermophoresis correlates with symptoms manifestation in patients (Figure 1). Further measurements suggest a previously unknown component in plasma, capable of modulating the affinity of AAT to the target. Our work highlights the possibility of assay development in the natural environment of blood plasma with thermophoresis with the promise to significantly improve the management of AAT deficiency.

**Keywords:** protein binding assays, blood plasma, microscale thermophoresis.

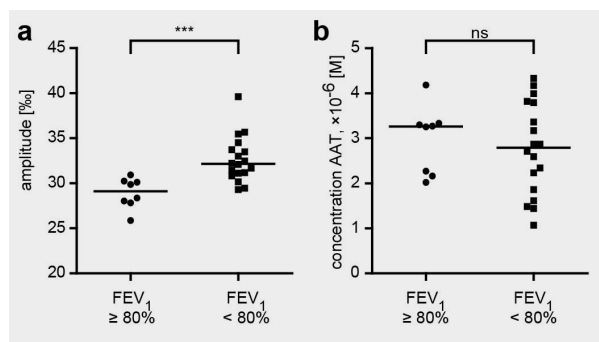


**Figure 1:** The novel assay we developed allows us to measure a parameter that is sensitive to both concentration and affinity of the analyzed molecule in blood plasma. We called this parameter an amplitude. The amplitude (a) correlates with symptoms manifestation better than concentration alone (b). FEV<sub>1</sub> – forced expiratory volume in 1 second. \*\*\* -  $p < 0.001$ .

## References:

1. T. Dau, E.V. Edeleva *et al.* Quantitative analysis of protease recognition by inhibitors in plasma using microscale thermophoresis. *Sci. Rep.* **6**, 35413; doi: 10.1038/srep35413 (2016)

# Bioengineered 3D Skin with biodegradable Poly (lactic acid)-poly (ethylene glycol) Encapsulated Interleukin-10 to Avoid Immune Rejection

Saurabh Dixit<sup>1</sup>, Rajnish Sahu<sup>1</sup>, Shree R. Singh<sup>1</sup> and **Vida A. Dennis<sup>1</sup>**

<sup>1</sup> Center for NanoBiotechnology & Life Sciences Research, Alabama State University, 915 South Jackson Street, Montgomery, AL, 36104, USA

## Abstract:

Current commercial skin replacements provide some protection and reestablishing epidermal and dermal layers, but are unable to resolve the issue of graft rejection. Stem cells have the capacity to transform into different tissues and organ systems of the body, thus making them exceptional for tissue engineering. However, they lack proliferative capacity which prevents their biomedical applicability. Induced pluripotent stem cells (iPSCs) are the most recent advancement made in the area of cell biology wherein reprogramming somatic cells provides an exciting alternative to using embryonic stem cells, and reducing the likelihood of immune rejection. Recent data shows that mesenchymal and embryonic stem cells are able to avoid immune rejection by producing interleukin 10 (IL-10) and suppressing T-cell proliferation and pro-inflammatory cytokines. We have successfully encapsulated IL-10 in biodegradable Poly (lactic acid)-poly (ethylene glycol) nanoparticle (PLA-PEG-IL-10), demonstrated its slow release profile and functional capacity to inhibit LPS-induced pro-inflammatory TNF in differentiated keratinocytes and macrophages. PLA-PEG is FDA approved, immunologically inert and biocompatible, and PLA-PEG-IL-10 can be integrated in a matrix of a 3D human skin reconstruction model to avoid immune rejection. Our current development of 3D skin reconstructs consist of a "dermis" with fibroblasts iPSCs embedded in a collagen I matrix, an "epidermis", which is comprised of stratified, differentiated keratinocytes and a functional basement membrane, which separates epidermis from dermis. Our 3D human skin model will facilitate engineering immune-tolerant skin grafts for biomedical applications.

**Keywords:** 3D bioengineered skin, keratinocytes, PLA-PEG, IL-10, TNF, ELISA, biodegradable nanopartilces.

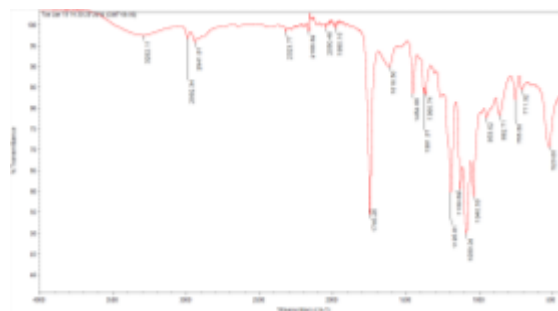
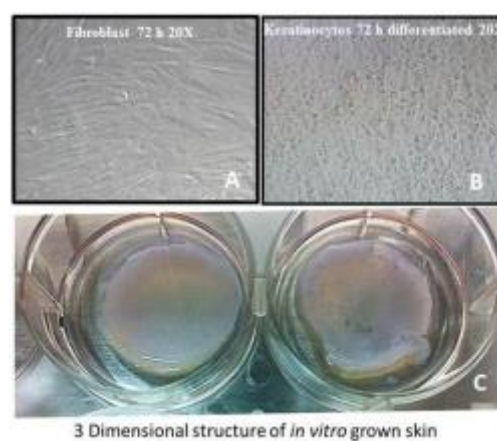


Fig. 1: FT-IR profile of encapsulated IL-10



**Figure 2:** Figure illustrating differentiated keratinocytes in culture and a 3D in vitro generated bioengineered skin. Our goal is to develop 3D skin infused with biodegradable encapsulated IL-10 to aid in skin regeneration and to avoid immunological rejection..

# Implementation of a new computational strategy in the design of more effective molecularly imprinted polymers

Ghada AlTaher<sup>1</sup>, Tarek M. Madkour<sup>2</sup>

<sup>1</sup>American University in Cairo, Nanotechnology graduate program, Cairo, Egypt

<sup>2</sup>American University in Cairo, Department of chemistry, Cairo, Egypt

## Abstract:

In the last few decades, Molecularly Imprinted Polymers (MIPs) emerged as potential substitutes to enzymes/proteins in chemical sensing applications. They are polymer based and thus, more stable and much cheaper.

MIP networks contain nano-scaled cavities that could bind complimentary analytes during chemical sensing. However MIPs are not as highly specific as enzymes/proteins, owing to the deterioration of many cavities during the synthesis stages (Figure 1). Literature usually focused on creating binding sites that can bind strongly with the template. It has been manifested that this is not always enough!

This research adopted a novel strategy in order to induce the formation of nano-scaled cavities that not only could bind strongly to a particular template, but also resisted deterioration.

Research methodology started by a theoretical computational approach followed by its validation in the experimental investigations.

The theoretical approach relied on the creation of a library of monomers (MIP building blocks), followed by a three-staged screening process based on conformational analysis and binding energy scores, in order to select the best two scoring candidates, which were employed in the synthesis of two new MIPs. Finally, The binding capacities (towards glucose) of the MIPs were compared against a control MIP.

Results showed that the new MIPs had higher binding capacities over the control, and the characterization methods employed (SEM, FTIR, BET) showed clear morphological, functionality, and porosity differences between them.

In conclusion, the adopted strategy was successful in designing MIPs that are more specific and economic for the next generation of chemical sensors.

**Keywords:** MIPs, computational modeling, molecular dynamics, nano-scaled cavities, binding energy, conformational analysis.

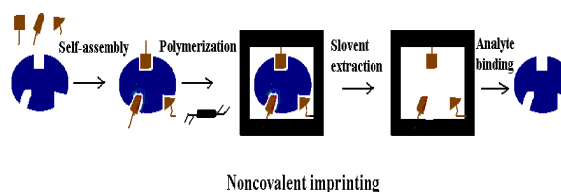


**Figure 1:** The current research investigates the implementation of a novel computational strategy, in order to effectively create nano-scaled cavities that can resist the detrimental effects caused by the different stages of non-covalent polymeric imprinting (Self assembly, crosslinking, polymerization, and template removal).

## References:

1. Lorenzo, R., Carro, A., Lorenzo, C., Concheiro, A. (2011), To Remove or Not to Remove? The challenge of extracting the template to make the cavities available in molecularly imprinted polymers (MIPs), *Int. J. Mol. Sci.*, 12, 4327-4347.
2. Yan, H., Row, H. (2006), Characteristic and synthetic approach of molecularly imprinted polymer, *Int. J. Mol. Sci.*, 7, 155-187.

**Posters Session II:  
NanoMaterials for Energy and  
Environment / Nanoelectronics/  
NanoPhotonics**

# All solid-state planar MoO<sub>x</sub>/Ag micro-supercapacitors with high performance

Ming-Xun Jiang,<sup>1</sup> Ke Teng,<sup>1</sup> Sheng-Wei Lee,<sup>1,2,3\*</sup>

<sup>1</sup>Institute of Materials Science and Engineering, National Central University, Taoyuan, Taiwan

<sup>2</sup>Department of Mechanical Engineering, National Central University, Taoyuan, Taiwan

<sup>3</sup>Department of Chemical and Materials Engineering, National Central University, Taoyuan, Taiwan

## Abstract:

The influences of the geometric configuration of all solid-state multilayered MoO<sub>x</sub>/Ag micro-supercapacitors on their specific energy and specific power have been investigated. The equivalent series resistance were extracted from the experimental electrochemical impedance spectroscopy (EIS) measurements performed on gold current collectors with different interdigitated patterns (varying the finger interspace, width, length, and number of interdigitated fingers shown in Figure 1). The results show that the geometric configuration plays a key-role on the electrochemical performances of the micro-capacitor (Figure 2), and that the specific power is enhanced by a reduction of the interspace. The multilayered MoO<sub>x</sub>/Ag micro-supercapacitor with an optimal geometric configuration was found to exhibit higher maximum energy density and maximum power density than those obtained for other solid-state supercapacitors. At a scan rate of 1 Vs<sup>-1</sup>, a volumetric capacitance  $\sim 45 \text{ Fcm}^{-3}$  is obtained for MoO<sub>x</sub>/Ag multilayer electrodes, which is much higher than the bare MoO<sub>x</sub> electrode. The EIS results also confirm that the electrical conductivity of MoO<sub>x</sub> is improved due to the incorporation of silver. The multilayered MoO<sub>x</sub>/Ag micro-supercapacitor also shows good long-term cycling stability. This fabrication process allows the multilayered MoO<sub>x</sub>/Ag micro-supercapacitor to be integrated with miniaturized electronic devices, to meet the need for microscale energy storage.

**Keywords:** micro-supercapacitors, MoO<sub>x</sub>/Ag, equivalent series resistance, electrochemical impedance spectroscopy, power density, long-term cycling stability volumetric capacitance, microscale energy storage.

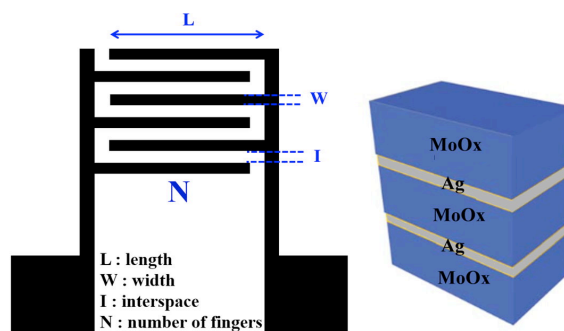


**Figure 1:** Schematic drawing of the symmetric interdigital micro-supercapacitor and stacked multilayers of MoO<sub>x</sub> and silver deposited by sputtering.

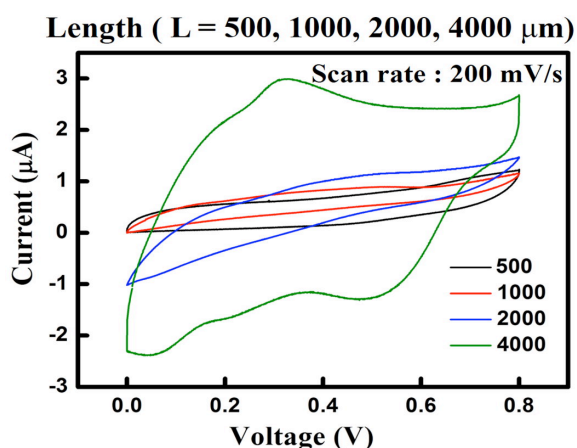


**Figure 2:** Cyclic voltammetry (CV) curves of the planar MoO<sub>x</sub>/Ag micro-supercapacitors with different lengths at scan rate of 200 mVs<sup>-1</sup>.

## References:

1. D. Pech, M. Brunet, T. M. Dinh, K. Armstrong, J. Gaudet, D. Guay (2013), Influence of the configuration in planar interdigitated electrochemical micro-capacitors, *J. Power Sources* 230, 230-235.

# Thermoelectric Properties of Zinc Antimonide Thin Film

C. Woo,<sup>1,\*</sup> H. Shim,<sup>1</sup> S. Han<sup>1</sup>

<sup>1</sup> Korea Institute Of Machinery & Materials, Department of Nanomechanics, Daejeon, Korea

## Abstract:

The zinc antimonide compound  $Zn_xSb_y$  is one of the most efficient thermoelectric materials known at high temperatures, due to its exceptional low thermal conductivity. For this reason, it continues to be the focus of active research, especially on its glass-like atomic structure. However, before practical use in actual surroundings such as near a vehicle manifold, it is imperative to analyze the thermal reliability of these materials. Herein we present the thermal cycling behavior of  $Zn_xSb_y$  thin films in nitrogen ( $N_2$ ) purged or ambient atmosphere.  $Zn_xSb_y$  thin films were prepared by co-sputtering, and reached a power factor of  $1.39 \text{ mW m}^{-1} \text{ K}^{-2}$  at  $321 \text{ }^\circ\text{C}$ . The high temperature *in-situ* XRD patterns and TEM results shows that the degradation in thermoelectric performance of  $Zn_xSb_y$  thin film with increasing number of thermal cycling comes from structural, morphological and compositional changes. In particular, the fluidity of Zn atoms in  $Zn_xSb_y$  thin film matrix during the thermal cycling give rise to morphological and compositional changes, such as nano inclusions or voids, which leads to degradation of the thermoelectric performance over thermal cycling. Moreover, these changes are more developed under atmospheric measurement condition, which generate thermally decomposed Zn or other impurity phase. For instance, the ZnO coating layer, which comes from oxidation of thermally decomposed Zn from the  $Zn_xSb_y$  thin film, keep the thermoelectric performance for a while by blocking the Zn evaporation from the  $Zn_xSb_y$  thin film. However,  $Zn_xSb_y$  thin film eventually was broken by growth of Zn fiber to relieve the thermal stress, which followed by Zn agglomeration with further atmospheric thermal cycling. These results provide insight for the needs for the proper encapsulation of the  $Zn_xSb_y$  surface that does not degrade thermoelectric performance with repeated thermal cycling.

**Keywords:** zinc antimonide, thermoelectric thin film, thermal cycle, thermoelectric properties and measurement, RF magnetron co-sputtering.

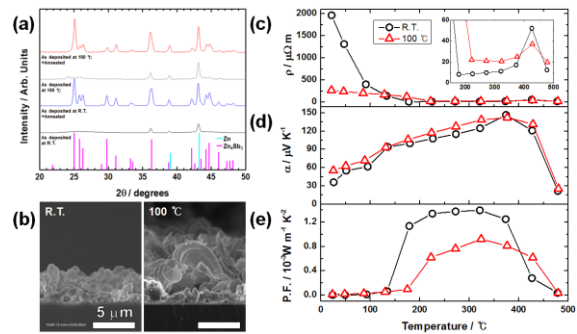


**Figure 1:** XRD patterns of sample deposited on the substrate at (a) room temperature (*type A*, gray line, Zn + amorphous  $Zn_4Sb_3$  ( $a-Zn_4Sb_3$ )), and  $100 \text{ }^\circ\text{C}$  (*type B*, light gray line, Zn +  $Zn_4Sb_3$ ). The blue and red lines indicate the XRD patterns of *type A* and *B* samples, respectively, after annealing. (b) Cross sectional FESEM images of *type A* (left) and *B* (right) samples. Thermoelectric properties of  $Zn_xSb_y$  thin film samples as a function of temperature: (c) resistivity ( $\rho$ ), (d) Seebeck coefficient ( $\alpha$ ), and (e) Power factor (P.F.) data.

## References:

1. Bell, E. (2008) Cooling, Heating, Generating Power, and Recovering Waste Heat with Thermoelectric Systems. *Science*, 321, 1457–1461.
2. Venkatasubramanian, R.; Siivola, E.; Colpitts, T.; O’Quinn, B. (2001) Thin-Film Thermoelectric Devices with High Room-temperature Figures of Merit. *Nature*, 413, 597–602.

# Electrochemical sensing of pesticides on disposable screen printed electrodes to detect water and environmental contamination

J. S. Noori,<sup>1,3</sup> M. Dimaki,<sup>1</sup> J. Mortensen,<sup>2</sup> W. E. Svendsen,<sup>1</sup>

<sup>1</sup> Technical University of Denmark, Department of Micro- and Nanotechnology, Kgs. Lyngby, DK

<sup>2</sup> Roskilde University, Department of Science and Environment, Roskilde, DK

<sup>3</sup>IPM – Intelligent Pollutant Monitoring, Kgs. Lyngby, DK

## Abstract:

There is an increasing demand for continuous monitoring of substances released in the environment. With today's portable accurate microelectronics and modern electrochemical detection methods, electrochemical measurements are the ideal candidate for contaminant detection. In order for the electrochemical techniques to be applicable in field settings, the targeted compound needs to initially be tested under controlled conditions and the different measurement parameters for the targeted element have to be found and optimized. In this work, the focus is to detect several pesticide compounds that have been reported to be present in the environment and develop a measuring protocol for each one separately. Currently, the focus is to detect Glyphosate by using voltammetric techniques. Different materials and geometries of screen printed electrodes were tested with voltammetric techniques to select the most suitable electrode and method to proceed with. The targeted detection limit is  $0.1\mu\text{gL}^{-1}$ . Initial testing results showed that water samples containing the same concentration ( $50\text{mgL}^{-1}$ ) of Glyphosate and tested on different electrodes will give different results, figure 1. The influence of the different electrode materials and design on the obtained signal is investigated. An initial estimate for the reduction peak of Glyphosate was made at around  $-0.65\text{V}$  when using carbon nanotube electrodes modified with gold nanoparticles. There are although interfering signals from other compounds which need to be identified. In addition, electrode surface modification is being investigated. All of these factors will allow resolving the challenge of using electrochemistry in real life applications. In addition, this study will allow combining the optimal sensors with the right devices to provide continuous measurements of the targeted pesticide concentrations in the environment.

**Keywords:** electrochemical sensing, screen printed electrodes, voltammetric measurements, pesticide, continuous measurement.

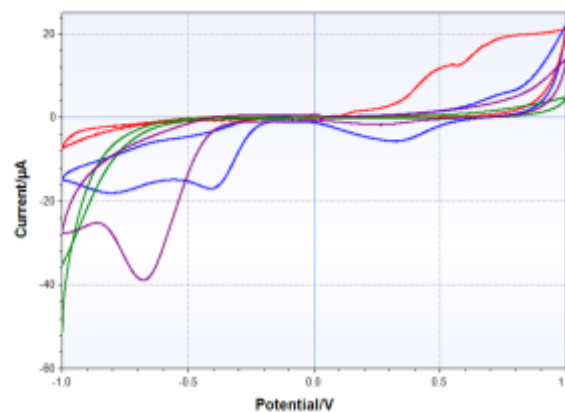


**Figure 1:** Illustration figure showing the different signals obtained when having same water sample, containing the same concentration,  $50\text{mgL}^{-1}$ , of Glyphosate, tested on different electrodes.

## References:

1. J. Wang, "Real-time electrochemical monitoring: Toward green analytical chemistry," *Acc. Chem. Res.*, vol. 35, no. 9, pp. 811–816, 2002.
2. K. I. M. R. Rogers and C. L. Gerlach, "a Status Report," *Env. Science and Technology*, vol. 30, no. 11, pp. 146–154, 1996.
3. M.-L. Tercier, J. Buffle, and F. Graziottin, "A Novel Voltammetric In-Situ Profiling System for Continuous Real-Time Monitoring of Trace Elements in Natural Waters," *Electroanalysis*, vol. 10, no. 6, pp. 355–363, 1998.

# A study on the modification of cellulose acetate membranes with graphene oxide nanofillers for water treatment

M. Mohamed<sup>1</sup>, A. Esawi<sup>2</sup>, R. Ramadan<sup>1</sup>

<sup>1</sup>Department of Chemistry, The American University in Cairo, AUC Avenue, New Cairo, Egypt

<sup>2</sup>Department of Mechanical Engineering, The American University in Cairo

## Abstract:

In this study, cellulose acetate (CA) ( $M_w = 52,000$  Da) membranes containing different amounts of graphene oxide (GO) were prepared by phase inversion (PI). Acetone was used as a solvent and N, N- dimethylformamide as a non-solvent, with a ratio of 4: 1, and deionized water as the coagulation medium. The membranes were prepared using a mixture of 19 wt.% CA with 0.025 to 0.1 wt.% GO. The effect of GO on membrane morphology was investigated by scanning electron microscopy (SEM), Fourier Transform Infrared spectrophotometer (FTIR), Brunauer-Emmett-Teller surface analysis (BET) and contact angle measurements. Salt rejection and permeation rates were tested using a 2000 ppm NaCl solution and 5000 ppm  $MgSO_4$  solution at a pressure of 24 bars using a dead-end filtration cell.

SEM cross sectional images showed proper dispersion of GO sheets in the polymeric matrix which implies the formation of strong hydrogen bonds between CA and GO sheets [1]. An increase in porosity of CA/GO membranes in comparison with the CA membrane was also noticed. In addition, finger-like macropores were formed indicating the instantaneous solvent-non-solvent exchange as a result of the hydrophilic nature of GO added (Figure 1). However, on increasing GO content to 0.1 wt. %, delayed demixing happened. It was found that permeation rates increased with increasing GO. This increase in GO increased the number of hydrophilic sites in the membranes which attracted water molecules and facilitated their movement through the membrane. As for salt rejection, the membrane with 0.05 wt.% GO showed the highest salt rejection value of 74% and 81% for 2000 ppm NaCl and 5000 ppm  $MgSO_4$  solutions respectively. This was explained by the decrease of the porosity at the membranes skin layer as a result of the addition of GO.[2]

**Keywords:** Cellulose acetate, graphene oxide, reverse osmosis, nanofiltration, water desalination.

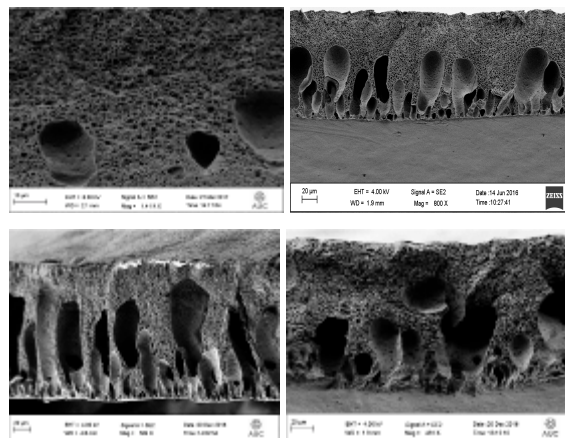


**Figure 1:** (a) 0 wt. %GO, (b) 0.025 wt. % GO, (c) 0.05 wt. %GO, (d) 0.1 wt. %GO

## References:

1. Ammar, A., Al-Enizi, A. M., AlMaa-deed, M. A., & Karim, A. (2016). Influence of graphene oxide on mechanical, morphological, barrier, and electrical properties of polymer membranes. *Arabian Journal of Chemistry*, 9(2), 274-286.
2. Ionita, M., Crica, L. E., Voicu, S. I., Pandeale, A. M., & Iovu, H. (2016). Fabrication of cellulose triacetate/ graphene oxide porous membrane. *Polymers for Advanced Technologies*, 27(3), 350-357.

# Control of Variable Speed Wind Turbine for A Stand Alone Load

A. Dahbi<sup>1,2,3\*</sup>, A. Reama<sup>2</sup>, N. Nait-Said,<sup>1</sup>, M. Nait-Said,<sup>1</sup>

<sup>1</sup> Batna University 2, Department of Electrical Engineering, LSP-IE' 05000, Batna, Algeria

<sup>2</sup> Department of system engineering, University of Paris-Est, ESIEE, Paris, France

<sup>3</sup> Unité de Recherche en Energies Renouvelables en Milieu Saharien (URERMS), Centre de Développement des Energies renouvelables (CDER), 01000, Adrar, Algeria

## Abstract:

This paper describes the modeling and control system of a variable speed wind turbine using Permanent Magnet Synchronous Generator (PMSG) associated to a Pulse Width Modulation (PWM) rectifier supplied a standalone load. The wind turbine is used to drive the PMSG in order to feed the isolated load. Our objectives are, maximizing the captured power in Wind energy conversion system (WECS) and controlling the delivered power to the load, for that, we applied a control strategy that allows sinusoidal current absorption to maximum the power from one hand, on the other hand, it ensures a good controlled electrical power according to different load requirements, all these are achieved by using only one converter, which reduce the cost and the system volume. Mathematical relations were studied and detailed. The dynamic performances are analyzed using simulation results under Matlab/Simulink then realized in real time using dSPACE 1104, the simulation results and realized results have shown that the proposed methodology is an efficient solution for different isolated load in the wind energy conversion system.

**Keywords:** protein Permanent-magnet synchronous generator (PMSG), Pulse width modulation (PWM), Wind energy conversion system (WECS).

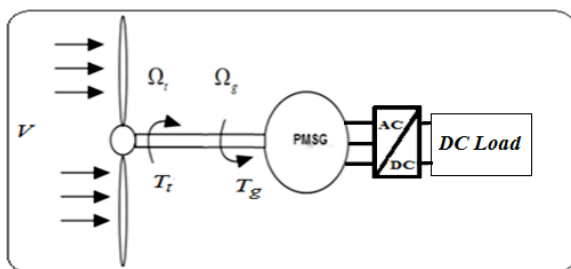


**Figure 1:** Global scheme of the WECS

## References:

1. Nayanar V, Kumaresan N, Ammasai Gounden N. A singlesensor-based MPPT controller for wind-driven induction generators supplying DC microgrid. IEEE Trans

Power Electron February 2016;31(2):1161-72.

2. Dahbi Abdeldjalil, Hachemi Mabrouk, Nait said Nasreddine, Nait Said Mohamed Said, A novel combined MPPT-pitch angle control for wide range variable speed wind turbine based on neural network, International journal of Hydrogen Energy, Vol 4 1, pp\_9427-9442, 2016.
3. Montoneri, A.J. Mahdi, W.H. Tang, L. Jiang, Q.H. Wu; " A Comparative Study on Variable-Speed Operations of a Wind Generation System Using Vector Control". *Proc ICREPQ'10, Granada (Spain), 2010.*
4. Dahbi Abdeldjalil, Hachemi Mabrouk, Nait said Nasreddine, Nait Said Mohamed Said, 'Realization and Control of a Wind Turbine Connected to the Grid by Using PMSG', Energy Conversion and Management, Vol 84; pp\_346–353, 2014.
5. Dahbi Abdeldjalil, Hachemi Mabrouk, 'Control of a Wind Turbine Based on PMSG and Connected to the Grid', International Review of Automatic Control (IREACO). Vol 5, No 5, pp\_553-559, Septembre 2012.
6. Dahbi Abdeldjalil, Nasreddine Nait-said, Messaoud Hamouda, Arama Fatima Zohra , ' Analysis of Different Converters Used In Wind Energy Conversion System'. 978-1-4799-7336-1/14/ IEEE Xplore, 2014.
7. Hanzo L. Power conversion and control of wind energy systems. IEEE Press; 2011 [Edition].
8. Dahbi Abdeldjalil, Hachemi Mabrouk, 'Influence of the parameters variations on the power injected to the network by wind turbine using PMSG', Acta Electrotehnica. Vol 54, No 1, pp\_31-44, 2013.
9. Yang Bo, Jiang Lin, Wang Lei, Yao Wei, Wu QH. Nonlinear maximum power point tracking control and modal analysis of DFIG based wind turbine. Electr Power Energy Syst, 2016;74:429-36.
10. Dahbi Abdeldjalil, Hachemi Mabrouk, Nait said Mohamed Said, Nait Said Nasreddine' Control and Realization of wind emulator

and the Effect of the Parameters Variations on the Efficiency of the Wind Turbine', Archives Des Sciences.Vol 66, No. 6; pp\_7-12, Jun 2013.

11. Harrouz, A. Dahbi, O. Harrouz, A. Bentiallah , 'Control of Wind Turbine based of PMSG Connected to Water Pumping System in South of Algeria'. IEEE Xplore, 10.1109/EFEA.2014.7059951, pp\_1-4, 2014.

# Ultrathin vertical plasmonic gaps

A. Manzi <sup>1,2,\*</sup>, L. Emeric <sup>3</sup>, A.S. Urban <sup>1,2</sup>, J. Feldmann <sup>1,2</sup>, J.-L. Pelouard <sup>3</sup>, C. Deeb <sup>3</sup>

<sup>1</sup>Ludwig-Maximilians-Universität, Chair for Photonics and Optoelectronics, Munich, Germany

<sup>2</sup>Nanosystems Initiative Munich (NIM), Munich, Germany

<sup>3</sup>Laboratoire de Photonique et de Nanostructures LPN—CNRS, Route de Nozay, 91460 Marcoussis, France

## Abstract:

Plasmonic cavities and nanoantennas have been reported as interesting tools to modify the photonic environment of emitters integrated in the vicinity of coupled plasmonic modes [1].

In these studies, we have investigated the gap-dependent resonances of plasmonic nanoantennas consisting of colloiddally synthesized metallic nanoparticles deposited on a gold film separated by an insulating layer deposited via atomic layer deposition (see Figure 1). The thickness of the spacer was varied accurately between 0.6 nm and several nanometers. In such a way, we were able to study the optical properties of these ultrathin vertical plasmonic gap nanoantennas and to understand how to tune the related parameters for application in light-emitting devices.

**Keywords:** nanoantennas, plasmonics, Purcell effect, fluorescence enhancement.

Processes Using Tunable Plasmonic Nanopatch Antennas, *Nano Lett.*, 14, 4797-4802

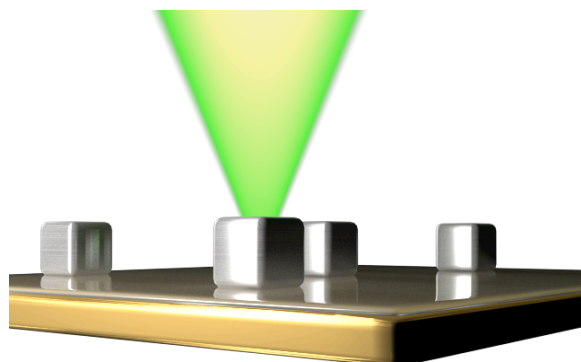


**Figure 1:** Schematic configuration of silver nanocubes placed on a gold film separated by an ultrathin insulating layer of controlled thickness.

## References:

1. A. Rose, T.B. Hoang, F. McGuire, J.J. Mock, C. Ciraci, D.R. Smith, and M.H. Mikkelsen. (2014) Control of Radiative

# Fabrication of magnetic vortex memory cell

M. Dhankhar,<sup>1,\*</sup> J. Sadilek,<sup>1</sup> M. Urbanek<sup>1</sup>, T. Sikola<sup>1</sup>

<sup>1</sup>Central European Institute of Technology, Brno University of Technology, Czech Republic

<sup>2</sup>Institute of Physical Engineering, Brno University of Technology, Czech Republic

## Abstract:

We present fabrication of a device which is capable to store four bit of information inside a single magnetic disk. The information inside of the disk is stored in a form of a magnetic vortex. Magnetic vortices are characterized by the sense of in-plane magnetization circulation and by the polarity of the vortex core, which leads to four possible stable configurations (vortex states). The device consist of a waveguide with permalloy disk on it and two electrodes connected to the disk. The waveguide serves for resonant vortex excitation and information writing via generation of magnetic field pulses, whereas the electrical contacts are used for readout of the vortex state via anisotropic magnetoresistance effect. Here we fabricate an array of permalloy disks with diameter ranging from 800nm - 4um and thickness of 35 – 50nm on 100nm thick gold waveguide and then contacting the disks by gold electrodes. The gold waveguide was fabricated on Silicon substrate with an insulating layer of silicon dioxide of 280nm by direct writing laser lithography using negative tone optical resist. The gold was then etched by ion beam etching technique. An insulating layer of silicon dioxide of 45nm was deposited on waveguide to make an insulation between waveguide and disks. Followed by sputtering of permalloy layer ( $\text{Ni}_{80}\text{Fe}_{20}$ ) and negative e-beam lithography of disks as shown in figure 1(a). The disks were then etched by ion beam etching technique and contacted with gold electrodes by positive e-beam lithography as shown in figure 1(b).

**Keywords:** fabrication, waveguide, contacting electrodes, magnetic vortex, anisotropic magnetoresistance, magnetic transmission x-ray microscopy, lithography, sputtering, etching

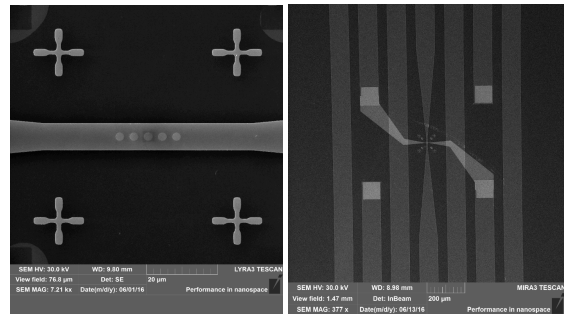


**Figure 1 (a) :** It shows the scanning electron microscope(SEM) image of permalloy disks on gold waveguide. Figure 1 (b) shows the SEM image of complete fabrication steps. It has gold waveguide with permalloy disks and contacting electrodes on disks.

## References:

1. Uhlř, V., Urbánek, M., Hladík, L., Spousta, J., Im, M.-Y., Fischer, P., Eibagi, N., Kan, J.J., Fullerton, E.E., and Sikola, T. Dynamic switching of the spin circulation in tapered magnetic nanodisks, *Nat. Nanotechnol.*, vol. 8, no. 5, pp. 341–346, May 2013.

# Effects of carbon dots on the growth of nanostructured NiCo<sub>2</sub>S<sub>4</sub> with different morphologies

Yuanyuan Huang,<sup>1,2</sup> Tielin Sh<sup>1,2</sup>i, Zirong Tang<sup>1,2</sup>

<sup>1</sup> State Key Laboratory of Digital Manufacturing Equipment and Technology, Huazhong University of Science and Technology, Wuhan 430074, China

<sup>2</sup> Wuhan National Laboratory for Optoelectronics, Huazhong University of Science and Technology, Wuhan 430074, China

## Abstract:

Metal sulfides have been applied to pseudocapacitors owing to their great electrochemical performance like high reversible capacity and high energy densities. However, some inevitable deficiencies such as the lower electronic conductivities, the volume change effect during redox reactions always lead to the poor cycleability and poor rate performances. To overcome these shortages, we use carbon dots (CDs) to adjust the morphology of nanostructured NiCo<sub>2</sub>S<sub>4</sub> during growth. Carbon dots, as a new class of 0D carbon nanomaterials have attracted vast attentions due to their unique properties in both physics and chemistry. NiCo<sub>2</sub>S<sub>4</sub>@CDs composite nanomaterials with optimal morphologies can increase the surface area and conductivity comparing the bare NiCo<sub>2</sub>S<sub>4</sub>. Meanwhile, CDs integrated NiCo<sub>2</sub>S<sub>4</sub> provides excellent interface for the interactions between electrolytes and electrodes. As the NiCo<sub>2</sub>S<sub>4</sub>@CDs composite has such perfect chemical performance, which can be used as the active materials for high performance supercapacitors. Fig. 1 shows our recent results, where a cheap, facile, and efficient way was used to fabricate NiCo<sub>2</sub>S<sub>4</sub>@CDs with different morphologies, the application of the material for supercapacitors is also under working.

**Keywords:** carbon dots, NiCo<sub>2</sub>S<sub>4</sub>, pseudocapacitors, morphologies, nanostructure

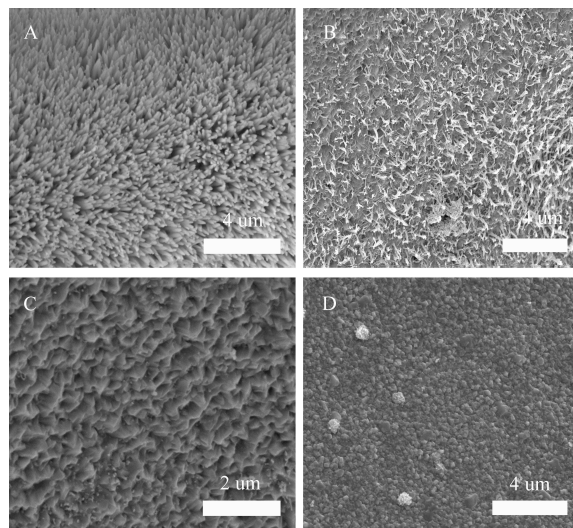


**Figure 1:** SEM images of the NiCo<sub>2</sub>S<sub>4</sub>@CDs with different amounts of CDs resulting in different morphologies.

## References:

1. Huang Y, Shi T, Jiang S, et al. Enhanced cycling stability of NiCo<sub>2</sub>S<sub>4</sub>@ NiO core-shell nanowire arrays for all-solid-state asymmetric supercapacitors. *Scientific Reports*, 2016, 6: 38620.
2. Wei J S, Ding H, Zhang P, et al. Carbon Dots/NiCo<sub>2</sub>O<sub>4</sub> Nanocomposites with Various Morphologies for High Performance Supercapacitors. *Small*, 2016, 12(43): 5927-5934.
3. Xiao Y, Lei Y, Zheng B, et al. Rapid microwave-assisted fabrication of 3D cauliflower-like NiCo<sub>2</sub>S<sub>4</sub> architectures for asymmetric supercapacitors. *RSC Advances*, 2015, 5(28): 21604-21613.

# Synthesis, Characterization and Application of Chitosan Beads-Supported Fe/Ag Bimetallic Nanoparticles for the Removal of Cadmium from Aqueous Solution

C. van der Horst,<sup>1,\*</sup> B. Silwana,<sup>2</sup> M. Makombe,<sup>3</sup> E. Iwuoha,<sup>1</sup> V. Somerset,<sup>4</sup>

<sup>1</sup> University of the Western Cape, SensorLab, Department of Chemistry, Bellville, South Africa

<sup>2</sup> Durham University, Department of Chemistry, Durham, United Kingdom

<sup>3</sup> Scientific Services Consulting Analytical Laboratory, Cape Town, South Africa

<sup>4</sup> Cape Peninsula University of Technology, Department of Chemistry, Bellville, South Africa

## Abstract:

Nowadays, water is the most important concern of this century, it is our common future and is important to preserve and guarantee this natural precious capital. However, the supply of good quality water becoming increasingly difficult in view of large scale pollution caused by agricultural, domestic and industrial activities. Many technologies including coagulation, membrane process, dialysis, foam flotation, osmosis, photocatalytic degradation and biological methods have been employed for the removal of toxic pollutants from water and wastewater. These technologies are effective but have some disadvantages such as expensive equipment, high operational and maintenance, high energy requirements, generation of toxic residual metal sludge and incomplete metal removal. On the other hand adsorption offers high efficiency, cost-effectiveness, easy handling and recovery of metals and other adsorbed species. Heavy metals are often found in wastewaters and the removal of these inorganic pollutants using bimetallic iron-based nanoparticles is still unclear. In this study, bimetallic iron-silver nanoparticles was chemically synthesized and impregnated into chitosan to form chitosan bimetallic iron-silver nanoparticles (CS/Fe-AgNPs) to remove heavy metals from wastewaters. The above CS/Fe-AgNPs beads were characterized using XRD, HRSEM, HRTEM, UV-VIS and FT-IR techniques. The HRTEM results shows that Fe/AgNPs and CS polymers are both spherical in shape with both Fe/AgNPs and CS polymers aligned on top of each other. The CS-Fe/AgNPs beads have a diameter of 5-10 nm. In the XRD pattern of chitosan/iron-silver nanocomposite, the presence of chitosan as well as bimetallic iron-silver peaks was observed. The values obtained for CS-Fe/AgNPs nanocomposite agreed well with the individual values obtained for both chitosan and Fe/AgNPs. In this study, chitosan iron-silver nanoparticles beads have been successfully prepared and it's efficiency in the removal of Cd(II) under ambient temperatures has

been evaluated. The removal rate of total Cd(II) from actual wastewater was 89.25%. Furthermore, the monolayer adsorption capacity of Cd(II) based on the Langmuir model was measured to be 90 mg/g. Results were satisfactory when employing the adsorbent for removal of Cd(II) from wastewater samples.

**Keywords:** Adsorption, Bioavailability, Monitoring, Wastewater.

## References:

1. Batisha, A.F. (2013), Sustainability of Water Purification Based on Nanotechnology, *Int. J. Sustain.*, 2, 12-24
2. Sharma, Y.C., Srivastava, V., Singh, V.K., Kaul, S.N., Weng, C.H. (2009), Nano-adsorbents for the removal of metallic pollutants from water and wastewater, *Environ. Technol.*, 30(6), 583-609.

# Environmental Remediation of water by novel CeO<sub>2</sub> nanoparticle photoelectrocatalysts.

R.Carvalho, A. Betts, J.Cassidy.

Dublin Institute of Technology, School of Chemical and Pharmaceutical Sciences, Dublin, IE

## Abstract:

CeO<sub>2</sub> nanoparticles were synthesized by a novel simple colloidal procedure. The impact of different factors like temperature and reactants concentration were varied experimentally, and optimized for CeO<sub>2</sub> nanoparticle synthesis. These nanoparticles were characterized by different techniques as UV-vis spectrometer, Raman, EDS, XRD, DLS and SEM to obtain information about absorption spectrum, elemental analysis, mean crystallite size, size distribution and morphology of nanoparticles. The data obtained by these analyses indicated that the colloidal method produces nanoparticles with a size range of 2-8nm.

Degradation of pollutants in wastewaters by photocatalysis is well known. In addition to this project the nanoparticles were utilized for photocatalytic degradation behavior of the anti-inflammatory Sodium Diclofenac and the dye methyl orange in aqueous solution. CeO<sub>2</sub> in both colloidal and powder forms were utilized as the catalyst under an irradiance of a solar simulator, which has given successful results. By utilizing this photocatalytic process in a Photo Fuel Cell (PFC) device, their rate of destruction may be greatly enhanced, at the same time producing useful electrical energy. This novel nanocrystalline visible-light active cerium oxide (ceria) photocatalysts will be incorporated onto a range of conductive surfaces for use as photoanodes in PFCs.

Their behavior in a PFC device will be assessed using selected wastewater pollutants and biomass-sourced compounds. A range of environmental conditions will be explored such as fuel/pollutant concentration level, electrolyte composition and pH variation, in order to determine the best performing catalyst/support/environment combination. A transition metal oxide-based air cathode will also be used (replacing expensive platinum) in conjunction with a modified PFC design, thus characteristics and mechanistic insights will be ascertained as a result. Direct comparison will be made with PFCs using a standard nanoparticulate TiO<sub>2</sub> photocatalyst.

**Keywords:** cerium dioxide, photocatalysis, wastewaters, PFC device, organic pollutants.

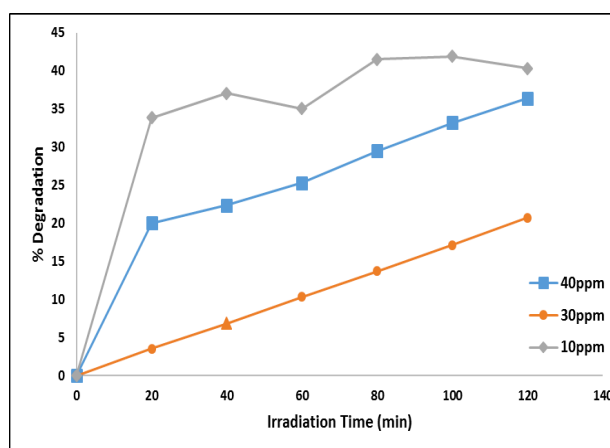


**Figure 1:** %Degradation of 10ppm, 30ppm and 40ppm sodium diclofenac over time under 20min UV irradiation.

## References:

1. A Garcia, R Espinosa, L Delgado, E Casals, E Gonzalez, V Puentes, C Barata, X Font, A Sanchez, *Desalination*, 269, 136 (2009)
2. P Enright, A J Betts, J F Cassidy, *Journal of Applied Electrochemistry*, 41, 345 (2011).
3. S K Mudili, S Wang, S Chen, C F Ng, C H A Huan, T C Sum, H S Soo, *Beilstein Journal of Nanotechnology*, 5, 517 (2014).

# Experimental Investigations on the Physical Properties of Tin Doped Indium Oxide Thin Films

H. Gueddaoui,<sup>1\*</sup> M. Ghemid<sup>1</sup>

<sup>1</sup> USTHB University, Faculty of Physics, LMSOM Laboratory, Algiers, Algeria

## Abstract:

Multi-layered tin indium doped oxide (ITO) films were deposited onto glass substrates by sol-gel spin coating process. The number of deposited layers was optimized in order to decrease the reflectance and to improve the optical transmittance in the visible range. Films properties were analysed with X-ray diffraction, optical and electrical measurements were also performed. A systematic investigation on the physical properties of ITO films was reported with respect to the number of deposited layers. Structural characterisation showed that obtained films are crystallized in cubic phases with 9–10 nm crystallite size and the determined lattice constant is nearly 10,1 Å, with orientation along the (222), (400), and (110) planes for all deposited films indicating stable cubic phase as reported in [1, 2].

Optical analysis of ITO showed high transparency and low reflectance in the visible range. The energy band gap of the multi-layered films as determined from absorption spectrum was ~ 3.7eV. The Drude-Lorentz classical model has been also used to fit the optical reflectance and transmittance.

Electrical measurements showed a clear dependence between sheet resistance and the deposited layers, the sheet resistance decreased from 114.5 MΩ to 4.35 MΩ for respectively 1 and 5 deposited layers.

**Keywords:** ITO, solar cells, sol-gel process, structural, electrical and optical properties.

## References:

1. P. C. Lansker, P. Petersson, G. A. Niklasson, C. G. Granqvist, (2013), Thin sputter-deposited gold films on In<sub>2</sub>O<sub>3</sub>:Sn, SnO<sub>2</sub>:In, TiO<sub>2</sub> and glass: Optical, electrical and structural effects, *Solar Energy Materials and Solar Cells.*, 117, 462-470.
2. A. Ayeshamariam, M. Kashif, M. Bououdina, U. Hashim, M. Jayachandran, M. E. Ali, (2014) Morphological, structural, and gas-sensing characterization of tin-doped indium oxide nanoparticles, *Ceramics International.*, 40, 1321-1328.

Media Partners

